Louisiana State University
LSU Digital Commons

LSU Doctoral Dissertations | Graduate School

2011

Semiconducting Polymers and Block Copolymers Prepared by Chain-Growth Living Polymerization

JinWoo Choi
Louisiana State University and Agricultural and Mechanical College

Follow this and additional works at: https://digitalcommons.lsu.edu/gradschool_dissertations

 Part of the Chemistry Commons

Recommended Citation
Choi, JinWoo, "Semiconducting Polymers and Block Copolymers Prepared by Chain-Growth Living Polymerization" (2011). *LSU Doctoral Dissertations*. 2308.
https://digitalcommons.lsu.edu/gradschool_dissertations/2308

This Dissertation is brought to you for free and open access by the Graduate School at LSU Digital Commons. It has been accepted for inclusion in LSU Doctoral Dissertations by an authorized graduate school editor of LSU Digital Commons. For more information, please contactgradetd@lsu.edu.

SEMICONDUCTING POLYMERS AND BLOCK COPOLYMERS PREPARED BY CHAIN-GROWTH LIVING POLYMERIZATION

A Dissertation

Submitted to the Graduate Faculty of the
Louisiana State University and
Agricultural and Mechanical College
in partial fulfillment of the
requirement for the degree of
Doctor of Philosophy

In

The Department of Chemistry

By

JinWoo Choi
B.S. Department of Chemistry, Korea University, Korea 2001
M.S. Department of Materials Chemistry, Korea University, Korea, 2003

August, 2011

DEDICATION

This dissertation is dedicated to my family and particularly to my mom with deep affection and praying who encourages me to finalize all my works. Whenever I was frustrated, she says I am a qualified person with certainty, saying the LORD always keeps me in safety.

I always keep in mind this phrase in the Bible, “In his heart a man plans his course, but the LORD determines his steps.” (Proverbs 16:9)

ACKNOWLEDGMENTS

I would like to truly appreciate my advisor Professor Evgueni E. Nesterov who made me finalize this work. Since having joined his group, I was always feeling that he tried to guide me to improve my knowledge to be a qualified organic/polymer Ph.D chemist. Although sometimes his advice and suggestions made me feel difficult, they eventually resulted in my Ph.D project. I would like to describe him as a great advisor with fruitful knowledge and kindness, a teacher and sometimes an engineer (he can fix almost any hardware in the lab such as a broken oven, poorly working exhaust fans on the roof-top of Choppin building, and even a partially broken car too!). He provided me with invaluable chances to acquire the field of conjugated polymers as my specialty area. Also, his great passion toward conjugated polymers allowed me to achieve exciting results that can provide a deeper understanding and develop my knowledge in the scientific research field. Indeed, I deeply respect him as a physical organic/polymer chemist as well as an advisor.

Specifically, I would like to extend a warm thank you to my advisory committee members: Professors Robin L. McCarley, M. Graća H. Vicente, Carol M. Taylor and Dimitri L. Nikitopolous for the kind guidance to complete this dissertation. I would like to thank our journal club co-chair, Professor David Spivak and his group members for giving me an opportunity to learn about fruitful ideas published in peer-reviewed journals every month and to exercise a technical research presentation for seminars, and interviews. This was a very enjoyable experience for me.

My deep appreciations go to the people who helped me to reach to the final pinnacle: Prof. Jayne Garno and Dr. Stephanie Daniels (our AFM study collaborators), Prof. Donghui Zhang and her group students (for GPC analysis), Prof. Paul Russo (for helpful discussion of light scattering results and polymer characterization), Dr. Rafael Cueto (for polymer characterization), Dr. Dale Treleaven (for NMR experiments), Prof. George Stanley (for helpful discussion of organometallic chemistry), Prof. Vince LiCata and his students (for

aqueous DSC studies), Dr. Henning Lichtenberg (for SAXS and WAXS measurements), my lab mate as well as friend Dr. Euiyong Hwang (for Electrochemical studies), Dr. Theshini Perera, Darina Polakova, Sang gil Yeum, Chang-uk Lee, Dr. Jiba Acharaya, Rajib Mondal, Deepa Pangeni, Brian Imsick, Carlos Chaves, Fan Huang and finally, Sourav Chatterjee (helping me out running SAXS and WASX measurements).

TABLE OF CONTENTS

LIST OF TABLES

LIST OF FIGURES

LIST OF SCHEMES

LIST OF ABBREVIATIONS AND SYMBOLS

acac - acetylacetonate
Ac_2O - acetic anhydride
CPs - conjugated polymers
Cy3 - Cyanine 3 dye
Cy5 - Cyanine 5 dye
DCM - dichloromethane
DMF - dimethylformamide
DMSO - dimethylsulfoxide
FTIR - Fourier Transform Infrared Spectroscopy
GRIM - Grignard Metathesis
GPC - gel permeation chromatography
HOMO - Highest Occupied Molecular Orbital
KCTP - Kumada Catalyst-Transfer Polycondensation
LCST - Lower Critical Solution Temperature
LDA - Lithium diisopropylamide
LUMO - Lowest Occupied Molecular Orbital
dppe - 1,2-bis(diphenylphosphino)ethane
dppf - 1,2-bis(diphenylphosphino)ferrocene
dppp - 1,3-bis(diphenylphosphino)propane
ppm - parts per million
P3HT - poly-(3-hexylthiophene)
P3AT - poly-(3-alkylthiophene)
PNIPAm - poly-(*N*-isopropylacrylamide)
PPV - poly-(*p*-phenylene vinylene)
PPE - poly-(*p*-phenylene ethynylene)
PF - polyfluorene
PPP - poly-(*p*-phenylene)
PPY - polypyrrole
PT - polythiophene
rr - regioregularity
TBAF - tetrabutylammonium fluoride
TBDMS – tert-Butyldimethylsilyl
TEA - triethylamine
TsCl - *p*-toluenesulfonyl chloride
TMS - tetramethyl silane or trimethylsilyl
UV/Vis - ultraviolet /visible
λ– lamda (wavelength)

ABSTRACT

Organic semiconducting polymers are the unique materials that considered a basis for the next generation of electronic and optoelectronic applications. However, high device performance of semiconducting polymers strongly depends on their molecular structure and nanoscale organization. Therefore, it is an essential task to develop robust and versatile synthetic approaches to build such well-defined semiconducting polymer materials.

This Ph.D. study aimed at design of state-of-the-art synthetic approaches towards organic semiconducting polymers via chain-growth living polymerization as well as development of polymer architectures which can self-organize into supramolecular nanoassemblies or allow external control of the polymer's properties.

First, we prepared a series of temperature-responsive water-soluble poly(*N*-isopropylacrylamide)-functionalized polythiophenes, and showed that their supramolecular organization and temperature control of their conformation and conjugation length was strongly dependent on the extent of regioregularity of the polythiophene backbone.

In order to improve the regioregularity, we developed a general approach to highly efficient external catalytic initiators for the synthesis of various semiconducting polymers. Extensive studies allowed better understanding of the unusual catalytic systems, and their behavior in chain-growth living polymerization reactions. Using this approach, we synthesized a variety of amphiphilic polythiophene block copolymers incorporating a low energy gap perylenedicarboximide (PDCI) unit to demonstrate the possibility to control supramolecular organization and photophysical properties of such systems by using external stimuli (such as solvent and temperature).

As part of our general studies towards design of near-infrared (NIR) fluorescent conjugated polymers, we developed a synthetic approach to a novel class of such materials which are based on cyanine dyes as monomeric repeating units. The obtained polymers showed a variety of properties (thermal stability, solubility, absorption and fluorescence in the NIR range) that may make them a useful class of NIR fluorescent conjugated polymers.

CHAPTER 1. A GENERAL OVERVIEW

1.1. Introduction to Conjugated Polymers (CPs) and CP-based Chemosensors

Conjugated polymers are macromolecules with alternating single and double carbon-carbon (or carbon-heteroatom) bonds and extended π-electron conjugation. After the discovery of highly conductive polyacetylene was made by Shirakawa, MacDiarmid and Heeger[1] over three decades ago, conducting polymers (also known as π-conjugated polymers) have received much attention from both academic and industrial communities due to the their unique electronic and optical properties which make them highly suitable for electronic and sensory devices.[2-6] In view of the general interest towards broad potential applications for manufacturing less expensive and flexible electronic devices, π-conjugated semiconducting polymers are considered highly promising functional polymers. For example, Philips introduced a first commercial LED (Light Emitting Diode) display based on conjugated polymers in 2002. During the three decades of research, various conjugated polymers such as polyacetylene, poly(*p*-phenylene) (PPP), poly(*p*-phenylene vinylene) (PPV), poly(*p*-phenylene ethynylene) (PPE), polythiophene (PT), poly(thienylene vinylene), polypyrrole, polyfluorene (PF), etc. have been synthesized and characterized. Chemical structures of typical conjugated polymers are shown in Figure 1. 1.[7]

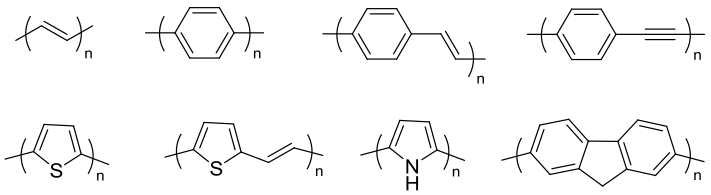

Figure 1. 1 Chemical structures of typical conjugated polymers.

This dissertation focuses mainly on the development of new synthetic pathways towards, as well as characterization of conjugated semiconducting polymers and studies of

their supramolecular organization (an additional research project described in the chapter 5 will deal with near infrared (NIR) π-conjugated polymer materials for sensing applications and potential photovoltaic devices). It is also focused on fundamental physical organic chemistry to better understand intermolecular and intramolecular energy transfer along the conjugated polymer backbone both in dilute solution and solid state. These phenomena are particularly important in the field of chemo- and biosensors development.

Generally, CP-based chemo- and biosensing represents a group of diverse methods to detect analytes. Fluorescence often acts as a sensitive optical transduction mechanism in which analyte binding events that lead to attenuation, enhancement, or wavelength shift in the emission can be used to make a functional sensor.[8] A chemically synthesized sensor consists of two interconnected functional groups - a receptor and a reporter group. When the two elements are in equilibrium, sensors can provide a real-time response which depends on the concentration of the analyte.

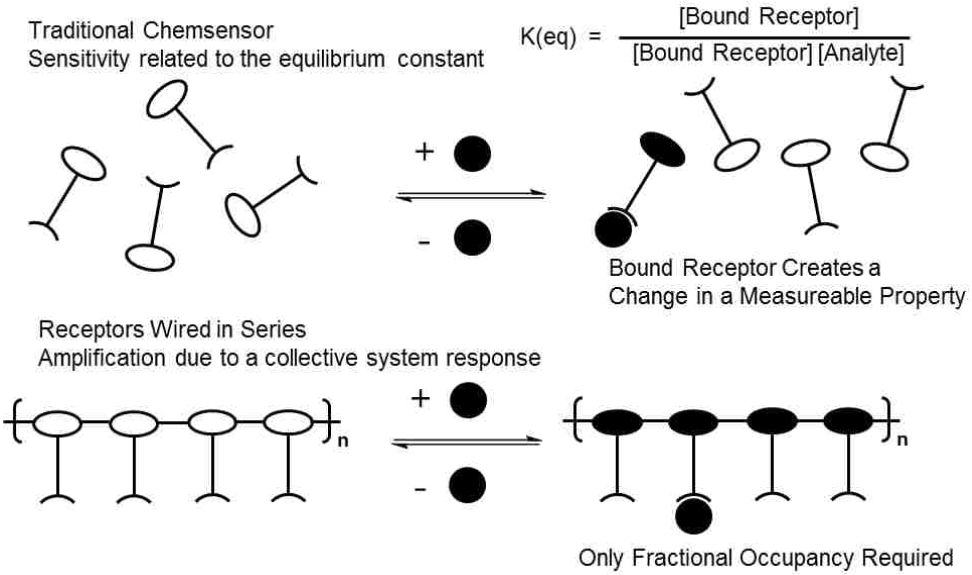

Figure 1. 2 Scheme of traditional monoreceptor and a wired polyreceptor system (adapted from ref 9).

To obtain a higher sensitivity, design of highly pre-organized receptors with high association constant that are able to overcome entropic penalty for complexation is required.

However, it is usual that preorganization and high association constant lead to slow dissociation kinetics, resulting in an irreversible response and in the ability to produce a reversible real-time response. Such approach has the disadvantage of introducing additional complexity into the sensor materials. On the other hand, in a conjugated polymer system, extended and collective electronic responses lead to significant signal *amplification*, resulting in a remarkable sensitivity. For example, even a single event the binding of an analyte in a supramolecular polymer system can yield a highly pronounced response that is far exceeding that produced by a similar interaction in an analogous small monomer system (Figure 1. 2).[9] Such amplified sensitivity in a supramolecular polymer system can give enormous advantages for conjugated polymer based sensing systems.

1.2. Chain-Growth Living Polymerization of Alkenes

Living polymerization methodology has expanded toward all of the chain-growth polymerization mechanisms such as cationic, anionic, free-radical and transition metal-catalyzed polymerizations. In the strictest sense, a living polymerization is a chain-growth polymerization that lacks irreversible chain-termination and chain-transfer steps.[10] Therefore, once chain growth is initiated, the polymer chain will continue to grow until complete consumtion of the monomers. After that, the active center will remain in active status, either until more monomers are added, in which case the chain growth will resume, or until a terminating agent is deliberately introduced. If initiation is complete and exchange between species of various reactivity is fast, the final average molecular weight of the polymer can be adjusted by varying the initial condition (DP = [Monomer]/$[Initiator]_o$, where DP =

degree of polymerization), while maintaining a narrow molecular weight distribution ($1.0 < M_w/M_n < 1.5$, where M_w = weight-average molecular weight and M_n = number-average molecular weight).[11] In a living system which uses a monofunctional initiator, only one site of chain-growth per polymer chain is dominant and consequently, the resulting macromolecule can be used as a polymeric building block. Living polymerization can produce precursor polymers which can be assembled into macromolecular assemblies that possess different structures and composition and exhibit novel properties. Theoretically, it would be ideal to keep the reacting end groups alive by supressing chain-transfer and chain-termination processes. However, in real living systems, chain-transfer and chain termination can occur to some degree and can be controlled by external conditions such as amount of monomers and initiators, reaction time, temperature, etc. In this case, the polymerization is called highly controlled living polymerization, and it is as synthetically useful as true living polymerization.

Of those controlled cationic, anionic, free-radical and transition metal-catalyzed living polymerization strategies, we will be focusing on transition metal-catalyzed living polymerization methods which have been widely employed for precise polymer synthesis. Not only can this process produce well-defined functional polymers, but it can also generate hybrids or conjugates with other (often biological) materials. Metal-catalyzed systems retain the advantages of conventional radical polymerization but distinguish themselves through catalytic, reversible halogen exchange equilibrium; the growing radical exists alongside a dormant species as a covalent precursor capped with a terminal halogen from an initiator. The catalyst dictates the selectivity, exchange rate, and control over the polymerization. Such catalysts enable a wider range of applications and target products, have low metal

content, could be readily removed from products, and provide recycling advantages. As some earlier examples, $RuCl_2(PPh_3)_3$[12-13], $FeCl_2(PPh_3)_2$[14] and $NiBr_2(PPh_3)_2$[15], showed enhanced catalytic activity and control through several modifications: electron-donating or resonance-enhancing groups, moderate bulkiness, heterochelation via a ligand, and halogen-donor additives. Figure 1. 3 illustrates an example of polymerization with methyl methacrylate (MMA) monomer, trichlorobromomethane (initiator) and $RuCl_2(PPh_3)_3$ (catalyst).

The first step in such polymerization (often referred to as Atom Transfer Radical Polymerization, ATRP) is the dissociation of the carbon-bromine bond in the initiator, catalyzed by the Ru(II) complex, which generates a reactive species that initiates propagation with MMA. This step involves oxidative addition which converts Ru(II) into Ru(III) while the catalyst accepts the bromine from the initiator.

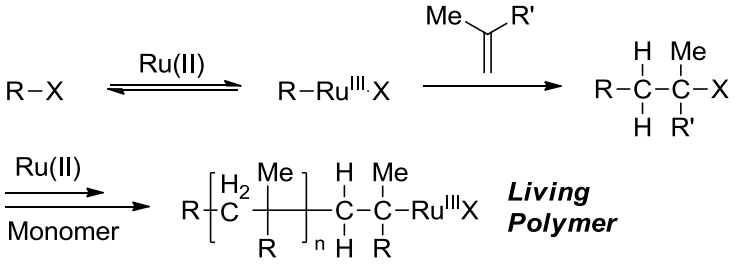

Figure 1. 3 An example of metal-catalyzed living polymerization via dormant species: a typical example with a Ru(II) catalyst (adapted from ref 13).

After numerous propagation steps, the intermediate ends up being capped with the bromine from the resulting Ru(III) species in the process of regenerating a dormant end and the Ru(II) catalyst. The overall process thus involves a reversible and dynamic equilibrium between the dormant species and the active carbon species, all mediated by a metal complex. The key to the living growth is a very low radical concentration, coupled with the

reversibility of its generation, thereby suppressing bimolecular radical termination prevailing in conventional radical polymerizations as generalized for other living or controlled polymerizations.

Metal catalysts are probably the most critical components in metal-catalyzed living polymerization, and over time have been developed hand in-hand with their systematic design, or an evolution of catalysts.[12,14,16] The required mode of action for the catalysis is the reversible activation of a dormant species or a terminal carbon-halogen bond, where it undergoes an oxidative addition and reductive elimination followed by abstraction/release of a halogen. Thus, central metals should afford formation of at least two valence states with one valence difference and should possess a moderate halogen affinity. Due to this reason, late transition metals such as iron, nickel, ruthenium, copper, etc. in a lower valence state are generally favored. However, some early transition metals have also been employed where the activation step is apparently triggered by an electron transfer from a catalyst to a dormant terminus, and thus a higher electron density on the metal center would be suitable.

1.2.1 Transition Metal Catalysts for ATRP. Ruthenium (Ru) complexes were the first class of catalysts for metal-catalyzed living polymerization, as first reported in 1995.[17] The ruthenium catalyst employed was a divalent Ru(II) complex, typically carrying two anionic ligands, such as halogens, conjugated carbanions, and phenoxy anions, as well as some neutral ligands as phosphines, amines, cymene, and carbenes. The large capacity of the coordination space and the inherent tolerance (low oxophilicity) to functional groups of the Ru(II) complexes allow coordination of various ligands, leading to wide possibilities in catalyst design based on the modulation of electron density and the steric environment at the ruthenium center. $RuCl_2(PPh_3)_3$ was the first example of dichloride ruthenium complexes

catalyzing living polymerization, which was originally proved to catalyze Kharasch addition reactions,[18] a model of the polymerization. Half-metallocene-type ruthenium complexes with indenyl[19] and pentamethylcyclopentadiene (Cp*)[20] ligands are representative active catalysts for living polymerization giving quite narrow molecular weight distributions and well-defined block copolymers.

In metal-catalyzed living polymerizations, copper (Cu) complexes have been widely used for various applications due to not only the superior catalysis and the detailed mechanistic understanding but also the low cost and easy handling of mixing a copper (I) halide with a ligand. Since the first discovery of living polymerization with CuCl/2,2′-bipyridyl (bpy) by Matyjaszewski,[21] various copper and ligand systems for ATRP have been developed. Typical examples of active catalysts are CuX or CuX_2 (X = halide) with cyclic ligand systems such as cyclam/DMCBCy (**1-1**), Me_6TREN(**1-2**),[22] *N,N,N′,N*′-tetrakis(2-pyridylmethyl)ethylendiamine (TPEN) (**1-3**) (Figure 1. 4).[21]

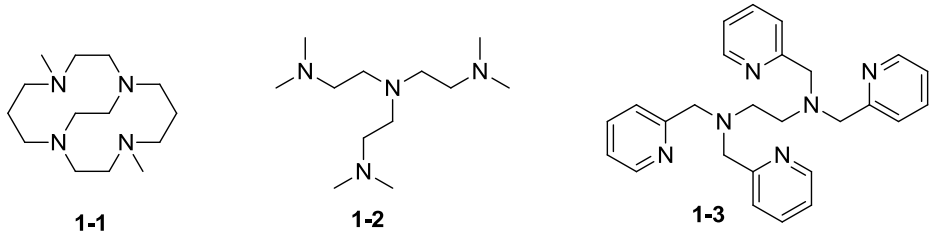

Figure 1. 4 Structures of cyclic ligands, cyclam/DMCBCy (**1-1**), Me_6TREN (**1-2**) and *N,N,N′,N*′-tetrakis(2-pyridylmethyl)-ethylendiamine (TPEN) (**1-3**).

Detailed structural studies indicate that the copper-ligand complex is in equilibrium between binuclear and mononuclear state in solution, and the latter is presumed to be a "real" activator. Because of such dynamic structural change and the flexible coordination by the multidendate ligand, the complex is stabilized during polymerization without suffering

from an extra coordination of solvents and monomers, which allows low amount of the copper catalyst. A milestone achievenment in copper-catalyzed living polymerization was the development of very efficient systems, where extremely small amount of catalyst (less than 10^{-6} mol %) is required to achieve living polymerization without deteriorating reaction rate and fine control.

The development of iron-based catalysts for living polymerization is currently important, because they possess a number of potentially beneficial features, e.g. they are safe, biocompatible, active, abundant, and inexpensive. In general, divalent iron complexes [Fe(II)] will be most suitable, and polymerization proceeds under an equilibrium between Fe(II) and Fe(III). Earlier examples in fact follow this concept, but systems starting from more stable trivalent complexes [Fe(III)] have been recently attracting attention from the applicational view point. The first example was iron(II) chloride with triphenylphosphine [$FeCl_2(PPh_3)_2$],[24] inspired by a similar ruthenium complex [$RuCl_2(PPh_3)_3$]. Some iron catalysts have been reported along with [$FeCl_2(PPh_3)_2$], such as a series of half-metallocene complexes with carbonyl and halogen[23] and an imidazolidene (*N*-heterocyclic carbene) iron halide,[26] which show enough tolerance to functional groups and induce living polymerization both in organic media and aqueous suspension.[27]

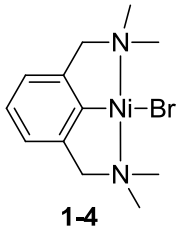

1-4

As attractive potential catalysts, nickel (Ni) complexes tend to undergo a two-electron transfer reaction rather than a one-electron redox reaction.[28] Nickel catalysts usually work only in a limited range of radical reactions such as Kharasch reaction. Nevertheless, its utility for living polymerization of alkenes was confirmed for some complexes at the earlier stage of its history. Some examples include bis(orthochelated) phenylnickel(II) (**1-4**)[29],

$Ni(PPh_3)_2Br_2$[30], and $Ni(PPh_3)_4$.[31]

Typically, divalent derivatives [Ni(II)] are employed to catalyze radical polymerizations via an equilibrium with a trivalent intermediate [Ni(III)]. A neutral Ni(II) acetylide complex structure induced living polymerization of MMA in conjunction with a simple organic halide such as $BrCCl_3$.[32] This long-living catalytic system allowed block copolymerization with selected monomers. Such a superior catalysis was rationalized by a dynamic structural change of the complex between "pseudo-tetrahedral" and "square planar" conformations.

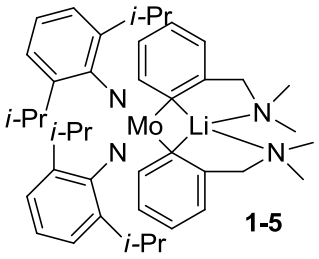

1-5

Molybdenum (Mo) complexes can also be candidates as catalysts for living polymerization because the metal displays a wide range of oxidation states ranging from -2 to 6. However, their utility has been less known for not only living polymerization but also Kharash reactions. Among them, a lithium molybdate (V) complex (**1-5**) was examined for living polymerization[33]. With a benzyl chloride initiator, it polymerized styrene into polystyrene, but the catalytic performance was rather poor and resulted in broad molecular weight distribution of the products (M_w/M_n 1.5~1.7), and low initiating efficiency (6-18%).

Although manganese (Mn) also can exist in a wide range of oxidation states (from -3 to 7), a few examples of Mn-based catalysts for living polymerization have been reported so far. The acetylacetonate manganese(III) complex [$Mn(acac)_3$] induces styrene polymerization when it is coupled with a benzyl bromide initiator.[34] One of the most common manganese complexes, a dinuclear carbonyl derivative [$Mn_2(CO)_{10}$] was found to show promising catalytic activity for living polymerizations.[33] Importantly, it was capable

of catalyzing, in conjunction with an iodide initiator, living polymerization of vinyl acetate to give controlled molecular weight, as the activity was high enough to reach high conversion and to generate high molecular weight polyvinylacetate.

Osmium (Os) complexes were also suggested as catalysts for living polymerizations due to its close affiliation with group VIII (i.e. Ru and Fe). The dichloride complex $[Os_2Cl_2(PPh_3)_3]$ indeed catalyzed the living polymerization of styrene with an alkyl bromide initiator to give narrow PDI (M_w/M_n 1.11).[36] Some complexes with rhodium (Rh), palladium (Pd), and rhenium (Re) have been reported in living alkene polymerization, yet there were few reports on the evolution of these complexes. A $[RhH_2(Ph_2N_3)(PPh_3)_2]$ complex for styrene polymerization was reported, with a poor performance ($M_w/M_n > 2$).[38] Rh(I) and Pd(0) are well-known to catalyze organic reactions, and usually the catalytic cycle involves an oxidative addition and a reductive elimination with two electron transfer. For this reason, these complexes might be less suitable for metal-catalyzed living polymerization via a single electron transfer.

1.2.2 Chain-Growth Living Polymerization Yielding π-Conjugated Semiconducting Polymers. In the previous section, various organometallic catalysts for living polymerizations of conventional alkene monomers were discussed. In this section, we will outline the nickel-catalyzed chain-growth living polymerization method that requires an alternative reaction mechanism to explain such unusual polymerization. Such processes are also called "Kumada" type intramolecular nickel-transfer reactions, in which the catalyst activates the end group of a polymer chain, followed by reaction with the monomer and transfer of the catalyst to the elongated polymer end group, in a manner similar to biological condensation polymerizations.

1.2.2.1. Polythiophene. Among the numerous conjugated polymers (CPs), polythiophene is one of the most widely used conjugated polymers with a broad variety of applications such as electrical conductors, nonlinear optical devices, polymer LEDs, batteries, electromagnetic shielding materials, photovoltaic materials, polymer electronic interconnects, nanoelectronic and sensory devices, etc.[39] Initially in the history of polythiophene, unsubstituted polythiophenes were synthesized via oxidative chemical polymerization.[40,41]

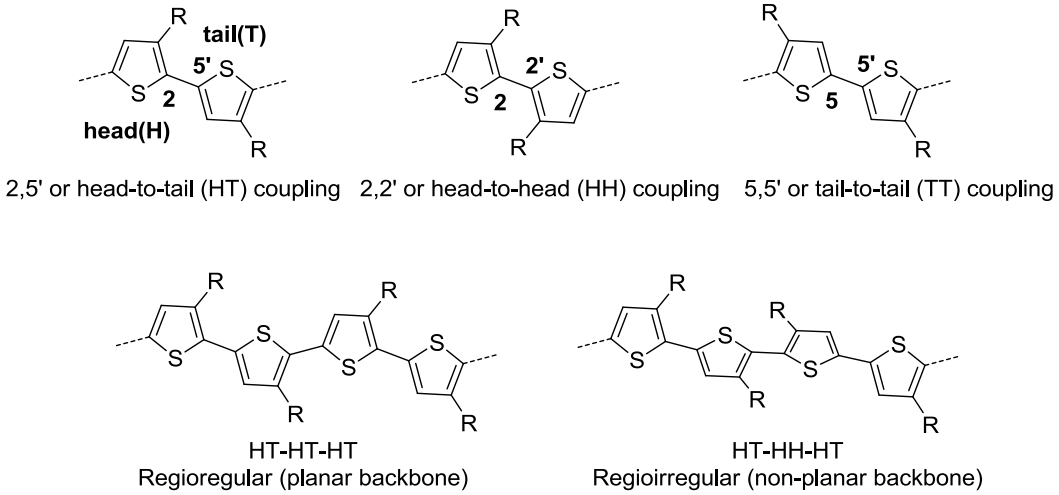

Figure 1. 5 General features of regioregular and regioirregular(regiorandom) poly(3-alkylthiophene)s.

They were found to be highly conductive, environmentally friendly, as well as thermally stable, yet practically insoluble in common organic solvents. In order to improve processibility in solution, soluble polythiophenes containing pendant side chains such as poly(3-alkylthiophenes) (P3ATs) were synthesized in the late 1980s by analogous methods used for the 2,5-coupled PT.[42] Typically, oxidative chemical and electrochemical methods create random (regiorandom) couplings in P3ATs, resulting in the less than 80% head-to-tail (HT) couplings (Figure 1. 5). Due to 3-alkyl thiophene being not a symmetrical molecule,

there are three relative orientations possible when two thiophene rings are coupled with each other at the positions 2 and 5. The first is 2-5' or head-to-tail coupling (HT), the second is 2-2' or head-to-head coupling (HH), and the third is 5-5' or tail-to-tail coupling (TT). The general structures of those couplings of 3-alkylthiophene are shown in Figure 1. 5.[44]

The loss of regioregularity during polymerization is due to multiple head-to-head (HH) and tail-to-tail (TT) couplings that cause sterically twisted conformations of polymer backbone, decresing the extent of π-conjugation. This leads to diminishing conductivity and loss of other desirable properties of PTs. Polymers that possess all three possible couplings in the backbone are denoted as *irregular, regiorandom* or non-HT. Irregularly substituted polythiophenes have structures where unfavorable H-H couplings induce sterically driven twists of thiophene rings, resulting in loss of π-electron conjugation while polymers that contain only head-to-tail (HT) couplings are denoted as *regioregular.* Regioregular poly-(3-substituted) thiophene can easily access low energy planar conformations, leading to high π-electron conjugation.

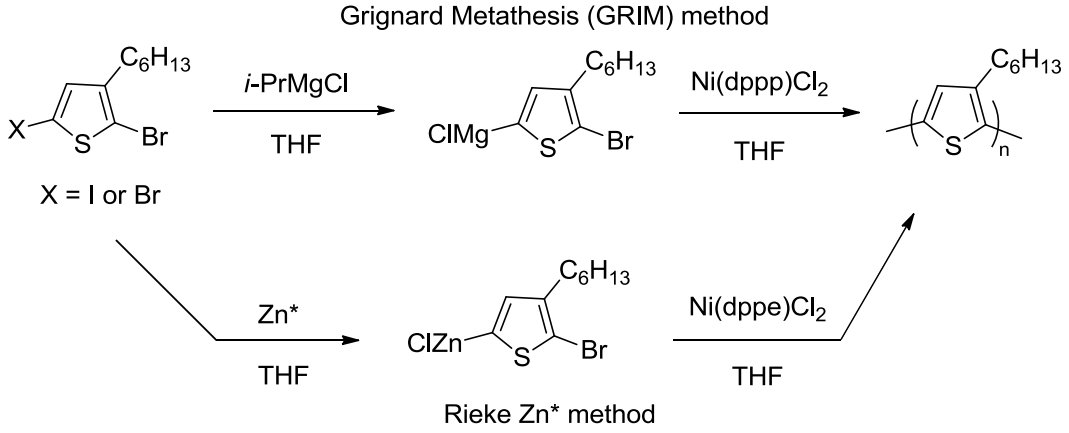

Scheme 1. 1 Typical methods for the synthesis of regioregular poly(3-hexylthiophene)s (P3HTs).

The early work of polymerization using Grignard metathesis (GRIM) with nickel

(diphenylphosphino)propane dichloride (Ni(dppp)Cl_2) (Scheme 1. 1) was carried out by McCullough et al., and became well-known as one of a few synthetic procedures for the preparation of regioregular poly(3-alkylthiophene)s, P3ATs.[45,46]

Simultaneously with the initial report by McCullough, Rieke et al.[47,48] reported an alternative synthesis of P3ATs (Scheme 1. 1). In that method, treating 2,5-dibromo-3-alkylthiophenes with highly reactive "Rieke zinc" (Zn*) yielded an intermediate organozinc reagent, which produced regioregular P3ATs when catalyzed with Ni(dppe)Cl_2, but the obtained results typically showed a very broad molecular weight distribution.[47-50]

However, Yokozawa et al. later reported that M_n of polymers increased in proportion to monomer conversion, with narrow polydispersities and was also controlled by the amount of the nickel catalyst. The M_n was proportional to the feed ratio of $[Grignard]_0/[Ni\ catalyst]_0$ when the polymerization was carried out at room temperature, and special care was taken to use exact amount of isopropylmagnesium chloride for *in situ* generation of Grignard monomer from the corresponding bromoiodothiophene (Scheme 1. 1), resulting in the PDI near 1.1 and M_n of 29,000.[51] McCullough and co-workers also reported that a similar zinc monomer and Grignard monomer from the corresponding dibromothiophene showed the same polymerization behavior.[53]

1.2.2.2. Mechanism of Ni-Catalyzed Polymierzation. The polymerization pathway is based on metal catalyzed cross-coupling reactions that involve a catalytic cycle of three consecutive steps: 1) oxidative addition, 2) transmetalation, and 3) reductive elimination. Until early 2000's, it was generally accepted that the nickel-catalyzed polymerization was likely a polycondensation that takes place via a stepwise (step-growth) reaction mechanism. However, in 2005 Yokozawa et al[54] suggested that the McCullough's nickel-catalyzed cross-

coupling polymerization (GRIM method) proceeds through a chain-growth mechanism when the polymerization is carried out at ambient temperature.

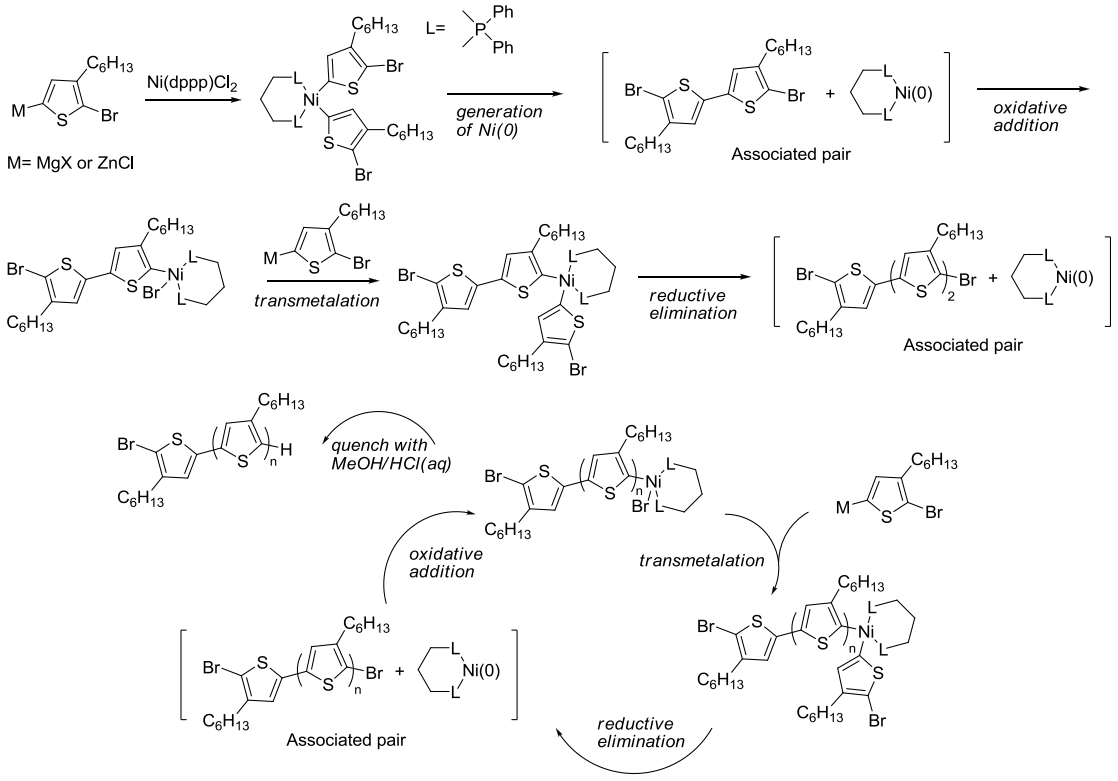

Scheme 1. 2 Mechanism of chain-growth polymerization proposed by McCullough et al. (adapted from ref 55)

Concomitantly, McCullough et al[55] also proposed that the polymerization was a chain-growth process occurring in a living fashion, depending on the reaction time, the amount of monomer and nickel catalyst to control the molecular weight, polydispersity (PDI) and regioregularity of the polythiophenes.

According to the proposed mechanism by McCullough et al. (Scheme 1. 2), in the first step 2 equivalents of Grignard monomer with Ni(dppp)Cl_2 give an organonickel species, and reductive elimination immediately occurs to produce an associated pair of the nickel(0) complex that was suggested to have a structure of a π-complex. Subsequently, rapid

oxidative addition to the nickel (0) center generates a new organonickel species.

Subsequent transmetalation with another Grignard monomer and the reductive elimination again produce an associated pair of the terthiophene and nickel (0). Subsequent growth of the polymer chain occurs by addition of one monomer at a time as shown in the reaction cycle, where the Ni(dppp) species is incorporated into the polymer chain as an end group via the formation of a π-complex. In this fashion, Ni(dppp)Cl_2 acts as an initiator rather than a catalyst, leading to the polymerization occurring at one end of the polymer chain. McCullough's and Yokozawa's suggestion of the mechanism as a living process was supported by two key experimental findings: firstly the increase of degree of polymerization upon increasing monomer conversion and molar ratio of the monomer to the nickel initiator, and secondly, addition of various Grignard reagents (R'MgX, X=halide) at the end of polymerized chain that result in end-functionalized polythiophenes with R' at the end, as well as all-conjugated diblock copolymers. Using this approach, McCullough et al. have synthesized a variety of end-group functionalized polythiophene derivatives[56,57], which strongly support the living nature of the nickel catalyzed polymerization.

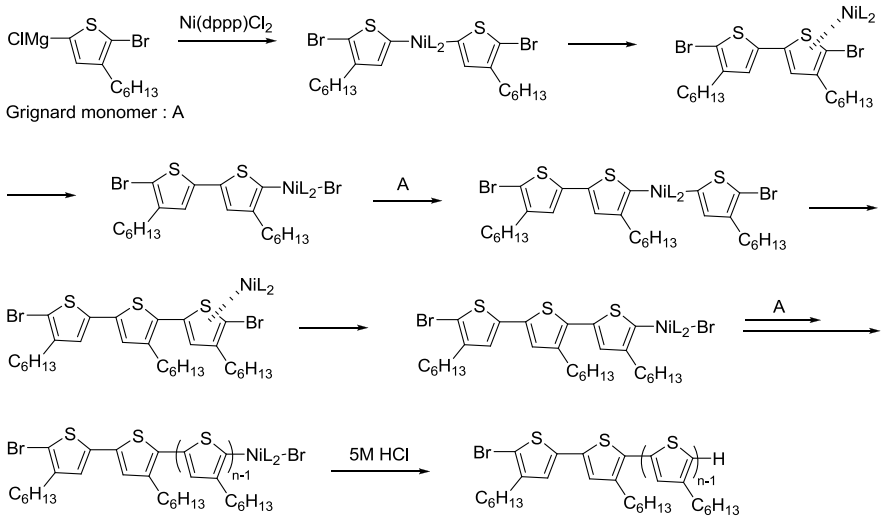

Scheme 1. 3 Mechanism of chain-growth polymerization proposed by Yokozawa et al. (adapted from ref 54).

In his closely related mechanism, Yokozawa also proposed that polymerization of the Grignard monomer proceeds in a chain-growth manner to afford regioregular poly-3-hexylthiophene (P3HT) with low polydispersity, in which M_n is controlled by the feed ratio of 2,5-dibromo-3-hexylthiophene to the nickel catalyst. After detailed study of the polymerization of Grignard monomer, he outlined four important points: (1) the polymer end groups are uniform among molecules, one end group being Br and the other being H; (2) the propagating end group is a polymer-Ni-Br complex; (3) one Ni species forms one polymer chain; and (4) the chain initiator is a dimer of Grignard monomer formed *in situ*. Based on this, he proposed an intramolecular nickel transfer polycondensation mechanism (Scheme 1. 3). In that mechanism, Ni(dppp)Cl_2 reacts with two equivalent of Grignard monomer, and the coupling reaction occurs with concomitant generation of a Ni(0) π-complex. The Ni(0) π-complex does not diffuse to the reaction mixture, rather it is inserted into the intramolecular C-Br bond. Another Grignard monomer reacts with this Ni species, followed by the coupling reaction and transfer of the Ni catalyst to the next carbon-Br bond. Chain-growth continues in a similar fashion in which the Ni catalyst always moves to the polymer end group.

A recent extensive mechanistic study of the nickel-catalyzed chain-growth polymerization of Grignard monomer by McNeil et al. additionally revealed that transmetalation is the rate-determining step of the catalytic cycle and Ar-Ni(II)-halide is the catalyst "resting state". Furthermore, the overall polymerization process strongly depends on the ligands at the Ni center (e. g. change from dppe to dppp resulted in the change of the rate-determining step) (Scheme 1. 4).[58,59]

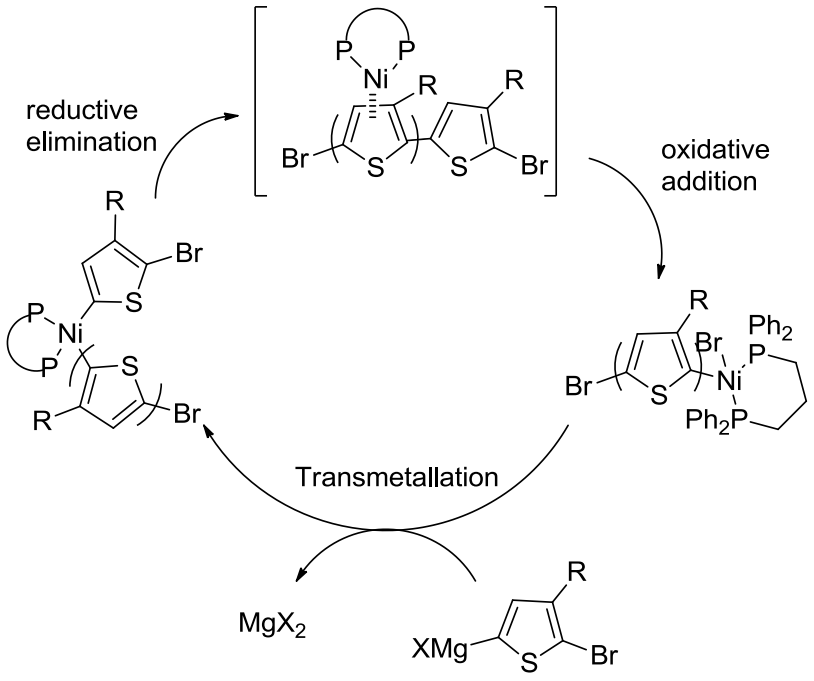

Scheme 1. 4 Mechanism of the chain-growth polymerization suggested by McNeil et al. (adapted from ref 59 and 60).

Recently, Kiriy et al.[60] and Luscombe et al.[61] reported direct polythiophene chain-growth by employing an externally prepared nickel (II) complex, opening an opportunity to directly immobilize conjugate polymer brushes on a target molecule. In the accepted polymerization mechanism, the polythiophene chains grow via intramolecular nickel transfer after addition of a Grignard monomer. The key point of externally-initiated "Kumada" catalyst-transfer polycondensation (KCTP) is using an externally addable nickel catalyst that can initiate thiophene chain-growth (Scheme 1. 5). As externally added catalyst can contain any molecular fragment, this allows growing conjugated polymer brushes on a non-conjugated platform or substrates. Since then, a number of synthetic methods (both in solution and in solid state) based on chain-growth of polymer brushes have been reported in literature.[62-67] However, enhancing catalytic activity in order to increase polymer length, and obtain narrow polydispersity (PDI) and control of regioregularity still remains an unsolved

problem.

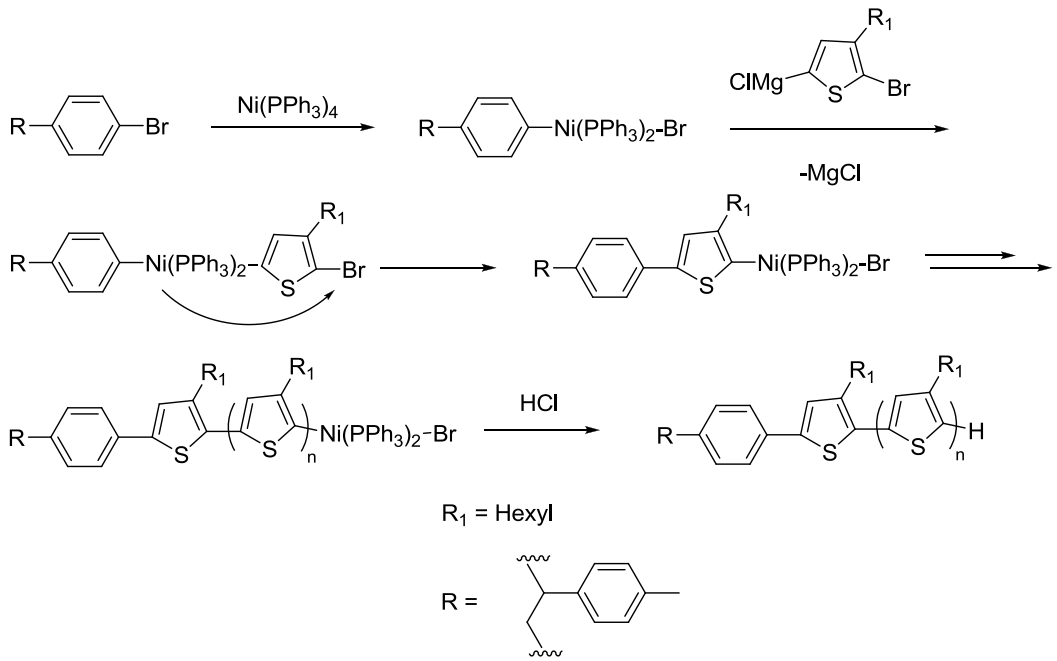

Scheme 1. 5 Polycondesation of thiophene initiated by an externally added Ni(II) initiator (adapted from ref 61).

Our achievements in development and studies of the highly efficient externally-initiated polymerization by using a novel externally-addable nickel catalyst are discussed in the Chapter 3. Our approach results in unprecedentedly high molecular weight, narrow polydispersity (PDI) and extremely high regioregular homo polythiophenes as well as block copolymers. Using this highly efficient, optimized catalytic system, we were also able to prepare thiophene polymer brushes from catalytic initiator covalently immobilized on various substrates such as glass, ITO, and etc.

1.2.2.3. Polyphenylene. In order to expand the limits of the living intramolecular catalyst-transfer chain-growth polymerization method, polymerization of various monomers incorporating phenylene, fluorene, carbazole, pyrrole, etc. units were performed for π-semiconducting polymers, however most of the earlier work demonstrated low molecular

weight and broad polydispersity. Also, different nickel catalytic systems (i.e. Ni(dppp)Cl_2, Ni(dppe)Cl_2, or Ni(dppf)$Cl)_2$) led to very similar results. Remarkably, addition of LiCl in a typical nickel-catalyzed chain-growth polymerization reaction produced poly(*p*-phenylene) with low polydispersity, and molecular weight could be controlled by changing feed ratio of the monomer and the nickel catalyst (Scheme 1. 6).[68]

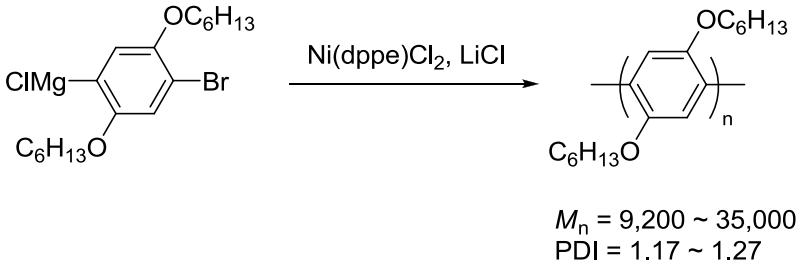

Scheme 1. 6 Chain-growth polymerization to yield poly(*p*-phenylene) initiated by nickel-catalyzed GRIM method (adapted from ref 68).

1.2.2.4. Polypyrrole. Polymerization of Grignard-type *N*-hexylpyrrole monomer with an additive LiCl and a nickel catalyst was performed to investigate the chain-growth living polymerization phenomena by the intramolecular nickel transfer.

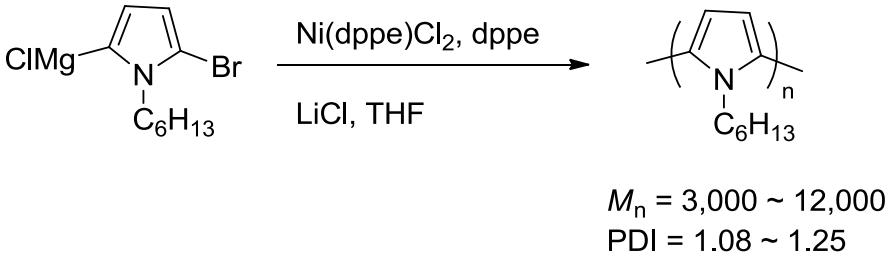

Scheme 1. 7 Chain-growth polymerization to yield polypyrrole by nickel-catalyzed GRIM method (adapted from ref 69).

This process resulted in the polypyrrole with a narrow molecular weight distribution (~1.11) and without low molecular weight oligomers. The conversion and feed ratio (monomer/catalyst) indicated that polymerization of pyrrole also took place in the living

polymerization fashion (Scheme 1. 7).[69]

1.2.2.5. Polyfluorene. Suzuki-Miyaura coupling conditions were employed to grow fluorene polymer chains. In this polymerization, stable arylpalladium complexes, Ar-Pd(II)-X (X = halide) served as an externally added initiator. Chain-growth polymerization of a fluorene monomer was carried out in the presence of $^{t}Bu_3PPd(Ph)Br$ as a catalyst to yield polyfluorene with a narrow polydispersity. A recent report by Geng and co-workers showed polymerization of Grignard-type fluorene monomer with $Ni(dppp)Cl_2$ catalyst. [71,72] (Scheme 1. 8).

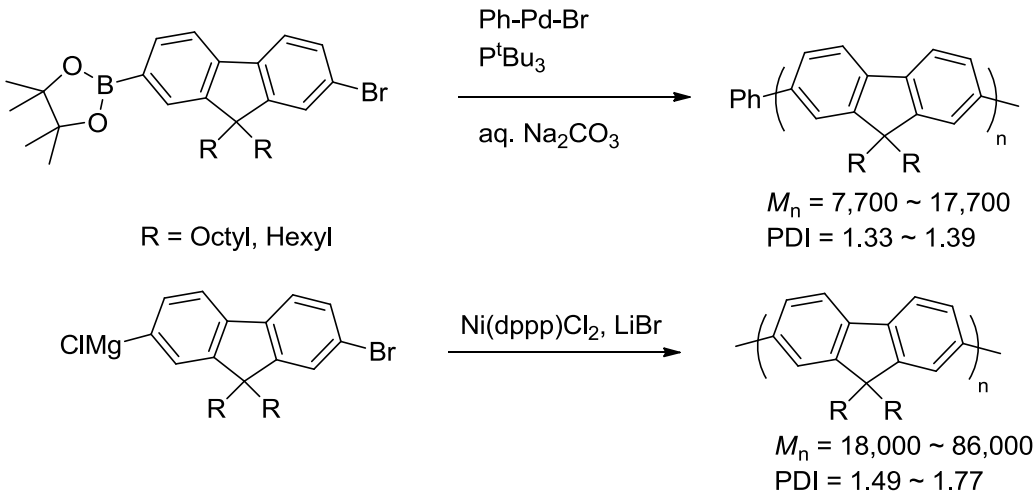

Scheme 1. 8 Chain-growth polymerization to yield polyfluorenes by Suzuki-Miyaura and nickel-catalyzed GRIM method (adapted from ref 70, 71and 72).

1.3. Conclusion

Conventional metal-catalyzed living polymerization techniques were reviewed here to show the broad scope of the conventional and chain-growth living polymerization and how it is applied for the synthesis of various semiconducting conjugated polymers.

One of these methods was used to prepare regioregular polythiophenes used in Chapter 2. This chapter discusses the research progress towards functionalized water-soluble

polythiophene derivatives that can undergo temperature-induced control of conformation and conjugation length depending on their regioregularity, which affect their photophysical properties.

Chapter 3 discusses our development of an externally-initiated polymerization through design of a highly efficient externally-addable nickel catalytic initiator. These results in polymers with unprecedentedly high molecular weights, narrow polydispersities (PDI) and extremely high regioregularities, as well as block copolymers. By using this highly efficient catalytic system, we were able to grow thiophene polymer brushes connected to aromatic molecules immobilized at solid substrates such as glass, ITO, etc. A detailed polymerization mechanism study using ^{31}P NMR spectroscopy and other approaches is also outlined in Chapter 3. The following Chapter 4 discusses the research progress on the design and study of supramolecular organization in stimuli-responsive amphiphilic polythiophene block copolymer architectures.

The final chapter 5 discusses the synthetic design and photophysical properties of conjugated polymers based on near-IR (NIR) cyanine dyes that can be used for potential biosensing applications or photovoltaic devices.

1.4. References

1. Chaing, C. K.; Fincher, C. R., Jr.; Park, Y. W.; Heeger, A. J.; Shirakawa, H.; Louis, E. J.; Gau, S. C.; MacDiarmid, A. G. *Phys. Rev. Letts*. **1977**, *39*, 1098-1101.

2. *Handbook of Conducting Polymers*, 2nd ed. (Eds: Skotheim, T. A.; Reynolds, J. R.; Elsenbaumer, R. L), Marcel Dekker, New York **1997.**

3. Feast, W. J.; Tsibouklis, J.; Pouwer, K. L.; Groenendaal, L.; Meijer. E. W. *Polymers*. **1996**, *37*, 5017-5047.

4. McQuade, D. T.; Pullen, A. E.; Swager, T. M. Conjugated Polymer-Based Chemical Sensors. *Chem. Rev.* **2000**, *100*, 2537–2574.

5. Thomas, S. W. III; Joly, G. D.; Swager, T. M. Chemical Sensors Based on Amplifying Fluorescent Conjugated Polymers. *Chem. Rev*. **2007**, *107*, 1339–1386.

6. Leclerc, M.; Faid, K. Electrical and optical properties of Processable Polythiophene Derivatives: Structure-Property relationships. *Adv. Mater*. **1997**, *9*, 1087-1094.

7. Patil, A. O.; Heeger, A. J.; Wudl, F. Optical Properties of conducting polymers. *Chem. Rev*. **1988**, *88*, 183-200.

8. Bissell, R. A.; de Silva, A. P.; Gunaratne, H. Q. N.; Lynch, P. L. M.; Maguire, G. E. M.; McCoy, C. P.; Sandanayake, K. R. A. S. Fluorescent PET (Photoinduced Electron Transfer) Sensors. *In Topics in Current Chemistry*, Springer-Verlag: Berlin Heidelberg, **1993**, *168*, 224.

9. Swager, T. M. The Molecular Wire Approach to Sensory Signal Amplification. *Acc. Chem. Res*. **1998**, *31*, 201-207.

10. Szware. M. 'Living' Polymers. *Nature*. **1956**, *178*, 1168-1169.

11. Quirk, R. P.; Lee, B. Experimental Criteria for Living Polymerizations. *Polym. Int.* **1992**, *27*, 359-367.

12. Higashimura, T,; Kamigaito, M.; Kato, M.; Hasebe, T.; Sawamoto, M. Living cationic polymerization of .alpha.-methylstyrene initiated with a vinyl ether-hydrogen chloride adduct in conjunction with tin tetrabromide. *Macromolecules* **1993**, *26*, 2670-2673.

13. Kamigaito, M.; Ando, T.; Sawamoto, M. Metal-catalyzed living radical polymerization: discovery and developments. *Chem. Rec.* **2004**, *4*, 159–175.

14. Ando, T.; Kamigaito, M.; Sawamoto, M. Iron(II) Chloride Complex for Living Radical Polymerization of Methyl Methacrylate. *Macromolecules* **1997**, *30*, 4507-4510.

15. Uegaki, H.; Kotani, Y.; Kamigaito, M.; Sawamoto, M. Nickel-Mediated Living Radical Polymerization of Methyl Methacrylate. *Macromolecules* **1997**, *30*, 2249-2253.

16. Matyjaszewski, K.; Xia, J. Atom Transfer Radical Polymerization. *Chem. Rev.* **2001**, *101*, 2921-2990.

17. Kato, M; Kamigaito, M.; Sawamoto, M; Higashimura, T. Polymerization of Methyl Methacrylate with the Carbon Tetrachloride / Dichlorotris- (triphenylphosphine) ruthenium(II)/Methylaluminum Bis(2,6-di-tert-butylphenoxide) Initiating System: Possibility of Living Radical Polymerization. *Macromolecules* **1995**, *28*, 1721-1726.

18. Matsumoto, H.; Nakano, T.; Nagai, Y. Radical reactions in the coordination sphere I.

Addition of carbon tetrachloride and chloroform to 1-olefins catalyzed by ruthenium(II) complexes. *Tetrahedron. Lett.* **1973**, *51*, 5147-5150.

19. Ando, T.; Kamigaito, M.; Sawamoto, M. Catalytic Activities of Ruthenium(II) Complexes in Transition-Metal-Mediated Living Radical Polymerization: Polymerization, Model Reaction, and Cyclic Voltammetry. *Macromolecules* **2000**, *33*, 5825-5829.

20. Watanabe, Y.; Ando, T.; Kamigaito, M.; Sawamoto, M. $Ru(Cp^*)Cl(PPh_3)_2$: A Versatile Catalyst for Living Radical Polymerization of Methacrylates, Acrylates, and Styrene. *Macromolecules* **2001**, *34*, 4370-4374.

21. Wang, J. -S.; Matyjaszewski, K. Controlled/"living" radical polymerization. atom transfer radical polymerization in the presence of transition-metal complexes. *J. Am. Chem. Soc*. **1995**, *117*, 5614-5615.

22. Braunecker, W. A.; Matyjaszewski, K. Recent mechanistic developments in atom transfer radical polymerization. *J. Mol. Cat. A: Chem.* **2006**, *254*, 155-159.

23. Tang, W.; Kwak, Y.; Braunecker, W. A.; Tsarevsky, N. V.; Coote, M. L.; Matyjaszewski, K. Understanding Atom Transfer Radical Polymerization: Effect of Ligand and Initiator Structures on the Equilibrium Constants. *J. Am. Chem. Soc.* **2008**, *130*, 10702-10713.

24. Ando, T.; Kato, M.; Kamigaito, M.; Sawamoto, M. Living Radical Polymerization of Methyl Methacrylate with Ruthenium Complex: Formation of Polymers with Controlled Molecular Weights and Very Narrow Distributions. *Macromolecules,* **1996**, *29*, 1070-1072.

25. Onishi, I.; Baek, K.-Y.; Kotani, Y.; Kamigaito, M.; Sawamoto, M. Iron-catalyzed living radical polymerization of acrylates: Iodide-based initiating systems and block and random copolymerizations. *J. Polym. Sci., Part A: Polym. Chem.* **2002**, *40*, 2033-2043.

26. Louie, J.; Grubbs, R. H. Highly active iron imidazolylidene catalysts for atom transfer radical polymerization. *Chem. Commun.* **2000**, 1479-1480.

27. Fuji, Y.; Ando, T.; Kamigaito, M.; Sawamoto, M. Iron-Catalyzed Suspension Living Radical Polymerizations of Acrylates and Styrene in Water. *Macromolecules* **2002**, *35*, 2949-2954.

28. Tsou, T. T.; Kochi, J. K. Mechanism of oxidative addition. Reaction of nickel(0) complexes with aromatic halides. *J. Am. Chem. Soc.* **1979**, *101*, 6319-6332.

29. Granel, C.; Dubois, Ph.; Jérôme, R.; Teyssié, Ph. Controlled Radical Polymerization of Methacrylic Monomers in the Presence of a Bis(ortho-chelated) Arylnickel(II) Complex and Different Activated Alkyl Halides. *Macromolecules* **1996**, *29*, 8576-

8582.

30. Kato, M.; Kamigaito, M.; Sawamoto, M.; Higashimura, T. Living polymerization of isobutyl vinyl ether with hydrogen iodide/iodine initiating system. *Macromolecules* **1984**, *17*, 265-268.

31. Uegaki, H.; Kamigaito, M.; Sawamoto, M. Living radical polymerization of methyl methacrylate with a zerovalent nickel complex, $Ni(PPh_3)_4$. *J. Polym. Sci. Part A: Polym. Chem.* **1999**, *37*, 3003-3009.

32. Shao, Q.; Sun, H.; Pang, X.; Shen, Q. A neutral Ni(II) acetylide-mediated radical polymerization of methyl methacrylate using the atom transfer radical polymerization method. *Eur. Polym. J.* **2004**, *40*, 97-102.

33. Brandts, J. A. M.; van de Geijn, P.; van Faassen, E. E.; Boersma, J.; van Koten, G. Controlled radical polymerization of styrene in the presence of lithium molybdate(V) complexes and benzylic halides. *J. Organomet. Chem.* **1999**, *584*, 246-253.

34. Endo, K.; Yachi, A. Molecular-weight-controlled polymerization of styrene with $Mn(acac)_3$ in combination with organic halides. *Polym. Bull.* **2001**, *46*, 363-369.

35. Koumura, K.; Satoh, K.; Kamigaito, M. Manganese-Based Controlled/Living Radical Polymerization of Vinyl Acetate, Methyl Acrylate, and Styrene: Highly Active, Versatile, and Photoresponsive Systems. *Macromolecules* **2008**, *41*, 7359-7367.

36. Braunecker, W. A.; Itami, Y.; Matyjaszewski, K. Osmium-Mediated Radical Polymerization. *Macromolecules* **2005**, *38*, 9402-9404.

37. Braunecker, W. A.; Brown, W. C.; Morelli, B. C.; Tang, W.; Poli, R.; Matyjaszewski, K. Origin of Activity in Cu-, Ru-, and Os-Mediated Radical Polymerizataion. *Macromolecules* **2007**, *40*, 8576-8585.

38. Kameda, N. Living Radical Polymerization of Methyl Methacrylate with a Rhodium(III) Complex–Organic Halide System in Dimethyl Sulfoxide. *Polym. J.* **2006**, *38*, 516-515.

39. McCullough, R. D. The Chemistry of Conducting Polythiophenes. *Adv. Mater*. **1998**, *10*, 93-116.

40. Yamamoto, T.; Sanechika, K.; Yamamoto, A. Polythiophene: Synthesis in aqueous medium and controllable morphology. *J. Poly. Sci. Polym. Lett. Ed*. **1980**, *18*, 9-12.

41. Lin, J. W. P.; Dudek, L. P. Synthesis and properties of poly(2,5-thienylene). *J. Poly. Sci. Polym. Lett. Ed.* **1980**, *18*, 2869-2873.

42. Elsenbaumer, R. L.; Jen, K. Y.; Oboodi, R. Processible and environmentally stable

conducting polymers. *Synth. Met*. **1986**, *15*, 169-174.

43. Sugimoto, R.; Takeda, S.; Gu, H. B.; Yoshino, K. Electrical and Optical Properties of Poly(3,4-dialkylthiophene). *Chem. Express*. **1986**, *1*, 635-639.

44. Osaka, I.; McCullough, R. D. Advances in Molecular Design and Synthesis of Regioregular Polythiophenes. *Acc. Chem. Res*. **2008**, *41*, 1202-1214.

45. McCullough, R. D.; Lowe, R. D. Enhanced electrical conductivity in regioselectively synthesized poly(3-alkylthiophenes). *J. Chem. Soc., Chem. Commun.* **1992**, 70-72.

46. McCullough, R. D.; Lowe, R. D.; Jayaraman, M.; Anderson, D. L. Design, synthesis, and control of conducting polymer architectures: structurally homogeneous poly(3-alkylthiophenes). *J. Org. Chem.* **1993**, *58*, 904-912.

47. Chen, T.; Rieke, R. D. The first regioregular head-to-tail poly(3-hexylthiophene-2,5-diyl) and a regiorandom isopolymer: nickel versus palladium catalysis of 2(5)-bromo-5(2)-(bromozincio)-3-hexylthiophene polymerization. *J. Am. Chem. Soc.* **1992**, *114*, 10087-10088.

48. Chen, T.; Wu, X.; Rieke, R. D. Regiocontrolled Synthesis of Poly(3-alkylthiophenes) Mediated by Rieke Zinc: Their Characterization and Solid-state Properties. *J. Am. Chem. Soc.* **1995**, *117*, 233-244.

49. Loewe, R. S.; Khersonsky, S. M.; McCullough, R. D. A Simple Method to Prepare Head-to-Tail Coupled, Regioregular Poly(3-alkylthiophenes) Using Grignard Metathesis. *Adv. Mater*. **1999**, *11*, 250-253.

50. Loewe, R. S.; Ewbank, P. C.; Liu, J.; Zhai, L.; McCullough, R. D. Regioregular, Head-to-Tail Coupled Poly(3-alkylthiophenes) Made Easy by the GRIM Method: Investigation of the Reaction and the Origin of Regioselectivity. *Macromolecules* **2001**, *34*, 4324-4333.

51. Miyakoshi, R.; Yokoyama, A.; Yokozawa, T. Synthesis of Poly(3-hexylthiophene) with a Narrow Polydispersity. *Macromol. Rapid. Commun.* **2004**, *25*, 1663-1666.

52. Sheina, E. E.; Liu, J.; Iovu, M. C.; Laird, D. W.; McCullough, R. D. Chain Growth Mechanism for Regioregular Nickel-Initiated Cross-Coupling Polymerizations. *Macromolecules* **2004**, *37*, 3526-3528.

53. Iovu, M. C.; Sheina, E. E.; Gil, R. R.; McCullough, R. D. Experimental Evidence for the Quasi-"Living" Nature of the Grignard Metathesis Method for the Synthesis of Regioregular Poly(3-alkylthiophenes). *Macromolecules* **2005**, *38*, 8649-8656.

54. Miyakoshi, R.; Yokoyama, A.; Yokozawa, T. Catalyst-Transfer Polycondensation. Mechanism of Ni-Catalyzed Chain-Growth Polymerization Leading to Well-Defined

Poly(3-hexylthiophene). *J. Am. Chem. Soc.* **2005**, *127*, 17542-17547.

55. Jeffries-El, M.; Sauve, G.; McCullough, R. D. Facile Synthesis of End-Functionalized Regioregular Poly(3-alkylthiophene)s via Modified Grignard Metathesis Reaction. *Macromolecules* **2005**, *38*, 10346-10352.

56. Jeffries-El, M.; Sauve, G.; McCullough, R. D. In-Situ End-Group Functionalization of Regioregular Poly(3-alkylthiophene) Using the Grignard Metathesis Polymerization Method. *Adv. Mater*. **2004**, *16*, 1017-1019.

57. Liu, J.; Sheina, E.; Kowalewski, T.; McCullough, R. D. Tuning the Electrical Conductivity and Self-assembly of Regioregular Polythiophene by Block Copolymerization: Nanowire Morphologies in New Di- and Triblock Copolymers. *Angew. Chem. Int. Ed*. **2002**, *41*, 329-332.

58. Lanni, E. L.; McNeil, A. Mechanistic Studies on Ni(dppe)Cl_2-Catalyzed Chain-Growth Polymerizations: Evidence for Rate-Determining Reductive Elimination. *J. Am. Chem. Soc.* **2009**, *131*, 16573-16579.

59. Lanni, E. L.; McNeil, A. Evidence for Ligand-Dependent Mechanistic Changes in Nickel-Catalyzed Chain-Growth Polymerizations. *Macromolecules* **2010**, *43*, 8039-8044.

60. Senkovskyy, V.; Khanduyeva, N.; Komber, H.; Oertel, U.; Stamm, M.; Kuckling, D.; Kiriy, A. Conductive Polymer Brushes of Regioregular Head-to-Tail Poly(3-alkylthiophenes) via Catalyst-Transfer Surface-Initiated Polycondensation. *J. Am .Chem. Soc,* **2007**, *129*, 6626-6632.

61. Bronstein, H. A.; Luscombe, C. K. Externally Initiated Regioregular P3HT with Controlled Molecular Weight and Narrow Polydispersity. *J. Am. Chem. Soc.* **2009**, *131*, 12894-12895.

62. Doubina, N.; Ho, A.; Jen, A. K.-Y.; Luscombe, C. K. Effect of Initiators on the Kumada Catalyst-Transfer Polycondensation Reaction. *Macromolecules* **2009**, *42*, 7670-7677.

63. Smeets, A.; Van den.; Bergh, K.; De Winter, J.; Gerbaux, P.; Verbiest, T.; Koeckelberghs, G. Incorporation of Different End Groups in Conjugated Polymers Using Functional Nickel Initiators. *Macromolecules* **2009**, *42*, 7638-7641.

64. Senkovskyy, V.; Tkachov, R.; Beryozkina, T.; Komber, H.; Oertel, U.; Horecha, M.; Bocharova, V.; Stamm, M.; Gevorgyan, S. A.; Krebs, F. C.; Kiriy, A. "Hairy" Poly(3-hexylthiophene) Particles Prepared via Surface-Initiated Kumada Catalyst-Transfer Polycondensation. *J. Am. Chem. Soc.* **2009**, *131*, 16445-16453.

65. Tkachov, R.; Senkovskyy, V.; Komber, H.; Sommer, J.-U.; Kiriy, A. Random Catalyst Walking along Polymerized Poly(3-hexylthiophene) Chains in Kumada

Catalyst-Transfer Polycondensation. *J. Am. Chem. Soc.* **2010**, *132*, 7803-7810.

66. Higashihara,T.;Takahashi, A.;Tajima, S.; Jin, S.;Rho,Y.;Ree,M.; Ueda, M. Synthesis of block copolymers consisting of poly(3-hexylthiophene) and polystyrene segments through ionic interaction and their self-assembly behavior. *Polym. J.* **2010**, *42*, 43-50.

67. Sontag, S.; Marshall, N.; Locklin, J. Formation of conjugated polymer brushes by surface-initiated catalyst-transfer polycondensation. *Chem. Commun,* **2009**, 3354-3356.

68. Miyakoshi, R.; Shimono, K.; Yokoyama, A.; Yokozawa, T. Catalyst-Transfer Polycondensation for the Synthesis of Poly(*p*-phenylene) with Controlled Molecular Weight and Low Polydispersity. *J. Am. Chem. Soc.* **2006**, *128*, 16012-16013.

69. Yokoyama, A.; Kato, A.; Miyakoshi, R.; Yokozawa, T. Precision Synthesis of Poly(*N*-hexylpyrrole) and Its Diblock Copolymer with Poly(*p*-phenylene) via Catalyst-Transfer Polycondensation. *Macromolecules* **2008**, *41*, 7271-7273.

70. Yokoyama, A.; Suzuki, H.; Kubota, Y.; Ohuchi, K.; Higashimura, H.; Yokozawa, T. Chain-Growth Polymerization for the Synthesis of Polyfluorene via Suzuki-Miyaura Coupling Reaction from an Externally Added Initiator Unit. *J. Am. Chem. Soc,* **2007**, *129*, 7236-7237.

71. Stefan, M. C.; Javier, A. E.; Osaka, I.; McCullough, R. D. Grignard Metathesis Method (GRIM): Toward a Universal Method for the Synthesis of Conjugated Polymers. *Macromolecules* **2009**, *42*, 30-32.

72. Huang, L.; Wu, S.; Qu, Y.; Geng, Y.; Wang, F. Grinard Metathesis Chain-Growth Polymerization for Polyfluorenes. *Macromolecules* **2008** *41*, 8944-8950.

CHAPTER 2. TEMPERATURE - INDUCED CONTROL OF CONFORMATION AND CONJUGATION LENGTH IN WATER - SOLUBLE FLUORESCENT POLYTHIOPHENE[1]

2.1. Introduction

The universal application of conjugated polymers (CPs) as signal-generating media in chemo- and biosensors is based on the efficient transport of excited states (excitons) along the isolated polymer chain. The exciton migration allows delivery of photoexcitation energy absorbed over large areas into low-energy gap sites created by the binding of analytes or other minor perturbations, resulting in significant signal amplification in sensory devices.[1-7] The process of intramolecular energy migration is strongly dependent on the extent of π-electron conjugation along the CP chain, which is determined by the ability of the polymer to achieve a highly planarized conjugated backbone conformation.[8-11] Furthermore, the CP backbone conformation can change as a result of intermolecular aggregation or interaction of an individual polymer chain with bioanalytical targets which can lead to a pronounced spectroscopic response, the phenomenon which provides a universal foundation for the development of biosensors and fluorescent biomarkers. For such applications, water soluble CPs are especially promising and were the subject of extensive studies in recent years.[12-19]

Among various classes of CPs, water-soluble polythiophenes (PTs) possessing solubilizing ionic or noncharged hydrophilic side chains are particularly interesting as they are highly susceptible to induced conformational changes of the conjugated backbone, which result in the wavelength shifts and intensity attenuations in absorption and fluorescence spectra and provide a simple basis for numerous bioanalytical applications.[20-28] Because of

[1] "Reproduced in part with permission from Choi, J.; Ruiz, C.; Nesterov, E. E., *Macromolecules* **2010**, *43*, 1964-1074., DOI: 10.1021/ma902136a, Copyright 2010 American Chemical Society."

the intrinsic hydrophobicity of the polythiophene conjugated backbone, even polymers substituted with hydrophilic solubilizing side groups tend to form intermolecular aggregates in dilute aqueous solutions as a way to minimize unfavorable contacts with solvent molecules. More planarized conformations of PTs tend to exhibit even stronger hydrophobic interchain interactions leading to significant intermolecular aggregation, whereas more twisted, lower conjugation length conformations show a smaller extent of aggregation.

Such planarization-induced aggregation results in interchain electronic delocalization leading to bathochromic shifts in absorption and emission spectra as well as diminished quantum efficiency of the polymer's fluorescence. These spectroscopic features are exactly the same as those caused by increasing conjugation length upon planarization of an isolated, non-aggregated polymer molecule. As the spectroscopic outcomes of both phenomena parallel each other, it is generally impossible to deconvolute the effect of extending π-electron conjugation length within isolated CP molecule upon its planarization from the effect of the planarization-induced intermolecular aggregation. This resulted in often controversial and contradictory interpretation of molecular mechanisms responsible for spectroscopic changes in water-soluble PTs.[29,30] From the fundamental standpoint, experimental differentiation between these two phenomena would be important as it could shed some light on the role of through-bond Dexter-type mechanism of intramolecular photoexcitation energy migration which in extended conjugated systems is often considered inefficient and inferior to its through-space Förster-type counterpart.[31-33]

Indeed, the through-bond intramolecular energy migration is expected to depend strongly on the extent of planarity of the conjugated polymer backbone and significantly

diminish upon the backbone twisting, while the dipole-induced dipole exciton hopping would be much less affected by the conformational twisting of the individual chain but will be dramatically enhanced due to the possibility of intermolecular energy migration in the three-dimensional polymer aggregates. Therefore, substantial variations of the intramolecular exciton migration efficiency upon induced conformational change in the conjugated backbone of the isolated PT chain would indicate an appreciable role of the through-bond mechanism.[11] From the practical standpoint, the ability to effectively control backbone conformation of the isolated conjugated PT chains in solution would add an extra variable in controlling the sensor behavior of the PT-based chemo- and biodetecting systems.

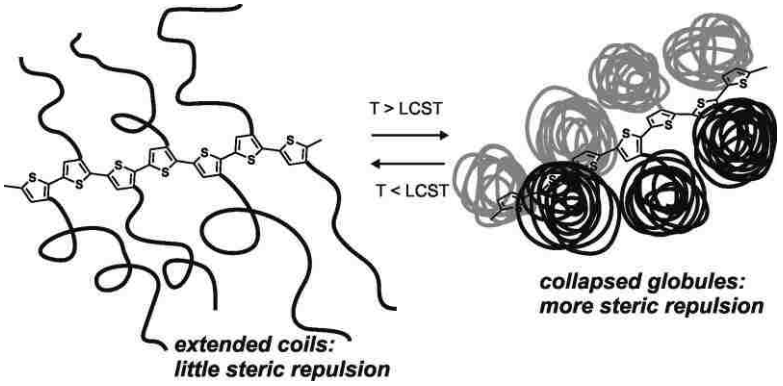

Figure 2. 1 Schematic illustration of the temperature-induced control of PT backbone conformation: grafted PNIPAm side chains collapse into sterically bulkier hydrophobic globular phase at temperatures above LCST, causing torsional twisting of the PT conjugated backbone (elements are not to scale).

In the search for possible model PT systems with electronic properties unaffected by aggregation in dilute solutions, and where the conjugated backbone conformation can be controlled by applying an external stimulus, we came across poly(*N*-isopropylacrylamide) (PNIPAm) grafted polythiophenes. PNIPAm is a unique temperature-responsive polymer which, due to its lower critical solution temperature (LCST) appearing in the physiological range (around 32 ℃), became very popular as a basis for the development of drug delivery and controlled release scaffolds as well as other biomedical applications.[34-36]

Below LCST, PNIPAm exists in the form of extended, hydrogen bond stabilized random coils, while above LCST it loses water and collapses into tight, hydrophobic globules.[37] The phase transition from coils to collapsed globules caused by increasing temperature occurs in the very narrow interval around LCST and, if polymer concentration in aqueous solution is sufficiently high, results in its aggregation and precipitation. Thus, grafting PNIPAm side chains at the β-position of each thienyl repeating unit in PT would provide a means for an effective control of the conjugated backbone conformation by using temperature as an external stimulus.

The schematic illustration of this approach is shown in Figure 2. 1. At lower temperature, the extended hydrated PNIPAm coils behave, within the proximity of the PT conjugated backbone, as smaller size substituents, which do not encounter significant steric repulsive interactions, and therefore allow the conjugated backbone to exist in a more planarized conformation with higher conjugation length. In addition, water-mediated hydrogen bonding between adjacent extended PNIPAm coils can further stabilize the planarized PT conformation. Above LCST, collapse of the side chains into hydrophobic globules effectively converts them to sterically bulky substituents; in order to accommodate these large-size substituents, the conjugated PT backbone must twist and bend into a conformation with lower conjugation length (Figure 2. 1). Since the PNIPAm phase transition is reversible, decreasing temperature below LCST would restore the original planarized conformation.

In the practical sense, this system would behave as a molecular thermometer, where spectroscopic change (absorption or fluorescence) can be used to report temperature of the surrounding medium.[38-40] Highly important is that the polymeric PNIPAm grafts would

provide an efficient insulation of the individual PT chains. Such insulation can prevent intermolecular electronic interactions between individual PT chains, therefore eliminating aggregation as a factor responsible for spectral properties change and leaving backbone conformation of the isolated PT molecules as the only contributing factor.

Recently, McCarley et al. have described a PNIPAm grafted regiorandom PT prepared by chemical oxidative polymerization; in that study, they observed some degree of temperature-induced conformational switching.[41] While the regiorandom nature of their material obviously precluded any significant conformational switching, it also raised a question of the role of regioregularity of the conjugated PT backbone in effecting the conformational control. In this chapter, we describe preparation and detailed studies of both regiorandom and regioregular PNIPAm-grafted fluorescent PTs and unexpectedly dramatic effect of small variations in regioregularity on the temperature-induced conformational switching. Such fine control over isolated polymer chain conformation in dilute solutions has not been demonstrated previously and serves to illustrate the relative importance of conformational effects for intramolecular energy migration in conjugated polymers.

2.2. Results and Discussion

Synthesis of PNIPAm-Grafted Copolymers. Three conjugated PT precursors **2-2~2-4** were prepared starting from the easily available TBDMS-protected dibromothiophene **2-1** (Scheme 2. 1) using nickel-catalyzed McCullough GRIM polymerization method.[42-45] When Ni(dppp)Cl_2 catalyst was used, regioregular polymers were obtained; a series of independent runs afforded the polymers with similar molecular weight and polydispersity values (as determined by GPC analysis) and regioregularities ranging from 89% to 92%.

The percentage of regioregularity in poly(3-alkylthiophene)s refers to the fraction of

head-to-tail (HT) coupled repeating units; thus, a 100% regioregular PT has 100% HT coupling, where a polymer with low percentage of HT coupling (50~80%) would be considered regiorandom.[44,45] Two of prepared polymers with HT fraction 89% and 92% were selected for further studies and designated here as **2-3** and **2-4** respectively. The percent regioregularity was determined by careful integration of the two signals between 2.5 and 3.5 ppm in ^{1}H NMR spectra; these signals belong to methylene protons of the 3-alkyl chain connected to the thienyl unit and ratio of their integral intensities serves as a reliable measure of regioregularity of 3-alkyl-substituted PTs (Since NMR signal integration can only be done with a certain degree of error, the percent regioregularities for **2-3**and **2-4** reported herein represent the lowest values for each polymer obtained from a few independent NMR experiments). [46-48]

In order to obtain regiorandom polymer **2-2**, McCullough GRIM polymerization was carried out in the same conditions, but using $Ni(PPh_3)_2Cl_2$ instead of $Ni(dppp)Cl_2$ as a catalyst. This afforded the polymer with 65% fraction of HT coupled repeating units. The fact that a simple change from bidentate (dppp) to monodentate (PPh_3) ligand in the nickel catalyst led to almost complete loss of regioregularity in the resulting PT has been documented previously;[47] the likely reason for this phenomenon seems to originate from the less strict steric requirements imposed by the monodentate ligand at the reactive metal center in the rate-limiting oxidative addition step during the chain-growth polymerization.[49]

Molecular weight of the regioregular polymers **2-3** and **2-4** was found to be higher than that of the random polymer **2-2** (corresponding to ~40 repeating units in **2-3** and **2-4** vs 30 repeating units for **2-2**); this reflected a more “living” nature of the polymerization involving the catalyst with a bidentate ligand.[50,51] In the next step, the TBDMS-protected

PTs were converted to macroinitiators **2-2~2-4** (Scheme 2. 2).

Scheme 2. 1 Synthesis of PNIPAm-grafted polythiophenes **2-8~10**

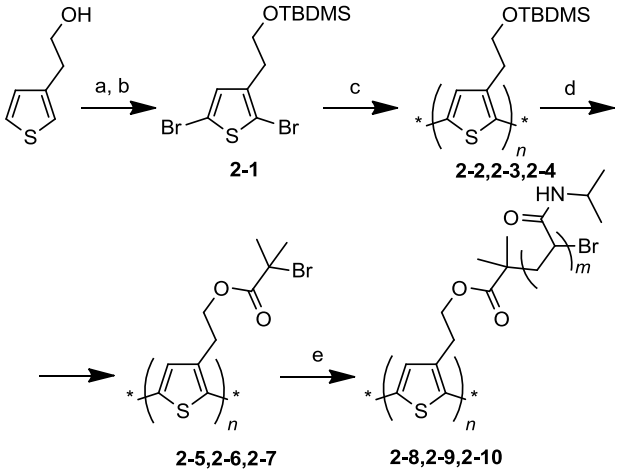

[a] Reagents and conditions: (a) NBS, THF, 0 ℃; (b) TBDMS-Cl, imidazole, DMF, 25 ℃, 80% over two steps; (c) *tert*-BuMgCl, THF, reflux, followed by $Ni(PPh_3)_2Cl_2$ cat. (for **2-3**), or $Ni(dppp)Cl_2$ cat. (for **2-3, 2-4**), reflux, 20-30%; (d) 2-Bromoisobutyryl bromide, TBAF, NEt_3, THF, 25 ℃, ~90%; (e) *N*-isopropylacrylamide, CuBr, 1,4,8,11-tetramethyl-1,4,8,11-tetraazacyclotetradecane, THF, 0 ℃, ~60-70%.

Finding appropriate experimental conditions for carrying out this transformation was a key issue, since both TBDMS protecting groups in **2-2~2-4** and 2-bromoisobutyryl groups in **2-5~2-7** serve as efficient solubilizing substituents for the corresponding polymers. However, conversion of **2-2~2-4** to the product polymers **2-5~2-7** occurs through the intermediate formation of OH-terminated side groups which are poor solubilizers for the polymers; polymer with a fraction of these groups exceeding some solubility threshold would become completely insoluble and simply precipitate from solution. In order to avoid precipitation during this transformation, a special strategy was developed to prevent substantial accumulation of OH-terminated side groups during the reaction. In particular, a dilute solution of tertrabutylammonium fluoride (TBAF) was very slowly added using a syringe pump to a THF solution of one of the polymers **2-2~2-4** mixed with an excess of triethylamine and 2-bromoisobutyryl bromide.[50,51] Employing these conditions allowed

avoiding the precipitate formation during the reaction and afforded soluble macroiniators **2-5~2-7** in almost quantitative yield. The completeness of side group transformation was monitored by ^{1}H NMR, and was close to 100% in all the runs.

Table 2. 1 Molecular weights and regioregularity of macroinitiators and target polymers

Polymer	M_n	D	%HT[a]
2-5	8,000	1.32	65
2-6	12,000	1.55	89
2-7	12,000	1.56	92
2-8	$1.16x10^5$	1.54	65
2-9	$1.46x10^5$	1.46	89
2-10	$1.71x10^5$	1.71	92

[a] Determined by ^{1}H NMR; [b] Determined by GPC in THF relative to polystyrene standards; [c] Determined by GPC in DMF using static light scattering method.

Finally, the PNIPAm-grafted polythiophenes **2-8~2-10** were prepared using the well-developed ATRP protocol.[53-55] Formation of the PNIPAm grafts was confirmed by ^{1}H NMR, and by significant increase of the polymers' molecular weights (Table 2. 1). On the basis of the approximate number of repeating units in the macroinitiators **2-5~2-7**, and assuming low polydispersity of the PNIPAm grafted side chains (which is a signature feature of "living" ATRP polymerization), one could estimate average molecular weight (M_n) of a side chain in **2-8~2-10**, to be around 3.5 kDa. The grafted polymers were found to be thermally stable in solid state and showed no thermal decomposition upon heating to ~600 ℃ as was revealed in TGA studies (Figure 2. 2). Not surprisingly, solid vacuum-dried polymer samples contained about 8 wt % of water, likely entrapped within the PNIPAm grafted chains. Loss of this water accounted for the experimentally observed ~10% weight reduction upon heating the solid samples in the range of 20-150℃ in TGA experiments; the

total weight loss was in good agreement with the water content obtained independently by Karl Fischer titration. Interestingly, at the temperatures above the decomposition point, the polymers showed rapid weight loss of almost 80 % of initial weight, possibly through depolymerization of the grafted side chains.

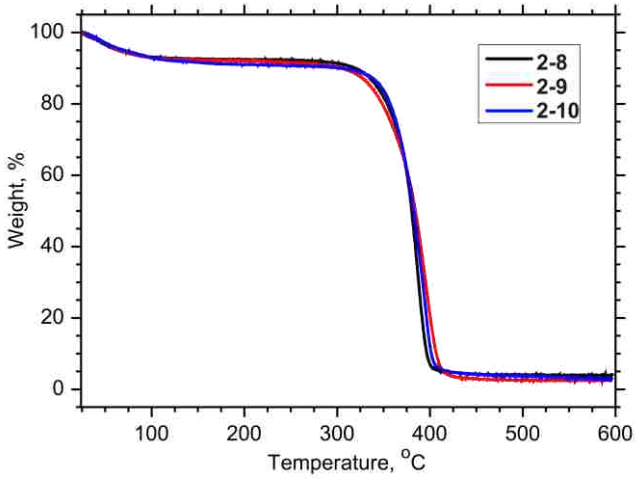

Figure 2. 2 TGA data for regiorandom copolymer **2-8** (black trace), regioregular copolymer **2-9** (red trace) and **2-10** (blue trace). The data were acquired at the heating rate of 10 ℃/min to 600 ℃ in nitrogen atmosphere.

Photophysical Properties of the Polymers. The PNIPAm-grafted copolymers **2-8~2-10** showed excellent solubility in water, as well as in variety of organic solvents (such as THF, chlorinated solvents, alcohols, etc.). At the same time, they were completely insoluble in aromatic solvents (toluene) and saturated hydrocarbons. As expected, increasing regioregularity from **2-5** to **2-7 (**and from **2-8** to **2-10**) resulted in pronounced bathochromic shifts in the absorption and fluorescence spectra acquired in dilute THF solutions (Table 2. 2 and Figure 2. 3).[47,56] The PNIPAm grafting in copolymers **2-8~2-10** did not seem to have profound impact on the polymers' backbone conformation and did not affect their electronic spectra in dilute THF solutions. Indeed, each pair of the macroinitiator precursor and the corresponding PNIPAm-graftred copolymers featured very

similar absorption and fluorescent spectra. However, PNIPAm grafting resulted in major increase in the fluorescent quantum yield (from around 10% in **2-5~2-8** to near 30% in **2-8~2-10**, Table 2. 2). Increasing fluorescence efficiency likely reflects good "insulating" properties of the PNIPAm grafts which reduce exposure of the PT backbone to solvent molecules and prevent vibrationally coupled radiationless deactivation of the excited state.

Both absorption and fluorescence spectra of grafted copolymers **2-8~2-10** acquired in aqueous solution were bathochromically shifted with respect to the same spectra in THF solution (Table 2. 3). The magnitude of the shift was relatively small (~15nm) for regiorandom copolymer **2-8** but was much larger (30~40 nm) for regioregular copolymers **2-9** and **2-10**. The bathochromic shifts likely reflect increasing conjugation length of the PT backbone in aqueous medium.

Table 2. 2 Spectral Properties of Polymers **2-5** ~ **2-10**

	solution[a]					
	in THF		in H_2O		thin film[b]	
polymer	$\lambda_{abs,}$ nm	$\lambda_{em,}$ nm (Φ, %)	$\lambda_{abs,}$ nm	$\lambda_{em,}$ nm (Φ, %)	$\lambda_{abs,}$ nm	$\lambda_{em,}$ nm (Φ, %)
2-5	417	549(10)			435	580
2-6	415	559(6)			510	641
2-7	434	566(6)			520	638
2-8	415	536(28)	430	545(9)	422	546
2-9	425	544(31)	457	573(4)	445	564
2-10	433	547(32)	476	573(4)	461	571

[a]at 20°C. [b] obtained by spin-casting from THF solution

Presumably, hydrophilic PNIPAm side chains benefit from strong stabilizing interactions with water molecules in the extended coil conformation and impose a more planarized PT backbone with longer conjugation length. The most striking difference between macroinitiator precursors **2-5~2-7** and PNIPAm-grafted copolymers **2-8~2-10** was found upon comparing their spin-cast film spectra. As expected, macroinitiators **2-5~2-7**

showed very significant aggregation in solid state, which resulted in large bathochromic shifts in absorption and fluorescence spectra and dramatic decrease of emission intensity. Such intermolecular aggregation is typical for soluble PTs and has been observed for polymers with a broad range of different substituents. Although all three precursor polymers **2-5~2-7** were substantially affected by intermolecular electronic interactions in solid films, the extent of such interactions was heavily dependent on the backbone regioregularity. The regioregular polymers **2-6** and **2-7** showed stronger tendency toward interchain aggregation due to the higher planarity of their conjugated backbones, while regiorandom polymer **2-5** showed much less pronounced aggregation-related spectroscopic changes in its spin-cast film (Figure 2. 3).

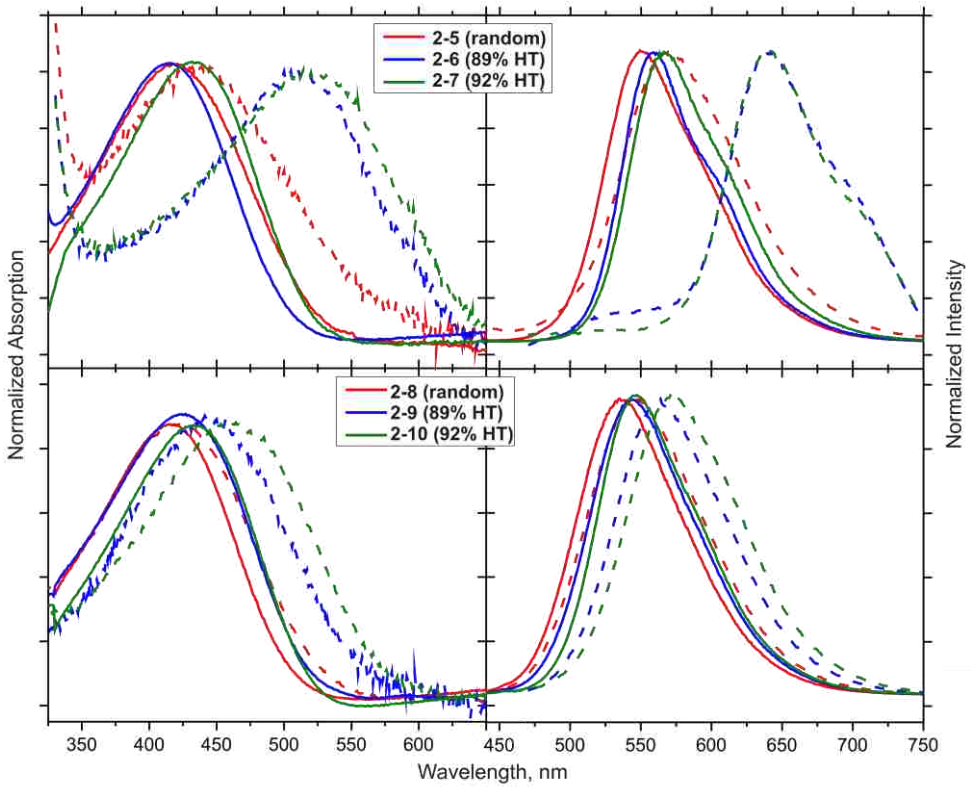

Figure 2. 3 Absorption and fluorescence spectra of precursor polymers **2-5~2-7** (top) and PNIPAM-grafted copolymers **2-8~2-10** (bottom). Solution spectra were acquired at 20 ℃ in THF (for **2-5~2-7**) and in water (for **2-8~2-10**). Concentration of all solutions was 0.15 mg/ml. Solid lines correspond to solution data, dash lines - to spin-cast films.

In stark contrast to macroinitiators **2-5~2-7**, PNIPAm-grafted copolymers **2-8~2-10** demonstrated practically no aggregation-related intermolecular electronic interactions in solid films prepared by spin-casting from THF solutions (Table 2. 2 and Figure 2. 3). This could be attributed to the presence of PNIPAm-grafted side chains which effectively "insulate" individual PT molecules and prevent interchain electronic communication upon aggregation in thin films. Depending on regioregularity of the PT backbone, small bathochromic shifts (relative to THF solution spectra) were observed in thin film spectra; the magnitude of the shifts was increasing with the increasing regioregularity. Remarkably, for each polymer **2-8~2-10** the magnitude of the bathochromic shift observed in spin-cast film spectra was similar to that of the spectra in aqueous solutions where it originated from enhanced backbone planarization (vide supra). It was likely that polymer backbone planarization (and possibly some supramolecular organization) also occurred upon spin-casting, thus resulting in more extended π-electron conjugation; the extent of planarization was consistent with the degree of regioregularity of the PT backbone. To further assess the "insulating" role of the PNIPAm grafted side chains in reducing interchain electronic interactions, a series of experiments were carried out in which the changes in the optical properties of PNIPAm-grafted polymers **2-8~2-10** were followed at different extents of aggregation. These studies can be performed by creating stable solutions of nanoscopic nonscattering particles, thereby allowing quantitative studies of the polymer optical properties in aggregated state.[57-59] This was accomplished by adding various amounts of toluene ("bad" solvent) to methanol ("good" solvent) solutions of the grafted copolymers **2-8~2-10** while keeping constant the polymer concentration in the final solutions (Figure 2. 4 and 2. 5). The aggregated particles of both regioregular and regiorandom grafted copolymers

displayed no appreciable changes in absorption spectra and showed only minor changes (small intensity decrease along with a slight bathochromic emission band shift, possibly due to PT backbone planarization occurring upon aggregation as discussed above). In contrast, the "noninsulated" precursor polymers **2-5~2-7** showed dramatic aggregation-related spectral changes as quality of solvent was gradually decreased (Figure 2. 4 and 2. 5; "good" solvent: chloroform; "bad" solvent: methanol). These spectral changes were found to be in agreement with the solution and thin-film spectral data for these polymers (Figure 2. 3).

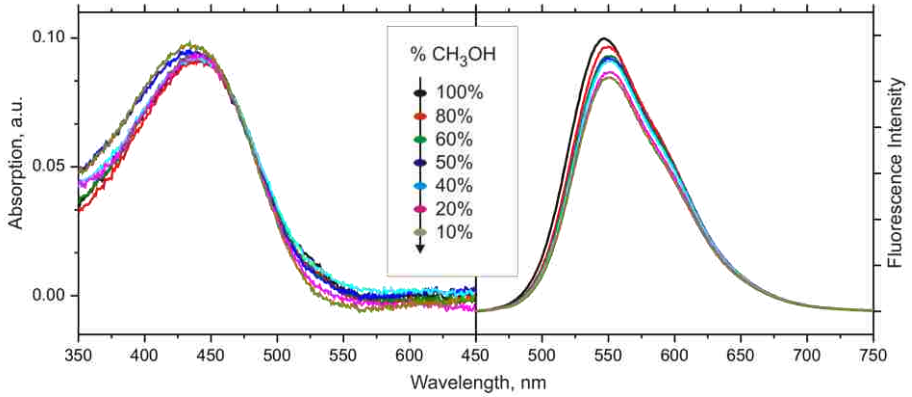

Figure 2. 4 Absorption and fluorescence spectra of polymers **2-10** acquired at 20°C in "good" - "bad" solvent mixtures with increasing fraction of a "bad" solvent ("good" solvent: methanol and "bad" solvent: toluene

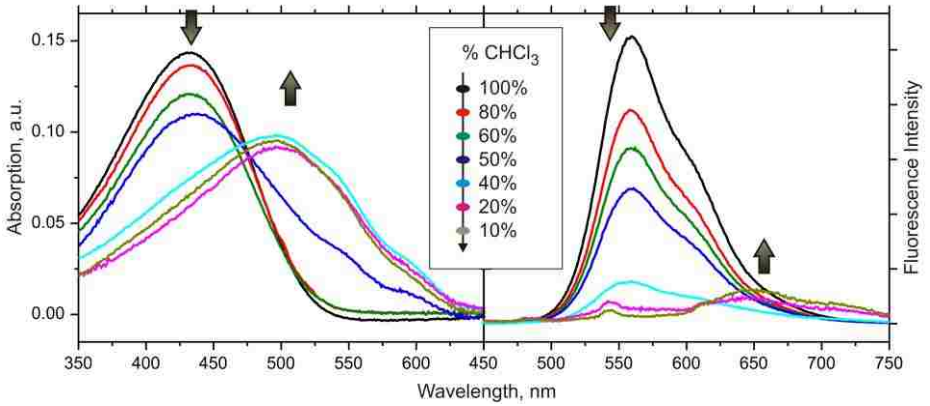

Figure 2. 5 Absorption and fluorescence spectra of polymers **2-7** acquired at 20°C in "good" - "bad" solvent mixtures with increasing fraction of a "bad" solvent ("good" solvent: chloroform, "bad" solvent : methanol)

Thus, it can be concluded that, owing to the "insulated" nature of the grafted

copolymers **2-8~10**, their spectral response in dilute solutions would be primarily due to the properties of individual isolated conjugated chains, with only minor (if any) influence of intermolecular electronic interactions.

Temperature-Dependent Spectroscopic Properties. All three grafted copolymers **2-8~2-10** exhibited temperature-induced spectral changes in dilute solutions which were consistent with the idea of the PT backbone conformational switching when grafted PNIPAm side chains collapse into globular phase at the temperatures above LCST. These changes included pronounced hypsochromic absorption and fluorescence spectral shifts as well as intensity increase of fluorescent emission upon heating the solutions (Figure 2. 6). These spectral changes were found to be completely reversible upon cooling the solutions. The magnitude of changes was strongly dependent on the extent of regioregularity of PT conjugated backbone, with random copolymer **2-8** displaying only small changes (consistent with previous observation by McCarley et al.[41]) and regioregular polymers showing much more pronounced changes. Thus, the highest regioregularity polymer **2-10** showed a 20 nm hypsochromic shift in absorption maximum as well as 16 nm shift in emission maximum when temperature was increased from 20 to 50 ℃, whereas the regiorandom polymer **2-8** displayed only smaller 8 nm absorption and emission shifts. The more pronounced spectral changes in regioregular polymer **2-10** were consistent with the notion of more planarized backbone conformation of this polymer in dilute solutions, which potentially allows larger conformational changes toward backbone twisting, in contrast to the regiorandom copolymer **2-8**.

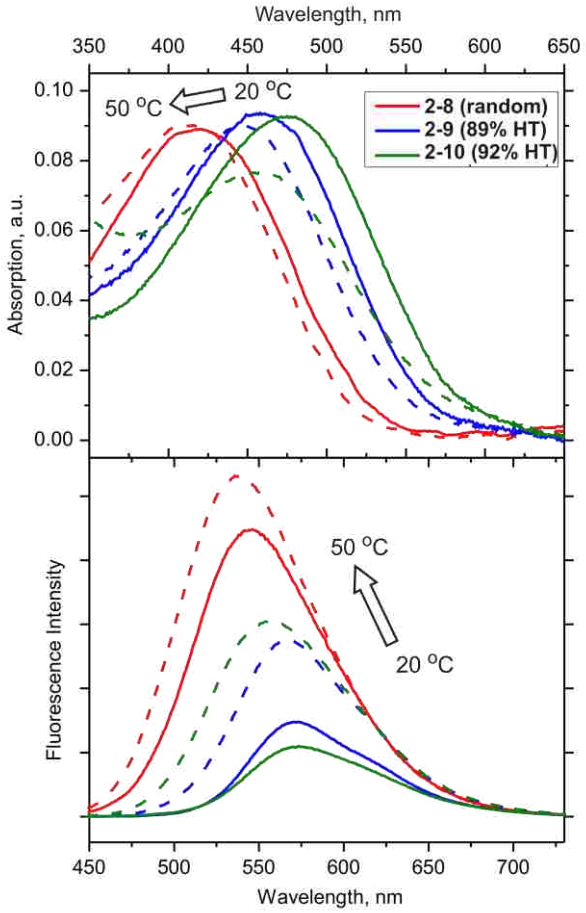

Figure 2. 6 Absorption (left) and fluorescence (right) spectra of PNIPAM-grafted copolymers **2-8, 2-9** and **2-10** in aqueous solution (concentration 0.15 mg/ml) at 20 ℃ (solid traces) and 50 ℃ (dash traces). The spectra are not normalized for intensity comparison purpose.

Surprisingly, two regioregular copolymers **2-9** and **2-10** showed strikingly different thermochromic behavior despite only a small 3% difference in regioregularity (Figure 2. 7). Clearly, the effect of conjugated backbone regioregularity on the extent of PT conformational twisting was not linear, and the relatively small increase in regioregularity could lead to dramatic effect on the ease and magnitude of the conformational twisting. Although thermochromism (temperature-induced spectral changes) is a well-documented phenomenon found both for solutions and thin films of regiorandom and regioregular PTs, it generally occurs in a much wider ($\geq$100 ^{o}C) range of temperatures and is related to

conformation-induced intermolecular aggregation, resulting in appearance of a new distinct absorption band; in many instances it is irreversible.[60-63] In contrast, the presently observed thermochromic behavior is completely different in nature and appearance as it originates from the reversible conformational switching of isolated conjugated polymer chains in a relatively narrow temperature interval. As such, it only results in spectral wavelength shifts, without appearance of a new absorption band. Indeed, the presently observed hypsochromic shifts upon heating solution of the regioregular copolymer **2-10** were very similar to those found by Kim and Swager for a surface-pressure-induced planar to perpendicularly twisted conformational transition of poly(*p*-phenyleneethynylene)s (PPEs) in Langmuir monolayer.[64] Although some caution should be exercised when drawing parallels between PTs and PPEs, extended π-electron conjugated nature of the planarized conformation of both classes of polymers makes such comparison viable. Further support in favor of the conformational switching was obtained from fluorescence lifetime measurements in dilute aqueous solution of **2-10** using the phase modulation technique. Both at 20 and 50 ^{o}C, the polymer emission decay was found to be double-exponential (Table 2. 3), likely indicating the presence of two independent decay pathways. The major, short-lived component showed values typical for PT polymers; the decrease from 0.56 ns at 20 ^{o}C to 0.51 ns at 50 ^{o}C was consistent with formation of a more twisted, less conjugated PT conformation at higher temperature.[65] This also paralleled the previous observations of a similar lifetime decrease in the more twisted, lower conjugation length conformations of PPEs[15] and their small-molecule congener.[66]

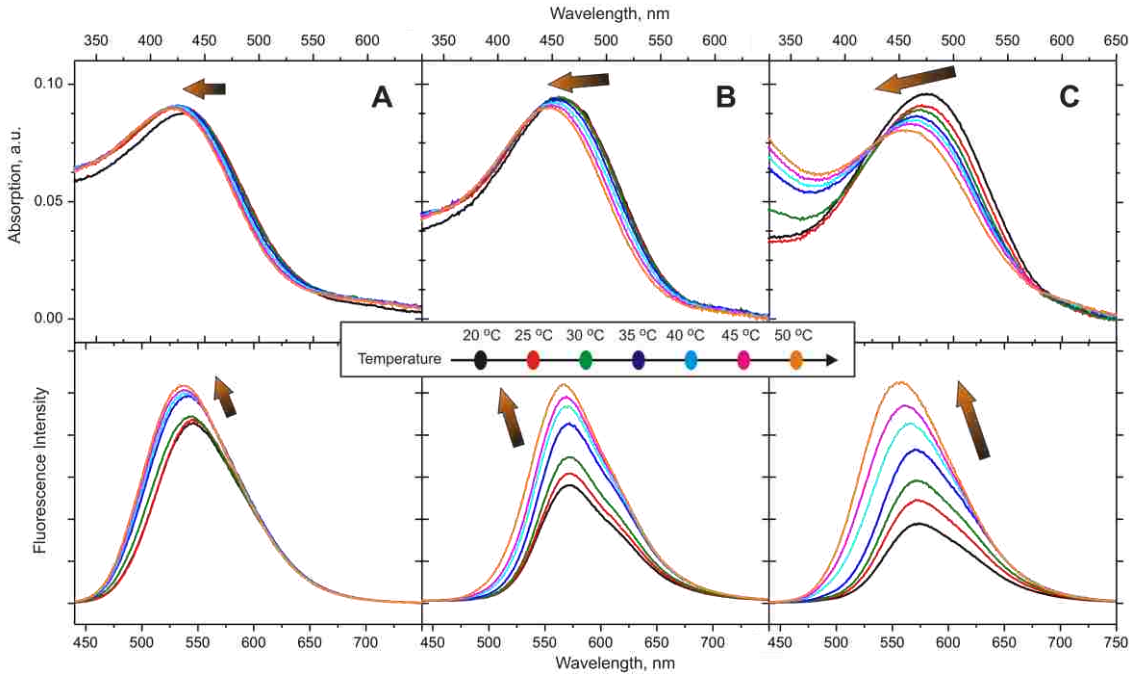

Figure 2. 7 Temperature-dependent absorption (top row) and corresponding fluorescence (bottom row) spectra of PNIPAM-grafted copolymers **2-8** (A), **2-9** (B) and **2-10** (C) in aqueous solution (concentration 0.15 mg/ml).

Increasing pre-exponential amplitude of the short-lived decay component was also in agreement with the increasing role of the short-lived decay pathway due to conformational twisting. The origin of the minor 3 ns decay component is not particularly clear. In many cases, the presence of a long-lived component indicates formation of exciplex-like species due to intermolecular aggregation.[67] However, the possibility of such electronic interactions seemed unlikely considering the "insulating" nature of the PNIPAm grafted side chains.

Table 2. 3 Fluorescent Lifetimes of Polymer **2-10** in Aqueous Solution[a]

Temp (°C)	τ_1 (ns)[b]	τ_2 (ns)[b]	χ^2
20	0.56(0.90)	3.18(0.10)	0.95
50	0.51(0.91)	3.34(0.08)	0.79

[a] Concentration 0.20 mg/ml. [b] Pre-exponential amplitude is given in parentheses (to add to 1.00).

Also, the relative contribution of the long-lived decay pathway consistently decreases with increasing temperature (Table 2. 3), which contradicts the data obtained from dynamic light scattering experiments (vide infra) that clearly indicate an increase in intermolecular aggregation as the temperature traverses through LCST. If intermolecular interactions are ruled out, and we assume that both decay components originate from isolated individual polymer chains, it could be possible that the short-lived component is associated with the fast coherent Dexter energy migration mechanism, while the long-lived component originates from the long-range incoherent exciton hopping.[68] In such case, the predominance of the short-lived component, especially at the higher temperature, does signify appreciable role of the conformation-dependent through-bond exciton migration process. The diminished conjugation length due to temperature-induced PT backbone twisting was also consistent with an almost 3-fold increase of emission intensity of **2-10** observed upon increasing the temperature from 20 to 50 ^{o}C (Figure 2. 7C). This was probably due to the shortening exciton diffusion length in the twisted conformation, which reduced the probability of excited state quenching with residual impurities or backbone defects. In contrast to PNIPAm-grafted copolymers, the precursor polymers **2-8~2-10** showed only subtle spectral changes when their THF solutions were studied in the same 20-50 ^{o}C temperature range, thus further supporting the uniqueness of the temperature-induced backbone conformational twisting in grafted copolymers **2-8~2-10** (Figure 2. 8).

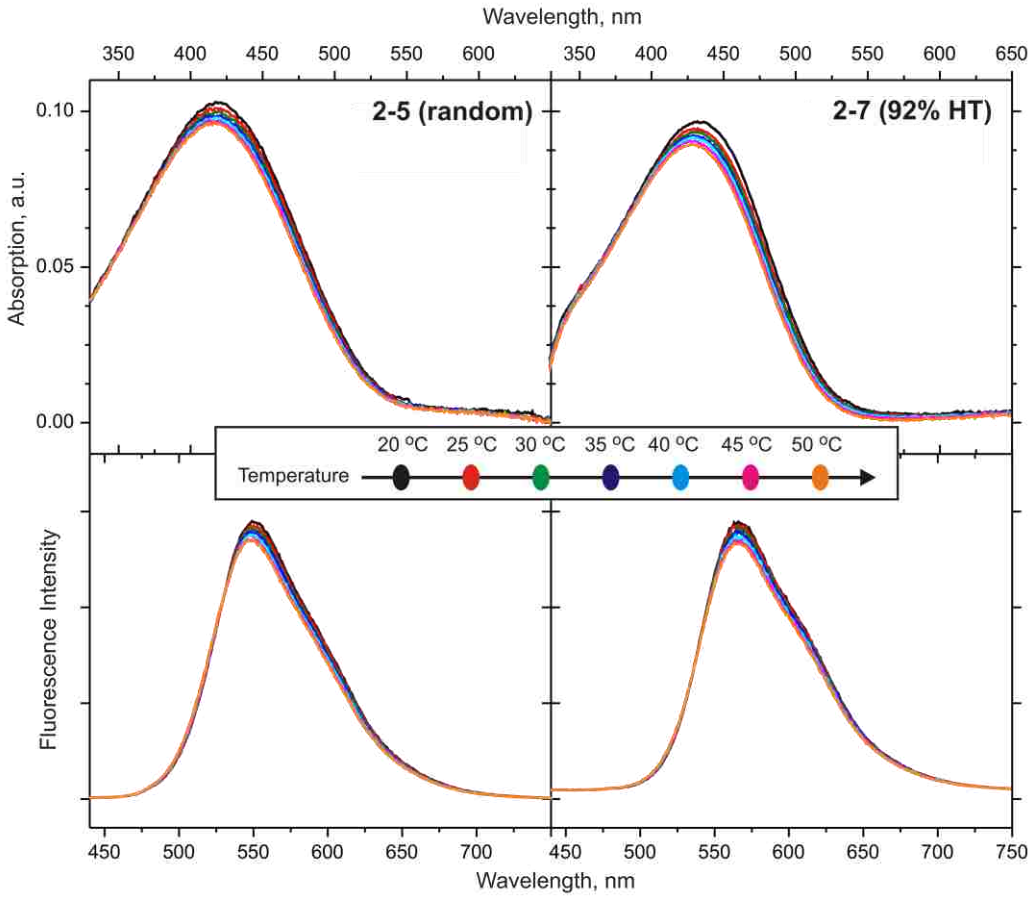

Figure 2. 8 Temperature-dependent absorption (*top row*) and corresponding fluorescence (*bottom row*) spectra of macroinitiator precursor regiorandom polymer **2-5** and regioregular **2-7** in THF solution (concentration 0.15 mg/ml)

Similarly, no substantial spectral changes were observed when THF was used instead of water as a solvent for grafted copolymers **2-8~2-10** (Figure 2. 9). Because the PNIPAm phase transition does not happen in THF, increasing temperature alone did not cause conformational twisting of the PT backbone in **2-8~10**; this emphasizes the critical role of the grafted PNIPAm side chains phase transition in the observed temperature-induced spectral changes. Since the PNIPAm phase transition occurs in a narrow temperature range around LCST, one would expect relatively sharp threshold change in the copolymers **2-8~2-10** spectral properties when the temperature traverses through LCST. Such threshold change occurring between 30 and 35 ^{o}C could indeed be observed in the case of regiorandom

copolymer **2-8** (Figure 2. 7A). However, in the increasingly more regioregular copolymers **2-9** and **2-10**, the change was found to become more continuous and spread over a broader temperature interval. Whereas some threshold change could still be noticed in the copolymer **2-9** (89% HT), it became completely continuous for the copolymer **2-10** (92% HT) (Figure 2. 7B, C).

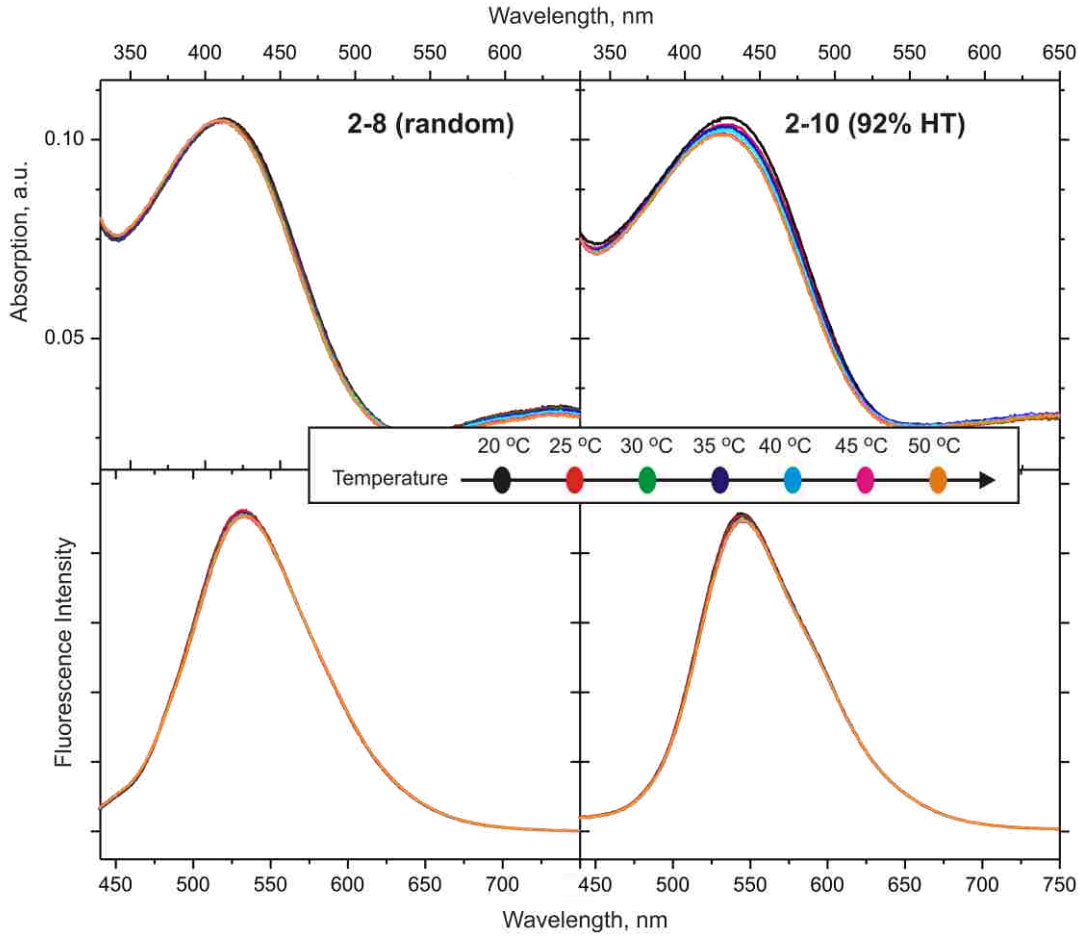

Figure 2. 9 Temperature-dependent absorption (*top row*) and corresponding fluorescence (*bottom row*) spectra of PNIPAm-grafted copolymers **2-8** and **2-10** in THF solution (concentration 0.15 mg/ml)

Thus, continuity of the temperature-induced spectral changes was strongly dependent on regioregularity of the PT backbone. Since neither parent precursor polymers **2-5~2-7** nor PNIPAm-grafted copolymers **2-8~2-10** showed appreciable temperature-

dependent spectral changes in THF solution, it was the PNIPAm phase transition in aqueous medium which had to be responsible for the conformational changes and observed spectral changes in the copolymers **2-8~10.** To gain deeper understanding of the continuous change phenomenon, differential scanning calorimetry (DSC) studies on dilute solutions of the copolymers **2-8~10** were carried out. The DSC experiments revealed that the PNIPAm phase transition occurred reversibly upon heating and cooling in the narrow temperature interval around LCST in all three grafted copolymers, independent of their regioregularity; this transition was associated with narrow endothermic (heating) and exothermic (cooling) peaks (Figure 2. 10).

An additional broad peak partially overlapping with the main narrow peak and corresponding to a phase transition in the 32-45 ^{o}C temperature range was particularly noticeable in DSC data for the copolymer **2-10**. This peak was found to be less pronounced (but still present) in DSC data for the less regioregular copolymer **2-9** and was seemingly absent in the case of regiorandom polymer **2-8** (Figure 2. 10).

The presence of this additional phase transition in solutions of regioregular grafted copolymers was an important feature likely related to the temperature-induced continuous spectral changes in these polymers. Important information about temperature-dependent behavior of the copolymers **2-8~10** was obtained from smallangle dynamic light scattering (DLS) studies.

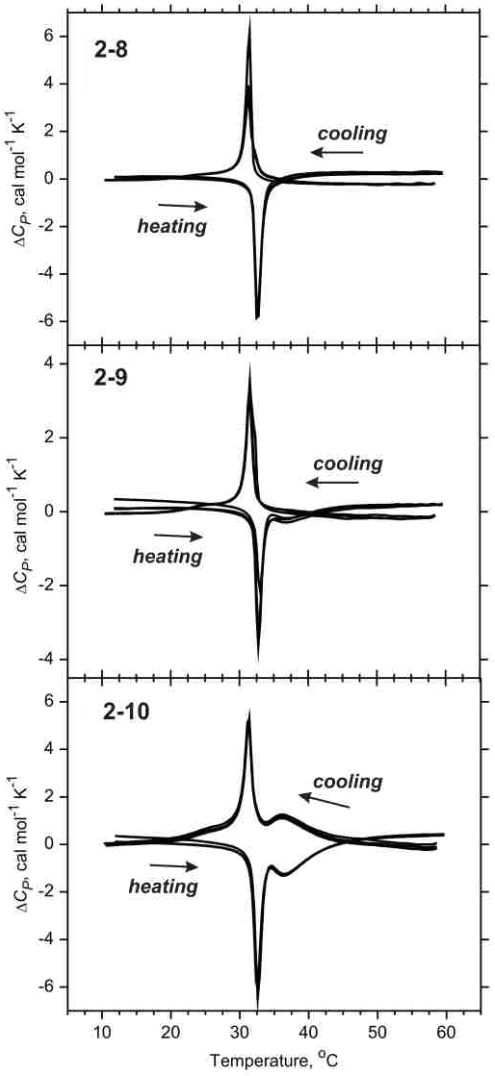

Figure 2. 10 DSC data for PNIPAm-grafted copolymers **2-8~2-10** in aqueous solution (concentration 0.25 mg/ml). Three repeated cycles of heating and cooling are shown for each polymer.

Analysis of DLS data (Figure 2. 11) revealed interesting temperature-induced features. Both regiorandom and regioregular copolymers **2-8** and **2-10** at 20 ^{o}C showed similar diffusion coefficients (around (1.2-1.3) $\times$ 10^{-11} m^2s^{-1}). Increasing temperature from 20 to 32 ^{o}C resulted in gradual and almost linear increase of the diffusion coefficients up to ~2 $\times$ 10^{-11} m^2s^{-1}. This increase can be associated with a continuous precollapse of the extended coils of PNIPAm grafted chains,[55] which decreases the polymer's radius of gyration and increases the apparent diffusion coefficient. Such "continuous" precollapse of grafted

PNIPAm side chains before the "precipitous" collapse at LCST was previously reported[69-71] and would result in increasing the effective steric size of the PNIPAm substituents in the vicinity of the PT conjugated backbone.

Therefore, it can be responsible for the continuous, gradual temperature-dependent PT backbone conformational twisting found for the regioregular copolymers **2-9** and **2-10** at the temperatures below LCST. This gradual PNIPAm side chains "precollapse" at the temperatures below LCST apparently could not affect the backbone conformation of the regiorandom copolymer **2-8**, in which case no spectral changes were observed in this temperature range. This was probably due to the already significantly twisted backbone conformation of this copolymer, which made any further twisting more unfavorable and requiring really major changes of the side chains (like the phase transition at LCST). The enhanced intermolecular interactions between PNIPAm-grafted side chains attached to the PT backbone in regioregular fashion were likely to intensify and "expand" the precollapse over longer temperature range, which explains the significant continuous spectral changes in regioregular copolymer **2-10** observed at the temperatures below LCST, in contrast to only the subtle changes in the regiorandom copolymer **2-8** (Figure 2. 7). Upon further heating, a sharp drop in diffusion coefficients was observed for both **2-8** and **2-10** copolymers in the very narrow 32-33 ^{o}C temperature range. Since this event occurred at exactly the same temperature as the major phase transition found in DSC studies (vide supra), it could be assigned to the extended coil-collapsed globule PNIPAm phase transition at LCST. It coincided with the threshold spectral changes observed in solution of the regiorandom polymer **2-8** (and, to some extent, in polymer **2-9**) originating from the backbone conformational twisting.

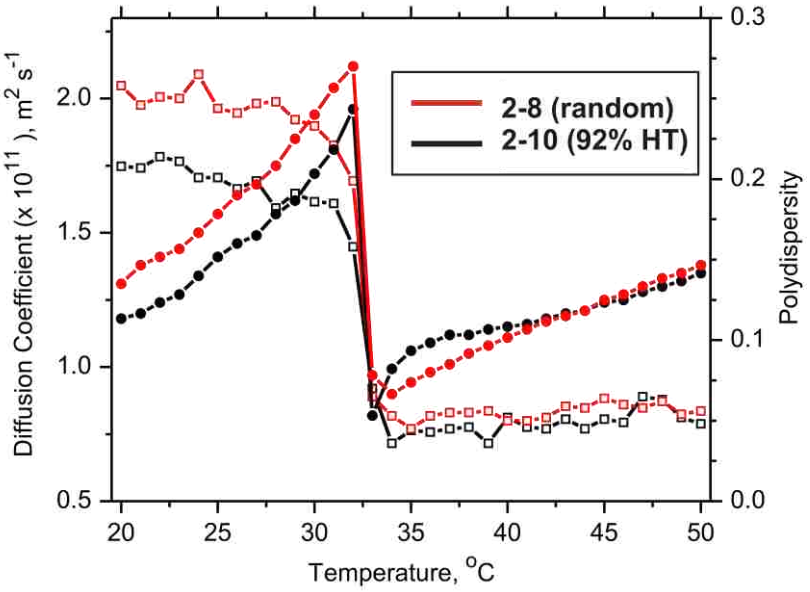

Figure 2. 11 Temperature-dependent small-angle DLS data for PNIPAm-grafted copolymers **2-8** and **2-10** in aqueous solution (concentration 0.5 mg/ml). Traces marked with solid circles use left *Y*-axis and represent diffusion coefficients; traces marked with squares use right *Y*-axis and correspond to DLS "polydispersity".

From general considerations, the PNIPAm phase transition from extended coil to collapsed globule at LCST was expected to diminish the effective size (radius of gyration) of an individual molecule and increase the diffusion coefficients. Thus, experimentally observed sharp decrease in diffusion coefficients at LCST surprisingly contradicted this assumption. Very likely, this drop reflected formation of intermolecular aggregates upon the PNIPAm grafted side chains precipitous collapse. The idea of loose aggregate formation is also in agreement with a sharp drop of DLS "polydispersity" from the values around 0.2-0.25 before LCST to 0.05 at the temperatures above this point (Figure 2. 11). The aggregate formation in aqueous solutions at the temperatures above LCST is driven by increasing hydrophobicity of the collapsed globule phase and is well-documented for PNIPAm polymers.[37] Because of the relatively short size of conjugated PT backbone in the present study (30-40 thienyl repeating units) and relatively large size of PNIPAm-grafted side chains,

it was unlikely that any noticeable folding of the PT chains could happen upon aggregation; it is more likely that the individual polymer chains formed loose side-by-side aggregates in their elongated wormlike conformation. Furthermore, these aggregates were likely to consist of only a small number of individual polymer molecules. Indeed, the calculated (using Stokes-Einstein equation) average hydrodynamic radius of the scattering particles in solution changed from 30 nm just before reaching LCST to 60 nm at the temperatures slightly above LCST. Even taking into account the very qualitative nature of this estimation (since the polymer particles could not be perfectly spherical), it would be safe to suggest that an average aggregate included no more than three polymer molecules.

As discussed above, such loose intermolecular aggregation could not directly affect the electronic properties of the copolymers **2-8~2-10** due to the PNIPAm grafts acting as efficient "insulator" for the conjugated PT backbone. It, however, could affect the conformation of the conjugated backbone as individual polymer chains would have to accommodate each other within the aggregated state. Interestingly, further temperature rise from 33 to 50 ^{o}C resulted in increasing effective diffusion coefficients as the polymer aggregates accommodated into more optimal intermolecular packing with decreasing overall dimensions. The increase was almost linear for the regiorandom copolymer **2-8**; however, it showed a much steeper, almost exponential increase in the 33-45 ^{o}C temperature range for the regioregular copolymer **2-10** (Figure 2. 11). This temperature range perfectly coincided with the temperature range where a second broad phase transition was observed for the aqueous **2-10** solution in DSC experiments (Figure 2. 10). On the basis of this observation, we hypothesize that this broad transition corresponds to the PT backbone conformational twisting as individual polymer chains try to better accommodate each other within the

aggregates; this explains the observed continuous spectral change for **2-10** in aqueous solution at the temperatures above LCST (Figure 2. 7). Although it was not possible a priori to anticipate that such a seemingly minor factor would cause such a significant conformational twisting of the regioregular polymer (of almost the same magnitude as the conformational change caused by the phase transition of grafted PNIPAm side chains), it can be easily understood considering the small energy required for twisting the regioregular PT backbone.

2.3. Conclusions

Reversible temperature-induced control of conjugated backbone conformation and conjugation length was demonstrated using a series of PNIPAm-grafted water-soluble fluorescent PTs. The grafted PNIPAm side chains provide an efficient "insulation" of the conjugated backbone, so the effect of intermolecular electronic interactions is greatly diminished to allow studies of the properties of electronically isolated CP molecules. The temperature-induced phase transition of the grafted side chains was responsible for the conformational twisting of the conjugated backbone at rising temperature, resulting in decreasing conjugation length, hypsochromic shifts in absorption and emission spectra, and increasing intensity of fluorescent emission along with a small drop in emission lifetime.

The extent of the temperature-induced conformational switching, as well as the magnitude and nature of spectroscopic changes, was found to be strongly dependent on the degree of regioregularity of the PT backbone. A regiorandom copolymer showed relatively small changes, which mostly occurred in a narrow temperature range around 32 ^{o}C corresponding to the PNIPAm phase transition.

In contrast, regioregular polymers showed much greater spectral changes which

occurred continuously in the temperature interval significantly exceeding that of the PNIPAm phase transition range. The effect of regioregularity was clearly not linear, as only a small increase in regioregularity (from 89% to 92%) led to very substantial difference in the extent of conformational switching. The enhanced continuous conformational and spectral changes in regioregular polymers are likely to be related to side-group driven aggregation, as was supported by the results of thermal and light-scattering experiments. It is possible that the PNIPAm-grafted copolymers of even higher regioregularity could demonstrate remarkably higher temperature-induced conformational switching control. In our studies, described in the following chapters, we developed a powerful catalytic system capable of producing PNIPAm-substituted polythiophenes with 100% regioregularity. Although in the course of this dissertation, we were not able to carry out the similar studies on such polymers, this still remains to be done, and will be done in the future research.

2.4. References

1. McQuade, D. T.; Pullen, A. E.; Swager, T. M. Conjugated Polymer-Based Chemical Sensors *Chem. Rev.* **2000**, *100*, 2537–2574.

2. Thomas III, S. W.; Joly, G. D.; Swager, T. M. Chemical Sensors Based on Amplifying Fluorescent Conjugated Polymers. *Chem. Rev.* **2007**, *107*, 1339-1386.

3. Swager, T. M. The Molecular Wire Approach to Sensory Signal Amplification. *Acc. Chem. Res*. **1998**, *31*, 201–207.

4. Bunz, U. H. F. Poly(aryleneethynylene)s: Syntheses, Properties, Structures, and Applications. *Chem. Rev.* **2000**, *100*, 1605-1644.

5. Chen, L.; McBranch, D. W.; Wang, H.-L.; Helgeson, R.; Wudl, F.; Whitten, D. G. Highly sensitive biological and chemical sensors based on reversible fluorescence quenching in a conjugated polymer. *Proc. Natl. Acad. Sci. USA.* **1999**, *96*, 12287-12292.

6. Finden, J.; Kunz, T. K.; Branda, N. R.; Wolf, M. O. Reversible and Amplified Fluorescence Quenching of a Photochromic Polythiophene. *Adv. Mater.* **2008**, *20*, 1998-2002.

7. Zhao, X.; Jiang, H.; Schanze, K. S. Polymer Chain Length Dependence of Amplified Fluorescence Quenching in Conjugated Polyelectrolytes. *Macromolecules* **2008**, *41*, 3422-3428.

8. Schwartz, B. J. Conjugated polymers as molecular materials: How Chain Conformation and Film Morphology Influence Energy Transfer and Interchain Interactions. *Annu. Rev. Phys. Chem.* **2003**, *54*, 141-172.

9. Averbeke, B. V.; Beljonne, D. Conformational Effects on Excitation Transport along Conjugated Polymer Chains. *J. Phys. Chem. A* **2009**, *113*, 2677-2682.

10. Collini, E.; Scholes, G. D. Coherent Intrachain Energy Migration in a Conjugated Polymer at Room Temperature. *Science* **2009**, *323*, 369-373.

11. Nesterov, E. E.; Zhu, Z.; Swager, T. M. Conjugation Enhancement of Intramolecular Exciton Migration in Poly(*p*-phenylene ethynylene)s. *J. Am. Chem. Soc.* **2005**, *127*, 10083-10088.

12. Rinto, M. R.; Schanze, K. S. Amplified fluorescence sensing of protease activity with conjugated polyelectrolytes. *Proc. Natl. Acad. Sci. USA* **2004**, *101*, 7505-7510

13. Liu, B.; Bazan, G. C. Homogeneous Fluorescence-Based DNA Detection with Water-Soluble Conjugated Polymers. *Chem. Mater.* **2004**, *16*, 4467-4476

14. Kim, I.-B.; Erdogan, B.; Wilson, J. N.; Bunz, U. H. F. Sugar–Poly(*para*-phenylene ethynylene) Conjugates as Sensory Materials: Efficient Quenching by Hg^{2+} and Pb^{2+} Ions. *Chem. Eur. J.* **2004**, *10*, 6247-6254.

15. Wosnick, J. H.; Mello, C. M.; Swager, T. M. Synthesis and Application of Poly(phenylene Ethynylene)s for Bioconjugation: A Conjugated Polymer-Based Fluorogenic Probe for Proteases. *J. Am. Chem. Soc.* **2005**, *127*, 3400-3405.

16. He, F.; Tang, Y.; Yu, M.; Wang, S.; Li, Y.; Zhu, D. Fluorescence-Amplifying Detection of Hydrogen Peroxide with Cationic Conjugated Polymers, and Its Application to Glucose Sensing. *Adv. Funct. Mater.* **2006**, *16*, 91-94.

17. Jiang, H.; Zhao, X.; Schanze, K. S. Amplified Fluorescence Quenching of a Conjugated Polyelectrolyte Mediated by Ca^{2+}. *Langmuir* **2006**, *22*, 5541-5543.

18. Liu, B.; Bazan, G. C. Optimization of the Molecular Orbital Energies of Conjugated Polymers for Optical Amplification of Fluorescent Sensors. *J. Am. Chem. Soc.* **2006**, *128*, 1188-1196.

19. Disney, M. D.; Zheng, J.; Swager, T. M.; Seeberger, P. H. Detection of Bacteria with Carbohydrate-Functionalized Fluorescent Polymers. *J. Am. Chem. Soc.* **2004**, *126*, 13343-13346.

20. Ho, H.-A.; Najari, A.; Leclerc, M. Optical Detection of DNA and Proteins with Cationic Polythiophenes. *Acc. Chem. Res.* **2008**, *41*, 168-178.

21. Ho, H. A.; Doré, K.; Boissinot, M.; Bergeron, M. G.; Tanguay, R. M.; Boudreau, D.; Leclerc, M. Direct Molecular Detection of Nucleic Acids by Fluorescence Signal Amplification. *J. Am. Chem. Soc.* **2005**, *127*, 12673-12676

22. Nilsson, K. P. R.; Å slund, A.; Berg, I.; Nyström, S.; Konradsson, P.; Herland, A.; Inganäs, O.; Stabo-Eeg, F.; Lindgren, M.; Westermark, G. T.; Lannfelt, L.; Nilsson, L. N. G.; Hammarström, P. Imaging Distinct Conformational States of Amyloid-β Fibrils in Alzheimer's Disease Using Novel Luminescent Probes. *ACS Chem. Biol.* **2007**, *2*, 553-560.

23. Sigurdson, C. J.; Nilsson, K. P. R.; Hornemann, S.; Manco, G.; Polymenidou, M.; Schwarz, P.; Leclerc, M.; Hammarström, P.; Wüthrich, K.; Aguzzi, A. Prion strain discrimination using luminescent conjugated polymers. *Nat. Methods* **2007**, *4*, 1023-1030.

24. Abérem, M. B.; Najari, A.; Ho, H.-A.; Gravel, J.-F.; Nobert, P.; Boudreau, D.; Leclerc, M. Protein Detecting Arrays Based on Cationic Polythiophene–DNA-Aptamer Complexes. *Adv. Mater.* **2006**, *18*, 2703-2707.

25. Tang, Y.; He, F.; Yu, M.; Feng, F.; An, L.; Sun, H.; Wang, S.; Li, Y.; Zhu, D. A Reversible and Highly Selective Fluorescent Sensor for Mercury(II) Using Poly(thiophene)s that Contain Thymine Moieties. *Macromol. Rapid Commun.* **2006**, *27*, 389-392.

26. Li, C.; Numata, M.; Takeuchi, M.; Shinkai, S. A Sensitive Colorimetric and Fluorescent Probe Based on a Polythiophene Derivative for the Detection of ATP. *Angew. Chem. Int. Ed.* **2005**, *44*, 6371-6374.

27. Nilsson, K. P. R.; Inganäs, O. Chip and solution detection of DNA hybridization using a luminescent zwitterionic polythiophene derivative. *Nat. Mater.* **2003**, *2*, 419-424.

28. Béra-Abérem, M.; Ho, H.-A.; Leclerc, M. Functional polythiophenes as optical chemo- and biosensors. *Tetrahedron* **2004**, *60*, 11169-11173.

29. Wang, M.; Zou, S.; Guerin, G.; Shen, L.; Deng, K.; Jones, M.; Walker, G. C.; Scholes, G. D.; Winnik, M. A. A Water-Soluble pH-Responsive Molecular Brush of Poly(*N*,*N*-dimethylaminoethyl methacrylate) Grafted Polythiophene. *Macromolecules* **2008**, *41*, 6993-7002.

30. Hoeben, F. J. M.; Jonkheijm, P.; Meijer, E. W.; Schenning, A. P. H. J. About Supramolecular Assemblies of π-Conjugated Systems. *Chem. Rev.* **2005**, *105*, 1491-1546.

31. Beljonne, D.; Pourtois, G.; Silva, C.; Hennebicq, E.; Hertz, L. M.; Friend, R. H.; Scholes, G. D.; Setayesh, S.; Müllen, K.; Brédas, J. L. Interchain vs. intrachain energy transfer in acceptor-capped conjugated polymers. *Proc. Nat. Acad. Sci. USA* **2002**, *99*, 10982-10987.

32. Nguyen, T.-Q.; Wu, J.; Doan, V.; Schwartz, B. J.; Tolbert, S. H. Control of Energy Transfer in Oriented Conjugated Polymer-Mesoporous Silica Composites. *Science* **2000**, *288*, 652-656.

33. Wang, C. F.; White, J. D.; Lim, T. L.; Hsu, J. H.; Yang, S. C.; Fann, W. S.; Peng, K. Y.; Chen, S. A. Illumination of exciton migration in rodlike luminescent conjugated polymers by single-molecule spectroscopy. *Phys. Rev. B* **2003**, *67*, 035202.

34. Mano, J. F. Stimuli-Responsive Polymeric Systems for Biomedical Applications. *Adv. Eng. Mater.* **2008**, *10*, 515-527.

35. Lyon, L. A.; Meng, Z.; Singh, N.; Sorrell, C. D.; St. John, A. Thermoresponsive microgel-based materials. *Chem. Soc. Rev.* **2009**, *38*, 865-874.

36. Jeong, B.; Kim, S. W.; Bae, Y. H. Thermosensitive sol-gel reversible hydrogels. *Adv. Drug Delivery Rev.* **2002**, *54*, 37-51.

37. Schild, H. G. Poly(*N*-isopropylacrylamide): experiment, theory and application. *Prog. Polym. Sci.* **1992**, *17*, 163-249.

38. Uchiyama, S.; Matsumura, Y.; de Silva, A. P.; Iwai, K. Fluorescent Molecular Thermometers Based on Polymers Showing Temperature-Induced Phase Transitions and Labeled with Polarity-Responsive Benzofurazans. *Anal. Chem.* **2003**, *75*, 5926-5935.

39. Creshaw, B. R.; Kunzelman, J.; Sing, C. E.; Andler, C.; Weder, C. Threshold Temperature Sensors with Tunable Properties. *Macromol. Chem. Phys.* **2007**, *208*, 572-580.

40. Shiraishi, Y.; Miyamoto, R.; Hirai, T. A Hemicyanine-Conjugated Copolymer as a Highly Sensitive Fluorescent Thermometer. *Langmuir* **2008**, *24*, 4273-4279.

41. Balamurugan, S. S.; Bantchev, G. B.; Yang, Y.; McCarley, R. L. Highly Water-Soluble Thermally Responsive Poly(thiophene)-Based Brushes. *Angew. Chem. Int. Ed.* **2005**, *44*, 4872-4876.

42. Loewe, R. S.; Khersonsky, S. M.; McCullough, R. D. A Simple Method to Prepare Head-to-Tail Coupled, Regioregular Poly(3-alkylthiophenes) Using Grignard Metathesis. *Adv. Mater.* **1999**, *11*, 250-253.

43. Loewe, R. S.; Ewbank, P. C.; Liu, J.; Zhai, L.; McCullough, R. D. Regioregular, Head-to-Tail Coupled Poly(3-alkylthiophenes) Made Easy by the GRIM Method: Investigation of the Reaction and the Origin of Regioselectivity. *Macromolecules,* **2001**, *34*, 4324-4333.

44. Osaka, I.; McCullough, R. D. Advances in Molecular Design and Synthesis of Regioregular Polythiophenes. *Acc. Chem. Res.* **2008**, *41*, 1202-1214.

45. Jeffries-El, M.; McCullough, R. D. Regioregular polythiophenes. *In Handbook of Conducting Polymers,* 3rd ed.; Skotheim, T. A., Reynolds, J. R., Eds.; CRC Press: Boca Raton, FL, **2007**; Vol. 1, pp 9-1-9-49.

46. Jeffries-El, M.; Sauvé, G.; McCullough, R. D. Facile Synthesis of End-Functionalized Regioregular Poly(3-alkylthiophene)s via Modified Grignard Metathesis Reaction. *Macromolecules* **2005**, *38*, 10346-10352

47. Chen, T.-A.; Wu, X.; Rieke, R. D. Regiocontrolled Synthesis of Poly(3-alkylthiophenes) Mediated by Rieke Zinc: Their Characterization and Solid-state Properties. *J. Am. Chem. Soc.* **1995**, *117*, 233-244.

48. Chen, T.; Rieke, R. D. The first regioregular head-to-tail poly(3-hexylthiophene-2,5-diyl) and a regiorandom isopolymer: nickel versus palladium catalysis of 2(5)-bromo-5(2)-(bromozincio)-3-hexylthiophene polymerization. *J. Am. Chem. Soc.* **1992**, *114*, 10087-10088.

49. Mao, Y.; Wang, Y.; Lucht, B. L. Regiocontrolled synthesis of poly(3-alkylthiophene)s by Grignard metathesis. *J. Polym. Sci., Part A: Polym. Chem.* **2004**, *42*, 5538-5547.

50. Iovu, M. C.; Sheina, E. E.; Gil, R. R.; McCullough, R. D. Experimental Evidence for the Quasi-"Living" Nature of the Grignard Metathesis Method for the Synthesis of Regioregular Poly(3-alkylthiophenes). *Macromolecules* **2005**, *38*, 8649-8656.

51. Miyakoshi, R.; Yokoyama, A.; Yokozawa, T. Catalyst-Transfer Polycondensation. Mechanism of Ni-Catalyzed Chain-Growth Polymerization Leading to Well-Defined Poly(3-hexylthiophene). *J. Am. Chem. Soc.* **2005**, *127*, 17542-17547.

52. Costanzo, P. J.; Stokes, K. K. Synthesis and Characterization of Poly(methyl acrylate) Grafted from Poly(thiophene) to Form Solid-State Fluorescent Materials. *Macromolecules* **2002**, *35*, 6804-6810.

53. Coessens, V.; Pintauer, T.; Matyjaszewski, K. Functional polymers by atom transfer radical polymerization. *Prog. Polym. Sci.* **2001**, *26*, 337-377.

54. Pyun, J.; Kowalewski, T.; Matyjaszewski, K. Synthesis of Polymer Brushes Using Atom Transfer Radical Polymerization. *Macromol. Rapid Commun.* **2003**, *24*, 1043-1059.

55. Balamurugan, S.; Mendez, S.; Balamurugan, S. S.; O'Brien II, M. J.; López, G. P. Thermal Response of Poly(*N*-isopropylacrylamide) Brushes Probed by Surface Plasmon Resonance. *Langmuir* **2003**, *19*, 2545-2549.

56. McCullough, R. D.; Lowe, R. D. Enhanced electrical conductivity in regioselectively synthesized poly(3-alkylthiophenes) *J. Chem. Soc. Chem. Commun.* **1992**, 70-72.

57. Kiriy, N.; J€ahne, E.; Adler, H.-J.; Schneider, M.; Kiriy, A.;Gorodyska, G.; Minko, S.; Jehnichen, D.; Simon, P.; Fokin, A. A.; Stamm, M. One-Dimensional Aggregation of Regioregular Polyalkylthiophenes. *Nano Lett*. **2003**, *3*, 707–712.

58. Langeveld-Voss, B. M. W.; Janssen, R. A. J.; Christiaans, M. P. T.; Meskers, S. C. J.; Dekkers, H. P. J. M.; Meijer, E. W. Circular Dichroism and Circular Polarization of Photoluminescence of Highly Ordered Poly{3,4-di[(*S*)-2-methylbutoxy]thiophene. *J. Am. Chem. Soc*. **1996**, *118*, 4908–4909.

59. Zahn, S.; Swager, T. M. Three-Dimensional Electronic Delocalization in Chiral Conjugated Polymers. *Angew. Chem. Int. Ed*. **2002**, *41*, 4225–4230.

60. Brustolin, F.; Goldoni, F.; Meijer, E. W.; Sommerdijk, N. A. J. M. Highly Ordered Structures of Amphiphilic Polythiophenes in Aqueous Media. *Macromolecules* **2002**, *35*, 1054-1059

61. Garreau, S.; Leclerc, M.; Errien, N.; Louarn, G. Planar-to-Nonplanar Conformational Transition in Thermochromic Polythiophenes: A Spectroscopic Study. *Macromolecules* **2003**, *36*, 692-697.

62. Lévesque, I.; Leclerc, M. Ionochromic and Thermochromic Phenomena in a Regioregular Polythiophene Derivative Bearing Oligo(oxyethylene) Side Chains. *Chem. Mater.* **1996**, *8*, 2843-2849.

63. Faïd, K.; Fréchette, M.; Ranger, M.; Mazarolle, L.; Lévesque, I.; Leclerc, M.; Chen, T.-A.; Rieke, R. D. Chromic Phenomena in Regioregular and Nonregioregular Polythiophene Derivatives. *Chem. Mater.* **1995**, *7*, 1390-1396.

64. Kim, J.; Swager, T. M. Control of conformational and interpolymer effects in conjugated polymers. *Nature.* **2001**, *411*, 1030-1034.

65. Theander, M.; Inganas, O.;Mammo,W.; Olinga, T.; Svensson, M.; Andersson, M. R. Photophysics of Substituted Polythiophenes. *J. Phys. Chem. B* **1999**, *103*, 7771–7780.

66. Levitus, M.; Schmieder, K.; Ricks, H.; Shimizu, K. D.; Bunz, U. H. F.; Garcia-Garibay, M. A. Steps To Demarcate the Effects of Chromophore Aggregation and Planarization in Poly(phenyleneethynylene)s. 1. Rotationally Interrupted Conjugation in the Excited States of 1,4-Bis(phenylethynyl)benzene. *J. Am. Chem. Soc*. **2001**, *123*, 4259–4265.

67. Pinto, M. R.; Kristal, B. M.; Schanze, K. S. A Water-Soluble Poly(phenylene ethynylene) with Pendant Phosphonate Groups. Synthesis, Photophysics, and Layer-by-Layer Self-Assembled Films. *Langmuir*. **2003**, *19*, 6523–6533.

68. Dias, F. B.; Knaapila, M.; Monkman, A. P.; Burrows, H. D. Fast and Slow Time Regimes of Fluorescence Quenching in Conjugated Polyfluorene−Fluorenone Random Copolymers: The Role of Exciton Hopping and Dexter Transfer along the Polymer Backbone. *Macromolecules.* **2006**, *39*, 1598–1606.

69. Zhulina, E. B.; Borisov, O. V.; Pryamitsyn, V. A.; Birshtein, T. M. Coil-globule type transitions in polymers. 1. Collapse of layers of grafted polymer chains. *Macromolecules.* **1991**, *24*, 140-149

70. Baulin, V. A.; Zhulina, E. B.; Halperin, A. Self-consistent field theory of brushes of neutral water-soluble polymers. *J. Chem. Phys.* **2003**, *119*, 10977-10988.

71. Zhang, W.; Zhou, X.; Li, H.; Fang, Y.; Zhang, G. Conformational Transition of Tethered Poly(*N*-isopropylacrylamide) Chains in Coronas of Micelles and Vesicles. *Macromolecules.* **2005**, *38*, 909-914.

CHAPTER 3. DEVELOPMENT OF HIGHLY EFFICIENT EXTERNAL INITIATOR FOR LIVING CHAIN-GROWTH POLYMERIZATION AND ITS APPLICATIONS IN PREPARATION OF CONJUGATED POLYMERS

3.1. Introduction

Polythiophenes (PTs) have emerged as conjugated polymers of choice for electronic and optoelectronic applications (such as thin-film transistors, photovoltaic cells and polymer light-emitting diodes)[1-3] and chemo- and biosensing devices.[4] The pressing need to fine-tune PT properties to meet the requirements of certain applications necessitates search for efficient synthetic methods to prepare PTs with desired and controlled molecular composition. Following the discovery by McCullough[5,6] and Yokozawa[7-8] that Ni(II) catalyzed Kumada polymerization of 5-bromo-2-thienylmagnesium monomers occurs as a quasi-"living" chain-growth process, its mechanism was studied in detail,[9-10] and a number of approaches have been developed to prepare variously functionalized highly regioregular PT polymers and copolymers with narrow polydispersity and high molecular weight.[11-14] Among the recent achievements was introduction of the externally initiated polymerization (by Kiriy[15] and Luscombe[16]) where stable aryl-Ni(II) initiating complexes can be used to carry out chain-growth polymerization. This method made possible simple incorporation of various aryl groups at one terminus of the resulting PT chain, as well as preparation of surface-immobilized PT brushes.[18,20]

We were particularly interested in amphiphilic PT block copolymers which incorporate low energy gap units as such systems provide unique opportunities to study photoexcitation energy transfer, as well as may lead to novel supramolecular architectures with interesting properties.[21] Introducing such π-conjugated units (e.g. perylenedicarboximide (PDCI)) can significantly alter the photophysical properties of conjugated polymers thus allowing, for example, to fine-tune their luminescence color in light-emitting devices. Despite some

significant achievements, controlled preparation of PTs with high molecular weight has not been demonstrated at the time we initiated this research (and until now). The major problem yet to be solved is the inavailability of simple, robust and efficient catalytic initiators capable of effecting such polymerization.

Therefore, to develop an efficient catalytic system that can provide PTs with high molecular weight, narrow polydispersity and 100% regioregularity, we focused on the studies of nickel catalyst coordinated with pendent ligands because previously it has been reported that even a simple change of ligands from 1,2-bis(diphenylphospino)ethane (dppe) to 1,3-bis(diphenylphospino)propane (dppp) in conventional living polymerization results in significant mechanistic changes.[9,10] Also, utilization of bidentate dppp instead of monodentate PPh_3 ligands at the Ni(II) catalytic center is strictly required to obtain regioregular PTs with high molecular weight.[11-14]

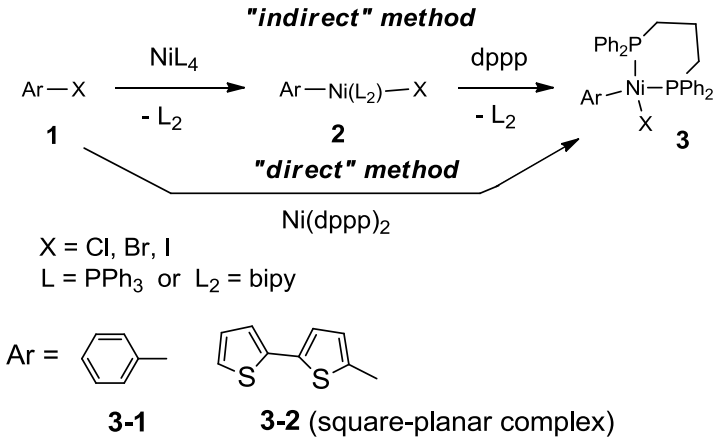

Scheme 3. 1 Preparation of External Catalytic Initiators **3**.

In the externally-initiated polymerization protocol previously developed by Kiriy[15] and Luscombe,[16] an external catalytic initiator was prepared in two steps, first by oxidative addition of Ar-X to the commercially available $Ni(PPh_3)$[7,8,16] or $Et_2Ni(bipy)$ [19] followed by

ligand exchange using dppp to obtain the resulting external initiator **3** with square-planar Ni(II) geometry (Scheme 3. 1, "indirect method").

This "indirect" method was relatively complex and could result in contamination of the final polymerization initiator **3** with the intermediate undesired ligands likely reducing the catalytic performance of the system. Therefore, we focused on a simple approach to prepare **3** through direct oxidative addition between Ar-X and $Ni(dppp)_2$. Because $Ni(dppp)_2$ is commercially unavailable and was previously deemed unreactive with Ar-X,[15] it has not received much attention. This Ni(0) compound can be easily prepared in a large scale following a simple literature procedure,[17] and can be stored for a long time without degradation. Furthermore, relative solubility of $Ni(dppp)_2$ in non-polar hydrocarbon solvents facilitates easy separation of the product **3** from the excess $Ni(dppp)_2$ by simply precipitating **3** with toluene-hexane mixture. Remarkably, generating **3** by this method turned out to furnish an unprecedentedly efficient catalytic system for Kumada "living" polymerization, which by all means surpassed the activity of the systems previously prepared by the "indirect" method **3**, allowing obtaining PT polymers and block copolymers with high molecular weight and narrow polydispersities in short reaction times. In this chapter, we present structural and reactivity studies on this unusual catalytic system.

3.2. Results and Discussion

3.2.1. Structural Studies on the Novel Catalytic System. To determine the scope of reactivity and limitations of $Ni(dppp)_2$-based catalytic systems, representative aryl halides such as chlorobenzene and 2-bromobithiophene were converted into the external Ni(II) initiator by reacting with excess $Ni(dppp)_2$ at room temperature for 24 h. ^{31}P NMR spectroscopy was used to monitor the conversion from the precursor molecules to the

external initiators in carefully kept anhydrous conditions. In an initial attempt, we tried to reproduce the literature two-step procedure by Luscombe starting from chlorobenzene.[16] Oxidative addition of chlorobenzene to $Ni(PPh_3)_4$ followed by ligand exchange using dppp was used to prepare the external initiator, **3-1** (Scheme 3. 1). The reaction was closely monitored by ^{31}P NMR. Concomitantly, we studied direct reaction between chlorobenzene and $Ni(dppp)_2$.

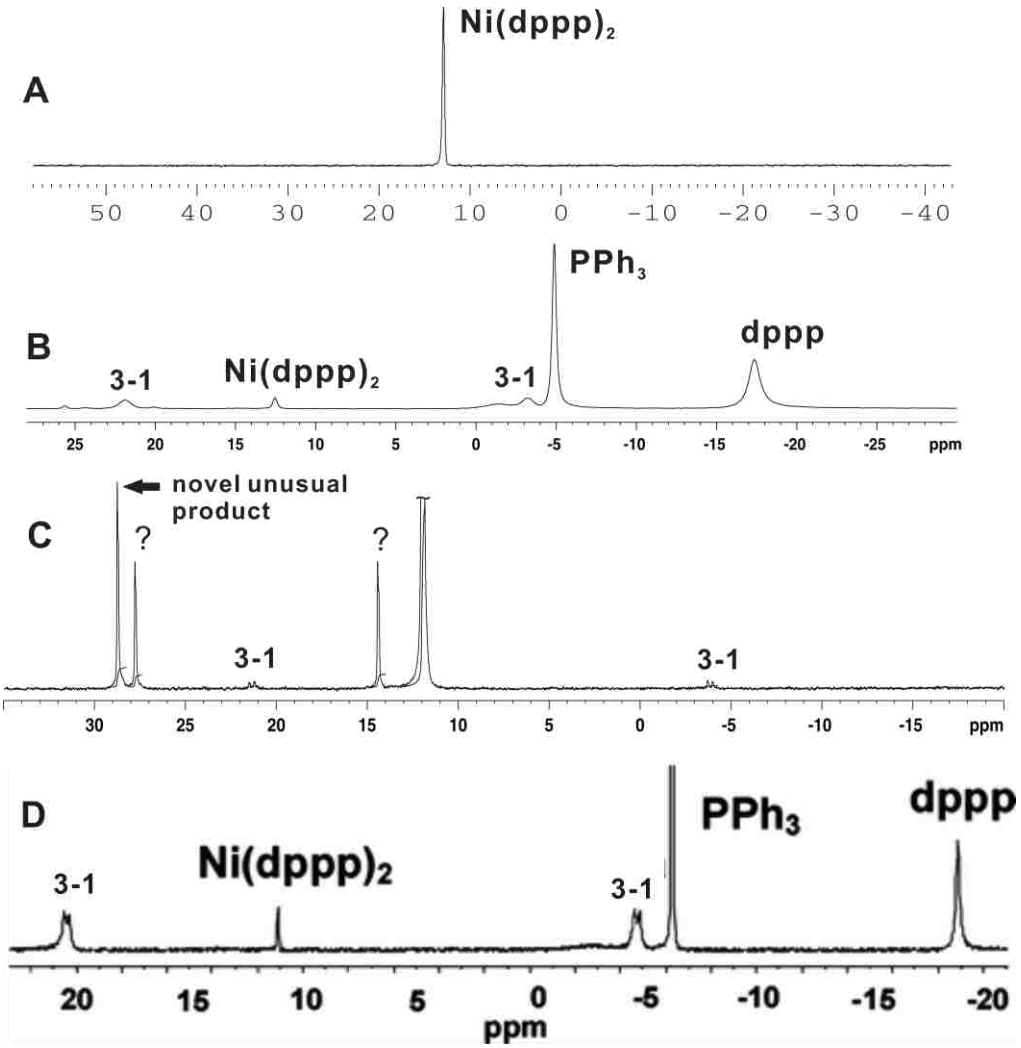

Figure 3. 1 ^{31}P NMR spectra of $Ni(dppp)_2$ in toluene (A) and the crude external initiator **3-1** (in chlorobenzene) prepared by the "indirect" method (B) and the "direct" method (C), as well as the crude ^{31}P NMR data by Luscombe et al.(D) (Reproduced in part with permission from ref 16).

Figure 3. 1 shows ^{31}P NMR data for Ni(dppp)$_2$ compound as well as for the external initiator, **3-1** prepared by the "indirect" literature method and the "direct" method. In good aggrement with the literature data, the "indirect" method resulted in appearance of a pair of ^{31}P signals associated with square-planar diamagnetic Ni(II) complex (Figure 3. 1B), similar to the previously observed result by Luscombe et al. (Figure 3. 1D).

In contrast, ^{31}P NMR data of the reaction mixture produced by the "direct" method showed a narrow singlet signal (28.8 ppm) and one pair of possibly interrelated signals (27.5 ppm and 14 ppm) as well (unfortunately, we have not been able to separate and identify the compound responsible for this pair of singlets). ^{31}P NMR signals of the square-planar diamagnetic Ni(II) complex **3-1** (two doublets) were also observed but as a minor admixture (Figure 3. 1C).

The formation in "direct" method of an unusual major product showing only one singlet in ^{31}P NMR spectrum was very surprising. Clearly, it was different from the expected square-planar complex **3-1** (which showed two doublets in its ^{31}P NMR spectrum due to inequivalency of two P atoms in such geometry). Furthermore, it was diamagnetic (which ruled out possibility of forming less usual but known tetrahedrally coordinated Ni(II) complex, as it would be paramagnetic[21,22]). The presence of only one singlet signal also indicated very high symmetry of this compound. Even more surprising was that the "direct" method unexpectedly gave this completely different result, as opposed to the expected squre-planar **3-1** product from the "indirect" method. Such unexpected results prompted us to further investigate the reaction to gain a better understanding of the structure and reactivity of this unusual product.

In further experiments, we selected 2-bromobithiophene as a model compound, as it

was more relevant for potential use in preparations of PTs, and could facilitate separation of the products. It could also allow to check the generality of the "direct" method. As before, we compared both "direct" and literature "indirect" method in preparation of the Ni(II) catalyst (Figure 3. 2).

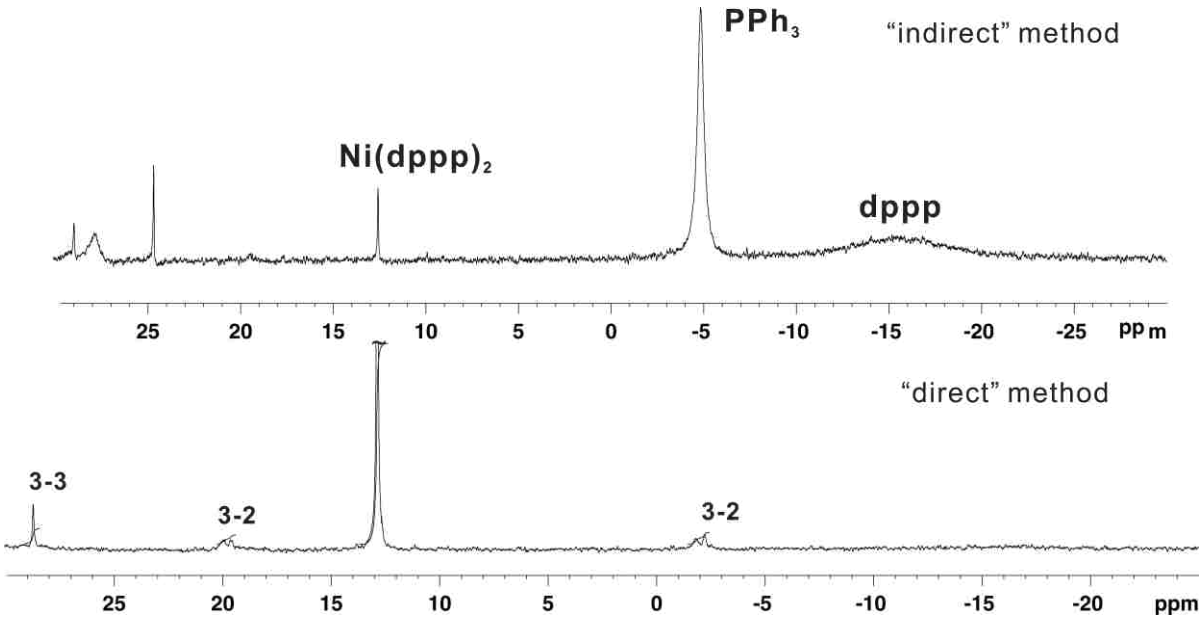

Figure 3. 2 ^{31}P NMR spectra of the crude reaction mixture (in toluene) prepared by the "indirect" method (top) and the "direct" method (bottom)

The obtained ^{31}P NMR data on crude reaction mixture in the case of the "direct" method showed a sharp singlet at 28.8 ppm (similar to the singlet obtained in the reaction of chlorobenzene with Ni(dppp)$_2$) and a pair of doublets (20 ppm and -2 ppm) certainly corresponding to the square-planar diamagnetic Ni(II) complex **3-2**. In contrast, the "indirect" method resulted in a mixture showing unidentifiable and hard to assign signals in the area between 25 and 29 ppm.

Although the "direct" method in the bromobithiophene case produced a mixture of at least two compounds (with both the square-planar Ni(II) complex **3-2** and a novel complex showing the singlet signal in its ^{31}P NMR spectrum being the major products), we were able

to separate and purify the latter compound by fractional precipitation (due to its lower solubility in toluene-hexane).

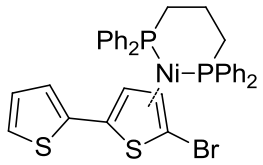

3-4 (a hypothetical π-complex)

In our initial analysis, we hypothesized that the unusual species obtained by "direct" reaction between Ar-X and $Ni(dppp)_2$ was a Ni(0) π-complex **3-4**. Although such complexes have been postulated as key intermediates in McCullough's and Yokozawa's mechanisms of living polymerization, they have never been experimentally observed. Assignment of **3-4** as a π-complex could explain its appearance as a singlet in ^{31}P NMR (due to roughly tetrahedral geometry of the Ni(0) center with the two equivalent P atoms owing to rapid rotation in the π-complex). Further evidence in favor of **3-4** being a Ni(0) π-complex could be obtained from variable temperature ^{31}P NMR experiments. Indeed, such a π-complex was expected to slow its molecular motion at lower temperatures, therefore breaking its high symmetry and showing some additional NMR splitting.

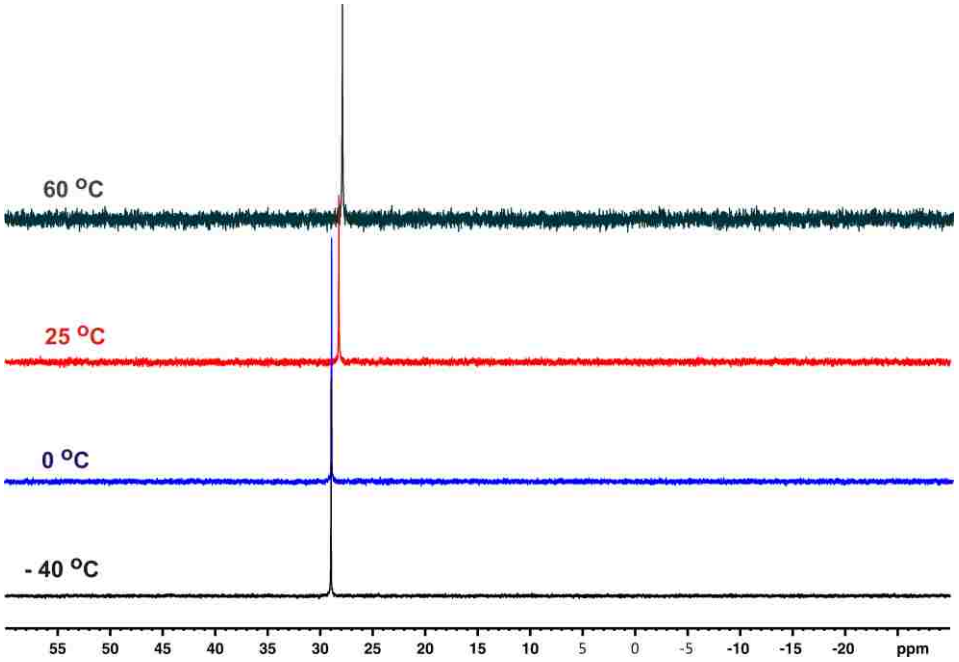

Figure 3. 3 Variable temperature ^{31}P NMR spectra of the bithiophene external initiator **3-3** (in toluene).

In reality, variable temperature ^{31}P NMR studies of the bithiophene external initiator showed that it was completely stable upon temperature variations in the range from 60^{o}C to -40^{o}C with a slight peak broadening at the higher temperature (Figure 3. 3). Clearly, we could not detect any additional splitting or substantial signal broadening even at -40^{o}C. Therefore, it was less likely for **3-3** to be an arene Ni(0) π-complex (which probably even would not survive at 60^{o}C). To determine if compound **3-3** was indeed a Ni(0) derivative, we carried out electrochemical studies. The studies were conducted in 3mM CH_3CN solution, using Pt working electrode and a standard 3-electrode set-up. For comparison purpose, we also studied $Ni(dppp)_2$ as an example of Ni(0) complex, and $Ni(dppp)Cl_2$ as a representative example of Ni(II) complex. The obtained cyclic voltammograms (CVs) of these compounds are shown in Figure 3. 4.

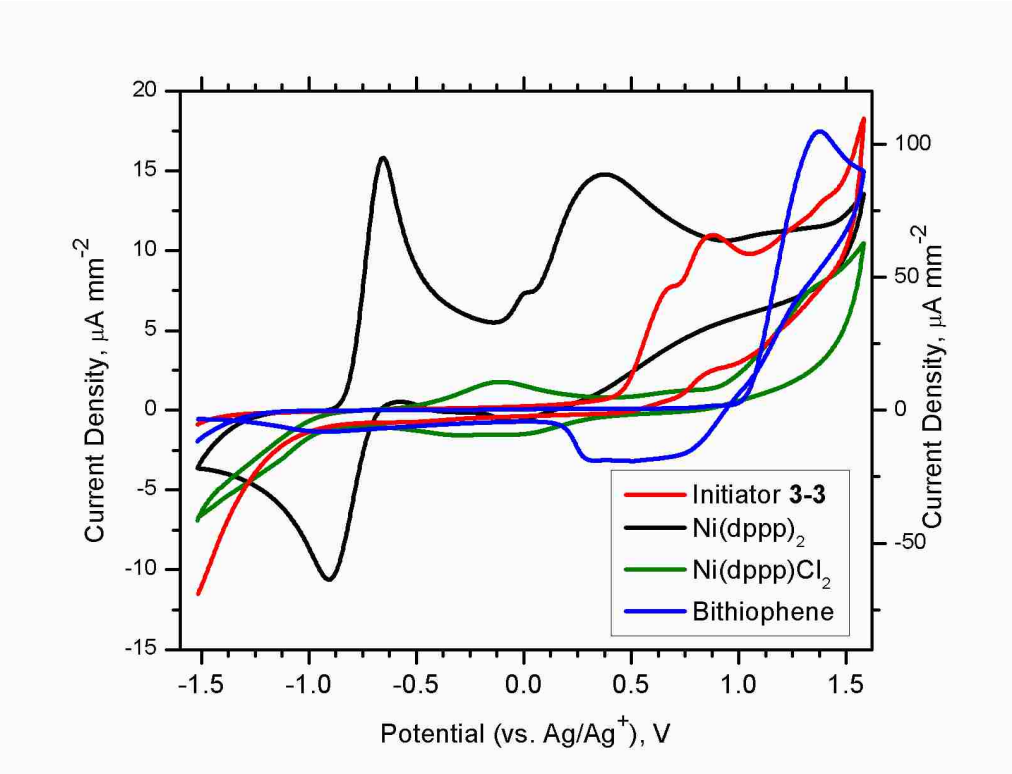

Figure 3. 4 Cyclic voltammograms of the bithiophene external nickel initiator **3-3**, and references compounds. Experiment conditions: 0.1M Bu_4NF_6 in CH_3CN, sweep rate 0.1V/s.

One could clearly see dramatic differences between the CVs of $Ni(dppp)_2$ and the compound **3-3**. $Ni(dppp)_2$ showed one reversible redox peak at $E_{1/2}$ –0.79 V (vs. Ag/Ag^+), likely corresponding to a Ni(0)/Ni(I) transition, and an irrerversible peak at E_p 0.57 V, likely due to a Ni(I)/Ni(II) oxidation. On the other hand, compound **3-3** did not show any peaks at lower potential where Ni(0)/Ni(I) was expected to be found. It showed an irreversible (or quasi-reversible) peak at E_p 0.88 V (vs. Ag/Ag^+), with a shoulder peak at at E_p 0.65 V (Figure 3. 4). The high potential of this peak can most likely rule out **3-3** as a Ni(0) π-complex. The oxidation peak potential was also not high enough to account for **3-3** as a Ni(III) complex (which, in addition, would be paramagnetic).

Therefore, we could safely assume that **3-3** was a Ni(II) complex. Indeed, there was some similiarity between CVs of **3-3** and $Ni(dppp)Cl_2$ (Figure 3. 4). If the compound **3-3** were to be a diamagnetic Ni(II) derivative, there could be only a few structural options. The most obvious one - square-planar complex **3-3** – can be completely ruled out. Furthermore, based on the only signal in its ^{31}P NMR spectrum, the compound **3-3** had to be of higher symmetry than **3-2** (but cannot be tetrahedral-coordinated as it then would be paramagnetic). The only structure that can satisfy these requirements is the square-pyramidal structure with two dppp ligands in a squre-planar arrangement, and with a bithiophene ligand in the axial position. Although such Ni(II) squre-pyramidal complexes are known,[24-26] they are not very common. A previously described complex most closely resembling **3-3** is compound **3-5** (Figure 3 .5).[27] Indeed, its ^{31}P NMR spectrum was described as a singlet at 23.3 ppm, which could not be resolved even upon cooling down to -90°C. An additional evidence in favor of the square-pyramidal structure for **3-3** came from analysis of its ^1H NMR spectrum (Appendix A-19~21). Although accurate integration of bithiophene signals was not possible

due to their low intensity and overlaps with the intense signals from PPh_3 groups, it seemed likely that there was 2:1 ratio of dppp to bithiophene groups, which satisfies the structure **3-3**.

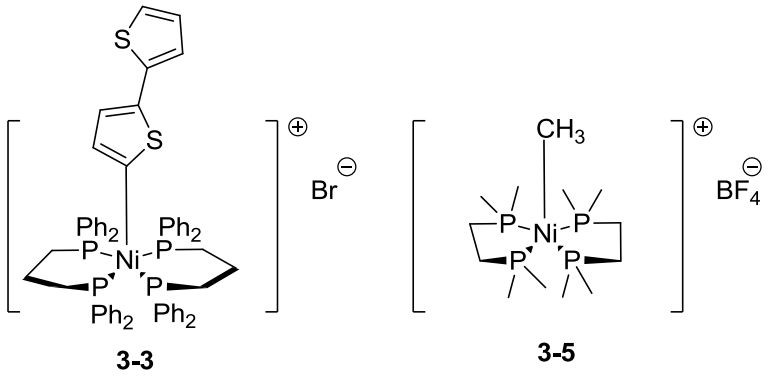

3-3 **3-5**

Figure 3. 5 Structure of square-pyramidal complex of the bithiophene nickel initiator the **3-3** and the known compound **3-5**.

Although complexes like **3-5** do not show very high stability, compound **3-3** did not show decomposition even upon heating to 60°C. Its extra stabilization could be related to electron-donating bithiophene ligand in the axial position, but further studies (including computational analysis) are required to decipher reasons for its particular stability. An extremely important question which naturally arises from the discussion above is why the square-pyramidal complex **3-3** could only be formed by the "direct" method (although together with the square-planar complex **3-2**), and was not found in the "indirect" method (where **3-2** was the only product). Furthermore, it is not obvious why **3-3** does not transform into **3-2**, even upon heating at 60°C. The most likely explanation should consider formation of both **3-2** and **3-3** as two independent parallel processes upon reaction of Ar-Hal with $Ni(dppp)_2$. Although **3-2** is likely to be thermodynamically more stable, there is a significant kinetic stabilization of **3-3** which hinders its conversion into **3-2**. This stabilization may come from the bidentate nature of the dppp ligand, and is not possible when monodentate ligand (e.g. PPh_3) is used. This can explain why structures similar to **3-3** have never been

observed in the "indirect" methods (where Ar-Hal reacts initially with $Ni(PPh_3)_4$ to form a square-planar complex Ar-$Ni(PPh_3)_2$-Hal). This explanation can serve only as an initial hypothesis, and more experimental and computational studies are necessary to prove it (obtaining X-ray crystal structure of **3-3** would be the best possible evidence, but unfortunately we have not been able so far to obtain a suitable quality single crystal).

3.2.2. 3-3 as External Catalytic Initiators of Chain-Growth Polymerization. With the availability of the unusual complex **3-3,** we attempted to use it as an external initiator of Kumada-type polycondensation of the Grignard monomer **3-6**, prepared *in situ* from the corresponding dibromide (Scheme 3. 2). To our surprise, the polymerization carried out at 35°C was very rapid and efficient – it was complete in less than 1h, and produced polymer **3-8** with high molecular weight and 100% regioregularity.

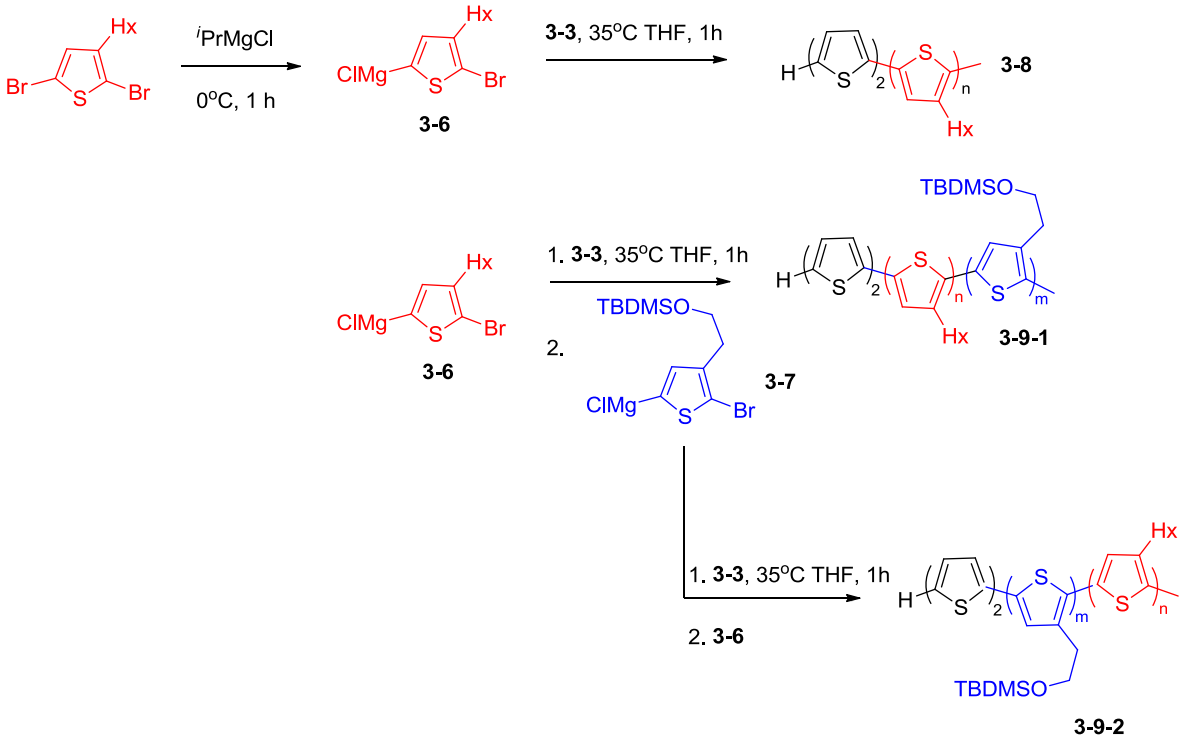

Scheme 3. 2 Homo poly-3-hexylthiophene (P3HT) and polythiophene diblock copolymers prepared by externally initiated chain-growth polymerization method.

Both the high reacitivity and the qualities of the resulting polymer completely surpassed our expectations: the complex **3-3** behaved as unprecedentedly efficient catalytic initiator. The higher reactivity of **3-3** could stem from the bithienyl ligand being in the axial position where it must have a higher nucleophilicity than the similar ligand in a square-planar complex (i.e. **3-2**). However, upon initiating polymerization reaction, it could easily be converted into a Ni(II) reaction center with square-planar geometry (as proposed in the mechanisms described in Chapter 1).

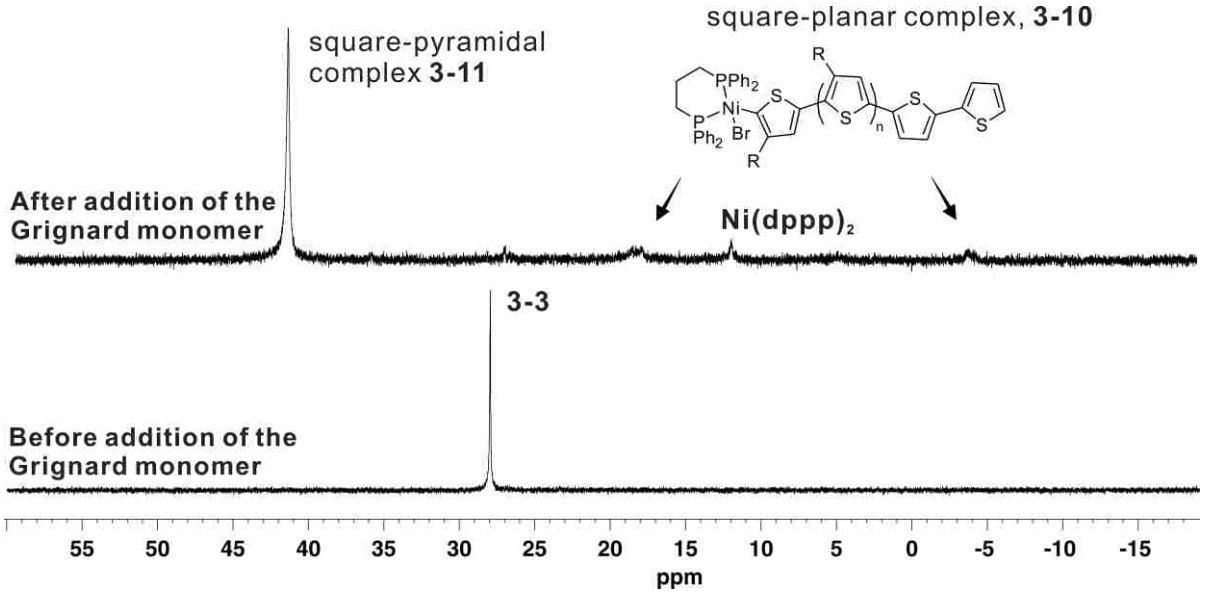

Figure 3. 6 ^{31}P NMR spectra of **3-3** (5mol% in THF at 35^{o}C) before and after addition of the Grignard monomer **3-6** solution.

In order to gain further mechanistic details on **3-3**-initiated Kumada polymerization process, a real-time ^{31}P NMR monitoring was performed during the process of polymerization. A relatively high concentration of **3-3** (5 mol%) was added to a freshly prepared Grignard monomer **3-6** solution to allow a chain-growth polymerization to start. As the experiment was carried out in an NMR tube, the ^{31}P NMR spectra could be acquired during polymerization. After addition of the Grignard monomer to a solution of **3-3** the

singlet at 27 ppm immediately disappeared, and a new broad singlet at 41.5 ppm was detected. In addition to this intense singlet, additional signals corresponding to $Ni(dppp)_2$ and a pair of signals from the square-planar Ni(II) were also evidenced (Figure 3. 6). The most striking observation was that the singlet at 41.5 ppm was very persistent – it stayed throughout the polymerization reaction, and still could be detected in 24h (albeit with diminished intensity) after starting the polymerization.

This result clearly demonstrated that the external initiator allows polymer chains to rapidly grow via Kumada catalyst-transfer polycondensation (KCTP)[12] pathway with repetitive transmetallation, reductive elimination and oxidative addition process until all the entire monomer is completely consumed. Considering the demonstrated stability of **3-3** towards conversion into **3-2,** it is unlikely that there is any equilibrium (or interconversion) between the square-planar **3-10** and square-pyramidal structures **3-11** of the active catalytic center during polymerization.

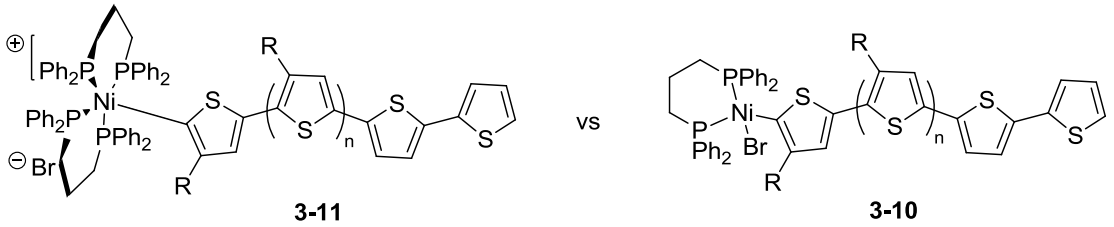

3-11 **3-10**

Figure 3. 7 Structures of squre-pyramidal reaction center **3-11** and square-planar reaction center **3-10**

It is possible that upon initiation of polymerization, it starts occurring through square-pyramidal active centers **3-11,** which correspond to the observed singlet at 41.5 ppm in ^{31}P NMR of the reaction mixture. As this center has elongated axial Ni-C bond with enhanced nucleophilicity of the carbon center, it also preserves the high polymerization activity (living character). The structural stability of the square-pyramidal Ni(II) center is maintained due to

the presence of two stabilizing dppp ligands. As the polymerization proceeds, some square-pyramidal centers could transform into square-planar centers **3-10,** as evidenced by the presence of the characteristic minor signals in ^{31}P NMR (Figure 3. 6). The square-planar active centers still can facilitate living chain-growth polymerization, but at a much slower rate (overall, this would result in some increase in polydispersity of the final polythiophene).

An essential information on the mechanism of Ni-catalyzed polymerization can be obtained from studies of the end group composition in polythiophenes by MALDI-TOF mass spectral analysis.[28] Upon end-group analysis of a series of polymers **3-8** obtained in 2-min intervals during **3-3** – initiated polymerization of the monomer **3-6**, we found presence of both H- and Br-terminated polymer chains, with an approximate ratio of Br to H termination 2 to 1 (Figure 3. 8).

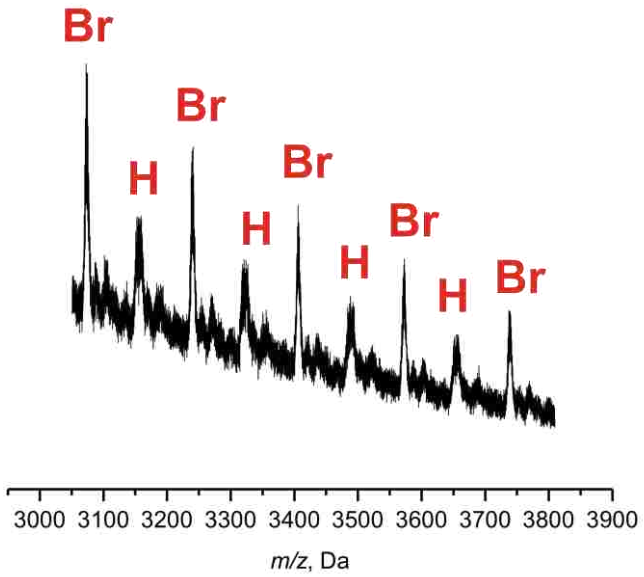

Figure 3. 8 End-group analysis of polythiophene **3-8** by MALDI-TOF (only low molecular weight region is shown).

Obviously, quenching of both active centers **3-10** and **3-11** with methanol would result in H-termination. On the other hand, Br-termination could occur if **3-11** existed in

equilibrium with a solvent cage stabilized contact pair of Br-terminated polythiophene/ $Ni(dppp)_2$ (indeed, $Ni(dppp)_2$) was also detected by ^{31}P NMR in the polymerization reaction mixture). The persistency of **3-11** after completion of the polymerization might indicate that **3-11** was indeed the "resting state" in the polymerization. In any case, considering complexity and controversial nature even of the "conventional" chain-growth polymerization mechanism, it was not surprising that our initial mechanistic findings on this novel catalytic initiator produced more questions than answers. What was clear is that the mechanistic features of this process are very complex, and will have to be studied in more detail in the course of future investigations.

To determine practical scope of this unusual catalytic system, a series of polymerization runs with 0.3 mol% of initiator **3-3** was carried out, and aliquots were taken every 2 min, quenched into methanol and analyzed by GPC and ^{1}H NMR spectroscopy.

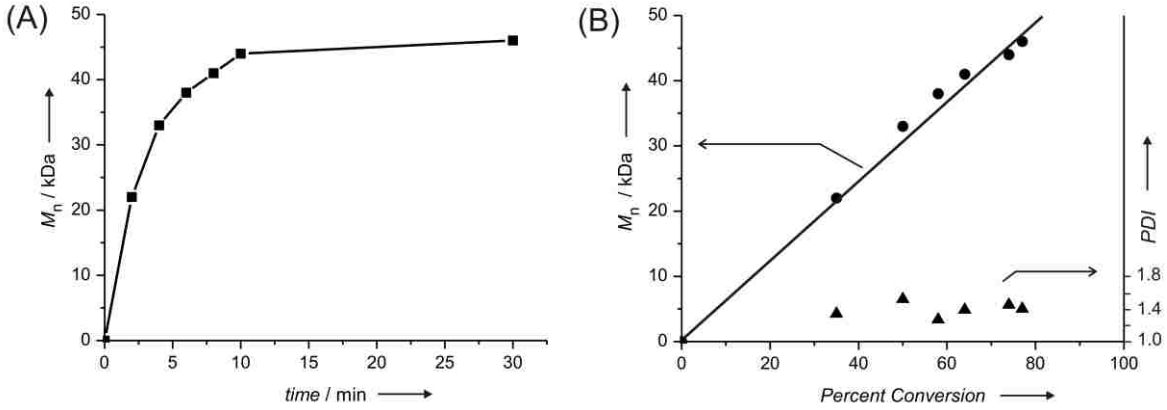

Figure 3. 9 Number average molecular weight (M_n) for **3-8** as a function of polymerization time (A); (M_n) and polydispersity (PDI) of P3HTs **3-8** as a function of monomer **3-6** conversion (B). Polymerization was carried out with 0.3 mol % of **3-3** as external initiator at 35 °C. M_n and PDI values were determined by GPC relative to polystyrene standards.

This controlled experiment revealed that the polymerization to form **3-8** was a true chain-growth "living" process. Indeed, the polymerization was very rapid and efficient: it

was practically complete in 10 min (Figure 3.9A). The linear dependence between M_n and percent conversion, along with narrow PDI and near 100% regioregularity, undoubtedly pointed to the "living" chain-growth polymerization mechanism (Figure 3. 9B). We did not find any evidence of reactive center transfer to another chain, and the only factor limiting the polymer molecular weight was the solubility of the polymer at the ambient conditions used for polymerization.

Test polymerization performed with 0.1mol% of the initiator **3-3** with Grignard monomer for 1 h at 35^{o}C followed by precipitating the crude polymer into methanol, and subsequent Soxhlet extraction with methanol, hexane, and chloroform afforded P3HT **3-8** with number average molecular weight (M_n) 48 kDa and polydispersity (PDI) 1.35 (by GPC) (Table 3. 1). One should notice slightly increase polydispersity of the polymer **3-8** which may be at the higher end of the results expected in living polymerization. The higher PDI values could indeed be a consequence of two simultaneously occurring polymerizations initiated by **3-10** and **3-11** active centers as discussed above.

Table 3. 1 Characterization of polymers **3-8** and **3-9.**

Polymers	mol% [a]	M_n, Da [b]	PDI [b]	% rr [c]
3-8	0.3	48,000	1.35	100
3-9-1[d]	0.4	70,000	1.27	100
3-9-2[d]	0.4	80,000	1.47	100

[a] Amount of **3-3** used in polymerization; [b] Determined by GPC relative to polystyrene standards; [c] Percent regioregularity (by ^{1}H NMR); [d] Ratio of poly(**3-6**) to poly(**3-7**) blocks 3.5:1 for **3-9-1**.and 1.5:1 for **3-9-2**.

The "living" nature of the highly efficient polymerization initiated by **3-3** allowed simple preparation of polythiophene diblock copolymers with high molecular weight in very short reaction times. Thus, polymerization with a sequential addition of two different Grignard monomers (e.g **3-6** and **3-7**) resulted in the polythiophene diblock copolymers **3-9-**

1 and **3-9-2** (Scheme 3.2) with very high molecular weight up to 80 kDa, narrow polydispersityies (PDI) and 100% regioregularity (Table 3. 1).

As control diblock copolymers, **3-9-1** and **3-9-2** were further functionalized with PNIPAm side chains to afford amphiphilic temperature-responsive block copolymers which will be discussed in detail in the next chapter. Furthermore, the choice of possible aryl groups is very broad, and in the next chapter we will demonstrate how this could be used to prepare complex block copolymer architectures.

3.3. Conclusions

We have developed a simple "direct" method to prepare square-pyramidal Ni(II) complex which can act as an external catalytic initiators for the unprecedentedly efficient "living" chain-growth Kumada polymerization. It can be used to prepare PT polymers and block copolymers incorporating various functional groups.

3.4. References

1. Ong, B. S.; Wu, Y.; Li, Y.; Liu, P.; Pan, H. Thiophene Polymer Semiconductors for Organic Thin-Film Transistors. *Chem. Eur. J.* **2008**, *14*, 4766-4778.

2. Cheng, Y.-J.; Yang, S.-H.; Hsu, C.-S. Synthesis of Conjugated Polymers for Organic Solar Cell Applications. *Chem. Rev.* **2009**, *109*, 5868-5923.

3. Perepichka, I. F.; Perepichka, D. F.; Meng, H.; Wudl, F. Light-Emitting Polythiophenes. *Adv. Mater.* **2005**, *17*, 2281-2305.

4. Thomas III, S. W.; Joly, G. D.; Swager, T. M. Chemical Sensors Based on Amplifying Fluorescent Conjugated Polymers. *Chem. Rev.* **2007**, *107*, 1339-1386.

5. Sheina, E. E.; Liu, J.; Iovu, M. C.; Laird, D. W.; McCullough, R. D. Chain Growth Mechanism for Regioregular Nickel-Initiated Cross-Coupling Polymerizations. *Macromolecules* **2004**, *37*, 3526-3528.

6. Iovu, M. C.; Sheina, E. E.; Gil, R. R.; McCullough, R. D. Experimental Evidence for the Quasi-"Living" Nature of the Grignard Metathesis Method for the Synthesis of Regioregular Poly(3-alkylthiophenes). *Macromolecules* **2005**, *38*, 8649-8656.

7. Miyakoshi, R.; Yokoyama, A.; Yokozawa, T. Catalyst-Transfer Polycondensation. Mechanism of Ni-Catalyzed Chain-Growth Polymerization Leading to Well-Defined Poly(3-hexylthiophene). *J. Am. Chem. Soc.* **2005**, *127*, 17542-17547.

8. Yokoyama, A.; Yokozawa, T. Converting Step-Growth to Chain-Growth Condensation Polymerization. *Macromolecules* **2007**, *40*, 4093-4101.

9. Lanni, E. L.; McNeil, A. Mechanistic Studies on Ni(dppe)Cl_2-Catalyzed Chain-Growth Polymerizations: Evidence for Rate-Determining Reductive Elimination. J. *J. Am. Chem. Soc.* **2009**, *131*, 16573-16579.

10. Lanni, E. L.; McNeil, A. J. Evidence for Ligand-Dependent Mechanistic Changes in Nickel-Catalyzed Chain-Growth Polymerizations. *Macromolecules* **2010**, *43*, 8039-8044.

11. Wu, P.-T.; Ren, G.; Li, C.; Mezzenga, R.; Jenekhe, S. A. Crystalline Diblock Conjugated Copolymers: Synthesis, Self-Assembly, and Microphase Separation of Poly(3-butylthiophene)-*b*-poly(3-octylthiophene). *Macromolecules* **2009**, *42*, 2317-2320

12. Beryozkina, T.; Senkovskyy, V.; Kaul, E.; Kiriy, A. Kumada Catalyst-Transfer Polycondensation of Thiophene-Based Oligomers: Robustness of a Chain-Growth Mechanism. *Macromolecules* **2008**, *41*, 7817-7823.

13. Ohshimizu, K.; Ueda, M. Well-Controlled Synthesis of Block Copolythiophenes. *Macromolecules* **2008**, *41*, 5289-5294.

14. Ouhib, F.; Khoukh, A.; Ledeuil, J.-B.; Martinez, H.; Desbrières, J.; Dagron-Lartigau. Diblock and Random Donor/Acceptor "Double Cable" Polythiophene Copolymers *via* the GRIM Method. *Macromolecules* **2008**, *41*, 9736-9743.

15. Senkovskyy, V.; Khanduyeva, N.; Komber, H.; Oertel, U.; Stamm, M.; Kuckling, D.; Kiriy, A. Conductive Polymer Brushes of Regioregular Head-to-Tail Poly(3-alkylthiophenes) via Catalyst-Transfer Surface-Initiated Polycondensation. *J. Am. Chem. Soc.* **2007**, *129*, 6626-6632.

16. Bronstein, H. A.; Luscombe, C. K. Externally Initiated Regioregular P3HT with Controlled Molecular Weight and Narrow Polydispersity. *J. Am. Chem. Soc.* **2009**, *131*, 12894-12895.

17. Corain, B.; Bressan, M.; Rigo, P. The behavior of nickel(0) diphosphine complexes towards unsaturated organic compounds. *J. Organomet. Chem.* **1971**, *28*, 133-136.

18. Khanduyeva, N.; Senkovskyy, V.; Beryozkina, T.; Horecha, M.; Stamm, M.; Uhrich, C.; Riede, M.; Leo, K.; Kiriy, A. Surface Engineering Using Kumada Catalyst-Transfer Polycondensation (KCTP): Preparation and Structuring of Poly(3-

hexylthiophene)-Based Graft Copolymer Brushes. *J. Am. Chem. Soc.* **2009**, *131*, 153-161.

19. Senkovskyy, V.; Tkachov, R.; Beryozkina, T.; Komber, H.; Oertel, U.; Horecha, M.; Bocharova, V.; Stamm, M.; Gevorgyan, S.; Krebs, F. C.; Kiriy, A. . "Hairy" Poly(3-hexylthiophene) Particles Prepared via Surface-Initiated Kumada Catalyst-Transfer Polycondensation. *J. Am. Chem. Soc.* **2009**, *131*, 16445-16453.

20. Sontag, S. K.; Marshall, N.; Locklin, J. Formation of conjugated polymer brushes by surface-initiated catalyst-transfer polycondensation. *Chem. Commun.* **2009**, 3354-3356.

21. Guan, Z.; Marshall, W. J. Synthesis of New Phosphine Imine Ligands and Their Effects on the Thermal Stability of Late-Transition-Metal Olefin Polymerization Catalysts. *Organometallics*, **2002**, *21*, 3580-3586.

22. Flapper, J.; Kooijman, H.; Lutz, M.; Spek, A. L.; Leeuwen, P. W. N. M.; Elsevier, C. J.; Kamer, P. C. J. Nickel and Palladium Complexes of New Pyridine-Phosphine Ligands and Their Use in Ethene Oligomerization. *Organometallics*, **2009**, *28*, 3272-3281.

23. Hoeben, F. J. M.; Jonkheijm, P.; Meijer, E. W.; Schenning, A. P. H. J. About Supramolecular Assemblies of π-Conjugated Systems. *Chem. Rev.* **2005**, *105*, 1491-1546.

24. Kohl, S. W.; Heinemann, F. W.; Hummert, M.; Weβhoff, H.; Grohmann, A. Tetra- and Triphosphane Pyridine Podands and Their Cobalt(II) and Nickel(II) Complexes. *Eur. J. Inorg. Chem.* **2006**, 3901-3910.

25. Curtis, C. J.; Miedaner, A.; Ellis, W. W.; Dubois, D. L. Measurement of the Hydride Donor Abilities of $[HM(diphosphine)_2]^+$ Complexes (M = Ni, Pt) by Heterolytic Activation of Hydrogen. *J. Am. Chem. Soc*. **2002**, *124*, 1918-1925.

26. DeDonno, T. A.; Rosen, W. Studies of a fifteen-membered tetraphosphorus macrocyclic ligand. *Inorg. Chem*. **1978**, *17*, 3714-3716.

27. Bochmann, M.; Hawkins, I.; Hursthouse, M. B.; Short, R. L. Synthesis of some Cationic 16- and 18-Electron Nickel Alkyl Phosphine Complexes containing Bidentate Ligands: Ligand-dependent Square-Planar, Trigonal-bipyramidal, and Square-pyramidal Co-ordination Geometries, their Reactions with CO and Alkynes, and the Crystal Structure of $[Ni(CH_2SiMe_3)(PMe_3)_3]BF_4$. *J. Chem. Soc. Dalton. Trans*. *1990*, 1213-1210.

28. Liu, J.; Loewe, R. S.; McCullough, R. D. Employing MALDI-MS on Poly(alkylthiophenes): Analysis of Molecular Weights, Molecular Weight Distributions, End-Group Structures, and End-Group Modifications. *Macromolecules* **1999**, *32*, 5777-5785.

CHAPTER 4. SUPRAMOLECULAR ORGANIZATION IN STIMULI- RESPONSIVE AMPHIPHILIC FLUORESCENT POLYTHIOPHENE BLOCK COPOLYMERS

4.1. Introduction

To design active materials for organic electronic devices such as photovoltaic materials based on π-conjugated polymers, deep understanding and ability to control the supramolecular organization of the individual π-conjugated molecules at the nanoscale is one of the most important challenges yet to be solved.[1]

Such distinct supramolecular organization assemblies in the solid state are often controlled by pre-organization in solution. Therefore, supramolecular organization process of the conjugated polymers in solution by self-assembly is an important initial step in developing rationally designed solid-film organic electronic materials, and in predicting and modifying their photophysical properties in solid state.

As one of the most important representative groups of conducting polymers, polythiophenes (PTs) have emerged as materials which are central for a wide variety of applications such as light-emitting diodes,[2] thin film transistors,[3,4] chemical sensory devices[5-7] and bulk heterojunction (BHJ) photovoltaic solar cells.[8] PTs exhibit complex optical and transport properties that are highly dependent on their nanoscale morphology which, in turn, is highly sensitive to external stimuli and backbone defects as well as minor variations in the polymer backbone conformation.

Extensive research efforts toward rational control over complex photophysical properties of polythiophenes and their block copolymers have been devoted in the recent years.[9-19] One of the most common ways to the physical and electronic properties of the PTs or even to prepare water-soluble polythiophene derivatives[30,31] is functionalization of

polythiophene backbone with various organic functional groups[20-25] or modified terminal alkyl pendant groups.[26-29]

Most noticeably, the intensive research efforts by McCullough et al. in the area of the synthesis of highly regioregular P3ATs opened new possibilities toward the facile preparation of termini-functionalized regioregular polythiophenes[32,33] that can be further integrated into even more complex polymeric architectures.[34-39] Although numerous synthetic approaches have been reported, recent milestone developments by Kiriy et al.[40] and Luscombe et al.[41] regarding externally initiated polymerization enabled conjugated polythiophene chains to incorporate a single initiating molecule, giving opportunity not only to incorporate various aryl groups at one terminus of the resulting PT chain, but to prepare surface-immobilized polymer brushes.

While searching for a versatile synthetic approach to build up complex amphiphilic conjugated polymer architectures, we developed a highly efficient catalytic system for externally initiated polymerization that enables preparation of complex polymeric structures of the desired conjugated polymer materials with an unprecedented degree of control. This catalytic system can yield not only polythiophene materials with exceptionally high molecular weight, 100% regioregularities and narrow polydispersities but also polythiophene block copolymer architectures[30] as well as surface-immobilized polymer brushes.[42]

Our main goal was to prepare stimuli-responsive amphiphilic polythiophenes which incorporate a fluorescent low energy gap unit. We hypothesized that such systems would exhibit dual-band fluorescent emission, which can be ratiometrically and reversibly controlled by applying external stimuli. Such an extended synthetic approach to build up the

amphiphilic fluorescent stimuli-responsive polythiophene block copolymers began with the selection of a suitable low-energy gap unit.

We chose the PDCI (perylenedicarboximide) unit as a single acceptor to incorporate into polythiophenes, due to its thermal stability, high fluorescent efficiency, and good match with polythiophene spectral properties.[43-45] By employing our novel highly efficient catalytic system (Chapter 3), we were able to prepare a series of amphiphilic polythiophene block copolymers incorporating a low energy gap PDCI unit and also demonstrated an efficient control of supramolecular organization that can alter spectroscopic responses by external stimuli such as temperature (both in solution and in solid state) and solvent polarity. Synthesized polythiophene block copolymers were found to show well-defined supramolecular architectures which could be assembled in a highly controlled manner.

Specifically, ratiometric fluorescent emission intensity change both in solution and in solid state exhibited clear and reversible thermochromic responses resulted from temperature-induced changes in supramolecular organization which could alter the extent of efficient energy migration towards a low energy gap unit. The polymers also demonstrated pronounced solvatochromic responses showing different behavior in a “non-selective” solvent relative to a “selective” solvent. A schematic cartoon showing the proposed solvent-controlled supramolecular organization is given in Figure 4. 1.

Such supramolecular organization can be readily controlled by altering the solvent composition or by applying other external stimuli. Such solvatochromic reorganization was completely reversible, demonstrating that the strategy can be used to control the photoluminescence properties of conjugated polymers without synthesizing entirely different polymer structures. In order to gain a better understanding of this supramolecular

organization in amphiphilic block copolymer architectures, further characterization of polymers by differential scanning calorimetry (DSC), both in solution and solid state, diffusion NMR experiments and AFM were carried out.

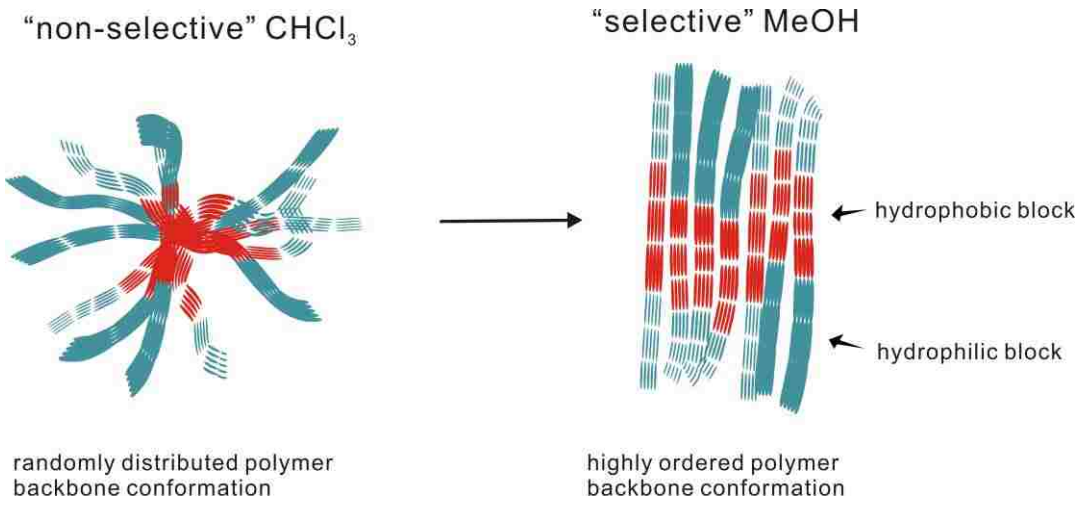

Figure 4. 1 Schematic illustration of supramolecular organization in amphiphilic polythiophene block copolymer **4-3-2** ("non-selective" chloroform and "selective" methanol).

In addition to solvent-controlled reorganization, we decided to use temperature as an additional external stimulus. In Chapter 2, we demonstrated that temperature can be used to effectively control conformation and conjugation length in fluorescent polythiophenes. Therefore, we decided to select poly(*N*-isopropylacrylamide) (PNIPAm)-functionalized polythiophene block as a hydrophilic segment, which not only renders the high water solubility for the polymers but adds the unique temperature-responsive properties to conjugated polymers. Simple conformational twisting of the conjugated backbone due to temperature-dependent phase transition in grafted PNIPAm side chains could modulate the overall change of electronic properties in the entire conjugated polymer system. Thus, with a simple variation of grafted PNIPAm brushes, a reversible and efficient control of the overall block copolymer supramolecular organization can be achieved.

4.2. Results and Discussion

4.2.1. Materials Synthesis. Synthesis of PDCI-incorporating polythiophene block copolymers was carried out using our new strategy described in Chapter 3. Indeed, our ability to successfully use this approach to prepare such copolymers acts as an excellent proof of the efficiency and generality of this strategy. The required diiodo-PDCI precursor **4-S1** was prepared in a few steps starting from commercially available bis-anhydride **4-PDCI1** (Scheme 4. 1). Our attempts to convert the diiodo-PDCI precursor **4-S1** into the corresponding bis-nickel initiator following the procedure described in Chapter 3, produced only the mono-nickel initiator **4-S2**. The assignment of **4-S2** as containing only one active Ni center was made by studying its ^{1}H NMR spectrum, as well as MALDI-TOF end-group analysis of the product of polymerization of the Grignard monomer **3-6** initiated by **4-S2**. Purification of **4-S2** was carried out by fractional reprecipitation from toluene-hexane mixture, and afforded **4-S2** as a dark-purple solid material relatively pure by ^{1}H and ^{31}P NMR (Figure 4. 2 and A-29).

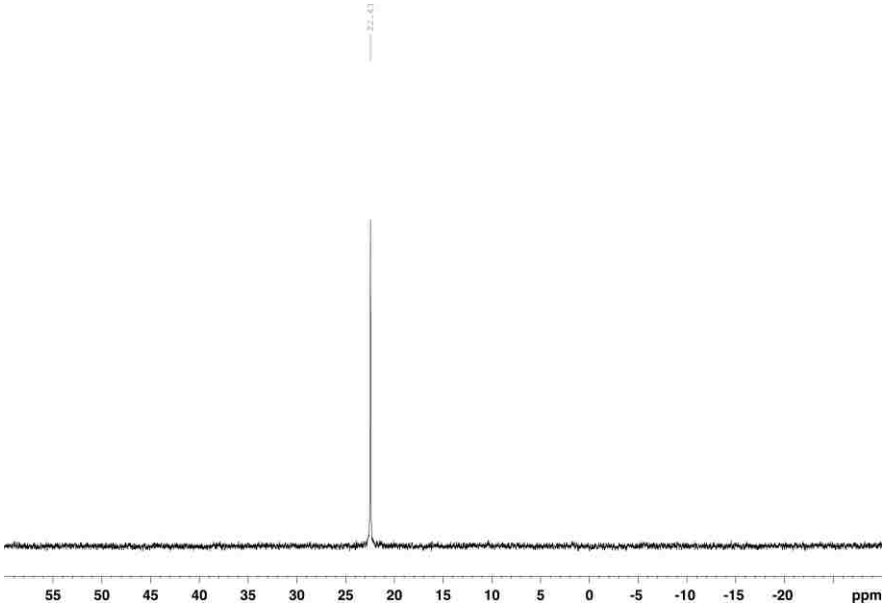

Figure 4. 2 ^{31}P NMR spectrum of the nickel PDCI external initiator **4-S2** (in THF)

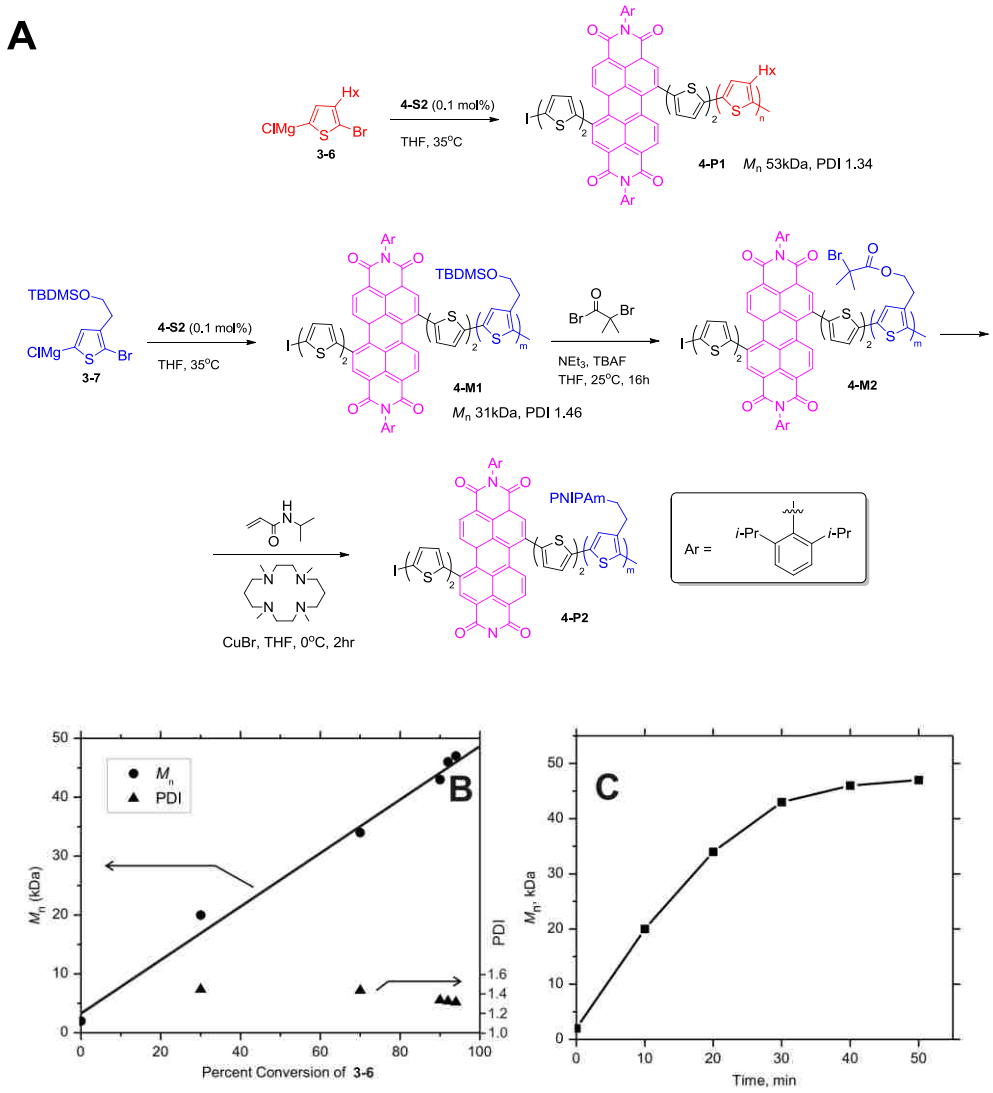

Figure 4. 3 Synthesis of PDCI-incorporating polythiophenes **4-P1** and **4-P2** (A); Number average molecular weight (M_n) and polydispersity (PDI) of **4-P1** as a function of monomer **3-6** conversion (B); (M_n) for **4-P1** as a function of polymerization time (C). Polymerization was carried out with 0.1 mol % of **4-S2** as external initiator at 35 °C. M_n and PDI values were determined by GPC relative to polystyrene standards.

Indeed, similar to the bithiophene catalytic initiator **3-3**, initiator **4-S2** exhibited ^{31}P NMR showing one singlet at 22.4 ppm (Figure 4. 2). Its ^{1}H NMR spectrum was consistent with the structure with one square-pyramidal Ni active center. Similar to the initiator **3-3**, the PDCI initiator **4-S2** was very efficient in carrying out living chain-growth polymerization of the Grignard monomer **3-6** (Figure 4. 3). Linear dependence of molecular weight M_n vs

percent conversion along with other attributes of living polymerization (near 100% regioregularity and narrow PDI) undoubtedly pointed to the same mechanism as discussed in Chapter 3 for the initiator **3-3**.

In order to prove incorporation of the PDCI unit in the polythiophene backbone, a relatively low molecular weight polymer to make possible accurate integration of the PDCI unit signals in ^{1}H NMR spectrum was prepared. The polymerization was carried out by the same protocol but was stopped (by pouring the crude reaction mixture into methanol) in only 10 min after starting the polymerization.

Remarkably, the obtained polymer showed M_n 24 kDa (by GPC) even in such a short polymerization time. After purification with preparative GPC to obtain only the narrow fraction corresponding to the polymer, ^{1}H NMR of a relatively concentrated polymer solution was acquired. Careful integration of the PDCI signals in the ^{1}H NMR spectrum resulted in M_n ~19 kDa (degree of polymerization 111) which agreed well with the M_n obtained by GPC (24kDa), therefore confirming the complete incorporation of the low energy gap PDCI unit into the conjugated chain (Figure 4. 4).

After we demonstrated possibility to use **4-S2** as an external catalytic initiator, we proceeded to prepare a series of PNIPAm-functionalized block copolymers **4-3-1**~**4-3-4**. This has been accomplished by allowing the initiator **4-S2** to react with one Grignard monomer (e.g. **3-6**) until completion of the polymerization followed by addition of the second Grignard monomer (**3-7**) and allowing enough time for the polymerization to form block copolymer **4-1-2** (Scheme 4. 1).

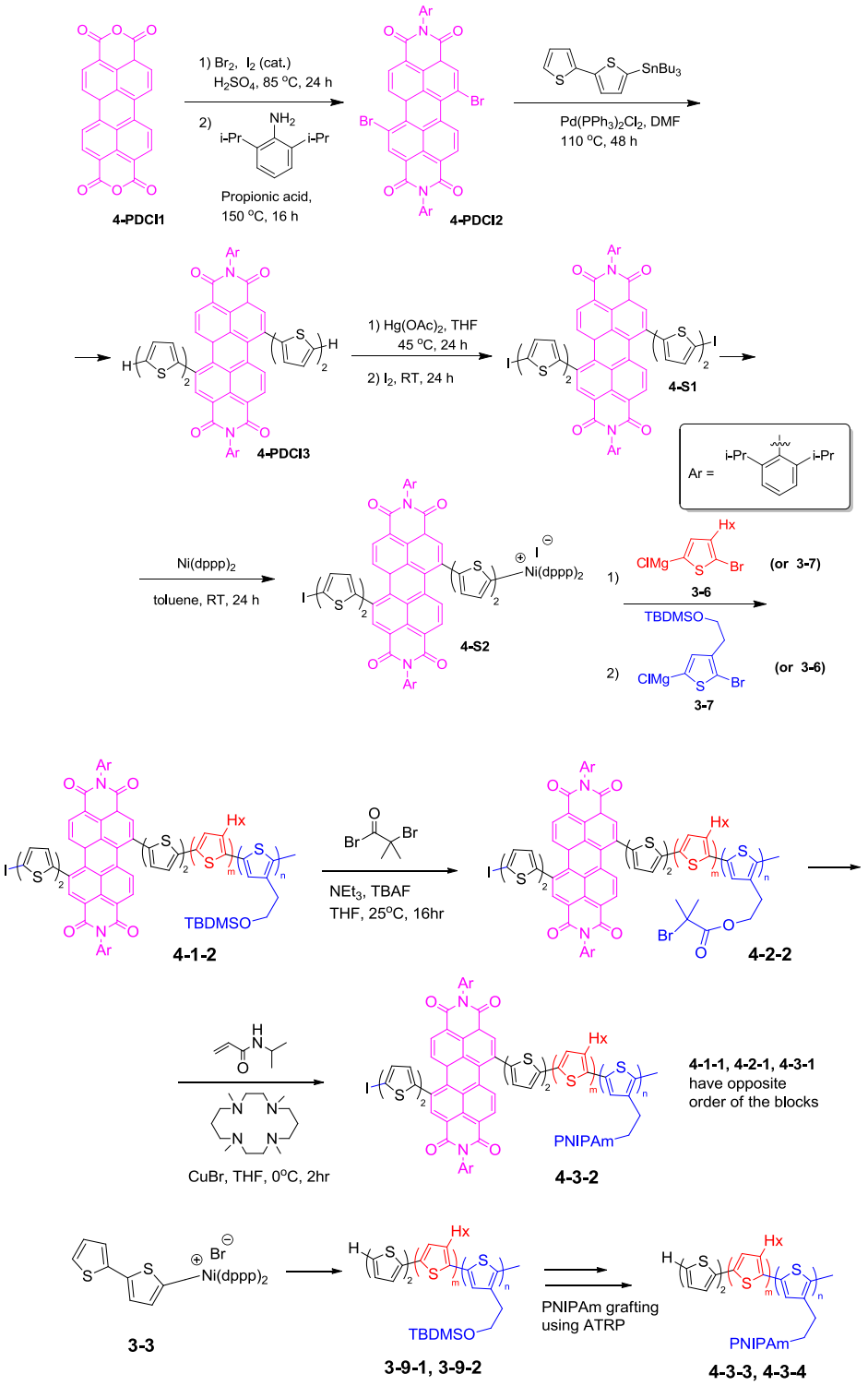

Scheme 4. 1 Synthesis of the external initiator (**4-S2**), precursor polymers (**4-1-1~4-1-4**) and post polymerization to graft poly (*N*-isopropylacrylamide) (PNIPAm) chains

The second block copolymer **4-1-1** was prepared following the same protocol but with reversed order of the Grignard monomers addition. For comparison purposes, two block copolymers **4-1-3** and **4-1-4** with different ratio of hydrophobic to hydrophilic blocks (to reflect that of **4-1-1** and **4-1-2**) were prepared using bithiophene external initiator **3-3** as described in Chapter 3. All four block copolymers were purified via Soxhlet extraction and characterized by ^{1}H NMR and GPC. Grafting the PNIPAm side chains to hydrophilic blocks was accomplished using the protocol developed for polymers described in Chapter 2.

The structures of both PDCI-incorporating block copolymers **4-3-1** and **4-3-2** and non-PDCI **4-1-3** and **4-1-4** are shown in Figure 4. 5 and their characterization data are given in Table 4. 1.

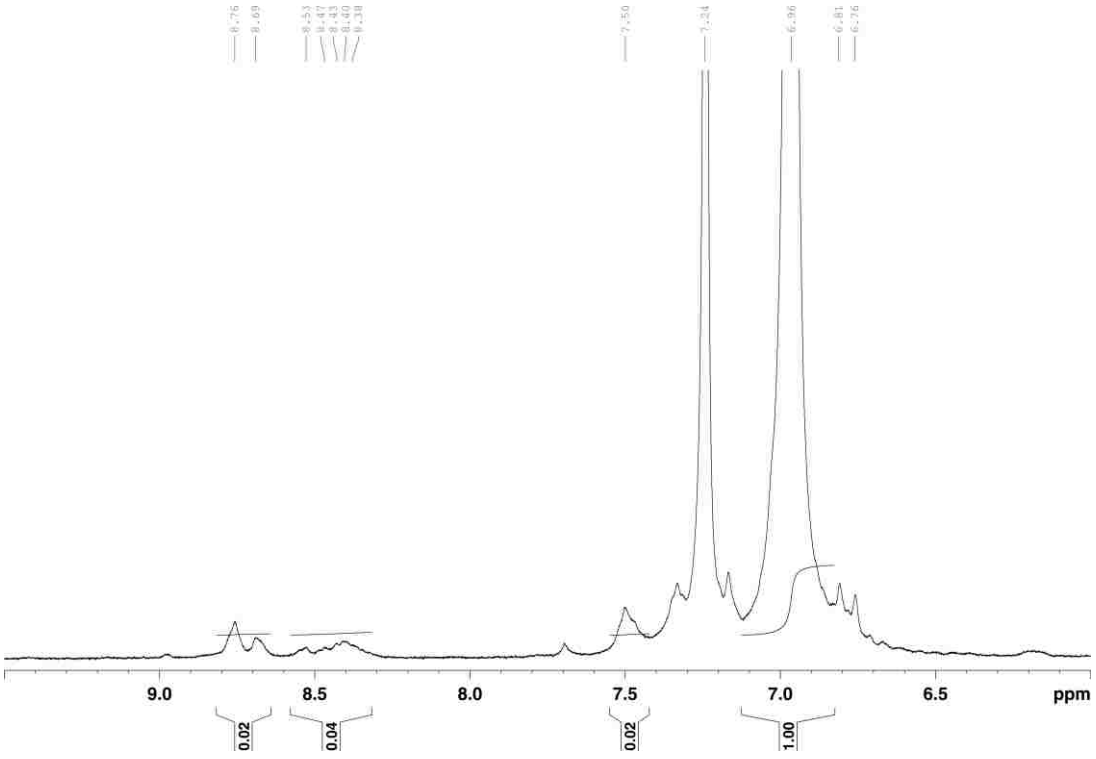

Figure 4. 4 Aromatic region of ^{1}H NMR spectrum low molecular weight **4-P1** (full spectrum is given in the Appendix **A-31**)

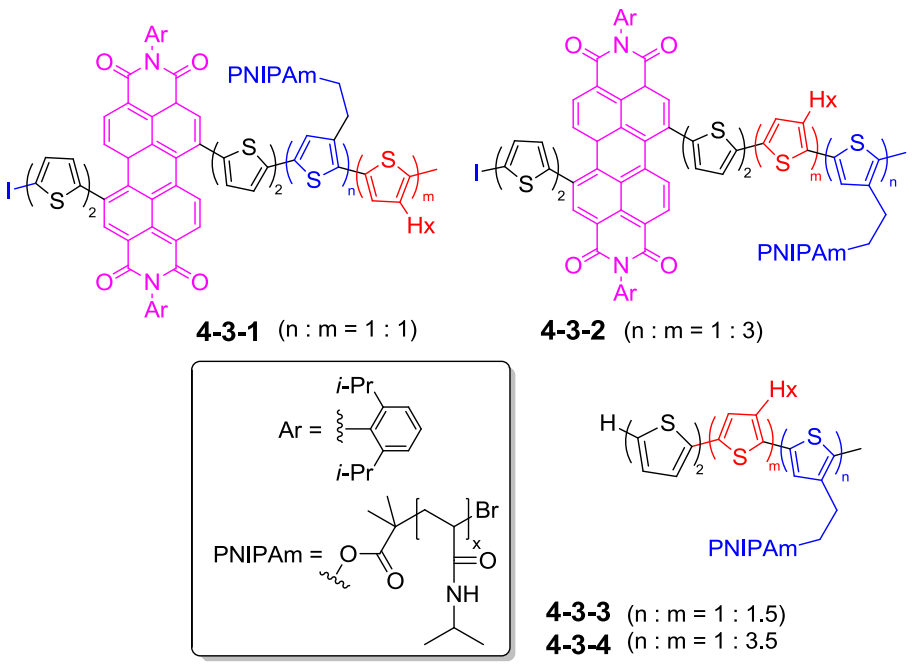

Figure 4. 5 Amphiphilic polythiophene block copolymers prepared in this study.

All four block copolymers were found to be completely soluble in practically any solvent (alcohols, ethers, water, chlorinated, aromatic solvents, DMF, and DMSO, except alkane solvents). Furthermore, most solvents including aqueous systems seem to be "good", i.e. the polymers showed no sign of precipitation of forming colloidal scattering particles.

Table 4. 1 Characterization of the amphiphilic polythiophene block copolymers and their precursors

Precursors	M_n[a]	D[b]	Block ratio[c] m : n	%HT[d]	Polymers	M_n[e]	D[b]
4-1-1	4.7×10^4	1.39	1:1	~100	**4-3-1**	1.43×10^6	2.25
4-1-2	4.4×10^4	1.43	3:1	~100	**4-3-2**	1.76×10^6	2.13
3-9-2	8.0×10^4	1.47	1.5:1	~100	**4-3-3**	2.1×10^6	2.78
3-9-1	7.0×10^4	1.27	3.5:1	~100	**4-3-4**	2.5×10^6	3.0

[a] Determined by GPC in THF relative to polystyrene (PS) standards, [b] Polydispersity index (PDI, M_w/M_n), [c] Determined by ^{1}H NMR (hydrophobic segment vs hydrophilic segment), [d] Head-to-Tail, % regioregularity, [e] Determined by GPC in DMF using multiangle light scattering method, d*n*/d*c*: 0.0548±0.0009 ml/g

4.2.2. Solvatochromism (Solvent-Dependent Spectroscopic Properties). Optical properties of the synthesized polythiophene block copolymers in different series of solvent systems were studied using UV/Vis and photoluminescence spectroscopy, which showed pronounced solvatochromism upon changing solvent polarity from "non-selective" chloroform to "selective" methanol.

To explore the solvatochromic behavior associated with hydrophobic and hydrophilic interactions as well as intermolecular aggregation, we investigated two different block copolymers, **4-3-1** and **4-3-2** in the various composition mixtures of "non-selective" chloroform and "selective" methanol solvents (Figure 4. 6). Gradual change in the solvent quality could be simply achieved by changing solvent composition. Due to the interplay of hydrophobic and hydrophilic interactions depending on the solvents polarity and their solvating ability the polymers displayed highly responsive solvatochromic changes.

The absorption λ_{max} of the polymer **4-3-1** in chloroform and in pure methanol appeared in the wavelength ranges typical for regioregular polythiophene derivatives - between 440~450 nm in $CHCl_3$ and at 565~570 nm in MeOH, respectively.

An apparent vibronic structure of the absorption band in methanol with the appearance of the characteristic shoulders (vibronic transitions) at higher wavelengths (~600 nm) is indicative of the molecularly ordered organization typically found in thin solid films of polythiophenes. Indeed, such degree of molecular order corresponds to the "parallel" organization schematically shown in Figure 4. 1. Upon gradual transition from pure chloroform to chloroform-methanol mixtures, the polymer **4-3-1** absorption band with λ_{max} 449 nm showed a gradual intensity decrease. At the same time, the band with λ_{max} 550 nm

started increasing its intensity and became visible at the composition of 60% chloroform and 40% methanol.

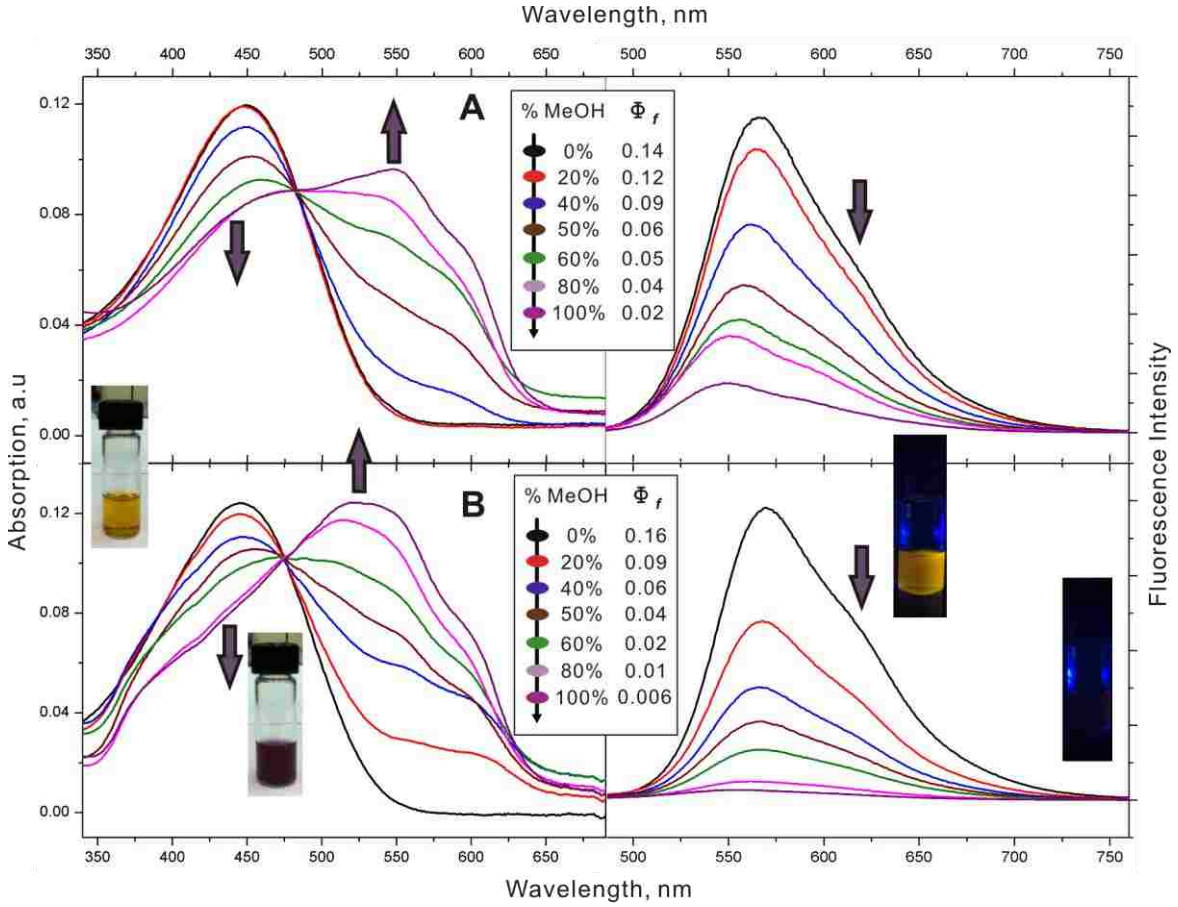

Figure 4. 6 Solvatochromism: absorption and fluorescence spectra change of **4-3-1**(A) and **4-3-2**(B) acquired at 20°C in "non-selective, $CHCl_3$" – "selective, MeOH" solvent mixtures upon increasing fraction of the "selective" solvent. Concentration of all solutions was 0.25mg/ml. Also given are fluorescent quantum yields. The images show visual appearance of the solutions of the polymer **4-3-2** in $CHCl_3$ and methanol and corresponding fluorescence images in the "black" backlight.

Overall, solvent transition from chloroform to methanol produced a large bathochromic shift (111 nm). In contrast to absorption spectra, fluorescent emission band (λ_{max} 567 nm) did not show any significant wavelength shift upon changing from chloroform to methanol. Concomitantly, fluorescent quantum efficiency (initially ay 14%) of **4-3-1** also showed gradual decrease upon increasing solvent polarity. Such diminished fluorescent

quantum yield (~90% decrease from pure $CHCl_3$ to pure methanol solution) could result from increasing intermolecular interactions between better aligned and molecularly ordered polymer molecules in the more planarized conformation which result in the fluorescence quenching. Furthermore, large bathochromic shift in the absorption spectrum corresponds to decreasing HOMO-LUMO gap, which also could result in the lower fluorescence quantum yield ("energy gap law").

The solvent-dependent spectral transitions between two absorption bands in **4-3-1** show a clear isosbestic point at 479 nm. The presence of the isosbestic point indicated that the spectral change reflected actual transition between two distinct supramolecular species, without participation of ill-defined species resulting from random, uncontrolled aggregation.

The solvatochromic behavior of the block copolymer **4-3-2** also showed similar transition between the two bands (Figure 4. 6B). It exhibited a gradual decrease of initial absorption band (λ_{max} 447 nm) upon adding CH_3OH with the most drastic change of the absorption spectrum occuring above the point where the ratio of chloroform and methanol was exactly the same, resulting in a pronounced new absorption band appearance (λ_{max} 575 nm, shoulder band 605 nm) with the large bathochromic shift (128 nm) after addition of excess amount of the "selective" solvent methanol.

The spectral transition also involved a clear isosbestic point at 474 nm. In comparison to polymer **4-3-1**, the transition between two absorption bands in **4-3-2** was more complete, i.e in pure methanol the residual shoulder from the lower wavelength (447 nm) band was much less evident than for the polymer **4-3-1**. The fluorescence spectra followed the same trend as for **4-3-1**, i.e. there was no significant spectral shift; instead the quantum yield gradually decreased from 16% in pure chloroform to 0.6% in pure methanol. The overall drop in

quantum yield (~30 fold) was more pronounced than for **4-3-1** (~10 fold) which was in good agreement with the "cleaner" transition in the absorption spectra. Most likely, such "clean" spectral transitions reflect the more compete interconversion between two distinct solvent-controlled supramolecular organizations in the block copolymer **4-3-2**. The reasons for the higher completeness of the structural transition are not obvious at this time. This could reflect both the opposite order of hydrophobic and hydrophilic blocks in the two copolymers and a higher degree of hydrophobicity (hydrophobic to hydrophilic segments ratio 3:1 in **4-3-2**) compared to the polymer **4-3-1** (hydrophobic to hydrophilic segments ratio 1:1).

Distinct supramolecularly organized species existing in dilute solutions result in a clear isosbestic point where these two completely different species coexist simultaneously. It confirms the presence of the two conformational forms, also documented by the characteristic color changes from yellow to purple. Their supramolecular morphologies were revealed in an AFM study, which clearly distinguished shrunken formations corresponding to the very unusual toroidal nanostructures and stretched nanostructures corresponding to the rough particles (*vide infra*).

4.2.3. Thermochromism (Temperature-Induced Spectroscopic Properties). An efficient exciton (excited states) migration in conjugated polymers both in solution and in solid state requires the presence of the highly ordered conjugated polymer backbone conformation or inclusion of low energy gap units in the polymer system. Such efficient energy migration can take place both intramolecularly and intermolecularly along the isolated conjugated polymer backbone.

To understand the efficient energy migration phenomena both in solution and in solid state, we demonstrated energy migration control in the amphiphilic polythiophene block

copolymer systems by applying temperature as an external stimulus. This led to ratiometric fluorescence changes both in solutions and solid state (spin-cast film).

Although thermochromism (temperature-induced spectroscopic change) of regioregular polythiophene derivatives is a well-known phenomenon documented to occur both in solution and in solid state,[48-52] it generally occurs in a wider temperature intervals ($\geq$100^{o}C). We previously demonstrated that PNIPAm-grafted fluorescent regioregular polythiophenes can undergo temperature-induced control of the conjugated backbone conformation and conjugation length (Chapter 2) in a relatively narrow temperature interval (20 ~ 50^{o}C). Thus, PNIPAm-grafted amphiphilic polythiophenes **4-3-1** and **4-3-2** incorporating a low energy gap perylenedicarboximide (PDCI) unit were found to exhibit a pronounced reversible thermochromic behavior in a narrow temperature interval (20 ~ 70^{o}C) including ratiometric response both in solution and solid state. The ratiometric behavior probably stems from the following reasons: 1) kinetically trapped block copolymer nanostructures resulted in the formation of supramolecular assemblies caused by the increasing glass transition temperature (T_g) of the hydrophobic segments;[53] 2) amplification of photoexcitation energy migration enhanced by well-defined supramlecular organization via three-dimensional intermolecular as well as intramolecular photoexcitation pathways.

Table 4. 2 Spectroscopic properties of amphiphilic polythiophene block copolymers **4-3-2** and **4-3-4** in thin films.

Polymers	Solid State (thin film) [a]					
	chloroform [b]		water [b]		methanol [b]	
	λ_{abs}, nm	λ_{ems}, nm	λ_{abs}, nm	λ_{ems}, nm	λ_{abs}, nm	λ_{ems}, nm
4-3-2	484	595(440)[c]	503	581(443)	549	622(469)
4-3-4	551	543	520	591	553	587

[a] At 20^{o}C. [b] Spin-cast from solutions in the indicated solvent. [c] Parenthesis indicates position of a second (lower intensity) band.

Two polythiophene block copolymers containing a terminal PDCI unit (hydrophobic : hydrophilic ratio 1 : 1 and 3 : 1) and two control polymers without a PDCI unit possessing a similar block ratio (1.5 : 1 and 3.5 : 1) were prepared. The properties of **4-3-1** and **4-3-2** were carefully compared to the control polymers **4-3-3** and **4-3-4** at various temperatures both in aqueous solutions and spin-cast solid films prepared from the three solvents ("non-selective" chloroform, "intermediate" water, and "selective" methanol).

All polymers were found to be well-soluble in water due to the hydrophilic PNIPAm grafts. In an aqueous solution, **4-3-1** showed absorption at λ_{max} 485 nm and correspond fluorescent emission at λ_{max} 606 nm) Its PDCI-lacking control polymer analogue **4-3-3** showed almost similar absorption (λ_{max} 485nm), on the other hand, its fluorescent emission spectrum displayed a less red-shifted band (λ_{max} 573nm) (Figures 4. 7 and 4. 8). Due to the relatively long conjugation lengths and different block ratio in the polymer backbone, the maxima of absorption and fluorescent bands of **4-3-2** and **4-3-4** were red-shifted compared to **4-3-1** and **4-3-3**. Also, the larger hydrophobic composition in the conjugated polymer backbone of **4-3-2** and **4-3-4** resulted in the appearance of a pronounced vibronic structure in the absorption spectra (Figure 4. 7B and D).

Most interestingly, reversible thermochromic ratiometric emission behavior of **4-3-2** was clearly evident (Figure 4. 8B). In this case, we presume that complicated combination of hydrophobic and hydrophilic interactions in the conjugated polymer backbone could control the exciton (excited states) migration towards a low energy gap PDCI unit, therefore attenuating the energy migration efficiency. On the other hand, separately prepared all-hydrophobic polymer analogue (**4-P1**) and all-hydrophilic polymer (**4-P2**), as well as **4-3-1** block copolymer only showed a single fluorescent emission band (λ_{max} 605nm).

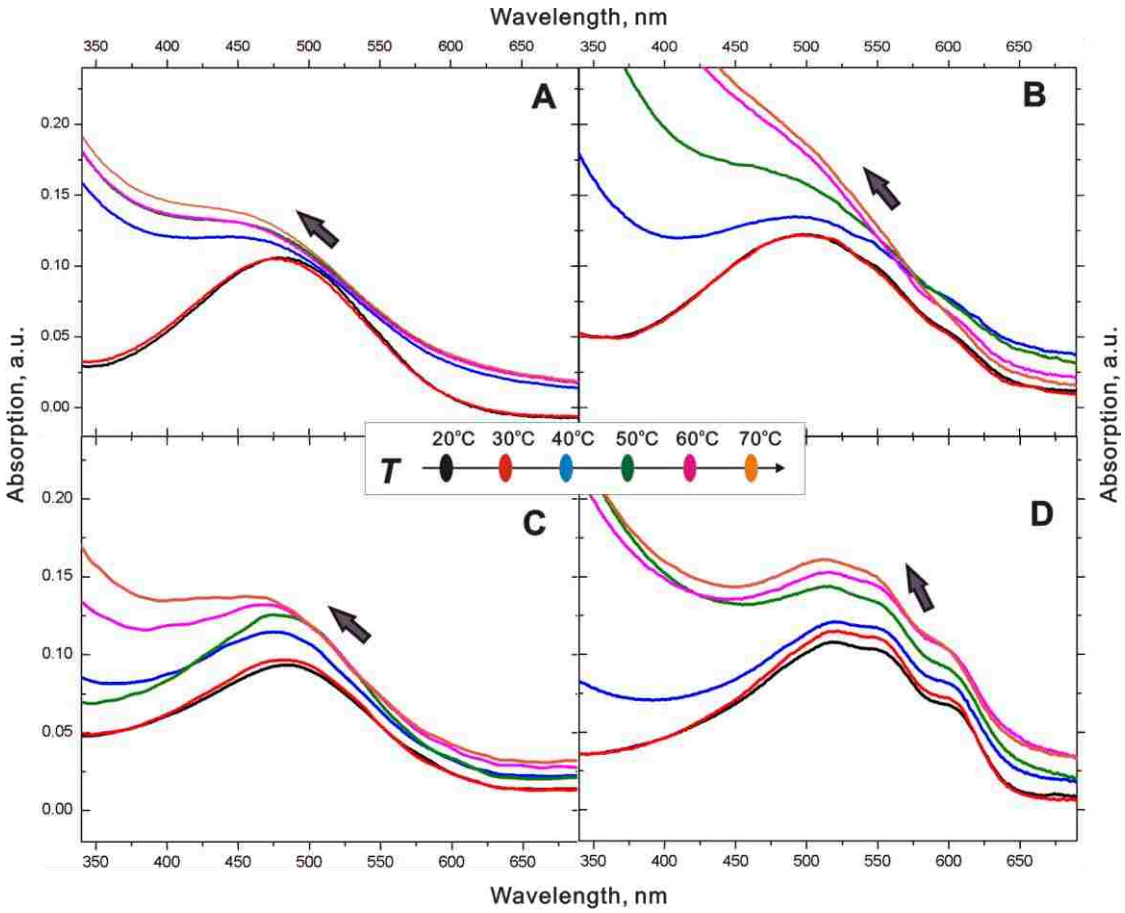

Figure 4. 7 Absorption spectra of **4-3-1**(A), **4-3-2**(B), **4-3-3**(C) and **4-3-4**(D) acquired in aqueous solution at variable temperatures. Concentrations of all solutions were (0.12~0.18 mg/ml). For the comparison purpose, the spectra were not normalized.

Increasing temperature (from 20 to 70^{o}C) resulted in the electronic band gap change of the conjugated polymer backbone, modulating absorption/fluorescent emission wavelength, and causing change in the band intensities. Our previous study of the PNIPAm-grafted polythiophenes found strong changes in the absorption and emission bands upon temperature variation (especially in the narrow temperature interval between 30 and 40 ^{o}C (LCST)). However, thermal responses obtained with the amphiphilic block copolymers were not similar to the earlier results due to the presence of hydrophobic blocks in the conjugated backbone (Figure 4. 7 and 4. 8). Upon temperature change, **4-3-1** showed hypsochromic shifts in both absorption (λ_{max} from 485 nm to 470 nm) and fluorescent emission (λ_{max} 605

nm to 599 nm) with accompanying intensity changes. However, at the a certain temperature (40^{o}C), the absorption spectra showed a drastic intensity change corresponding to increased hydrophobic nature of PNIPAm-grafted conjugated polymer backbone (leading to a turbid aqueous solution which caused strong light scattering) (Figure 4. 7).

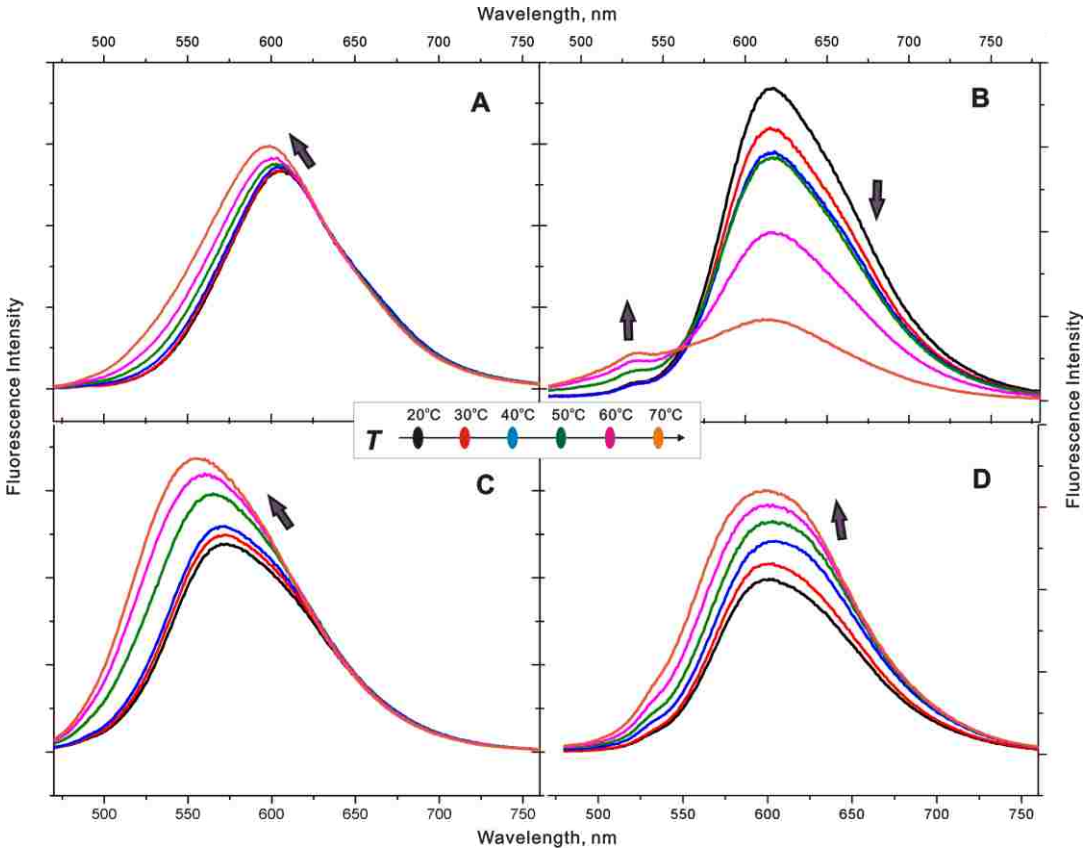

Figure 4. 8 Fluorescent emission spectra of **4-3-1**(A), **4-3-2**(B), **4-3-3**(C) and **4-3-4**(D) acquired in aqueous solution at variable temperatures. Concentrations of all solutions were (0.12~0.18 mg/ml). For the comparison purpose, the spectra were not normalized.

In the case of the block copolymer **4-3-2**, similar hypsochromic shift and intensity change of absorption spectrum in a dilute aqueous solution were observed. Increasing temperature resulted in a ratiometric change of the fluorescent emission spectrum. Below LCST, the blue-shifted emission band at λ_{max} 530 nm and the red-shifted emission at 620 nm showed a slight intensity change. Above LCST, the 620 nm emission band intensity

drastically decreased. At the same time, the 530 nm emission band increased its intensity. Indeed, a noticeable isosbestic point where two different species coexists clearly indicated presence of the two distinct supramolecularly organized structures similar to these observed in solvatochromic responses. Due to the absence of a PDCI unit in the conjugated backbone, control polymers **4-3-3** and **4-3-4**'s optical properties were quite similar to typical regular polythiophene derivatives.[54,55]

In "non-selective" chloroform and "selective" methanol solutions the block copolymer **4-3-2** also showed thermochromic responses; however, ratiometric emission behavior was not observed. An increasing fluorescent emission intensity caused by the intermolecular hydrogen bonding between PNIPAm-grafts in polymer backbone in methanol was observed while the chloroform solution did not show any emission intensity changes (Figure 4. 9).

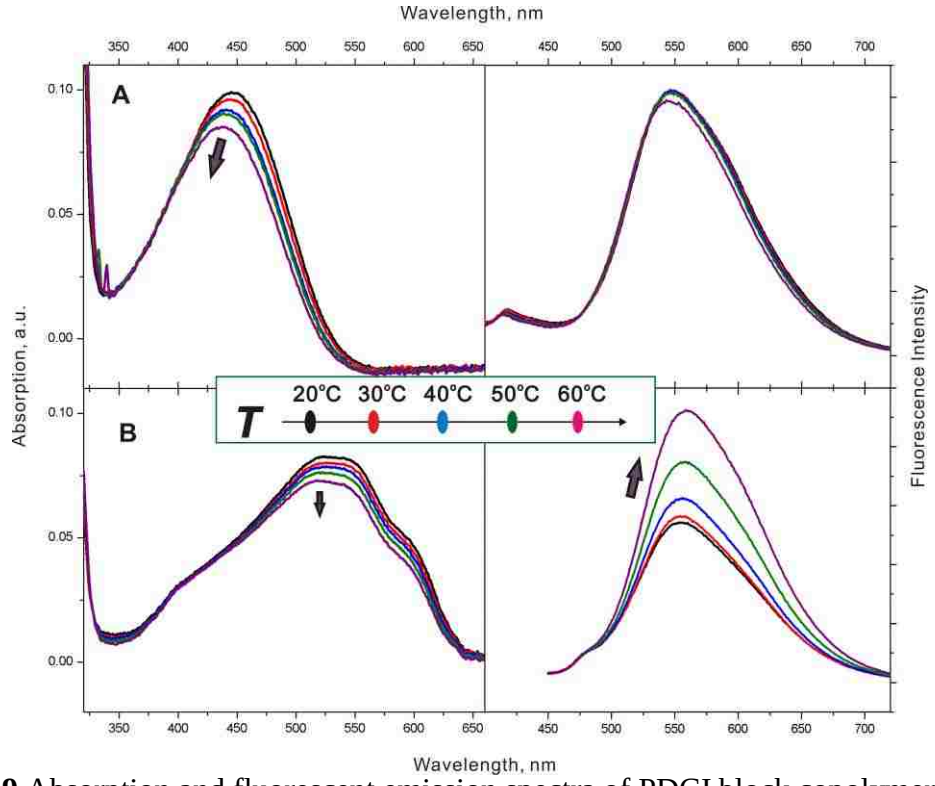

Figure 4. 9 Absorption and fluorescent emission spectra of PDCI block copolymer **4-3-2** solutions in "non-selective" chloroform (0.13mg/ml) (A) and "selective" methanol (0.11mg/ml) (B) at variable temperatures (20°C ~ 60°C)

Thus, distinct ratiometric thermochromic responses in polymer solutions were only dominant in aqueous solutions, although methanol solutions also displayed somewhat less pronounced temperature-induced responses. In contrary, the "non-selective" chloroform solution did not show any temperature-dependent fluorescent emission changes, indicating lack of interactions between hydrophilic and hydrophobic segments.

All four block copolymers **4-3-1** ~ **4-3-4** showed some thermochromic response in the temperature interval 20^{o}C ~ 70^{o}C when they were studied in spin-cast thin films. However, only the block copolymer **4-3-2** showed a relatively strong response. Therefore, we carried out studies of the spectroscopic behavior of **4-3-1** in solid state where three-dimensional intramolecular and intermolecular energy transfer can occur.

For comparison purpose, its non-PDCI analogue **4-3-4** was also studied. A spin-cast film of **4-3-2** prepared from a "non-selective" chloroform solution showed a hypsochromic shift in the absorption spectra upon increasing temperature (λ_{max} 498 nm at 20^{o}C vs. λ_{max} 480 nm at 70^{o}C) (Figure 4. 10A). On the other hand, the control block copolymer **4-3-4** displayed a highly red-shifted absorption band (λ_{max} 557 nm) (Figure 4. 10B) at 20^{o}C and showed only a slight blue shift upon increasing temperature to 70^{o}C. As expected, **4-3-2** showed highly temperature-responsive ratiometric fluorescent dual-bands (λ_{max} 599 nm and second band at 432 nm) (Figure 4. 11A). Interestingly, compared to the aqueous solution spectra at 20^{o}C, both dual-bands in a film of **4-3-2** spin-cast from "non-selective" chloroform solution showed relatively blue-shifted absorption wavelength which was in a good agreement with the previously observed solvatochromic responses (in pure chloroform solution). This allows each polymer chain to preserve energetically more stable (increased entropy status) supramolecular organization.

Upon increasing temperature, two dual fluorescent emission bands exhibited a gradual increase of the longer wavelength emission maxima and decrease of the smaller lower-wavelength band−a ratiometric behavior opposite to that observed in an aqueous solution (Figure 4. 11), probably due to the attenuation of photoexcitation energy migration or conformational kinks[56] in the conjugated polymer backbone. In contrast, control block copolymer **4-3-4** seemed to show a typical polythiophene fluorescent emission band (λ_{max} 540 nm) reported in literature.[54,55] Furthermore, its temperature response was almost negligible (Figure 4.12).

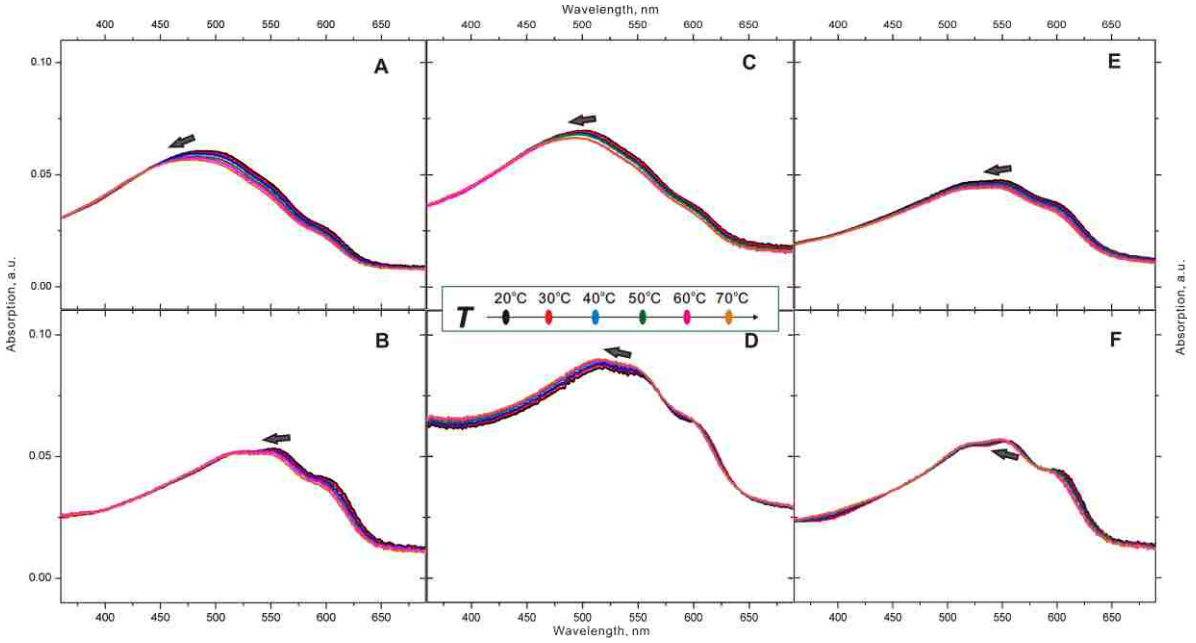

Figure 4. 10 Absorption spectra of PDCI block copolymer **4-3-2** in solid state **(**spin-cast film prepared from chloroform (A), water (C) and methanol (E) and control block copolymer **4-3-4** in solid state **(**spin-cast film prepared from chloroform (B), water (D) and methanol (F) at variable temperatures (20^{o}C ~ 70^{o}C).

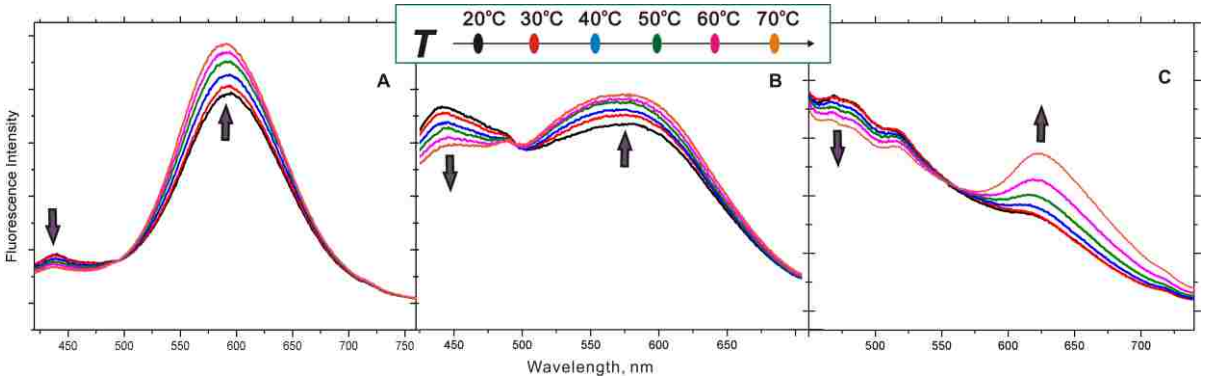

Figure 4. 11 Fluorescent emission spectra of PDCI block copolymer **4-3-2** in solid state **(**spin-cast film prepared from chloroform (A), water (B) and methanol (C) at variable temperatures (20°C ~ 70°C).

In the case of films of **4-3-2** spin-cast from water as an "intermediate" and MeOH as a "selective" solvent, the maxima of absorption and fluorescent emission spectra were observed at the longer wavelengths because such specific solvent systems enable polymer chains to be in a highly planarized conformation probably due to the intermolecular hydrogen bonding which leads to stronger intrachain association. This enhances the three dimensional energy migration in the conjugated polymer backbone.[57] The solid film spectra of **4-3-2** prepared from a water solution displayed broad absorption (λ_{max} 498 nm) and fluorescent emission dual bands (λ_{max} 540, 449 nm).

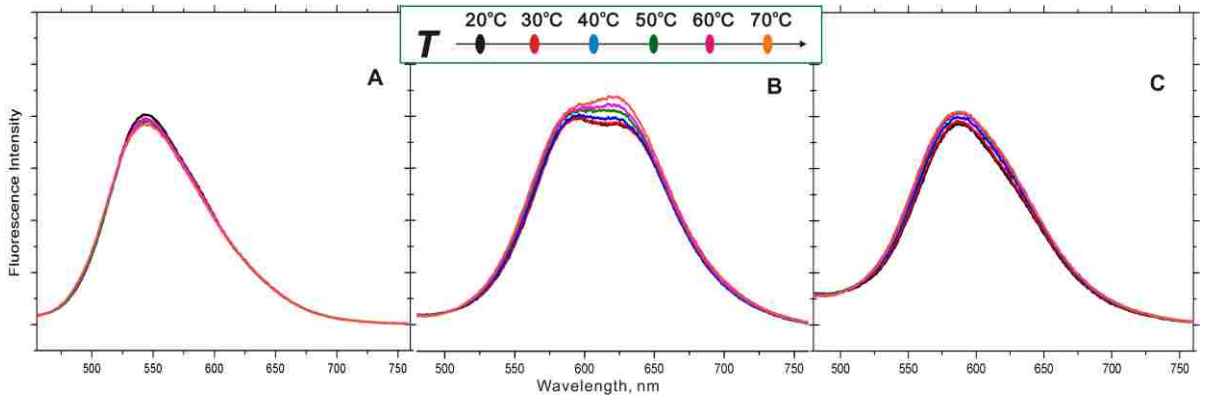

Figure 4. 12 Fluorescent emission spectra of the control block copolymer **4-3-4** in solid state **(**spin-cast film prepared from chloroform (A), water (B) and methanol (C)) at variable temperatures (20°C ~ 70°C).

Thermochromic responses were particularly pronounced in the case of thin films spin-cast from methanol both in absorption (λ_{max} 549 nm) and broad fluorescent emission dual bands (λ_{max} 624, 448 nm). The more intense fluorescence emission band (λ_{max} 624 nm) increased its intensity, while the smaller emission band (λ_{max} 448 nm) decreased the intensity upon increasing temperature (Figure 4. 11C). These results were also in good agreement with the data obtained with the thin film spin-cast from an aqueous solution. In contrast, thermochromic response of the **4-3-4** control polymer showed only a small monochromic change without ratiometric responses, therefore acting as a convincing evidence that no energy migration could be involved (Figure 4. 12C).

4.2.4. Diffusion NMR Study. Change of solvent- and temperature-induced supramolecular nanostructures are highly associated with the hydrophilic and hydrophobic interactions in amphiphilic block copolymer systems. Presumably, polymer size changes corresponding to increasing or decreasing amphiphilicity triggered by the interplay between PNIPAm-grafts and hydrophobic hexylthiophene units can be a driving force that defines such organization.

In order to assess possible influence of solvent and temperature on polymer organization, determination of diffusion coefficients by pulse-gradient NMR in "non-selective" chloroform and "selective" methanol solvents was performed, displaying the size changes in association with both the thermochromic and solvatochromic responses (Table 4. 3).

The interplay between hydrophilic and hydrophobic blocks interactions resulted in the diffusion coefficient differences of 100-fold between polymers in the "non-selective" chloroform and "selective" methanol solutions. In an aqueous solution, diffusion coefficients

showed a 10-fold change upon increasing temperature from 20°C to 70°C. These results reflect both the much larger size of supramolecular nanostructures existing in methanol as compared to the "non-selective" solvent chloroform, and significant decrease in the nanostructures size upon increasing temperature in an aqueous solution.

Table 4. 3 Diffusion coefficients obtained in pulse-gradient NMR experiments

Polymer	D_{app} (Diffusion Coefficient) m^2s^{-1} [a]		
	$CHCl_3$	$CHCl_3$:MeOH(1:1 mixture)	MeOH
4-3-1	3.68×10^{-9}	1.50×10^{-9}	7.20×10^{-11}
4-3-2[b]	3.79×10^{-9}	1.40×10^{-9}	1.22×10^{-11}

[a] All measurements were conducted at 20°C. [b] Diffusion coefficients in an aqueous solution were as follows: 5.36×10^{-9} (20°C) and 8.04×10^{-8} (70°C)

4.2.5. Differential Scanning Calorimetry (DSC). A dilute aqueous solution of the **4-3-2** copolymer showed a particularly pronounced ratiometric emission behavior and therefore it was choson to study the continuous phase transition in association with hydrophilic and hydrophobic interactions. DSC studies on dilute solutions of **4-3-2** showed very broad endothermic and exothermic peaks (Figure 4. 13), which were strikingly different from the DSC data previously obtained for the PNIPAm-functionalized polythiophenes (very narrow endothermic and exothermic peaks) (Figure 2. 10 in Chapter 2). In that earlier case, the major narrow DSC peaks corresponded mostly to the phase transition in the PNIPAm grafts. On the other hand, very broad DSC bands in the case of **4-3-2** probably cannot be explained as originating from a similar PNIPAm transition.

Indeed, a broad-temperature (35 ~ 55°C) phase transition observed upon heating most likely corresponds to the reorganization of one distinct supramolecular assembly (existing at a lower temperature) to another distinct supramolecular assembly (existing at a higher

temperature). Furthermore, this thermal transition perfectly coincides with the spectroscopic ratiometric changes observed for this polymer in its aqueous solution (*vide supra*).

Upon reverse cooling, the high temperature favored supramolecular organization slowly returns back to the low-temperature favored supramolecular organization. The noisy, jittering trace of the DSC peak corresponding to the cooling process is particularly noteworthy and reflects the "difficulties" in the reverse reorganization. It is likely that this structural reorganization cannot happen instantaneously; it requires longer time (and numerous "trials and errors") for the system to accommodate itself into a lower-temperature supramolecular nanostructure.

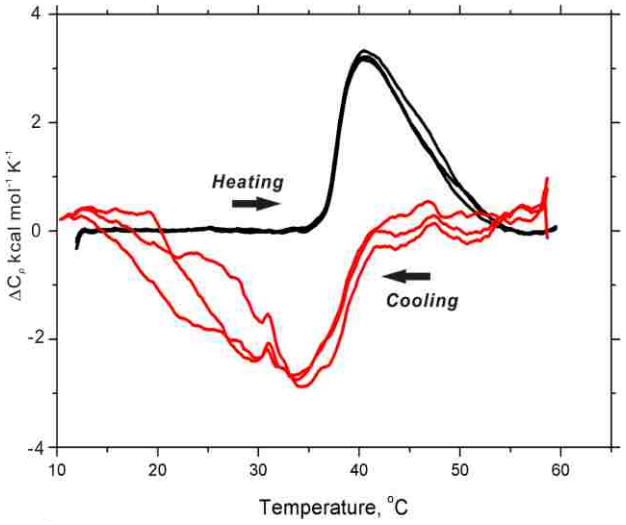

Figure 4. 13 DSC data for the PNIPAm-grafted polythiophene diblock copolymer **4-3-2** in aqueous solution (0.15 mg/ml). Three repeated cycles of heating and cooling are shown.

4.2.6. AFM (Atomic Force Microscopy) Study. Single component amphiphilic molecules, including polymers, are able to self-assemble into various supramolecular nanostructures, however, complicated entropic or kinetic parameters and amphiphilic interactions should be taken into account to understand the self-assembly mechanism. Generally, supramolecular organization of block copolymers in solution is driven by the

incompatibility of one block with the solvent. In certain cases, a block copolymer nanostructure might involve kinetically trapped species, resulting in the formation of aggregates caused by the increasing hydrophobicity in the segment of an isolated block copolymer, specifically when the glass transition temperature (T_g) of the insoluble block is higher than room temperature.[53]

In order to better understand the solvatochromic behavior of the amphiphilic block copolymers, we decided to study individual supramolecular nanostructures by acquiring AFM images of the films prepared by spin-casting from very dilute solutions of the polymer **4-3-2** ranging from the "non-selective" chloroform to the "selective" methanol solvents. The polymer **4-3-2** was chosen because it showed pronounced ratiometric responses triggered both by solvents and temperature. Due to the "non-selective" nature of chloroform solvent, both hydrophilic and hydrophobic segments in macromolecular chains randomly move whereas increased amphiphilic interactions may result in unusual nanostructures.

An AFM image in Figure 4.14 (A) shows toroidal (doughnut-shaped) nanostructures which are highly unusual and have been rarely observed before[58,59] due to the less stable structures associated with the energy penalty for bending.[60] An AFM image acquired from the film obtained from solution in the "intermediate" water solvent showed a mixture of small globular micelles and growing doughnut-shaped micelles (Figure 4.14 (B)).

In contrast, an AFM image obtained from the "selective" methanol solution exhibited more typical globular (micellar) nanostructures. It is likely that many macromolecules tend to form shapeless particles when they are dissolved in a "non-selective" solvent whereas they self-organize into toroidal (doughnut-shaped) particles driven by complicated aggregation.

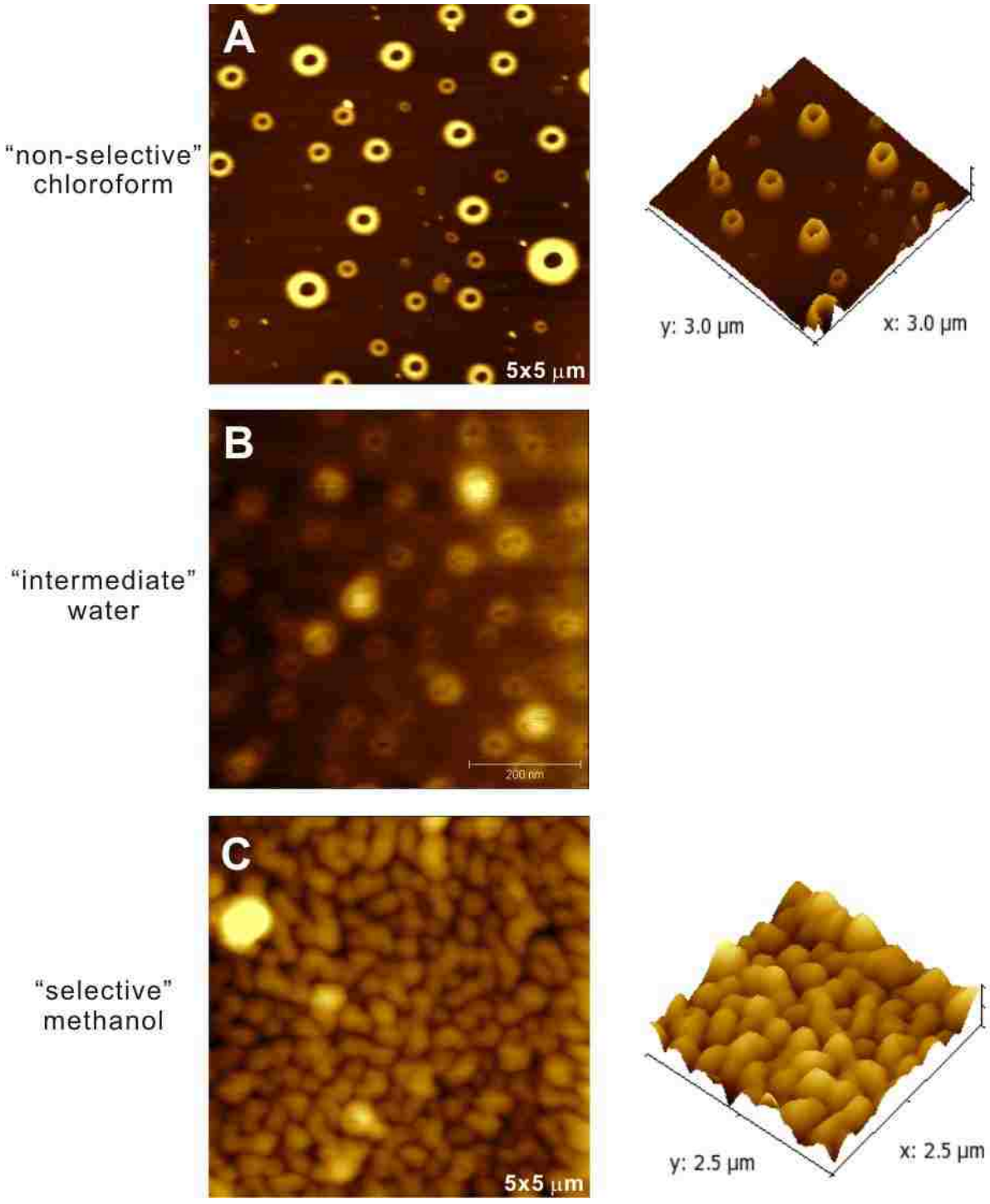

Figure 4. 14 AFM images obtained from the films on mica surface prepared by spin-casting from "non-selective" chloroform (3×10^{-3} mg/ml) (**A**), "intermediate" water (3×10^{-3} mg/ml) (**B**) and "selective" methanol ($3x10^{-3}$ mg/ml) (**C**) solutions.

Interestingly, intermolecular hydrogen bonding with water molecules is generally stronger than that of other solvents (i.e. polar protic and aprotic solvents such as methanol, ethanol, DMF, DME, etc.), however, the AFM images (Figure 4. 14) and photophysical properties in various solvents attest to the fact that aqueous solution may be less stronger than methanol solution in stabilizing amphiphilic block copolymer supramolecular nanostructures.

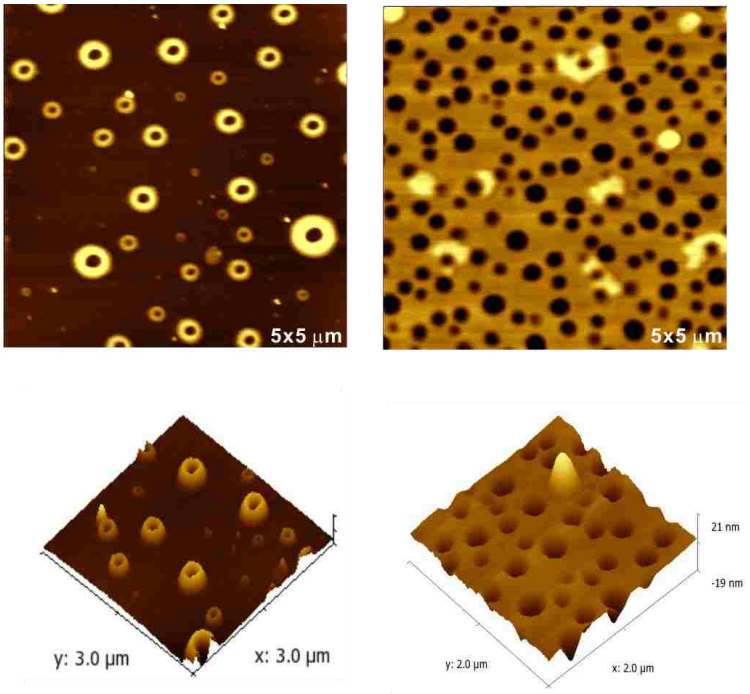

Figure 4. 15 AFM images of polymer **4-3-2** films on mica surfaces prepared from dilute chloroform ($3x10^{-3}$ mg/ml, left) and concentrated chloroform ($3x10^{-1}$ mg/ml, right) solutions.

It was suggested that the unusual toroidal nanostructure formation can be explained by a conventional process of intra- or intermicellar coalescence mechanism[61,62] or a vesicle growth mechanism.[60] The obtained doughnut-shaped micellar structures were in excellent agreement with the vesicle growth mechanism which assumes that a spherical micelle enters

a solvent-philic stage ("semivesicle" state) followed by diffusion of solvent inside the core, then a spontaneous growth of the semivesicle occurs to become a toroidal micelle in solution.

The studies of films obtained from chloroform solutions of two different concentrations showed distinct toroidal nanostructures obtained at lower concentration, while films with cylindrical pores were obtained from a high-concentration solution (Figure 4.15). This indicated a growing stage of spherical micelles at high concentration chloroform solution (3×10^{-1} mg/ml), however only a very dilute concentration allowed to accelerate the nucleation process which can result in growth of toroidal micelles. A correlation with interactions of aggregated blocks as well as glass transition temperature (T_g) may be involved in this process caused by solvent quality. In order to gain deeper understanding of the correlation between block copolymers and glass transition temperature, a study of temperature-dependent AFM morphology is currently in progress in collaboration with Dr. Jayne Garno group.

4.3. Conclusions

We have successfully synthesized a series of amphiphilic polythiophene block copolymers incorporating a terminal low energy gap PDCI unit, and demonstrated an unusual control over supramolecular organization which can cause spectroscopic responses by applying external stimuli such as temperature or solvent polarity in both solution and solid state. Well-defined supramolecular organization phenomena associated with solvatochromic and thermochromic behavior were observed by AFM as unique toroidal (doughnut-shaped) and micellar nanostructures.

4.4. References

1. Hoeben, F. J. M.; Jonkheijm, P.; Meijer, E. W.; Schenning, A. P. H. J. About Supramolecular Assemblies of π-Conjugated Systems. *Chem. Rev*. **2005**, *105*, 1491-1546.

2. Huitema, H. E. A.; Gelinck, G. H.; van der Putten, J. B. P. H.; Kuijk, K. E.; Hart, C. M.; Cantatore, E.; Herwig, P. T.; van Breemen, A. J. M. M.; de Leeuw, D. M. Plastic transistors in active-matrix displays. *Nature* **2001**, *414*, 599.

3. Sirringhaus, H.; Tessler, N.; Friend, R. H. Integrated Optoelectronic Devices Based on Conjugated Polymers. *Science* **1998**, *280*, 1741-1744.

4. Sirringhaus, H.; Brown, P. J.; Friend, R. H.; Nielsen, M. M.; Bechgaard, K.; Langeveld-Voss, B. M. W.; Spiering, A. J. H.; Janssen, R. A. J.; Meijer, E. W.; Herwig, P.; de Leeuw, D. M. Two-dimensional charge transport in self-organized, high-mobility conjugated polymers. *Nature* **1999**, *401*, 685-688.

5. Muccini, M. A bright future for organic field-effect transistors. *Nat. Mater.* **2006**, *5*, 605-613.

6. Thomas III, S. W.; Joly, G. D.; Swager, T. M. Chemical Sensors Based on Amplifying Fluorescent Conjugated Polymers. *Chem. Rev*. **2007**, *107*, 1339-1386.

7. Bernier, S.; Garreau, S.; Bera-Aberem, M.; Gravel, C.; Leclerc, M. A Versatile Approach to Affinitychromic Polythiophenes. *J. Am. Chem. Soc.* **2002**, *124*, 12463-12468.

8. Kim, K.; Liu, J.; Namboothiry, M. A. G.; Carroll, D. L. Roles of donor and acceptor nanodomains in 6% efficient thermally annealed polymer photovoltaics. *Appl. Phys. Lett.* **2007**, *90*, 163511.

9. Jenekhe, S. A.; Chen, X. L. Self-Assembled Aggregates of Rod-Coil Block Copolymers and Their Solubilization and Encapsulation of Fullerenes. *Science* **1998**, *279*, 1903-1907.

10. Mena-Osteritz, E.; Meyer, A.; Langeveld-Voss, B. M. W.; Janssen, R. A. J.; Meijer, E. W.; Ba¨uerle, P. Two-Dimensional Crystals of Poly(3-alkyl-thiophene)s: Direct Visualization of Polymer Folds in Submolecular Resolution. *Angew. Chem. Int. Ed.* **2000**, *39*, 2679-2684.

11. Apperloo, J. J.; Janssen, R. A. J.; Malenfant, P. R. L.; Fre´chet, J. M. J. Interchain Delocalization of Photoinduced Neutral and Charged States in Nanoaggregates of Lengthy Oligothiophenes. *J. Am. Chem. Soc.* **2001**, *123*, 6916-6924.

12. Westenhoff, S.; Abrusci, A.; Feast, W. J.; Henze, O.; Kilbinger, A. F. M.; Schenning, A. P. H. J.; Silva, C. Supramolecular Electronic Coupling in Chiral Oligothiophene Nanostructures. *Adv. Mater.* **2006**, *18*, 1281-1285.

13. Tu, G.; Li, H.; Forster, M.; Heiderhoff, R.; Balk, L. J.; Sigel, R.; Scherf, U. Amphiphilic Conjugated Block Copolymers: Synthesis and Solvent-Selective Photoluminescence Quenching. *Small.* **2007**, *3*, 1001-1006.

14. Pan, H.; Liu, P.; Li, Y.; Wu, Y.; Ong, B. S.; Zhu, S.; Xu, G. Unique Polymorphism of Oligothiophenes. *Adv. Mater.* **2007**, *19*, 3240-3243.

15. Kiriy, N.; Jahne, E.; Alder, H.-J.; Schneider, M.; Kiriy, A.; Gorodyska, G.; Minko, S.; Jehnichen, D.; Simon, P.; Fokin, A. A.; Stamm, M. One-Dimensional Aggregation of Regioregular Polyalkylthiophenes. *Nano. Lett*. **2003**, *3*, 707-712.

16. Scherf, U.; Gutacker, A.; Koenen, N. All-Conjugated Block Copolymers. *Acc. Chem. Res*. **2008**, *41*, 1086-1097.

17. Park, S-J.; Kang, S-G.; Fryd, M.; Saven, J. G.; Park, S. J. Highly Tunable Photoluminescent Properties of Amphiphilic Conjugated Block Copolymers. *J. Am .Chem. Soc.* **2010**, *132*, 9931-9933.

18. Yokozawa, T.; Yokoyama, A. Chain-Growth Condensation Polymerization for the Synthesis of Well-Defined Condensation Polymers and π-Conjugated Polymers. *Chem. Rev*. **2009**, *109*, 5595-5619.

19. Zhang, Y.; Tajima, K.; Hirota, K.; Hashimoto, K. Synthesis of All-Conjugated Diblock Copolymers by Quasi-Living Polymerization and Observation of Their Microphase Separation. *J. Am. Chem. Soc*, **2008**, *130*, 7812-7813.

20. Van Hutten, P. F.; Gill, R. E.; Herrera, J. K.; Hadziioannou, G. Structure of Thiophene-Based Regioregular Polymers and Block Copolymers and Its Influence on Luminescence Spectra. *J. Phys. Chem*. **1995**, *99*, 3218-3224.

21. Levesque, I.; Leclerc, M. Ionochromic and Thermochromic Phenomena in a Regioregular Polythiophene Derivative Bearing Oligo(oxyethylene) Side Chains. *Chem. Mater*. **1996**, *8*, 2843-2848.

22. Levesque, I.; Bazinet, P.; Roovers, J. Optical Properties and Dual Electrical and Ionic Conductivity in Poly(3-methylhexa(oxyethylene)oxy-4-methylthiophene). *Macromolecules* **2000**, *33*, 2952-2957.

23. Hong, X. M.; Collard, D. M. Liquid Crystalline Regioregular Semifluoroalkyl-Substituted Polythiophenes. *Macromolecules* **2000**, *33*, 6916-6917.

24. Sakurai, S.-I.; Goto, H.; Yashima, E. Synthesis and Chiroptical Properties of Optically Active, Regioregular Oligothiophenes. *Org. Lett*. **2001**, *3*, 2379-2382.

25. de Boer, B.; van Hutten, P. F.; Ouali, L.; Grayer, V.; Hadziioannou, G. Amphiphilic, Regioregular Polythiophene. *Macromolecules* **2002**, *35*, 6883-6887.

26. Bjornholm, T.; Greve, D. R.; Reitzel, N.; Hassenkam, T.; Kjaer, K.; Howes, P. B.; Larsen, N. B.; Bogelund, J.; Jayaraman, M.; Ewbank, P. C.; McCullough, R. D. Self-Assembly of Regioregular, Amphiphilic Polythiophenes into Highly Ordered π-Stacked Conjugated Polymer Thin Films and Nanocircuits. *J. Am. Chem. Soc*. **1998**, *120*, 7643-7644.

27. Yu, J.; Holdcroft, S. Solid-State Thermolytic and Catalytic Reactions in Functionalized Regioregular Polythiophenes. *Macromolecules* **2000**, *33*, 5073-5079.

28. Stokes, K. K.; Heuze, K.; McCullough, R. D. New Phosphonic Acid Functionalized, Regioregular Polythiophenes. *Macromolecules* **2003**, *36*, 7114-7118.

29. Mattu, J.; Johansson, T.; Holdcroft, S.; Leach, G. W. Highly Ordered Polymer Films of Amphiphilic, Regioregular Polythiophene Derivatives. *J. Phys. Chem. B* **2006**, *110*, 15328-15337.

30. Choi, J.; Nesterov. E. E. Pentacoordinate Ni(II) Complexes as Highly Efficient Initiators of Chain-Growth Polymerization: a Versatile Route to Conjugated Polymers. *Angew. Chem. Int. Ed*. **2011** *(submitted)*

31. Balamurugan, S. L.; Bantchev, G. B.; Yang, Y.; McCarly, R. L. Highly Water-Soluble Thermally Responsive Poly(thiophene)-Based Brushes. *Angew. Chem. Int. Ed*. **2005**, *44*, 4872-4876.

32. Jeffries-EL, M.; Sauve, G.; McCullough, R. D. Facile Synthesis of End-Functionalized Regioregular Poly(3-alkylthiophene)s via Modified Grignard Metathesis Reaction. *Macromolecules* **2005**, *38*, 10346-10354.

33. Jeffries-EL, M.; Sauve, G.; McCullough, R. D. In-Situ End-Group Functionalization of Regioregular Poly(3-alkylthiophene) Using the Grignard Metathesis Polymerization Method. *Adv. Mater.* **2004**, *16*, 1017-1020.

34. Liu, J.; Sheina, E.; Kowalewski, T.; McCullough, R. D. Tuning the Electrical Conductivity and Self-Assembly of Regioregular Polythiophene by Block Copolymerization: Nanowire Morphologies in New Di- and Triblock Copolymers. *Angew. Chem. Int. Ed.* **2002**, *41*, 329-332.

35. Liu, J.; Tanaka, T.; Sivula, K.; Alivisatos, A. P.; Fréchet, J. M. J. Employing End-Functional Polythiophene To Control the Morphology of Nanocrystal−Polymer Composites in Hybrid Solar Cells. *J. Am. Chem. Soc.* **2004**, *126*, 6550-6551.

36. Radano, C. P.; Scherman, O. A.; Stingelin-Stutzmann, N.; Muller, C.; Breiby, D. W.; Smith, P.; Janssen, R. A. J.; Meijer, E. W. Crystalline−Crystalline Block Copolymers of Regioregular Poly(3-hexylthiophene) and Polyethylene by Ring-Opening Metathesis Polymerization. *J. Am. Chem. Soc*. **2005**, *127*, 12502-12503.

37. Sivula, K.; Ball, Z. T.; Watanabe, N.; Fréchet, J. M. J. Amphiphilic Diblock Copolymer Compatibilizers and Their Effect on the Morphology and Performance of Polythiophene: Fullerene Solar Cells. *Adv. Mater.* **2006**, *18*, 206-210.

38. Dai, C.-A.; Yen, W.-C.; Lee, Y.-H.; Ho, C.-C.; Su, W.-F. Facile Synthesis of Well-Defined Block Copolymers Containing Regioregular Poly(3-hexyl thiophene) via Anionic Macroinitiation Method and Their Self-Assembly Behavior. *J. Am. Chem. Soc*. **2007**, *129*, 11036-11038.

39. Chen, X.; Gholamkhass, B.; Han, X.; Vamvounis, G.; Holdcroft, S. Polythiophene-*graft*-Styrene and Polythiophene-*graft*-(Styrene-*graft*-C_{60}) Copolymers. *Macromol. Rapid Commun.* **2007**, *28*, 1792-1797.

40. Senkovskyy, V.; Khanduyeva, N.; Komber, H.; Oertel, U.; Stamm, M.; Kuckling, D.; Kiriy, A. Polymer Brushes of Regioregular Head-to-Tail Poly(3-alkylthiophenes) via Catalyst-Transfer Surface-Initiated Polycondensation. *J. Am .Chem. Soc,* **2007**, *129*, 6626-6634.

41. Bronstein, H. A.; Luscombe, C. K. Externally Initiated Regioregular P3HT with Controlled Molecular Weight and Narrow Polydispersity. *J. Am. Chem. Soc.* **2009**, *131*, 12894-12895.

42. Hwang, E.; Choi, J.; Lusker, K.; Garno, J. C.; Nesterov. E. E. Grafting of Surface-Immobilized Nanopatterned Polythiophenes by Surface-initiated Living Polymerization. *Adv. Mater.* **2011** *(in preparation to submission)*

43. Schmidt-Mende, L.; Fechtenkotter, A.; Mullen, K.; Moons, E.; Friend, R. H.; MacKenzie, J. D. Self-Organized Discotic Liquid Crystals for High-Efficiency Organic Photovoltaics. *Science.* **2001**, *293*, 1119-1122.

44. Ranke, P.; Bleyl, I.; Simmerer, J.; Haarer, D.; Bacher, A.; Schmidt, H. W. Electrolumineseence and electron transport in a perylene dye *App. Phys. Lett.* **1997**, *71*, 1332-1334.

45. Ehli, C.; Mateo-Alonso, A.; Prato, M.; Schmidt, C.; Backes, C.; Hauke, F.; Hirsch, A. Manipulating single-wall carbon nanotubes by chemical doping and charge transfer with perylene dyes. *Nat. Chem,* **2009**, *1*, 243-249.

46. McQuade, D. T.; Pullen, A. E.; Swager, T. M. Conjugated Polymer-Based Chemical Sensors. *Chem. Rev.* **2000**, *100*, 2537-2574.

47. Chen, L.; McBranch, D. W.; Wang, H.-L.; Helgeson, R.; Wudl, F.; Whitten, D. G. Highly sensitive biological and chemical sensors based on reversible fluorescence quenching in a conjugated polymer. *Proc. Natl. Acad. Sci. USA.* **1999**, *96*, 12287-12292.

48. Yang, C.; Orfino, F. P.; Holdcroft, S. A Phenomenological Model for Predicting Thermochromism of Regioregular and Nonregioregular Poly(3-alkylthiophenes). *Macromolecules* **1996**, *29*, 6510-6517.

49. Brustolin, F.; Goldoni, F.; Meijer, E. W.; Sommerdijk, N. A. J. M. Highly Ordered Structures of Amphiphilic Polythiophenes in Aqueous Media. *Macromolecules* **2002**, *35*, 1054-1059.

50. Garreau, S.; Leclerc, M.; Errien, N.; Louarn, G. Planar-to-Nonplanar Conformational Transition in Thermochromic Polythiophenes: A Spectroscopic Study. *Macromolecules* **2003**, *36*, 692-697.

51. Lévesque, I.; Leclerc, M. Ionochromic and Thermochromic Phenomena in a Regioregular Polythiophene Derivative Bearing Oligo(oxyethylene) Side Chains. *Chem. Mater.* **1996**, *8*, 2843-2849.

52. Faïd, K.; Fréchette, M.; Ranger, M.; Mazarolle, L.; Lévesque, I.; Leclerc, M.; Chen, T.-A.; Rieke, R. D. Chromic Phenomena in Regioregular and Nonregioregular Polythiophene Derivatives. *Chem. Mater.* **1995**, *7*, 1390-1396.

53. Nicolai, T.; Colombani, O.; Chassenieux, C. Dynamic polymeric micelles *versus* frozen nanoparticles formed by block copolymers. *Soft. Matter.* **2010**, *6*, 3111-3118.

54. Chen, T.-A.; Wu, X.; Rieke, R. D. Regiocontrolled Synthesis of Poly(3-alkylthiophenes) Mediated by Rieke Zinc: Their Characterization and Solid-State Properties. *J. Am. Chem. Soc.* **1995**, *117*, 233-244.

55. McCullough, R. D. Chemistry of Conducting Polythiophenes. *Adv. Mater.* **1998**, *10*, 93-116.

56. Collini, E.; Scholes, G. D. Coherent Intrachain Energy Migration in a Conjugated Polymer at Room Temperature. *Science*. **2009**, *323*, 369-372.

57. Nesterov. E. E.; Zhu, Z.; Swager, T. M. . Conjugation Enhancement of Intramolecular Exciton Migration in Poly(*p*-phenylene ethynylene)s. *J. Am. Chem. Soc.* **2005**, *127*, 10083-10088.

58. Pochan, D.; Chen, Z. Cui. H, Hales. Qi, K.; Wooley, K. L. Toroidal Triblock Copolymer Assembliees. *Science* **2004***, 306,* 94-97.

59. Hung, H.; Chung, B.; Jung, J.; Park, H.; Chang, T. Toroidal Micelles of Uniform Size from Diblock Copolymers. *Angew. Chem. Int. Ed.* **2009**, *48*, 4594-4597.

60. He, X.; Schimid, F. Spontaneous Formation of Complex Micelles a Homogeneous Solution. *Phys. Rev. Lett.* **2008**, *100*, 137802.

61. Van der Schoot, P.; Wittmer, J. P. Linear aggregation revisited:Rods, rings and worms. *Macromol. Theory Simul.* **1999**, *8*, 428-432.

62. In, M;Aguerre-Chariol, O.; Zana, R. Closed-Looped Micelles in Surfactant Tetramer Solutions. *J. Phys. Chem. B* **1999**, *103*, 7747-7750.

CHAPTER 5. POLY(CYANINE)S–NEAR-INFRARED (NIR) FLUORESCENT CONJUGATED POLYMERS

5.1. Poly(cyanine)s - NIR Fluorescent CPs – an Introduction

Fluorescent conjugated polymers (CPs) attract tremendous amount of interest as a versatile platform for chemo- and biosensing applications and optoelectronic devices.[1] The efficient photoexcitation energy transport taking place both in dilute solution and in the aggregated form of CPs allows funnelling the energy collected over large areas into the low energy gap sites resulting in significant amplification in sensing devices,[2,3] or tuning the luminescence color in light-emitting devices.[4,5] Some fluorescent polymers, such as water-soluble polythiophenes, display substantial conformational flexibility of their conjugated backbone which makes them an outstanding platform for designing biosensors and biomarkers. Conformational twisting of the conjugated backbone results in disruption of the π-electron conjugation and decreasing conjugation length which is accompanied by hypsochromic shifts in the absorption and fluorescence spectra. Subsequent binding to a bioanalytical target may lead to the backbone planarization and the bathochromic spectral shifts. Owing to the efforts of Leclerc,[6-8] Nilsson,[9,10] and others,[11,12] the approach based on this phenomenon was successfully used in the design of polythiophene biosensors and imaging agents. Whereas such detectors operate in the visible spectral range, availability of the conformationally flexible fluorescent CPs operating in the near-infrared (NIR) region would open wider possibilities for practical applications. The advantages of the NIR region (700-1100 nm) for biosensors are numerous and well documented;[13,14] among them are lower background absorption and fluorescence, decreased light scattering, etc. However, development of NIR fluorescent, low energy gap CPs faces numerous challenges. A popular design scheme utilizes alternating donor-acceptor conjugated backbone pattern; such design

can yield CPs with very low energy gap and intense NIR absorption.[15,16] Although such polymers proved useful for enhancing light capturing efficiency of organic solar cells, they commonly are only weakly fluorescent due to the dominance of low-emissive charge-transfer states. An attractive approach to NIR fluorescent CPs employs highly fluorescent π -conjugated small-molecule dyes as repeating units in the CP backbone. Previously this approach was realized with squaraines[18,19], porphyrins[20,21], BODIPY dyes[22,23], perylenediimides[24], etc. The resulting oligomers and polymers commonly show intense NIR absorption and fluorescence, and proved useful as an alternative to "conventional" fluorescent CPs.

Polymethine cyanine dyes have been known for one and a half century, and represent a unique family of fluorescent markers with wide-spread applications.[25] These charged molecules incorporate two heterocyclic units interconnected by a polymethine bridge with odd number of π -conjugated carbons. Their electronic structure is unique in a sense that, unlike most polyenes, they possess completely delocalized conjugated bridge with absolutely no bond-length alternation.[27,28] As their ground and excited state geometries are close to each other, these dyes exhibit narrow absorption and fluorescence bands with small Stokes shift. [29] Although the π - conjugated electrons in cyanine dyes are heavily delocalized within the polymethine bridge, the terminal heterocyclic aromatic moieties also participate in the π -electron delocalization. For example, increase in conjugation length with accompanying bathochromic spectral shifts was observed when naphthalene aromatic termini (as in benzindocyanine compounds) were used instead of benzene units (as in indocyanine dyes).[30]

5.2. Results and Discussion

Encouraged by this observation, we hypothesized that linking indocyanines as monomeric units into a poly(cyanine) chain will produce fluorescent conjugated polymers with the extended π - electron delocalization, therefore shifting their absorption and emission into the NIR wavelength region.[31] Due to the relative conformational flexibility around the bonds which interconnect the adjacent monomeric repeating units, photophysical properties of the polymers could be very sensitive to the environment, making such polymers highly suitable for sensing applications. In addition, these polymers as intrinsic cationic polyelectrolytes would be suitable for biodetection owing to their enhanced binding to negatively charged biomolecules such as DNA.

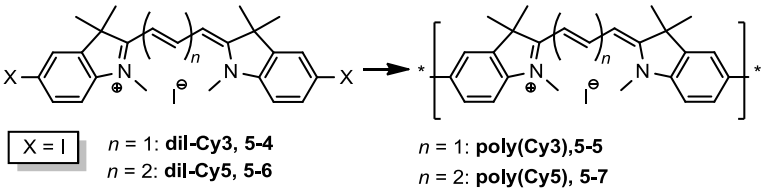

Scheme 5. 1 Synthesis and GPC characterization of poly(cyanine) conjugated polymers **5-5** and **5-7**. Polymerization conditions: $Ni(COD)_2$, COD, 2,2′-bipy, DMF, 60°C, 24 h.

As a proof of concept, we decided to prepare poly(cyanine)s incorporating simple Cy3 and Cy5 repeating units (Scheme 5. 1). In naming the polymers, we followed the notation introduced by Waggoner for the related family of indocyanine fluorescent biomarkers.[32] Thus, "poly(Cy3)" stands for a conjugated polymer consisting of indocyanine ("Cy") repeating units which incorporate a three-carbon ("3") conjugated bridge. Novel polymers poly(Cy3), **5-5** and poly(Cy5), **5-7** were conveniently prepared by employing Yamamoto polymerization[33] of easily available diiodo-substituted monomeric precursors diI-

Cy3 and diI-Cy5 (Scheme 5. 1). Although formation of the polymers was evident unfortunately, we were unable to determine the molecular weight of the prepared materials due to the polycationic nature of the polymers. This nature prevented us from using MALDI-TOF measurements (as it provides m/z data which do not change with the number of the repeating units for charged polymers). The highly charged nature of these polymers also precluded using GPC to determine molecular weight (as they either remain trapped in the columns, or show unreliable retention times). Determination of molecular weight of the obtained polymer materials is still in progress (attempts include using ultracentrifugation, osmometry, etc).

Both poly(Cy3) and poly(Cy5) were found to be well soluble in alcohols (methanol, ethylene glycol, etc.) and in polar aprotic solvents such as acetonitrile, DMF, and DMSO. While these polymers could not be dissolved in water directly, stable aqueous solutions could be prepared by mixing their concentrated methanol solutions with water. Both polymers showed reasonable thermal stability in solid state; thus no substantial degradation was found in TGA studies at the temperatures below 200 °C (Figure 5. 1).

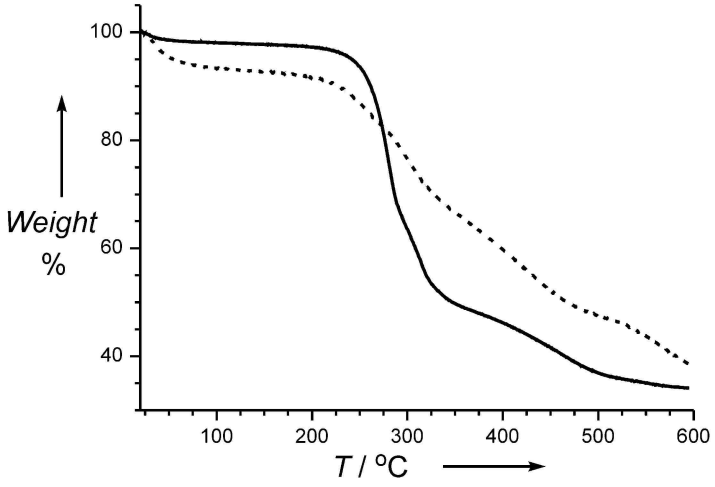

Figure 5. 1 TGA data for **5-5** (solid trace) and **5-7** (dash trace). The data were acquired at the heating rate of 10 °C min^{-1} in nitrogen atmosphere.

Below the decomposition temperature, the polymers experienced a first-order phase transition which manifested itself as a broad endothermic peak in differential scanning calorimetry (DSC) experiments centered at around 80 ℃ for poly(Cy3) and around 95 ℃ for poly(Cy5) (Figure 5. 2); this phase transition could be attributed to melting the polymers. Lack of sharp melting point indicated highly amorphous nature of the solid polymers which likely reflected the large variety of conformations of the conjugated backbone in solid state (*vide infra*).

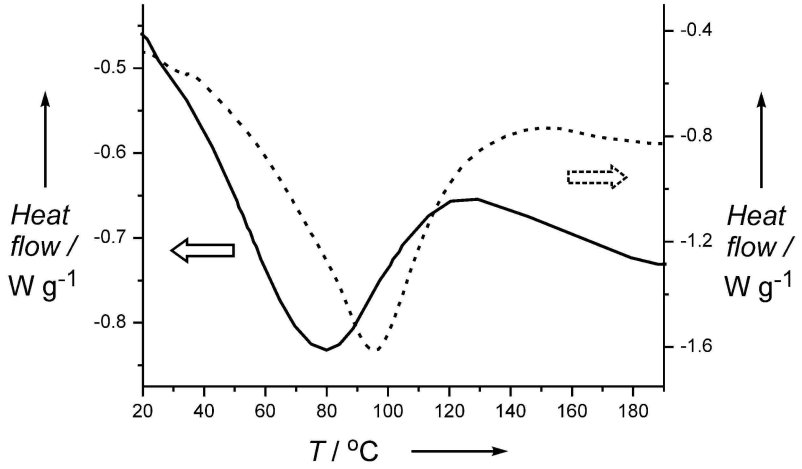

Figure 5. 2 DSC data for **5-5** (solid trace) and **5-7** (dash trace). The data were acquired at the heating rate of 10 ℃ min^{-1} in nitrogen atmosphere.

To study π-electron delocalization in poly(cyanine)s and to determine the effect of increasing conjugation length on optical properties, computational analysis was performed on nonamer of Cy3 as a reasonable model for poly(Cy3). The initial conformational search was performed with Monte-Carlo molecular mechanics method, followed by geometry optimization at the semiempirical (AM1) level and single-point Franck-Condon geometry excited-state ZINDO computation. The computation revealed an extended-chain geometry with dihedral angle between the completely planar Cy3 adjacent repeating units ranging between 35 to 45° (Figure 5. 3). Such moderate dihedral twist did not preclude extensive

delocalization of the molecular orbitals participating in the electronic excitation. Such delocalization should lead to longer conjugation length and bathochromic spectral shifts. Indeed, comparison of the ZINDO computational results for the nonamer and corresponding monomeric Cy3 molecule (X = H, n = 1 in Scheme 5. 1) revealed a noticeable 0.30 eV bathochromic shift in an absorption spectrum (from 485 to 549 nm) along with an 8-fold increase in the oscillator strength of the major electronic transitions contributing to the excitation.

Figure 5. 3 Optimized geometry and delocalized molecular orbitals involved into one of the electronic configurations (MO599 → MO615) describing the Franck-Condon excitation of the nonamer of Cy3 as a theoretical model for poly(Cy3). Ground-state geometry was optimized at the AM1 level following the Monte-Carlo conformational search; single-point excited state computation was performed with ZINDO.

In good agreement with the computational analysis, optical spectra of the poly(cyanine) polymers displayed noticeable bathochromic shifts relative to the corresponding monomeric dyes (Figure 5. 4 and Table 5. 1). The monomer – polymer optical energy gap change for the compounds in dilute solutions (determined as a long-wavelength offset of the absorption bands) was 0.34 eV for poly(Cy3) and 0.23 eV for poly(Cy5). Also in agreement with the computational data, the polymers showed 5 (for poly(Cy3)) and 10 (poly(Cy5)) times increase in the oscillator strength (determined from the

integration of the absorption spectra[34]). The polymers' optical spectra were significantly broadened as compared to the corresponding monomers and appeared to consist of at least two overlapping bands. Thus, absorption spectrum of poly(Cy3) showed two maxima: one at 569 nm was just slightly red-shifted relative to that of Cy3 (544 nm), whereas the second maximum (at 615 nm) showed a substantial 71 nm bathochromic shift (Figure 5. 4a).

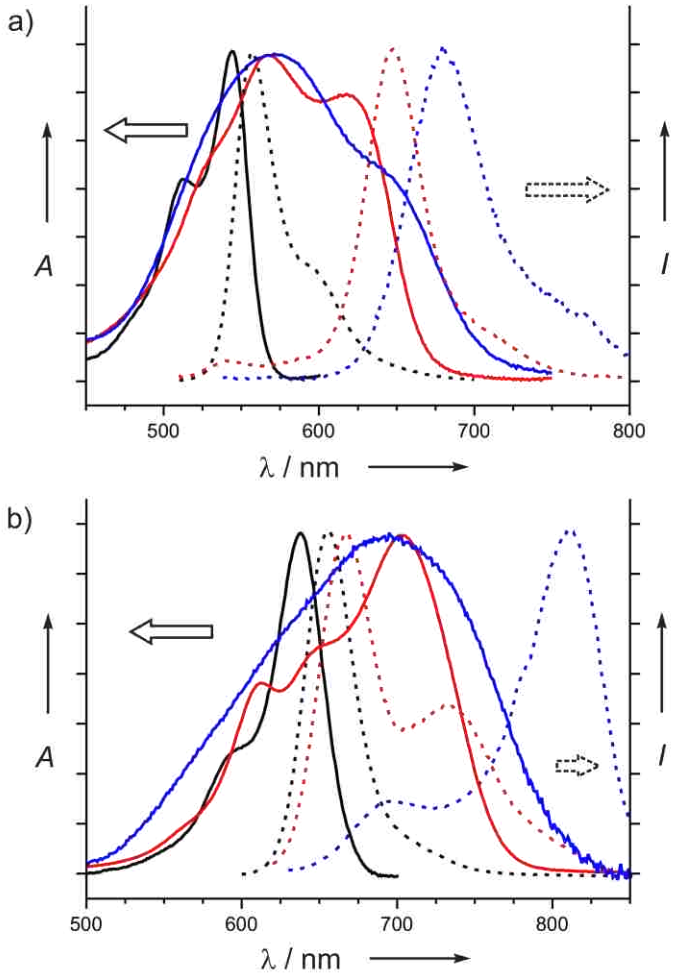

Figure 5. 4 Normalized absorption and fluorescence spectra of Cy3 / poly(Cy3) (a) and Cy5 / poly(Cy5) (b) compounds. Solid traces correspond to absorption, and dash traces – to fluorescence spectra. Trace color: black – Cy3 (Cy5) solution in methanol, red – poly(Cy3) (poly(Cy5)) solution in methanol, blue – poly(Cy3) (poly(Cy5)) spin-cast thin films.
Table 5. 1 Photophysical properties of poly(cyanine)s and corresponding monomeric cyanine dyes.

	Cy3	Poly(Cy3)	Cy5	Poly(Cy5)
E_g^{opt} [eV] [a]	2.18	1.84	1.85	1.62
ε [mol^{-1} cm^{-2}] [b]	1.1×10^5	2.7×10^5	1.0×10^5	6.0×10^5
f [c]	1.0	4.8	0.7	7.3
Φ [%] [d]	14	16	8	1

[a] Optical energy gap, determined as a long-wavelength offset of the absorption spectra in methanol; [b] Extinction coefficient (per repeating unit for the polymers); [c] Electronic transition oscillator strength; [d] Fluorescence quantum yield in methanol solution.

Similar appearance was found for the absorption spectrum of poly(Cy5): a monomer-like band with the maximum at 649 nm (vs. 638 nm for Cy5), and a significantly red-shifted band with the maximum at 705 nm. Like the absorption spectra, polymers' emission spectra also displayed two overlapping bands. Since the relative intensity of emission bands is strongly affected by intramolecular energy migration, a higher intensity band often originates from the lower energy sites. Thus, efficient energy migration in poly(Cy3) led to dominating red-shifted emission band at 648 nm, with a low-intensity residual band at ~540 nm. In contrast to poly(Cy3), fluorescence spectrum of poly(Cy5) clearly showed two bands, with the more intense band at 666 nm and a red-shifted less intense band at 732 nm (Figure 5. 4b).

The origin of the dual-band absorption and fluorescence spectra of poly(cyanine)s is currently not clear. It is known that monomeric cyanine dyes are prone to aggregation even in solution, resulting in the aggregates both with hypsochromically and bathochromically shifted new absorption bands (so called *H* and *J* aggregates).[35-37] Thus, the dual absorption and fluorescence bands could result from such aggregation. Typically, the aggregation behavior is strongly affected by concentration, resulting in concentration dependence of the aggregation-related spectroscopic features.[38-40] With both poly(Cy3) and poly(Cy5), normalized absorption spectra showed only a slight change upon a 32-fold increase in the polymers' concentration (Figure 5. 5).

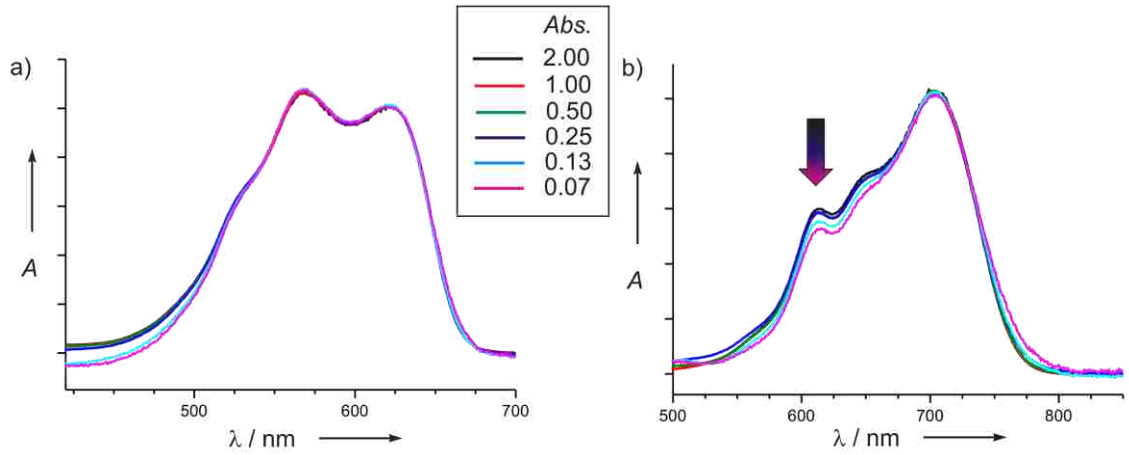

Figure 5. 5 Normalized absorption spectra of **5-5** (a) and **5-7** (b) at different concentrations in methanol. The trace colors correspond to the absorbance values shown in the square box.

Furthermore, the polymers' absorption spectra followed Beers' law in this concentration range (optical density change from 0.063 to 2.00). In addition to concentration, aggregation behavior often depends on temperature;[41] however no appreciable spectral change was observed upon increasing temperature of the dilute polymer solutions from 20 to 50 ℃ (Figure 5. 6). Therefore, the dual-band nature of the poly(cyanine) spectra cannot be attributed to intermolecular aggregation. Considering the initially proposed conformational flexibility of the poly(cyanine)s, it is more likely that appearance of the two bands indicate the presence of two distinct types of chromophores in the conjugated backbone: one with a lower and another with a higher conjugation length.

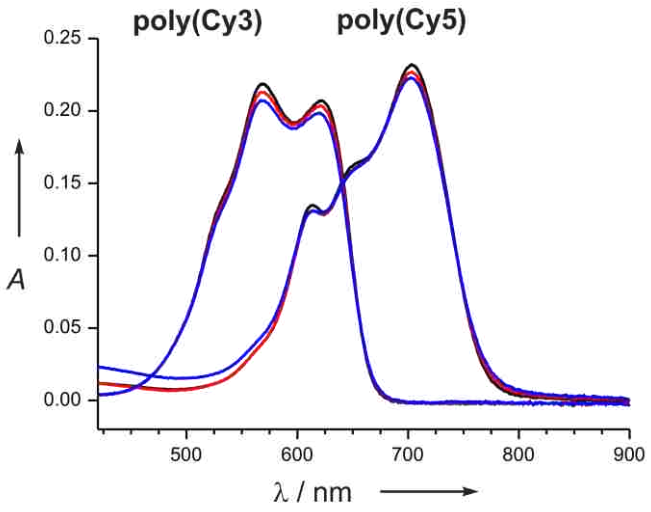

Figure 5. 6 Absorption spectra of poly(Cy3) and poly(Cy5) in methanol solution at 20 ℃ (black traces), 35 ℃ (red traces), and 50 ℃ (blue traces).

The existence of "kinks" and other conformational defects leading to electronically isolated conjugated subunits in the polymer backbone is commonly postulated for CPs.[46] Thus it is possible that statistical distribution of such conjugated subunits within the individual poly(cyanine) chains could be reflected in the presence of the two spectral bands. Intramolecular energy transfer from the higher to the lower energy subunits would occur as an exciton hopping by dipole - induced dipole mechanism and result in the experimentally observed redistribution of the emission band intensities.[43,44] Such energy redistribution agreed well with the excitation spectra of poly(Cy3) and poly(Cy5) which showed excitation bands at the same wavelengths as those in the absorption spectra, but of different relative intensities. Whereas a red-shifted band dominated fluorescence spectrum of poly(Cy3) due to complete energy transfer to the lower energy backbone subunits, the presence of two emission bands with comparable intensities in the fluorescence spectrum of poly(Cy5) in methanol solution (Figure 5. 4b) opened an interesting possibility to control their ratio by changing environment. Changing viscosity of the environment by choosing a more viscous

solvent was the simplest test. Retarding molecular motion in the more viscous solvents would slow excited state decay through non-radiative channels (by preventing molecular vibration and double-bond isomerisation[45,46,48]).

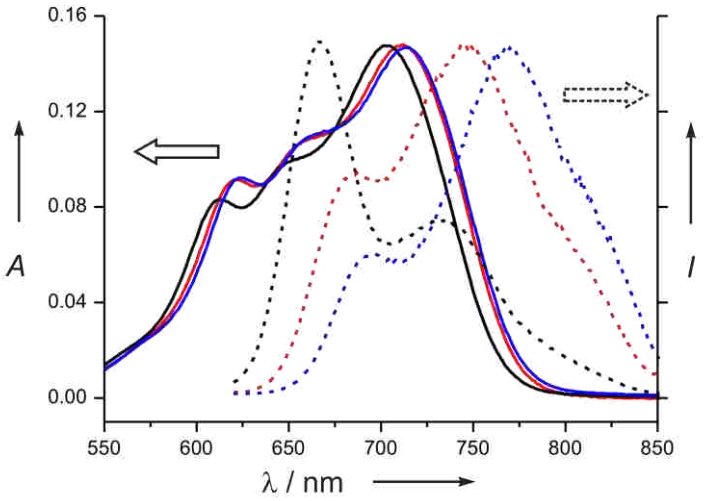

Figure 5. 7 Absorption (solid traces) and normalized fluorescence (dash traces) spectra of poly(Cy5) solutions in methanol (black traces), ethylene glycol (red traces), and glycerol (blue traces). Fluorescence spectra were acquired at 600 nm excitation.

This would increase the exciton lifetime to enable more efficient energy migration to the lower energy chromophore subunits, resulting in higher intensity of the longer-wavelength emission band, and (possibly) its further bathochromic shifting. In excellent agreement with this prediction, switching from methanol (viscosity η 0.59 mPa s) to ethylene glycol (η 13.5 mPa s) to glycerol (η 945 mPa s) had the profound effect on the poly(Cy5) spectra (Figure 5. 7). While the absorption maxima showed only moderate bathochromic shifts (indicating only a small change in the polymer conformation), complete reversion of relative intensities was observed for the two emission bands, along with significant bathochromic shift of these bands. While gaining deeper insight into this behavior requires further extensive studies (which are currently being carried out), such dramatic response on changing environment could be a valuable property in designing

fluorescent bio- and chemosensors.

Interestingly, both poly(cyanine)s showed no substantial aggregation features (formation of new spectral bands) even in thin films. Their thin-film featureless broad absorption spectra generally matched the solution spectra and appeared to be a superposition of the absorption bands from numerous subunit chromophores in the conjugated backbone (Figure 5. 4).

As expected, due to the three-dimensionally enhanced exciton migration in solid films,[47,48] thin-film emission spectra originated from the lowest energy gap subunits, and therefore were dramatically red-shifted compared to solution spectra (especially for poly(Cy5)).

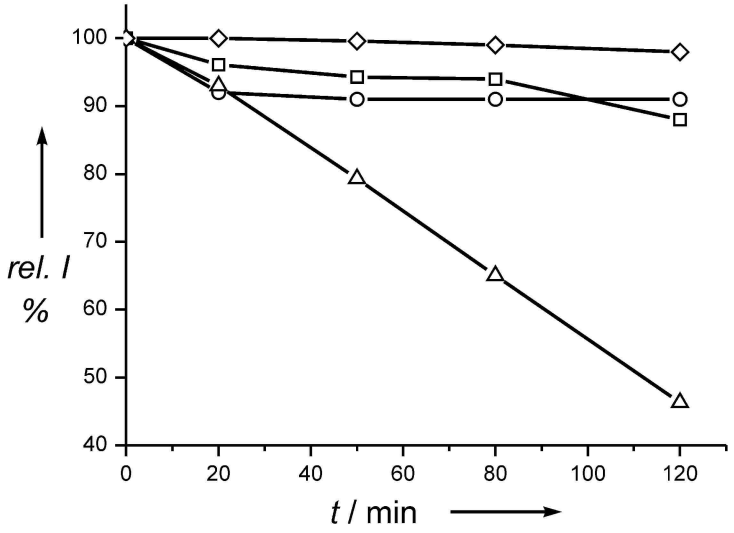

Figure 5. 8 Change in integrated fluorescent intensity of cyanine compounds upon continuous irradiation with 18 mW cm^{-2} monochromatic light (550 nm for Cy3 / poly(Cy3), 650 nm for Cy5 / poly(Cy5)) in air-exposed methanol solutions. Cy3 – squares, poly(Cy3) – circles, Cy5 – triangles, poly(Cy5) – diamonds.

In addition to NIR spectral characteristics, poly(cyanine)s showed exceptional stability against photodegradation. Rapid photobleaching is a known drawback of NIR cyanine dyes.[49,50] Both poly(Cy3) and poly(Cy5) were remarkably stable upon intense

irradiation of their air-exposed methanol solutions (Figure 5. 8). Thus, irradiation of poly(Cy5) with 650 nm monochromatic light of 18 mW cm^{-2} power density for 2 h led to practically no change in its fluorescence intensity.

In contrast, the fluorescence intensity of Cy5 solution dropped by more than 50% after irradiation in the same conditions. Future practical applications of poly(cyanine)s will definitely benefit from this increased photostability.

5.3. Conclusions

Two poly(cyanine)s – representatives of a novel class of highly soluble polycationic NIR fluorescent CPs – have been prepared and characterized. These exceptionally photostable polymers with significant electronic delocalization exhibited dual-band absorption and fluorescence spectra which showed dramatic response on changing environment. These features will benefit potential applications of poly(cyanine)s as NIR fluorescent chemo- and biodetectors, optoelectronic materials, etc. However, further studies on fundamental properties and practical applications of this new family of fluorescent CPs will be required in the future.

5.4. References

1. *Handbook of Conducting Polymers*, 3rd ed., Vol. 2 (Eds: Skotheim, T. A.; Reynolds, J. R.), CRC Press, Boca Raton, 2007.

2. Thomas III, S. W.; Joly, G. D.; Swager, T. M. Chemical Sensors Based on Amplifying Fluorescent Conjugated Polymers. *Chem. Rev*. **2007**, *107*, 1339-1386.

3. Swager, T. M. The Molecular Wire Approach to Sensory Signal Amplification. *Acc. Chem. Res*. **1998**, *31*, 201-207.

4. Ego, C.; Marsitzky, D.;Becker, S.; Zhang, J.; Grimsdale, A. C.; Müllen, K.; MacKenzie, J. D.; Silva, C.; Friend,e R. H. Attaching Perylene Dyes to Polyfluorene: Three Simple, Efficient Methods for Facile Color Tuning of Light-Emitting Polymers. *J. Am. Chem. Soc*. **2003**, *125*, 437-443.

5. Grimsdale, A. C.; Chan, K. L.; Martin, R. E.; Jokisz, P. G.; Holmes, A. B. Synthesis of Light-Emitting Conjugated Polymers for Applications in Electroluminescent Devices. *Chem. Rev*. **2009**, *109*, 897-1091.

6. Ho, H.-A.; Najari, A.; Leclerc, M. Optical Detection of DNA and Proteins with Cationic Polythiophenes. Optical Detection of DNA and Proteins with Cationic Polythiophenes. *Acc. Chem. Res*. **2008**, *41*, 168-178.

7. Béra-Abérem, M.; Ho, H.-A.; Leclerc, M. Functional polythiophenes as optical chemo- and biosensors. *Tetrahedron* **2004**, *60*, 11169-11173.

8. Abérem, M. B.; Najari, A.; Ho, H.-A.; Gravel, J.-F.; Nobert, P.; Boudreau, D.; Leclerc, M. Protein Detecting Arrays Based on Cationic Polythiophene–DNA-Aptamer Complexes. *Adv. Mater*. **2006**, *18*, 2703-2707.

9. Nilsson, K. P. R.; Inganäs, O. Chip and solution detection of DNA hybridization using a luminescent zwitterionic polythiophene derivative. *Nat. Mater*. **2003**, *2*, 419-424.

10. Nilsson, K. P. R.; Å slund, A.; Berg, I.; Nyström, S.; Konradsson, P.; Herland, A.; Inganäs, O.; Stabo-Eeg, F.; Lindgren, M.; Westermark, G. T.; Lannfelt, L.; Nilsson, L. N. G.; Hammarström, P. Imaging Distinct Conformational States of Amyloid-β Fibrils in Alzheimer's Disease Using Novel Luminescent Probes. *ACS Chem. Biol*. **2007**, *2*, 553-560.

11. Feng, F.; He, F.; An, L.; Wang, S.; Li, Y.; Zhu, D. Fluorescent Conjugated Polyelectrolytes for Biomacromolecule Detection. *Adv. Mater*. **2008**, *20*, 2959-2964.

12. Li, C.; Numata, M.; Takeuchi, M.; Shinkai, S. A Sensitive Colorimetric and Fluorescent Probe Based on a Polythiophene Derivative for the Detection of ATP. *Angew. Chem. Int. Ed*. **2005**, *44*, 6371-6374.

13. Terpetschnig, E.; Wolfbeis, O. S. *in Near-Infrared Dyes for High Technology Applications, NATO ASI Series*, Vol. 52 (Eds: Daehne, S.; Resch-Genger, U.; Wolfbeis, O. S.), Kluwer Academic Publishers, Dordrecht, 1998, pp. 161-182.

14. Becker, A.; Hessenius, C.; Licha, K.; Ebert, B.; Sukowski, U.; Semmler, W.; Wiedenmann, B.; Grötzinger, C. Receptor-targeted optical imaging of tumors with near-infrared fluorescent ligands. *Nat. Biotechnol*. **2001**, *19*, 327-331.

15. Bundgaard, E.; Krebs, F. C. Low band gap polymers for organic photovoltaics. *Sol. En. Mater. Sol. Cells* **2007**, *91*, 953.

16. Kroon, R.; Lenes, M.; Hummelen, J. C.; Blom, P. W. M.; Boer, B. de. Small Bandgap Polymers for Organic Solar Cells. *Polym. Rev*. **2008**, *48*, 531-582.

17. Cheng, Y.-J.; Yang, S.-H.; Hsu, C.-S. Synthesis of Conjugated Polymers for Organic

Solar Cell Applications. *Chem. Rev*. **2009**, *109*, 5868-5923.

18. Ajayaghosh, A. Chemistry of Squaraine-Derived Materials: Near-IR Dyes, Low Band Gap Systems, and Cation Sensors. *Acc. Chem. Res*. **2005**, *38*, 449-459.

19. Ajayaghosh, A. Donor–acceptor type low band gap polymers: polysquaraines and related systems. *Chem. Soc. Rev*. **2003**, *32*, 181-191.

20. Duncan, T. V.; Susumu, K.; Sinks, L. E.; Therien, M. J. Exceptional Near-Infrared Fluorescence Quantum Yields and Excited-State Absorptivity of Highly Conjugated Porphyrin Arrays. *J. Am. Chem. Soc*. **2006**, *128*, 9000-9001.

21. Ghoroghchian, P. P.; Frail, P. R.; Susumu, K.; Blessington, D.; Brannan, A. K.; Bates, F. S.; Chance, B.; Hammer, D. A.; Therien, M. J. Near-infrared-emissive polymersomes: Self-assembled soft matter for *in vivo* optical imaging. *Proc. Natl. Acad. Sci. U. S. A*. **2005**, *102*, 2922-2927.

22. Donuru, V. R.; Vegesna, G. K.; Velayudham, S.; Meng, G.; Liu, H. *J*. Deep-red emissive conjugated poly(2,6-BODIPY-ethynylene)s bearing alkyl side chains. *Polym. Sci., Part A: Polym. Chem*. **2009**, *47*, 5354-5366.

23. Alemdaroglu, F. E.; Alexander, S. C.; Ji, D.; Prusty, D. K.; Börsch, M.; Herrmann, A. Poly(BODIPY)s: A New Class of Tunable Polymeric Dyes. *Macromolecules* **2009**, *42*, 6529-6536.

24. Yan, Q.; Zhao, D. Conjugated Dimeric and Trimeric Perylenediimide Oligomers. *Org. Lett*. **2009**, *11*, 3426-3429.

25. Mishra, A.; Behera, R. K.; Behera, P. K.; Mishra, B. K.; Behera, G. B. Cyanines during the 1990s: A Review. *Chem. Rev*. **2000**, *100*, 1973-2011.

26. Fabian, J.; Nakazumi, H.; Matsuoka, M. Near-infrared absorbing dyes. *Chem. Rev*. **1992**, *92*, 1197-1226.

27. Tolbert, L. M.; Zhao, X. Beyond the Cyanine Limit: Peierls Distortion and Symmetry Collapse in a Polymethine Dye. *J. Am. Chem. Soc*. **1997**, *119*, 3253-3258.

28. Ohira, S.; Hales, J. M.; Thorley, K. J.; Anderson, H. L.; Perry, J. W.; Brédas, J.-L. A New Class of Cyanine-like Dyes with Large Bond-Length Alternation. *J. Am. Chem. Soc*. **2009**, *131*, 6099-6101.

29. R. C. Benson, H. A. Kues, Absorption and fluorescence properties of cyanine dyes. *J. Chem. Eng. Data* **1977**, *22*, 379-383.

30. Mujumdar, S. R.; Mujumdar, R. B.; Grant, C. M.; Waggoner, A. S. Cyanine-Labeling Reagents: Sulfobenzindocyanine Succinimidyl Esters. *Bioconjugate Chem*. **1996**, *7*,

356-362.

31. Geiger, T.; Benmansour, H.; Fan, B.; Hany, R.; Nüesch, F. Low-Band Gap Polymeric Cyanine Dyes Absorbing in the NIR Region. *Macromol. Rapid Commun*. **2008**, *29*, 651-658.

32. Mujumdar, R. B.; Ernst, L. A.; Mujumdar, S. R.; Lewis, C. J.; Waggoner, A. S. Cyanine dye labeling reagents: Sulfoindocyanine succinimidyl esters. *Bioconjugate Chem*. **1993**, *4*, 105-111.

33. Yamamoto, T.; Morita, A.; Miyazaki, Y.; Maruyama, T.; Wakayama, H.; Zhou, Z.; Nakamura, Y.; Kanbara, T.; Sasaki, S.; Kubota, K. Preparation of π-conjugated poly(thiophene-2,5-diyl), poly(p-phenylene), and related polymers using zerovalent nickel complexes. Linear structure and properties of the π-conjugated polymers. *Macromolecules* **1992**, *25*, 1214-1223.

34. Turro N. J. *Modern Molecular Photochemistry*, University Science Books, Sausalito, CA, 1991.

35. Hannah, K. C.; Armitage, B. A. DNA-Templated Assembly of Helical Cyanine Dye Aggregates: A Supramolecular Chain Polymerization. *Acc. Chem. Res*. **2004**, *37*, 845-853.

36. Gadde, S.; Batchelor, E. K.; Kaifer, A. E. Controlling the Formation of Cyanine Dye H- and J-Aggregates with Cucurbituril Hosts in the Presence of Anionic Polyelectrolytes. *Chem. Eur. J*. **2009**, *15*, 6025-6031.

37. Kim, J. S.; Kodagahally, R.; Strekowski, L.; Patonay, G. A study of intramolecdular H-complexes of novel bis(heptamethine cyanine) dyes. *Talanta*. **2005**, *67*, 947-954.

38. Yao, S.; Beginn, U.; Gress, T.; Lysetska, M.; Würthner, F. Supramolecular Polymerization and Gel Formation of Bis(Merocyanine) Dyes Driven by Dipolar Aggregation. *J. Am. Chem. Soc.* **2004**, *126*, 8336-8348.

39. Takahashi, D.; Oda, H.; Izumi, T.; Hirohashi, R. Substituted effects on aggregation phenomena in aqueous solution of thiacarbocyanine dyes. *Dyes Pigm*. **2005**, *66*, 1-6.

40. Rösch, U.; Yao, S.; Wortmann, R.; Würthner, F. Fluorescent H-Aggregates of Merocyanie Dyes. *Angew. Chem. Int. Ed*. **2006**, *45*, 7026-7030.

41. Wang, M.; Silva, G. L.; Armitage, B. A. DNA-Templated Formation of a Helical Cyanine Dye J-Aggregate. *J. Am. Chem. Soc*. **2000**, *122*, 9977-9986.

42. Scholes, G. D.; Rumbles, G. Excitons in nanoscale systems. *Nat. Mater*. **2006**, *5*, 683-696.

43. Beljonne, D.; Pourtois, G.; Silva, C.; Hennebicq, E.; Hertz, L. M.; Friend, R. H.; Scholes, G. D.; Setayesh, S.; Müllen, K.; Brédas, J. L. Interchain vs. intrachain energy transfer in acceptor-capped conjugated polymers. *Proc. Nat. Acad. Sci. U. S. A.* **2002**, *99*, 10982-10987.

44. Nguyen, T.-Q.; Wu, J.; Doan, V.; Schwartz, B. J.; Tolbert, S. H. Control of Energy Transfer in Oriented Conjugated Polymer-Mesoporous Silica Composites. *Science.* **2000**, *288*, 652-656.

45. Dietzek, B.; Brüggemann, B.; Pascher, T.; Yartsev, A. Pump-Shaped Dump Optimal Control Reveals the Nuclear Reaction Pathway of Isomerization of a Photoexcited Cyanine Dye. *J. Am. Chem. Soc*. **2007**, *129*, 13014-13021.

46. Martini, I.; Hartland, G. V.; Ultrafast Investigation of Vibrational Relaxation in the S_1 Electronic State of HITC. *J. Phys. Chem*. **1996**, *100*, 19764-19770.

47. Levitsky, I. A.; Kim, J. ; Swager, T. M. Energy Migration in a Poly(phenylene ethynylene): Determination of Interpolymer Transport in Anisotropic Langmuir−Blodgett Films. *J. Am. Chem. Soc*. **1999**, *121*, 1466-1472.

48. Levitsky, I. A.; Kim, J.; Swager, T. M. Mass and Energy Transport in Conjugated Polymer Langmuir−Blodgett Films: Conductivity, Fluorescence, and UV−Vis Studies. *Macromolecules* **2001**, *34*, 2315-2319.

49. Song, F.; Peng, X.; Lu, E.; Zhang, R.; Chen, X.; Song, B. Syntheses, spectral properties and photostabilities of novel water-soluble near-infrared cyanine dyes. *J. Photochem. Photobiol. A*. **2004**, *168*, 53-57.

50. Johnson, J. R.; Fu, N.; Arunkumar, E.; Leevy, W. M.; Gammon, S. T.; Piwnica-Worms, D.; Smith, B. D. Squaraine Rotaxanes: Superior Substitutes for Cy-5 in Molecular Probes for Near-Infrared Fluorescence Cell Imaging. *Angew. Chem. Int. Ed.* **2007**, *46*, 5528-5531.

CHAPTER 6. EXPERIMENTAL

6.1. Experimental Details

All reactions were performed under an atmosphere of dry nitrogen. Melting points were determined in open capillaries and are uncorrected. Column chromatography was performed on silica gel (Sorbent Technologies, 60 Å, 40-63μm) slurry packed into glass columns. THF, ether, toluene, dichloromethanem and hexane were dried by passing through activated alumina, and DMF – by passing through activated molecular sieves, using a PS-400 Solvent Purification System from Innovative Technology, Inc. The water content of the solvents was periodically controlled by Karl Fischer titration (using a DL32 coulometric titrator from Mettler Toledo). Isopropylmagnesium chloride (2.0M solution in THF) was purchased from Acros Organics. All other reagents and solvents were obtained from Aldrich and Alfa Aesar and used without further purification.

^{1}H NMR spectra were acquired at 250 and 400 MHz and are reported in ppm downfield from tetramethylsilane (TMS). ^{31}P NMR spectra were acquired at 161 MHz and are reported in ppm relative to 80% aqueous H_3PO_4 as external standards.

UV-visible spectra were recorded on Varian Cary 50 UV-Vis spectrophotometer supplied with a temperature-controlled multicell holder. Fluorescence studies were carried out with a PTI QuantaMaster4/2006SE spectrofluorimeter equipped with a water-heated cell holder connected to a Neslab RTE-7 thermostat for variable-temperature experiments. Fluorescence quantum yields were determined using ethanol solution of Coumarin 6 (Φ = 0.78[1]) as standards.

Thermogravimetric analysis (TGA) of solid polymer samples was performed using TGA 2950 from TA Instruments (New Castle, DE) at the heating rate of 10°C min^{-1} in a

nitrogen atmosphere. Solid-state differential calorimetry (DSC) experiments were performed with DSC 2920 from TA Instruments (New Castle, DE) at the heating rate 10℃ min^{-1} in a nitrogen atmosphere. Aqueous solution DSC experiments were performed on a MicroCal VP-DSC. Buffer baselines were subtracted to obtain the excess heat capacity curves, which were analyzed using the manufacturer supplied MicroCal Origin DSC software, Version 5.0.

GPC analyses of polymers were performed with Agilent 1100 chromatograph equipped with two PLgel 5 μm MIXED-C and one PLgel 5 μm 1000 Å columns connected in series, using THF as a mobile phase, and calibrated against polystyrene standards. GPC data for side chain grafted copolymers were acquired with Agilent 1200 chromatograph series equipped with three Phenogel 5 μm, 300 X 7.8 mm columns (100 Å, 1000 Å, and Linear(2)) connected in series, using 0.1M LiBr solution in DMF as a mobile phase, and Wyatt Optilab rEX multiangle light scattering detector. The specific refractive index increment (d*n*/d*c*) was measured from a series of polymer solutions in 0.1M LiBr in DMF with different polymer concentrations using a Wyatt Optilab rEX differential refractometer.

Thin-film polymer samples were spin-casted at 1500~4000 rpm from variable solutions using Laurell Technologies WS-400B-6NPP spin processor.

Water content in polymers was determined by dissolving a vacuum dried polymer sample in anhydrous dichloromethane (water content 1.8ppm) with subsequent Karl Fischer titration using a DL32 coulometric titrator (Mettler Toledo).

All electrochemical experiments were performed using an Autolab PGSTAT 302 potentiostat from Eco Chemie using a standard three-electrode system with Pt button electrode (diameter 2 mm, CH Instruments, Inc.), $Ag/AgNO_3$ non-aqueous reference electrode, and a Pt gauze counter electrode.

High resolution mass spectra were obtained at the LSU Department of Chemistry Mass Spectrometry Facility using an ESI method, and a peak matching protocol to determine the mass and error range of the molecular ion, or a MALDI-TOF method with tert-thiophene matrix.

Dynamic Light Scattering (DLS) Measurements were carried out with a Zetasizer nano ZS instrument (Malvern Instruments, Malvern, U.K.). This system is equipped with a 4 mW He/Ne laser at a wavelength of 632.8 nm and measures the particle size using noninvasive backscattering at a detection angle of 173. Temperature (20^{o}C~50^{o}C) was controlled by the instrument (Thermoelectric cooling/heating). At least 12 measurements of the correlation time of scattered light intensity, G(τ), were averaged for each sample. The data were fitted to equation 1, where B is baseline, A is amplitude, q is the scattering vector, τ is delay time and D is the diffusion coefficient:

$$G(\tau) = B + Ae^{-2q2D\tau} \qquad (1)$$

The hydrodynamic radius (R_H) of the scattering particles is inversely proportional to the diffusion coefficient D and the solvent viscosity (η), as shown in the Stokes–Einstein equation (eq 2), where k_B is Boltzmann's constant and T denotes the absolute temperature:

$$R_H = k_B T (6\pi\eta D)^{-1} \qquad (2)$$

Frequency-domain lifetime fluorescent measurements were performed using a Spex Fluorolog-3 spectrofluorometer (model FL3-22TAU3; HORIBA Jobin Yvon, Edison, NJ). Fluorescent decay times were measured using a variable frequency phase-modulation technique. The system used a 450W Xe arc lamp light source and a Hamamatsu R928 PMT detector operating at 950 V. Full-sized 1cm quartz cells were placed in a carousel thermostated cell holder and used with a 450 nm excitation. The emission was collected

through a 500 nm long pass filter. Thirty-eight logarithmically spaced frequencies were collected over a frequency range of 10 ~ 174.6 MHz using five averages and a 10 s integration time at each frequency. Frequency-domain measurements were collected versus Ludox, a scatter reference solution, which showed lifetime of 0 ns. Constant phase and modulation errors of 0.5^{o} and 0.005 were used in analyses for consistency and ease of day-to-day data interpretation.

Photobleaching experiments were performed using a monochromatic irradiation produced by a Newport 66353 300W Xe lamp, controlled by a Newport 68945 Digital Exposure Controller through an electromechanical shutter. The monochromic light of a required wavelength (550 nm for **Cy3** / **poly(Cy3)** and 650 nm for **Cy5** / **poly(Cy5)**) was selected using a Newport 77250 high throughput monochromator. The incident light intensity was measured by a Newport 70260 Radiant Power Meter equipped with a Newport 70268 probe, and adjusted to the same value (18 mW cm^{-2}) for all experiments. Samples were prepared as solutions in methanol with the same optical density (~ 0.1 a.u.) at irradiation wavelength for the corresponding pairs monomer / polymer and were irradiated in an open rectangular quartz fluorescence cuvette (1 cm path length) for specified periods, after which fluorescence spectra were acquired to determine the extent of photobleaching.

6.2. Synthesis of Water-Soluble PNIPAm-Grafted Polythiophene Copolymers

2,5-Dibromo-3-(2-hydroxyethyl)thiophene. NBS (6.75 g, 37.9 mmol) was added in a few small portions over period of 30 min to a stirred at 0 ℃ solution of 4.82 g (37.6 mmol) of 2-(3-thienyl)ethanol in 50 ml of THF. After the addition was completed, the reaction mixture was stirred at 0 ℃ for 2 h, poured into water, extracted with diethyl ether (3 × 50 ml), washed with water and dried over Na_2SO_4. The resulting solution was filtered through a short plug of silica gel eluted with ether, and concentrated in vacuo to afford 6.0 g (84%) of

the resulting compound as yellowish oil. The ^{1}H NMR data were consistent with those published in literature.[2]

2-[(2,5-dibromothiophen-3-yl)ethyloxy]-*tert*-butyldimethylsilane (**2-1**). Imidazole (4.9 g, 73.0 mmol) was added to a solution of 6.0 g (29.0 mmol) of the precursor compound in 60 ml of DMF and the resulting mixture was stirred at room temperature for 15 min. This was followed by addition of 5.2 g (35.0 mmol) of TBDMS-Cl in 10 ml of DMF. The reaction mixture was stirred for 16 h at room temperature, poured into water-ice mixture, extracted with hexane (3 × 60 ml), the organic fraction was washed with water, and dried over Na_2SO_4. Concentration in vacuo afforded crude product that was purified by column chromatography on silica gel (eluent hexane – EtOAc 3:1) to yield 8.0 g (95%) of **2-1** as colorless oil, R_f 0.8 ^{1}H NMR (250 MHz, $CDCl_3$) δ 6.85 (s, 1H), 3.75 (t, J = 6.8 Hz, 2H), 2.75 (t, J = 6.8Hz , 2H), 0.87 (s, 9H), 0.00 (s, 6H). HRMS *m/e* 397. $[M+H]^+$ (calcd for $C_{25}H_{18}IO_2$ 477.0351).

Polymer 2-3. A solution of *tert*-BuMgBr (0.9 ml of 1,4 M solution in THF-toluene, 1.25 mmol) was added dropwise to a solution of 0.5 g (1.25 mmol) of **2-1** in 20 ml of THF, and the resulting mixture was stirred at reflux conditions for 2 h. A catalytic amount of Ni(dppp)Cl_2 (6 mg) was added in one portion and the reaction mixture was stirred at reflux conditions for 20 h. Precipitation into 120 ml of methanol resulted in a dark red polymer which was placed into a Soxhlet extractor, and extracted successively with methanol, hexane, and $CHCl_3$. The chloroform fraction yielded 0.12 g (20%) of **2-3** as dark-red solid material, M_n (GPC, vs. polystyrene) 12000, D 1.55. ^{1}H NMR (400 MHz, $CDCl_3$) δ 7.08 (s, 1H), 3.89 (s, 2H), 2.99 (s, 2H), 0.99 (s, 9H), 0.00 (s, 6H). Polymer **2-4** was prepared following the procedure for polymer **2-3**.

Regiorandom polymer **2-2** was prepared following the same procedure but using catalytic

amount of $Ni(PPh_3)_2Cl_2$ instead of $Ni(dppp)Cl_2$. M_n (GPC, vs. polystyrene) 8000, *D* 1.32. ^{1}H NMR (400 MHz, $CDCl_3$) δ 7.02 (s, 1H), 3.81 (s, 2H), 2.87 (s, 2H), 0.86 (s, 9H), 0.07 (s, 6H).

Polymer 2-6. A solution of tetrabutylammonium fluoride (2 ml of 0.1 M solution in THF, 0.26 mmol) was added dropwise over the period of 2 h (syringe pump) to a mixture of 50 mg (0.24 mmol) of polymer **2-3**, 0.48 g of 2-bromoisobutyryl bromide (0.26 ml, 2.4 mmol), 36 µl of triethylamine (0.26 mmol) in 20 ml of THF at room temperature, and the resulting mixture was stirred at room temperature for 16 h. Precipitation into methanol and washing with acetone yielded in 45mg (90%) of **2-3** as dark red solid material, M_n (GPC, vs. polystyrene) 12000, *D* 1.55. ^{1}H NMR (400 MHz, $CDCl_3$) δ 7.17 (s, 1H), 4.47 (s, 2H), 3.23 (s, 2H), 1.93 (s, 6H).

Polymers **2-5** and **2-7** were prepared exactly following the procedure for **2-3** starting from **2-2** and **2-4**, respectively. **2-5**: M_n (GPC, vs. polystyrene) 8000, *D* 1.32. ^{1}H NMR (400 MHz, $CDCl_3$) δ 7.16 (s, 1H), 4.40 (s, 2H), 3.11 (s, 2H), 1.93 (s, 6H). **2-7**: M_n (GPC, vs. polystyrene) 12000, *D* 1.56. ^{1}H NMR (250 MHz, $CDCl_3$) δ 7.17 (s, 1H), 4.48 (s, 2H), 3.22 (s, 2H), 1.93 (s, 6H).

Polymer 2-9. An air-free flask was charged with 20 mg (0.14 mmol) of CuBr, 1.5 g (14.0 mmol) of *N*-isopropylacrylamide, and 31 mg (0.14 mmol) of 1,4,8,11-tetramethyl-1,4,8,11-tetraazacyclotetradecane, evacuated and backfilled with Ar 3 times, filled with 10 ml of THF, cooled in an ice bath, and purged with Ar for 10 min. After 15 min, a separately prepared and degassed in an air-free flask solution of 40 mg (0.14 mmol based on repeating unit) of **2-6** in 35 ml of THF was added dropwise via cannula. The resulting mixture was stirred at 0 ℃ for 2.5 h, then it was poured into 200 ml of hexane to precipitate a crude polymer

product. The precipitate was thoroughly washed twice with diethyl ether, redissolved in THF, and precipitated into hexane. Finally, this precipitate was redissolved in THF and filtered through a short plug of silica gel eluted with THF to remove catalyst. The THF solution was again precipitated from hexane and dried in vacuo to afford 0.9 g (66%) of **2-9** as bright yellow solid material, M_n (GPC using light-scattering detector) 1.46 × 10^5, *D* 1.46. ^{1}H NMR (250 MHz, $CDCl_3$) δ 6.8-6.2 (br. s, 1H), 3.98 (s, 1H), 2.47 (s, 1H), 2.2-1.62(br. s, 2H) 1.13 (s, 6H).

Polymers 2-8 and **2-10** were prepared following the same procedure starting from **2-5** and **2-7**, respectively. **2-8**: M_n (GPC using light-scattering detector) 4.54 × 10^5, *D* 1.88. ^{1}H NMR (250 MHz, $CDCl_3$) δ 6.8-6.2 (br. s, 1H), 3.98 (s, 1H), 2.47 (s, 1H), 2.2-1.62(br. s, 2H) 1.13 (s, 6H). **2-10**: M_n (GPC using light-scattering detector) 1.71 × 10^5, *D* 1.71. ^{1}H NMR (250 MHz, $CDCl_3$) δ 6.8-6.2 (br. s, 1H), 3.98 (s, 1H), 2.47 (s, 1H), 2.2-1.62(br. s, 2H) 1.13 (s, 6H).

6.3. Synthesis of Thiophene Polymers and Block Copolymers by Externally-Initiated Chain-Growth Living Polymerization.

Bis[1,3-bis(diphenylphosphino)propane]nickel(0) (**Ni(dppp)$_2$**) was prepared following the literature procedure.[3] To a vigorously stirred mixture of 1.50 g (5.84 mmol) of nickel(II) bis(acetylacetonate) (Ni(acac)$_2$) and 4.82 g (11.7 mmol) of 1,3-bis(diphenylphosphino)-propane (dppp) in 80 ml of ether and 15 ml of toluene, a solution of *i*-Bu_3Al (19.8 ml of 1.0 M solution in hexanes, 19.8 mmol) was added slowly over a 1 h period (syringe pump) in Ar atmosphere. The resulting mixture was stirred at room temperature for 24 h, and during this period the solution color changed from bright-green to bright-red. The reaction mixture was left to stay unperturbed for additional 24 h, and the resulting precipitate was filtered under argon, and washed with excess ether to give 3.5 g (68%) of the product as a

bright-orange solid material, mp 281 ℃, decomp. (lit.[3] mp 281-283 ℃).

Crude External Initiator (3-2) (the "Indirect" method): To $Ni(PPh_3)_4$ (0.11g, 0.1mmol) chlorobenzene was added in a 20mL vial at room temperature followed by addition of dppp (55mg, 0.1mmol). The mixture was stirred for 5 hr and was allowed to stay unperturbed for 24hr.

Crude External Initiator (3-2) (the "Direct" method): To $Ni(dppp)_2$ (80mg, 0.09mmol) chlorobenzene was added in a 20 mL vial at room temperature. The mixture was stirred for 5 hr and was allowed to stay unperturbed for 24hr.

External Bithiophene Initiator (3-3): 2-Bromobithiophene (0.10 g, 0.4 mmol) was added to a solution of 1.06 g (1.2 mmol) of $Ni(dppp)_2$ in 25 ml of toluene at room temperature. The resulting mixture was stirred at 35 ℃ for 24 h and was left without stirring for additional 24 h. After precipitating into hexanes, the precipitate was collected and thoroughly washed with the mixture of toluene-hexanes to afford 0.20 g (44%) of **3-3** as a yellowish-green solid, mp 126-130 ℃, decomp. ^{1}H NMR (400 MHz, THF-D_8) δ 7.85 - 7.72 (m, 16H), 7.71 - 7.60 (m, 1 H), 7.52 - 7.30 (m, 24H), 7.25 - 7.0 (m, 4H), 2.60 - 2.40 (m, 8H), 2.00 - 1.75 (m, 4H). ^{31}P NMR (161 MHz, THF-D_8) δ 28.2 (s).

General Procedure for Externally-Initiated "Living" Kumada Polymerization: Poly(3-hexylthiophene), P3HT: Polymer (3-8).

A solution of *i*-PrMgCl (0.75 ml of 2.0 M solution in THF, 1.5 mmol) was added dropwise to a stirred solution of 0.49 g (1.5 mmol) of 2,5-dibromo-3-hexylthiophene in 22 ml of THF at 0 ℃, and the resulting solution was stirred for 1 h at this temperature to yield a solution of Grignard reagent **3-6**. A solution of 5.1 mg (4.5 μmol) of the initiator **3-3** in 2 ml of toluene was added to the Grignard reagent solution and the reaction mixture was stirred at 35 ℃ for 1 h. Precipitation into 120 ml of methanol resulted in a crude dark-purple polymer which

was placed into a Soxhlet extractor, and extracted successively with methanol, hexane, and $CHCl_3$. The chloroform fraction yielded 0.10 g (40%) of **3-8** as a dark-purple solid, M_n 48 kDa, PDI 1.35 (GPC, vs. polystyrene). ^{1}H NMR (400 MHz, $CDCl_3$) δ 6.96 (s, 1H), 2.85 – 2.65 (m, 2H), 1.75 - 1.10 (m, 8H), 0.95 - 0.75 (m, 3H).

Block Copolymer 3-9-1 A solution of *i*-PrMgCl (0.38 ml of 2.0 M solution in THF, 0.77 mmol) was added dropwise to a stirred solution of 0.25 g (0.77 mmol) of 2,5-dibromo-3-hexylthiophene in 15 ml of THF at 0 ℃, and the resulting solution was stirred for 1 h at this temperature to yield solution of the Grignard reagent **3-6**. A solution of 3.45 mg (3.06 μmol) of complex **3-3** in 2 ml of toluene was added to the Grignard reagent solution and the reaction mixture was stirred at 35 ℃ for 1 h. A solution of the Grignard reagent **3-7** (prepared separately at 0 ℃ from 1.53 g (3.83 mmol) of 2-[(2,5-dibromothiophen-3-yl)ethoxy]-*tert*-butyldimethylsilane in 30 ml of THF and 1.92 ml (3.83 mmol) of 2.0 M solution of *i*-PrMgCl in THF) was added dropwise over the period of 1 min, and the resulting solution was stirred at 35 ℃ for additional 4 h. Precipitation into 150 ml of methanol resulted in a crude dark-purple polymer which was placed into a Soxhlet extractor, and extracted successively with methanol, hexane, and $CHCl_3$. The chloroform fraction yielded 0.11 g (12%) of **3-9-1** as a dark-purple solid material, M_n 70 kDa, PDI 1.27 (GPC, vs polystyrene). ^{1}H NMR (250 MHz, $CDCl_3$) δ 7.06 (broad s, 0.29 H), 6.96 (s, 1 H), 3.95 - 3.75 (m, 0.57H), 3.07 - 2.91 (m, 0.57H), 2.85 - 2.64 (m, 2H), 1.80 - 1.52 (m, 2H), 1.50 - 1.15 (m, 6H), 0.98 - 0.74 (m, 5.61H), 0.10 - 0.03 (m, 1.74H). Based on the ^{1}H NMR data, the ratio of P3HT to poly[3-(TBDMSO-ethyl)thiophene] blocks was ~3.5:1.

Block Copolymer 3-9-2 A solution of *i*-PrMgCl (0.77 ml of 2.0 M solution in THF, 1.53 mmol) was added dropwise to a stirred solution of 0.61 g (1.53 mmol) of 2-[(2,5-

dibromothiophen-3-yl)ethoxy]-*tert*-butyldimethylsilane in 25 ml THF, at 0 ℃, and the resulting solution was stirred for 1 h at this temperature to yield solution of the Grignard reagent **3-7**. A solution of 6.9 mg (6.1 μmol) of initiator **3-3** in 2 ml of toluene was added to the Grignard reagent solution and the reaction mixture was stirred at 35 ℃ for 1 h. A solution of the Grignard reagent **3-6** (prepared separately at 0 ℃ from 0.5 g (1.53 mmol) of 2,5-dibromo-3-hexylthiophene in 22 ml of THF and 0.77 ml (1.53 mmol) of 2.0 M solution of *i*-PrMgCl in THF) was added dropwise over the period of 1 min, and the resulting solution was stirred at 35 ℃ for additional 2 h. Precipitation into 150 ml of methanol resulted in a crude dark-purple polymer which was placed into a Soxhlet extractor, and extracted successively with methanol, hexane, and $CHCl_3$. The chloroform fraction yielded 0.03 g (5%) of **3-9-2** as a dark-purple solid material, M_n 80 kDa, PDI 1.47 (GPC, vs polystyrene). ^{1}H NMR (250 MHz, $CDCl_3$) 7.06 (broad s, 0.67H), 6.96 (s, 1H), 3.95 - 3.75 (m, 1.33H), 3.07 - 2.91 (m, 1.33H), 2.85 - 2.64 (m, 2H), 1.80 - 1.52 (m, 2H), 1.50 - 1.15 (m, 6H), 0.98 - 0.74 (m, 9.03H), 0.10 - 0.03 (m, 4.02H). Based on ^{1}H NMR, the ratio of P3HT to poly[3-(TBDMSO-ethyl)thiophene] blocks was ~1.5:1.

6.4. Synthesis of Amphiphilic Polythiophene Block Copolymers Incorporating a Low Energy Gap PDCI Unit

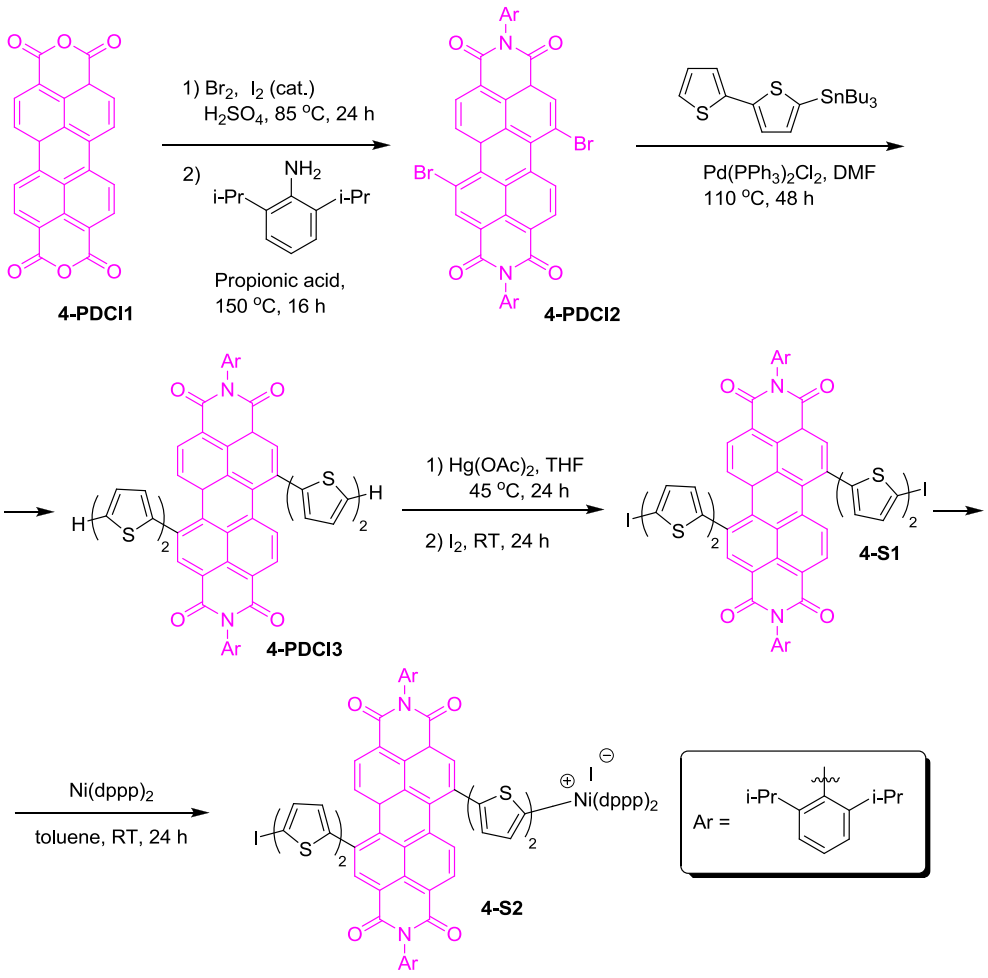

***N,N'*-Bis(2,6 - diisopropylphenyl) - 1,7 – dibromoperylene - 3,4:9,10 - tetracarboxylic acid bisimide (4-PDCI2)** was prepared following literature protocols.[4,5] A suspension of 10.0 g (25.5 mmol) of perylene-3,4:9,10-tetracarboxylic acid bisanhydride (**4-PDCI1**) in 80 ml of concentrated sulfuric acid was stirred for 12 h at room temperature, followed by addition of 0.24 g (0.93 mmol) of iodine. The reaction mixture temperature was brought to 85 ℃, and bromine (8.73 g, 54.6 mmol) was added dropwise over a period of 8 h. After the addition was complete, the reaction mixture was stirred at 85 ℃ for additional 10 h and allowed to cool to room temperature. After the excess bromine was removed by blowing a gentle stream of N_2 through the reaction mixture, water (70 ml) was added carefully. The

resulting precipitate was separated by filtration, washed successively with 90 ml of 86% sulfuric acid and a large amount of water and dried in vacuo to give 11.1 g (79%) of crude dibromoperylene bisanhydride as a red solid. A suspension of 5.0 g (9 mmol) of the crude dibromoperylene bisanhydride, 8.0 g (8.5 ml, 45 mmol) of 2,6-diisopropylaniline in 55 ml of propionic acid was refluxed at 150 ℃ over 16 h, and then allowed to cool down to room temperature. The resulting precipitate was separated by filtration, and washed successively with water, saturated aqueous $NaHCO_3$, and water. The crude product was dried in vacuum oven at 85 ℃ over 12 h, and purified by chromatography on silica gel (eluent $CHCl_3$ - hexanes = 5:1) to afford 4.5 g (58%) of **4-PDCI2** as a bright-orange solid. ^{1}H NMR (250 MHz, CD_2Cl_2) δ 9.53 (dd, J_1 = 6.6, J_2 = 1.6 Hz, 2H), 8.93 (d, J = 1.3 Hz, 2H), 8.71 (dd, J_1 = 6.6, J_2 = 1.6 Hz, 2H), 7.45 (t, J = 7.6 Hz, 2H), 7.28 (d, J = 7.6 Hz, 4H), 2.66 (septet, J = 6.8 Hz, 4H), 1.07 (d, J = 6.8 Hz, 24H). The ^{1}H NMR spectrum was in a good agreement with the literature data.[4]

***N,N′*-Bis(2,6-diisopropylphenyl)-1,7-bis(2,2′-bithiophen-5′-yl)perylene-3,4:9,10-tetracarboxylic acid bisimide (4-PDCI3)**. A mixture of 0.5 g (1.78 mmol) of 5-(tributylstannyl)-2,2′-bithiophene, 0.6 g (0.69 mmol) of **4-PDCI2** and 97 mg (0.14 mmol, 20 mol %) of $Pd(PPh_3)_2Cl_2$ in 10 ml of DMF was stirred at 110 ℃ in a sealed air-free flask for 48 h. After allowing to cool to room temperature, the resulting mixture was filtered through a short silica gel column eluted with chloroform, and concentrated in vacuo. The crude product was additionally purified by column chromatography on silica gel (eluent $CHCl_3$ – MeOH = 5:1) to afford 0.34 g (48%) of **4-PDCI3** as a black color crystalline material, mp >300 ℃. ^{1}H NMR (400 MHz, CD_2Cl_2) δ 8.79 (d, J = 6.6 Hz, 2H), 8.54 - 8.49 (m, 2H), 8.39 (d, J = 6.6Hz, 2H), 7.57 - 7.53 (m, 2H), 7.40 (t, J = 8.1 Hz, 2H), 7.35 - 7.26 (m,

10H), 7.10 - 7.09 (m, 2H), 2.81 - 2.76 (m, 4H), 1.19 -1.18 (m, 24H).

***N,N′*-Bis(2,6-diisopropylphenyl)-1,7-bis(5-iodo-2,2′-bithiophen-5′-yl)perylene-3,4:9,10-tetracarboxylic acid bisimide (4-S1)**. A solution of 0.16 g (0.15 mmol) of **4-PDCI3** and 0.29 g (0.90 mmol) of $Hg(OAc)_2$ in 20 ml of THF was stirred at 45 ℃ for 24 h. After allowing the reaction mixture to cool to room temperature, a solution of 0.27 g (1.05 mmol) of iodine in 1 ml of THF was added dropwise, and the resulting mixture was stirred at room temperature for 24 h. The reaction mixture was washed with saturated $Na_2S_2O_3$ solution to remove excess of iodine, washed with H_2O, extracted with CH_2Cl_2, and dried over Na_2SO_4. Concentration in vacuo resulted in a crude product that was further purified by column chromatography on silica gel (eluent CH_2Cl_2 – hexanes = 3:1) to yield 0.15 g (78%) of **4-S1** as a black color crystalline material, mp >300 ℃. ^{1}H NMR (400 MHz, CD_2Cl_2) δ 8.66 - 8.65 (m, 2H), 8.39 - 8.34 (m, 2H), 8.27 (d, *J* = 8.0 Hz, 2H), 7.44 - 7.41 (m, 3H), 7.30 - 7.25 (m, 5H), 7.16 - 7.12 (m, 4H), 6.85 - 6.82 (m, 2H), 2.68 - 2.66 (m, 4H), 1.07-1.05 (m, 24H). HRMS *m/e* 1291.107$[M+H]^+$ (calcd for $C_{64}H_{48}I_2N_2O_4S_4$ 1291.065)

PDCI Initiator (4-S2). A mixture of 0.27 g (0.30 mmol) of $Ni(dppp)_2$ and 0.13 g (0.10 mmol) of **4-S1** was placed in an air-free flask, and repeatedly evacuated and backfilled with argon gas. Anhydrous toluene (4 ml) was added to the reaction mixture and the homogenous solution was stirred at room temperature for 5 h, and then was left unperturbed for 24 h. After adding hexane, the precipitated solid was separated by centrifugation and washed thoroughly with a hexane-toluene mixture to afford 0.2g (91%) of **4-S2** as dark purple solid material, mp >300 ℃. ^{1}H NMR (400 MHz, in THF-D_8) δ 8.80 - 8.65 (m, 2H), 8.60 - 8.35 (m, 4H), 8.07~7.92.(m, 2H), 7.85 - 7.68 (m, 18H), 7.67 - 7.59 (m, 1H), 7.51 - 7.12 (m, 33H), 2.9 - 2.7 (m, 4H), 2.51 - 2.41 (m, 8H), 1.99 - 1.75 (m, 4H), 1.25 - 1.01 (m, 24H), ^{31}P NMR (162

MHz, in THF-D_8) δ 22.4 (s).

High M_n P3HTs-PDCI (4-P1) A solution of *i*-PrMgCl (0.75 ml of 2.0 M solution in THF, 1.5 mmol) was added dropwise to a stirred solution of 0.49 g (1.5 mmol) of 2,5-dibromo-3-hexylthiophene in 22 ml of THF at 0 ℃, and the resulting solution was stirred for 1 h at this temperature. External catalytic initiator **4-S2** (3.35mg, 1.54 μmol) in 1 ml of toluene was added and the reaction mixture was stirred at 35 ℃ for 1 h. Precipitation into 120 ml of methanol resulted in a crude dark-purple polymer which was placed into a Soxhlet extractor, and extracted successively with methanol, hexane, and $CHCl_3$. The chloroform fraction yielded 0.1g (33%) of **4-P1** as a dark-purple solid, M_n (GPC, vs. polystyrene) 53000, PDI 1.34. ^{1}H NMR (400 MHz, $CDCl_3$) δ 6.96 (s, 1H), 2.78 (t, J = 8.0 Hz, 2H), 1.75 - 1.60 (m, 2H), 1.45 - 1.33 (m, 6H), 0.93 - 0.85 (m, 3H).

Low M_n P3HTs-PDCI (4-P1) A solution of *i*-PrMgCl (0.77 ml of 2.0 M solution in THF, 1.5 mmol) was added dropwise to a stirred solution of 0.50 g (1.53 mmol) of 2,5-dibromo-3-hexylthiophene in 22 ml of THF at 0 ℃, and the resulting solution was stirred for 1 h at this temperature to yield a solution of Grignard reagent **3-6**. A solution of 4.7 mg (2.2 μmol) of complex **4-S2** in 2 ml of toluene was added to the Grignard reagent solution and the reaction mixture was stirred at 35 ℃ for 10 min. Precipitation into 120 ml of methanol resulted in a crude dark-purple polymer which was placed into a Soxhlet extractor, and extracted successively with methanol, hexane, and $CHCl_3$. The resulting polymer was purified by preparative GPC. M_n (GPC, vs. polystyrene) 24,000 and determined molecular weight by NMR 19,000. ^{1}H NMR (400 MHz, $CDCl_3$) δ 8.77 - 8.67 (br.d, 2H), 8.55 - 8.35 (m, 4H), 6.96 (s, 111H), 2.78 (t, 222H), 1.75 - 1.60 (m, 222H), 1.45 - 1.33 (m, 666H), 0.93 - 0.85 (m, 333H).

Polymer 4-M1 was prepared following the procedure for polymer **4-P1**. A reaction of *i*-PrMgCl (0.75 ml of 2.0 M solution in THF), 0.60 g (1.5 mmol) of 2-[(2,5-dibromo-thiophen-3-yl)ethoxy]-*tert*-butyldimethylsilane, and 3.35 mg (1.54 μmol) of **4-S2** afforded 0.12 g (40%) of **4-M1** as a dark-purple solid material, M_n (GPC, vs. polystyrene) 31,000, *D* 1.46. ^{1}H NMR (400 MHz, $CDCl_3$) δ 7.05 (br. s, 1H), 3.94 - 3.80 (m, 2H), 3.10 - 2.93 (m, 2H), 0.87 (br. s, 9H), 0.01 (br. s, 6H).

PDCI Polythiophene Block Copolymer 4-1-2. A solution of *i*-PrMgCl (0.77 ml of 2.0 M solution in THF, 1.53 mmol) was added dropwise to a stirred solution of 0.5 g (1.53 mmol) of 2,5-dibromo-3-hexylthiophene in 22 ml of THF at 0 °C, and the resulting solution was stirred for 1 h at this temperature. External catalytic initiator **4-S2** (46.8 mg, 21.5 μmol) in 2 ml of toluene was added and the reaction mixture was stirred at 35 °C for 1 h. A solution of Grignard reagent **3-7** (prepared separately at 0°C from 0.61 g (1.53 mmol) of 2-[(2,5-dibromothiophen-3-yl)ethoxy]-*tert*-butyldimethylsilane and 0.77 ml (of 2.0 M solution in THF) of *i*-PrMgCl in 22 ml of THF) was added dropwise, and the resulting solution was stirred at 35 °C for additional 4 h. Precipitation into 250 ml of methanol resulted in a crude dark-purple polymer which was placed into a Soxhlet extractor, and extracted successively with methanol, hexane, and $CHCl_3$. The chloroform fraction afforded 0.11g (18%) of **4-1-2** as a dark-purple solid material, M_n (GPC, vs polystyrene) 44kDa, PDI 1.43. ^{1}H NMR (250 MHz, $CDCl_3$) δ 7.13 - 6.90 (m, 1.33H), 3.95 - 3.81 (m, 0.66H), 3.07 - 2.93 (m, 0.66H), 2.84 - 2.69 (m, 2H), 1.80 - 1.52 (m, 2H), 1.50 - 1.15 (m, 6H), 0.98 - 0.78 (m, 5.97H), 0.03 (br. s, 1.98H). Based on ^{1}H NMR, the ratio of P3HT to poly[3-(TBDMSO-ethyl)thiophene] blocks was ~3:1.

PDCI Polythiophene Block Copolymer 4-1-1. A solution of *i*-PrMgCl (0.77 ml of 2.0 M

solution in THF, 1.53 mmol) was added dropwise to a stirred solution of 0.61 g (1.53 mmol) of 2-[(2,5-dibromothiophen-3-yl)ethoxy]-*tert*-butyldimethylsilane in 22 ml of THF at 0 ℃, and the resulting solution was stirred for 1 h at this temperature. External catalytic initiator **4-S2** of 46.8 mg (21.5 μmol) in 2 ml of toluene was added and the reaction mixture was stirred at 35 ℃ for 1 h. A solution of Grignard reagent **3-6** (prepared separately at 0℃ from 0.5 g (1.53 mmol) of 2,5-dibromo-3-hexylthiophene and 0.77 ml (of 2.0 M solution in THF) of *i*-PrMgCl in 22 ml of THF) was added dropwise, and the resulting solution was stirred at 35 ℃ for additional 4 h. Precipitation into 250 ml of methanol resulted in a crude dark-purple polymer which was placed into a Soxhlet extractor, and extracted successively with methanol, hexane, and $CHCl_3$. The chloroform fraction yielded 0.07 g (11%) of **4-1-1** as a dark-purple solid material, M_n (GPC, vs polystyrene) 47kDa, PDI 1.39. ^{1}H NMR (250 MHz, $CDCl_3$) δ 7.10 - 6.86 (m, 2H), 3.95 - 3.76 (m, 2H), 3.12 - 2.88 (m, 2H), 2.88 - 2.65 (m, 2H), 1.80 - 1.52 (m, 2H), 1.50 - 1.12 (m, 6H), 1.00 - 0.74 (m, 12H), 0.01 (br. s, 6H). Based on ^{1}H NMR, the ratio of poly[3-(TBDMSO-ethyl)thiophene] to P3HT blocks was ~1:1.

Macroinitiator 4-2-2. A solution of tetrabutylammonium fluoride (4.25 ml of 0.1 M solution in THF, 0.42 mmol) was added dropwise over the period of 2 h (syringe pump) to a mixture of 92 mg (0.38 mmol based on repeating unit) of polymer **4-1-2**, 2-bromoisobutyryl bromide 0.47 ml, (3.8 mmol), 60 μl of triethylamine (0.42 mmol) in 35 ml of THF at room temperature, and the resulting mixture was stirred at room temperature for 16 h. Precipitation into methanol and washing with acetone yielded in 93mg (89%) of **4-2-2** as dark purple solid material, M_n (GPC, vs polystyrene) 44kDa, PDI 1.43. ^{1}H NMR (250 MHz, $CDCl_3$) δ 7.10-6.86 (m, 1.33H), 4.43-4.34 (m, 0.66H), 3.25-3.16 (m, 0.66H), 2.88-2.65 (m, 2H), 1.93(s, 1.95H), 1.80-1.52 (m, 2H), 1.50-1.12 (m, 6H), 1.00-0.74 (m, 3H).

Macroinitiator 4-2-1, **4-2-3**, **4-2-4** and **4-M2** were prepared exactly following the procedure for **4-2-2** starting from **4-1-1**, **3-9-2**, **3-9-1** and **4-M1** respectively. **4-2-1**: M_n (GPC, vs polystyrene) 47kDa, PDI 1.39. ^{1}H NMR (250 MHz, $CDCl_3$) δ 7.19-6.86 (m, 2H), 4.51-4.36 (br.s, 2H), 3.25-3.16 (m, 2H), 2.85-2.71 (m, 2H), 1.93(s, 6H), 1.80-1.52 (m, 2H), 1.50-1.12 (m, 8H), 1.00-0.74 (m, 3H). **4-2-3**: M_n (GPC, vs polystyrene) 80kDa, PDI 1.47. ^{1}H NMR (250 MHz, $CDCl_3$) δ 7.10-6.86 (m, 1.65H), 4.43-4.34 (m, 1.32H), 3.95-3.76 (m, 1.32H), 2.88-2.65 (m, 2H), 1.93(s, 3.9H), 1.80-1.52 (m, 2H), 1.50-1.12 (m, 6H), 1.00-0.74 (m, 3H). **4-2-4**: M_n (GPC, vs polystyrene) 70kDa, PDI 1.27. ^{1}H NMR (250 MHz, $CDCl_3$) δ 7.10-6.86 (m, 1.29H), 4.43-4.34 (m, 0.57H), 3.28-3.16 (m, 0.57H), 2.88-2.65 (m, 2H), 1.93(s, 1.98H), 1.80-1.52 (m, 2H), 1.50-1.12 (m, 6H), 1.00-0.74 (m, 3H). **4-M2**: M_n (GPC, vs polystyrene) 31kDa, PDI 1.46. ^{1}H NMR (250 MHz, $CDCl_3$) δ 7.17 (s, 1.H), 4.05-4.40 (t, 2H), 3.3-3.15 (t, 2H), 1.93(s, 6H).

Amphiphilic Polythiophene Block Copolymer 4-3-2. An air-free flask was charged with 25.8 mg (0.18 mmol) of CuBr, 2.03 g (18.0 mmol) of *N*-isopropylacrylamide, and 46.2 mg (0.18 mmol) of 1,4,8,11-tetramethyl-1,4,8,11-tetraazacyclotetradecane, evacuated and backfilled with Ar 3 times, filled with 10 ml of THF, cooled in an ice bath, and purged with Ar for 10 min. After 15 min, a separately prepared and degassed in an air-free flask solution of 50 mg (0.18 mmol based on repeating unit) of **4-2-2** in 35 ml of THF was added dropwise via cannula. The resulting mixture was stirred at 0 ℃ for 2.5 h, then it was poured into 200 ml of hexane to precipitate a crude polymer product. The precipitate was thoroughly washed twice with diethyl ether, redissolved in THF, and precipitated into hexane. Finally, this precipitate was redissolved in THF and filtered through a short plug of silica gel eluted with THF to remove catalyst. The THF solution was again precipitated from hexane

and dried in vacuo to afford 1.42 g (70%) of **4-3-2** as purple red solid material, M_n (GPC using light-scattering detector) 1.76 × 10^6, *D* 2.13. ^{1}H NMR (250 MHz, $CDCl_3$) δ 6.8-6.2 (br. s, 1H), 3.98 (s, 1H), 2.47 (s, 1H), 2.2-1.62(br. s, 2H) 1.13 (s, 6H).

Amphiphilic Polythiophene Block Copolymers 4-3-1, **4-3-3**, **4-3-4** and **4-P2** were prepared following the same procedure **4-3-2** starting from **4-2-1**, **4-2-3** and **4-2-4** respectively. **4-3-1**: M_n (GPC using light-scattering detector) 1.43 × 10^6, *D* 2.25. ^{1}H NMR (250 MHz, $CDCl_3$), **4-3-3**: M_n (GPC using light-scattering detector) 2.1 × 10^6, *D* 2.78, **4-3-4**: M_n (GPC using light-scattering detector) 2.5 × 10^6, *D* 3.0. ^{1}H NMR spectra of all polymers are identical.

Polymer 4-P2 was prepared following the same procedure **4-3-2** staring from **4-M2**. **4-P2**: M_n (GPC using light-scattering detector) 1.03 × 10^6, *D* 1.93.

6.5. Synthesis of Cyanine Dyes Based Conjugated Polymers

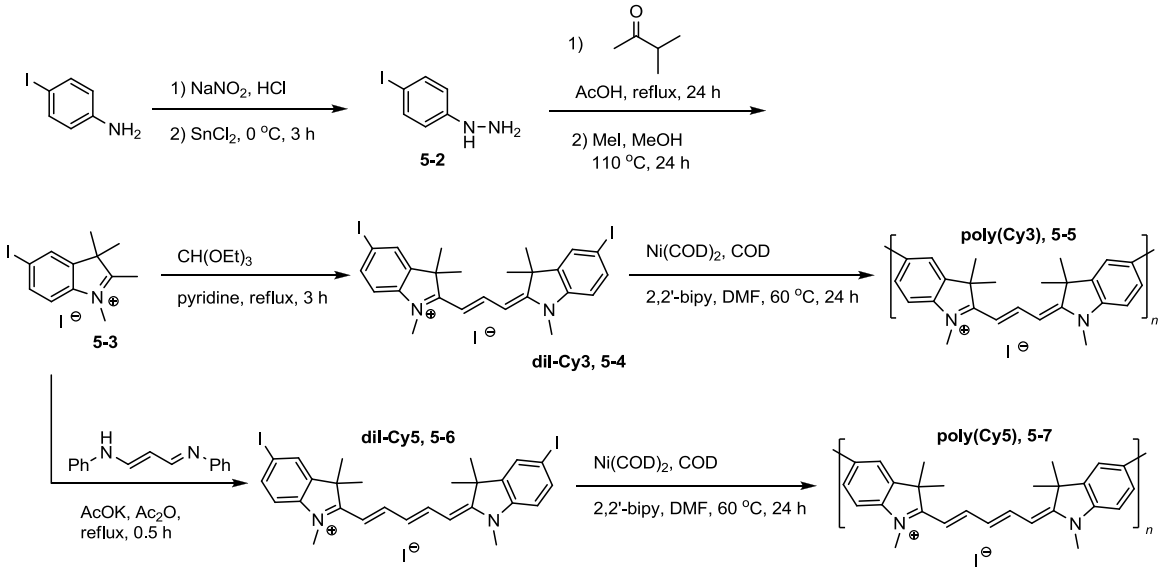

(4-Iodophenyl)hydrazine (**5-2**) was prepared following a general literature procedure.[6] A

solution of 2.0 g (9.1 mmol) of 4-iodoaniline in 40 ml of conc. HCl was prepared upon heating, and cooled down to 0 ^{o}C. An aqueous solution of 0.7 g (10.0 mmol) of $NaNO_2$ was added dropwise, and the reaction mixture was stirred at 0 ℃ for 1 h. Then a solution of 12.3 g (54.4 mmol) of $SnCl_2 \times 2H_2O$ in 10 ml of HCl was added dropwise over 15 min that resulted in immediate formation of a beige precipitate. The resulting mixture was stirred for 3 h at 0 ^{o}C, and quenched with 50% NaOH aqueous solution until pH 14. The organic product was extracted with ethyl acetate, washed with water and dried over Na_2SO_4. Concentration in vacuo resulted in 1.14 g (crude yield: 53%) of a crude product as a bright beige solid, which was used for the next step without further purification. ^{1}H NMR (250 MHz, $CDCl_3$) δ 7.49 (d, *J* = 8.77 Hz, 2H), 6.62 (d, *J* = 8.77 Hz, 2H), 5.25 (bs, 1H), 3.65(bs, 2H).

5-Iodo-1,2,3,3-tetramethylindolium iodide (**5-3**) was prepared following a literature procedure.[7] A mixture of 1.08 g (4.6 mmol) of **5-2**, 5 ml of acetic acid, and 0.42 g (0.52 ml, 4.9 mmol) of isopropyl methyl ketone was refluxed for 3 h. The resulting solution was then diluted with water and $NaHCO_3$ was added until pH 7. The crude indole compound was extracted with ethyl acetate, and the extract was concentrated in vacuo to yield brown oil which was dissolved in 10 ml of methanol, 1.31 g (9.2 mmol) of iodomethane was added and the resulting mixture was heated in a sealed tube at 110 ℃ for 24 h. The product precipitate was filtered, washed with chloroform and recrystallized from a mixture of DMSO and chloroform to afford 0.73 g (31%) of **5-3** as a red solid. ^{1}H NMR (250 MHz, DMSO-D_6) δ 8.28 (d, *J* = 1.6 Hz, 1H), 8.00 (dd, J_1 = 1.6 Hz, J_2 = 8.4 Hz, 1H), 7.70 (d, *J* = 8.4Hz, 1H), 3.91 (s, 3H), 2.71 (s, 3H), 1.50 (s, 6H).

2-[3-(1,3-Dihydro-5-iodo-1,3,3-trimethyl-2H-indol-2-ylidene)-1-propenyl]-5-iodo-1,3,3-

trimethyl-3H-indolium iodide (**diI-Cy3, 5-4**) was prepared following the literature procedure[7] from 0.27 g (0.63 mmol) of **5-3**, 0.28 g (0.32 ml, 1.90 mmol) of triethyl orthoformate in 2 ml of pyridine to yield 0.093 g (41%) of diI-Cy3 as a green crystalline material. ^{1}H NMR (400 MHz, DMSO-D_6) δ 8.29 (t, *J* = 13.4 Hz, 1H), 8.02 (s, 2H), 7.79 (d, *J* = 8.5 Hz, 2H), 7.28 (d, *J* = 8.5 Hz, 2H), 6.41 (d, *J* = 13.4 Hz, 2H), 3.60 (s, 6H), 1.67 (s, 12H).

2-[5-(1,3-Dihydro-5-iodo-1,3,3-trimethyl-2H-indol-2-ylidene)-1,3-pentadienyl]-5-iodo-1,3,3-trimethyl-3H-indolium iodide (**diI-Cy5, 5-6**) was prepared following the published general procedure.[8] A mixture of 0.20 g (0.47 mmol) of **5-3**, 0.054 g (0.24 mmol) of 3-anilinoacrolein anil and 0.23 g (2.35 mmol) of potassium acetate in 5ml of acetic anhydride was refluxed for 30 min. The resulting green precipitate was collected by filtration, washed with cold ethanol, and recrystallized from methanol to afford 0.10 g (60%) of diI-Cy5 as green crystalline material, mp 273-274 °C. ^{1}H NMR (250 MHz, DMSO-D_6) δ 8.32 (t, *J* = 13.0 Hz, 2H), 8.04 (s, 2H), 7.73 (d, *J* = 8.4 Hz, 2H), 7.21 (d, *J* = 8.4 Hz, 2H), 6.54 (t, *J* = 13.0 Hz, 1H), 6.25 (d, *J* = 13.0 Hz, 2H), 3.56 (s, 6H), 1.67 (s, 12H). HRMS m/e 635.0419 ($[M+H]^+$) (calcd for $C_{27}H_{29}I_2N_2$ 635.0415).

Poly(Cy3), 5-5. A mixture of 0.082g (0.11 mmol) of diI-Cy3, 8.8 mg (10 μl, 0.08 mmol) of 1,5-cyclooctadiene (COD), 23.4 mg (0.15 mmol) of 2,2′-bipyridyl and 41.2mg (0.15 mmol) of $Ni(COD)_2$ in 2ml of anhydrous DMF was stirred in a sealed air-free flask at 65 °C for 24 h. After allowing to cool to RT, most of DMF was removed in vacuo, and the product was precipitated into the mixture of methanol – hexane (1:9) to yield crude polymer as a dark-purple solid. The crude product was placed into a Soxhlet extractor, and extracted successively with chloroform, acetone and methanol. The methanol fraction yielded 40 mg

(~60%) of poly(Cy3) as a dark-purple solid material, ^{1}H NMR (400 MHz, DMSO-D_6) δ 8.45-8.30 (m, 1H), 8.03 (br. s, 2H), 7.94-7.80 (m, 2H), 7.60-7.50 (m, 2H), 6.55-6.40 (m, 2H), 3.72 (br. s, 6H), 1.80 (br. s, 12H)

Poly(Cy5), 5-7 was prepared following the procedure described above for poly(Cy3). Reaction of 0.080 g (0.10 mmol) of diI-Cy5, 8.8 mg (0.08 mmol) of 1,5-cyclooctadiene (COD), 23.4 mg (0.15 mmol) of 2,2′-bipyridyl and 41.2 mg (0.15 mmol) of Ni(COD)$_2$ in 12 ml of anhydrous DMF yielded 45 mg (~80%) of poly(Cy5) as a dark-purple solid material, ^{1}H NMR (400 MHz, DMSO-D_6) δ 8.44-8.33 (m, 2H), 8.00 (br. s, 2H), 7.86-7.10 (m, 4H), 6.65-6.48 (m, 1H), 6.40-6.15 (m, 2H), 3.75-3.55 (m, 6H), 1.80-1.60 (m, 12H).

Reference compounds: **2-[3-(1,3-Dihydro-1,3,3-trimethyl-2H-indol-2-ylidene)-1-propenyl]-1,3,3-trimethyl-3H-indolium iodide (Cy3) and 2-[5-(1,3-dihydro-1,3,3-trimethyl-2H-indol-2-ylidene)-1,3-pentadienyl]-1,3,3-trimethyl-3H-indolium iodide (Cy5)** were prepared starting with 1,2,3,3-tetramethylindolium iodide following the procedures described above for diI-Cy3 and diI-Cy5, respectively. The characterization of the compounds (mp, ^{1}H NMR) was in agreement with the published literature data.[10]

6.6. References

1. Reynolds, G. A.; Drxhage, K. H. New coumarin dyes with regidized structure for flashlamp-pumped dye lasers. *Opt. Commun*. **1975**, *13*, 222-225.

2. Taranekar, P.; Qiao, Q.; Jiang, H.; Ghiviriga, I.; Schanze, K. S.; Reynolds, J. R. Hyperbranched Conjugated Polyelectrolyte Bilayers for Solar-Cell Applications. *J. Am. Chem. Soc.* **2007**, *129*, 8958-8959.

3. Corain, B.; Bressan, M.; Rigo, P. The behaviour of nickel(0) diphosphine complexes towards unsaturated organic compounds. *J. Organomet. Chem.* **1971**, *28*, 133-136.

4. Würthner, F.; Stepanenko, V.; Chen, Z.; Saha-Möller, C. R.; Kocher, N.; Stalke, D. Preparation and Characterization of Regioisomerically Pure 1,7-Disubstituted Perylene Bisimide Dyes. *J. Org. Chem.* **2004**, *69*, 7933-7939.

5. Liu, Y.; Li, Y.; Jiang, L.; Gan, H.; Liu, H.; Li, Y.; Zhuang, J.; Lu, F.; Zhu, D. Assembly and Characterization of Novel Hydrogen-Bond-Induced Nanoscale Rods. *J. Org. Chem.* **2004**, *69*, 9049-9054.

6. Olmsted, J. *J. Phys. Chem*. Calorimetric determinations of absolute fluorescence quantum yields. **1979**, *83*, 2581-2584.

7. Murphy, S.; Yang, X.; Schuster, G. B. Cyanine Borate Salts that Form Penetrated Ion Pairs in Benzene Solution: Synthesis, Properties, and Structure. *J. Org. Chem*. **1995**, *60*, 2411-2422.

8. Klotz, E. J. F.; Claridge, T. D. W.; Anderson, H. L. Homo- and Hetero-[3]Rotaxanes with Two π-Systems Clasped in a Single Macrocycle. *J. Am. Chem. Soc*. **2006**, *128*, 15374-15375.

9. Hamer F. M. *The Cyanine Dyes and Related Compounds*, Interscience Publishers, New York, 1964.

10. Sato, S.; Tsunoda, M.; Suzuki, M.; Kutsuna, M.; Takido-uchi, K.; Shindo, M.; Mizuguchi, H.; Obara, H.; Ohya, H. Synthesis and spectral properties of polymethine-cyanine dye-nitroxide radical hybrid compounds for use as fluorescence probes to monitor reducing species and radicals. *Spectrochim. Acta, Part A* **2009**, *71*, 2030-2039.

APPENDIX A: NMR SPECTRA

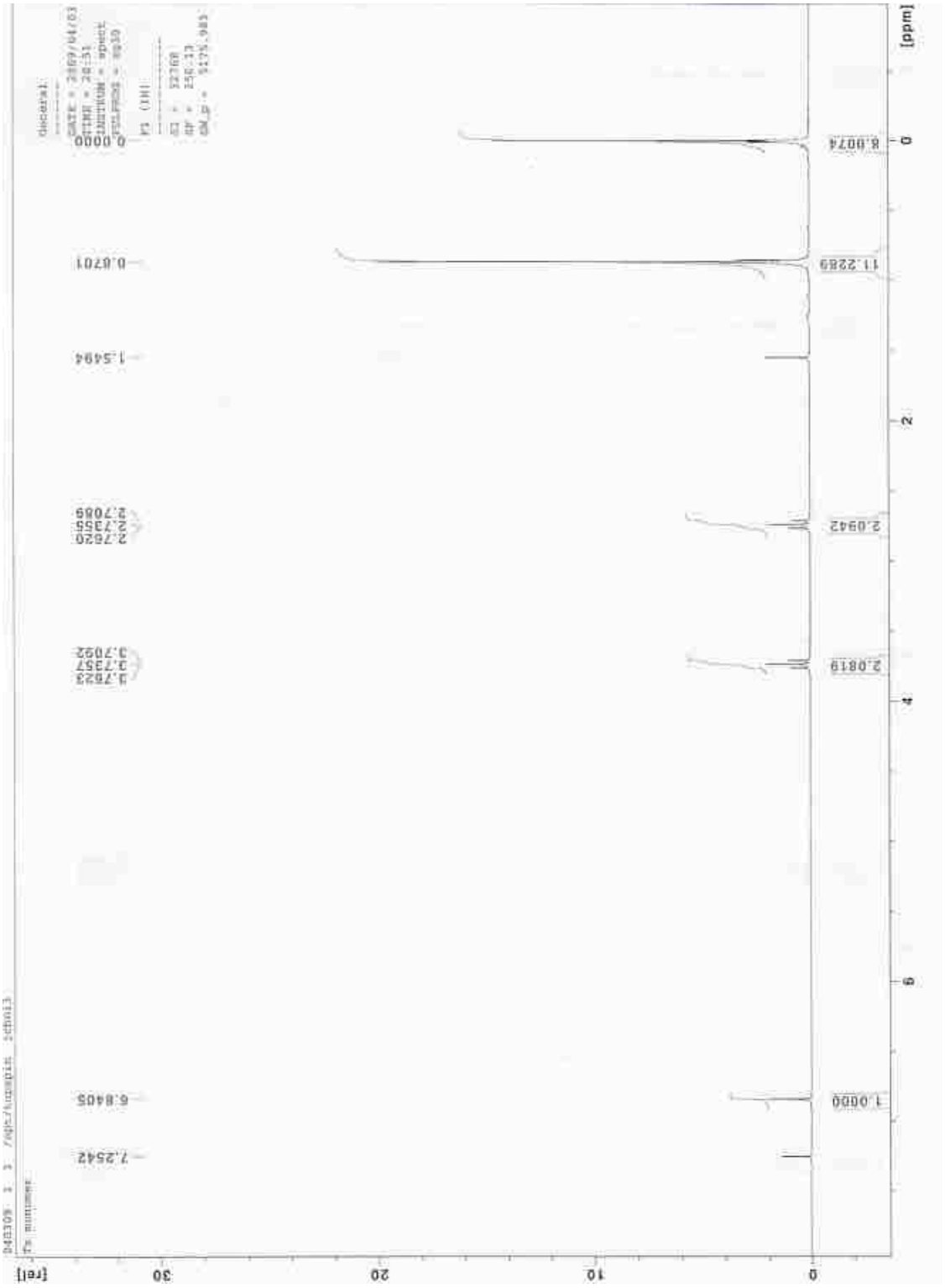

Figure A-1. ^{1}H NMR of compound **2-1** (250 MHz, $CDCl_3$)

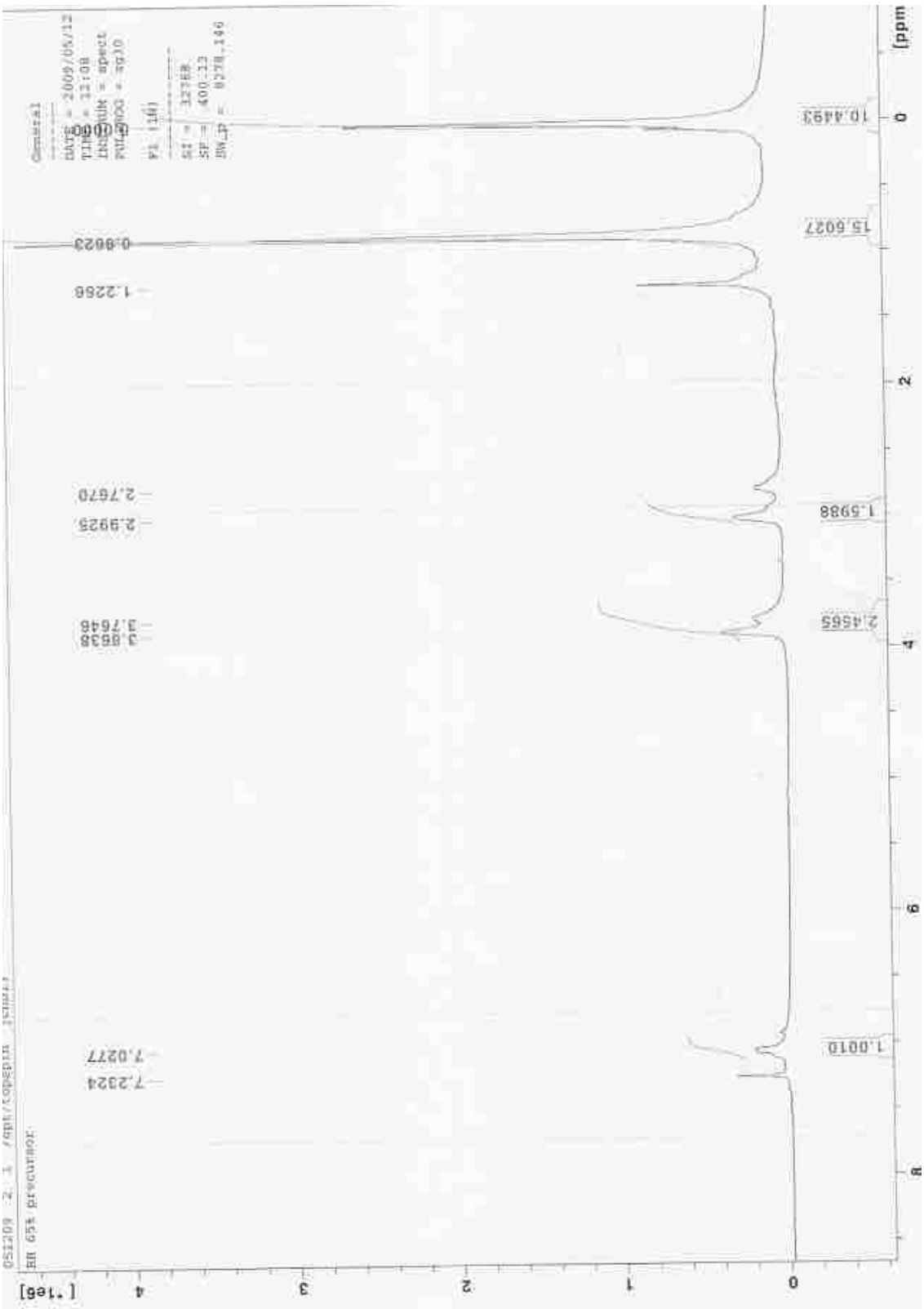

Figure A-2. ^{1}H NMR of polymer **2-2** (400 MHz, $CDCl_3$)

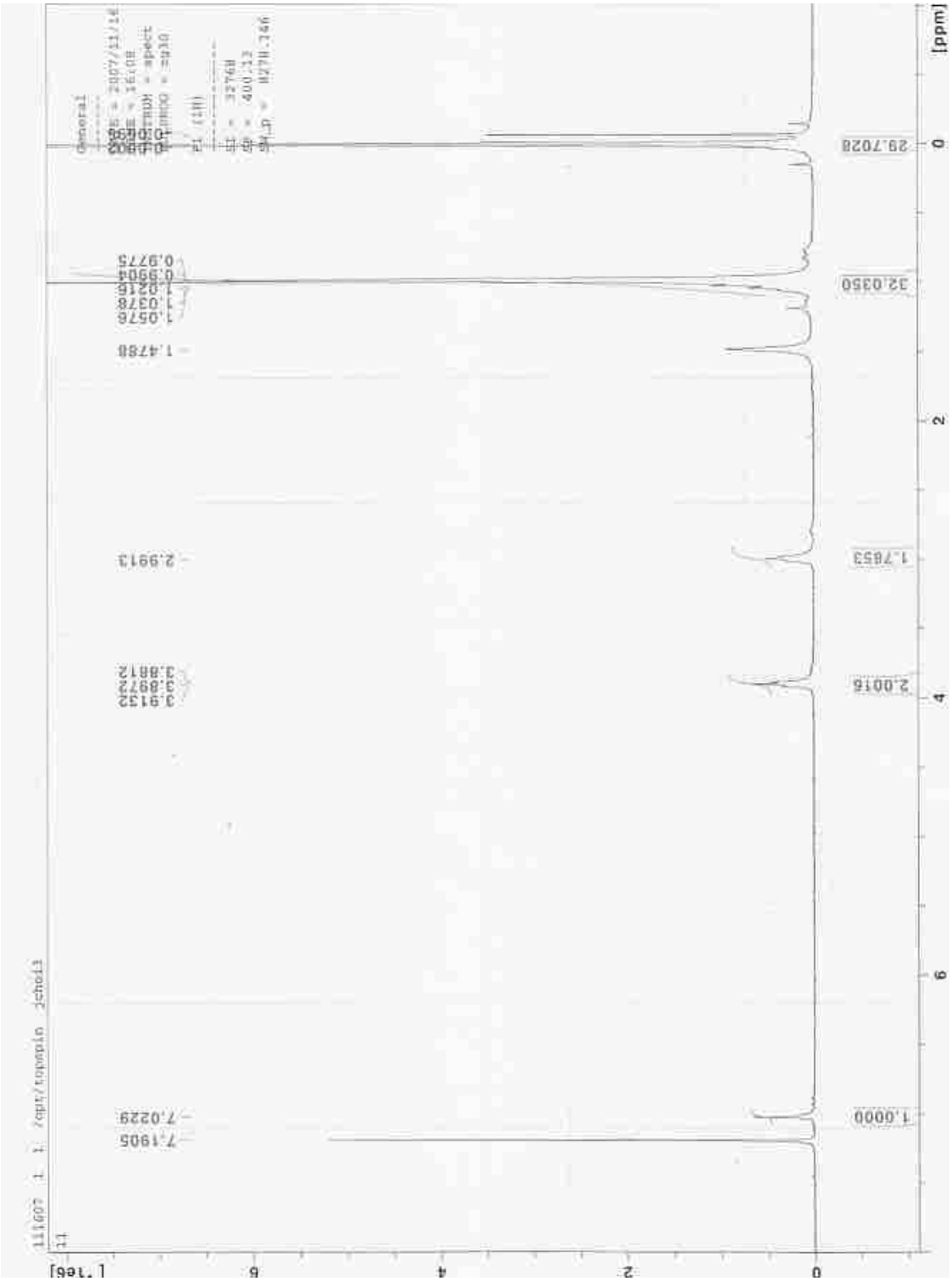

Figure A-3. ^{1}H NMR of polymer **2-3** (400 MHz, $CDCl_3$)

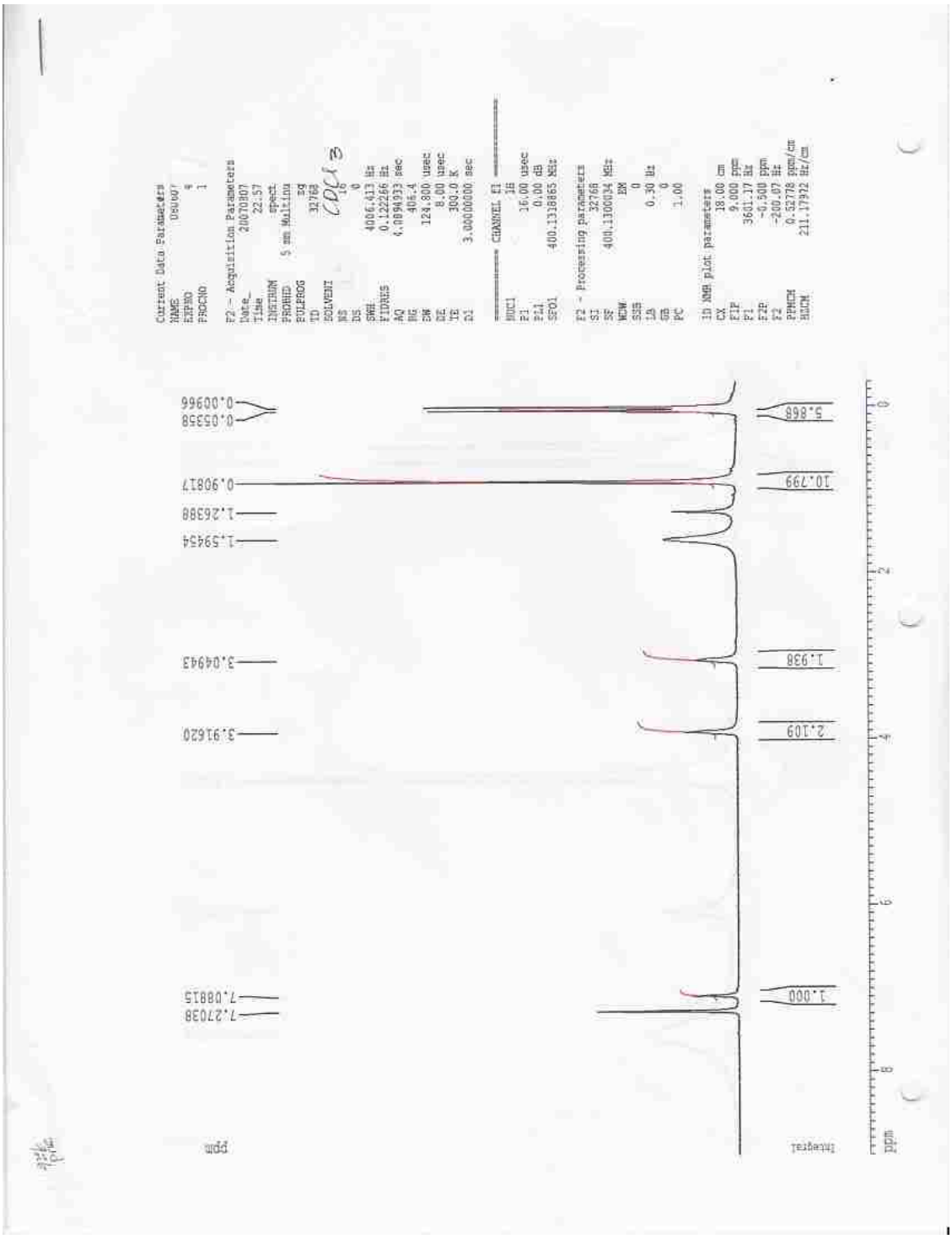

Figure A-4. ^{1}H NMR of polymer **2-4** (400 MHz, $CDCl_3$)

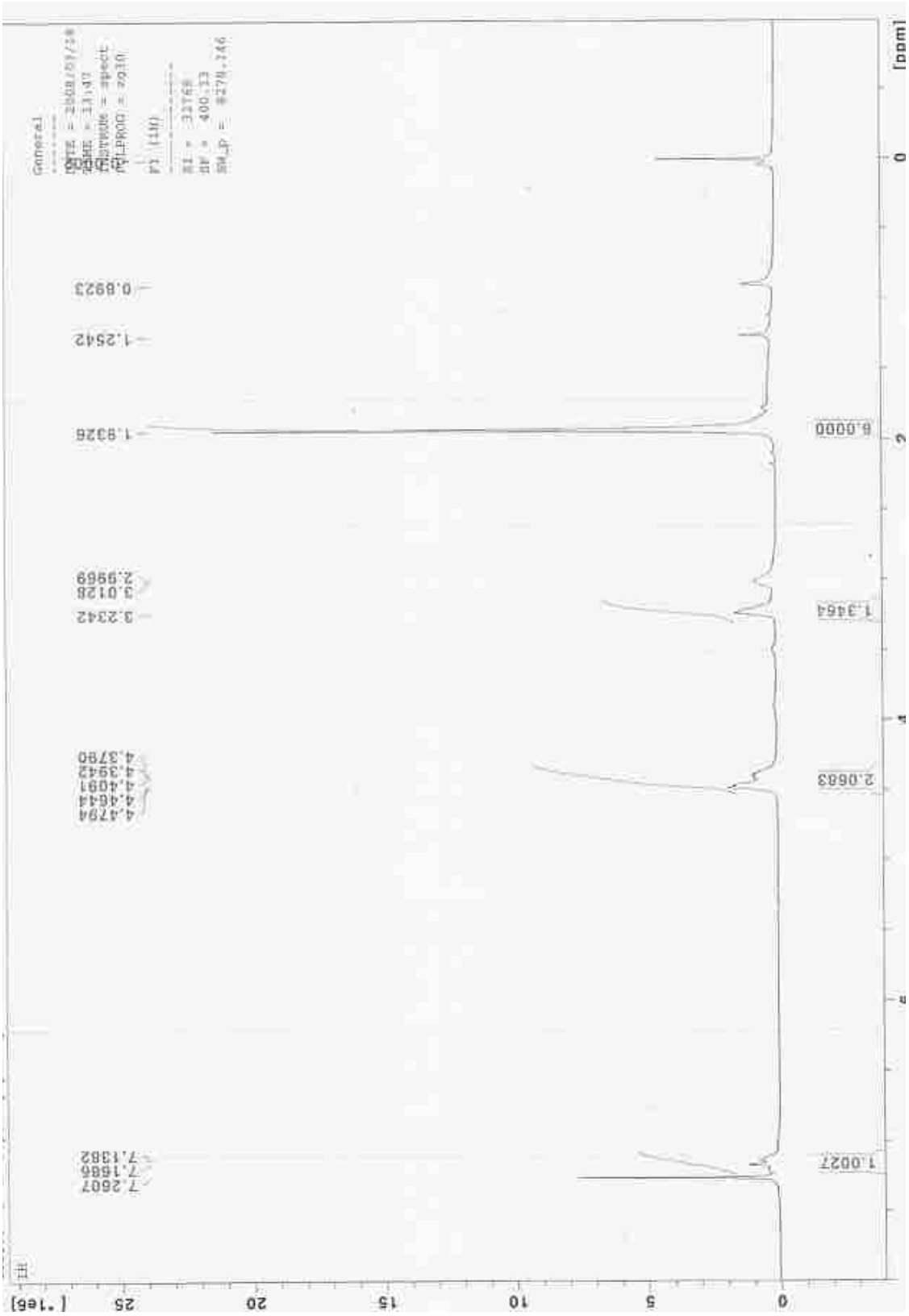

Figure A-5. ^{1}H NMR of polymer **2-5** (400 MHz, $CDCl_3$)

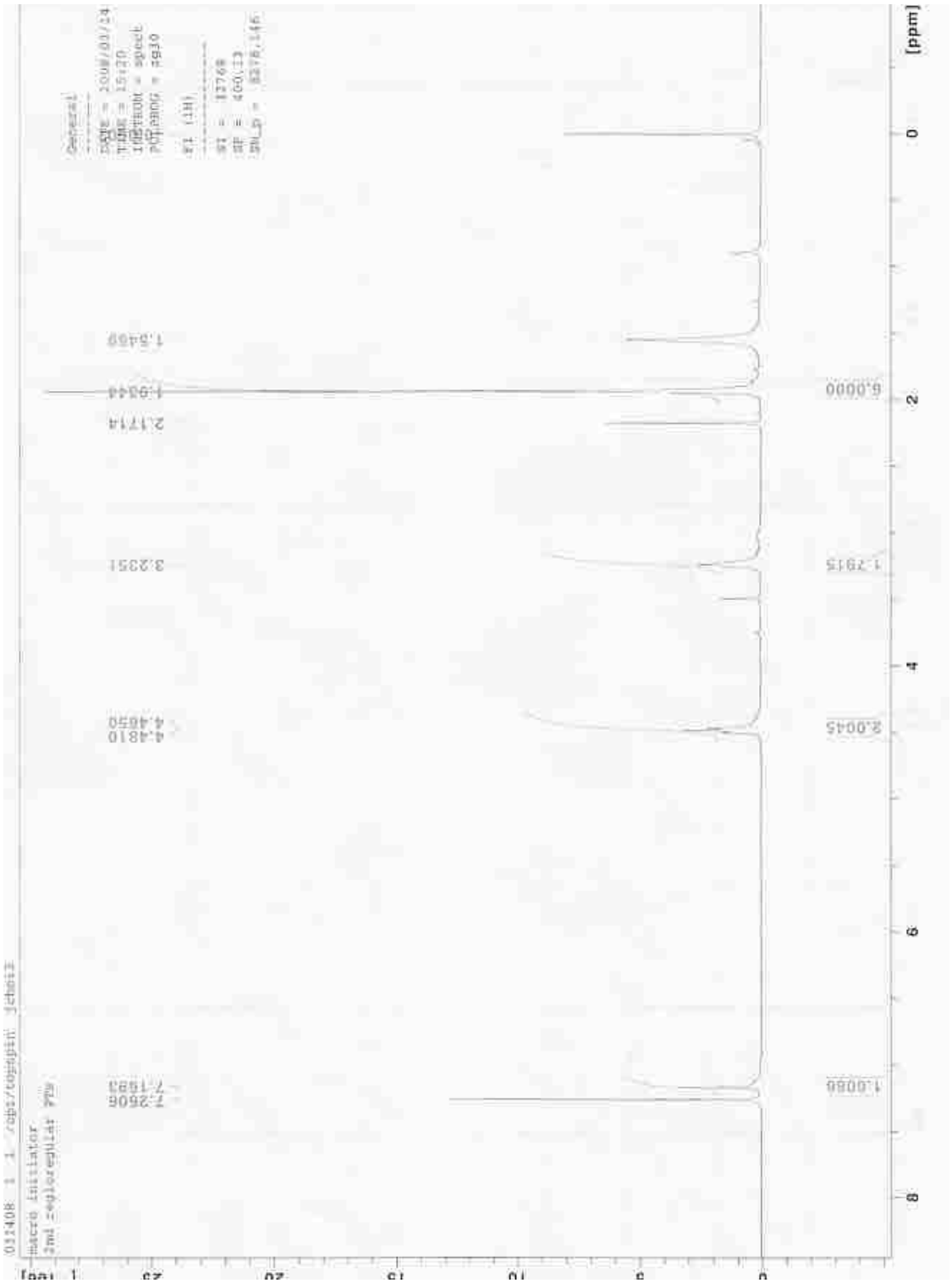

Figure A-6. ^{1}H NMR of polymer **2-6** (400 MHz, $CDCl_3$)

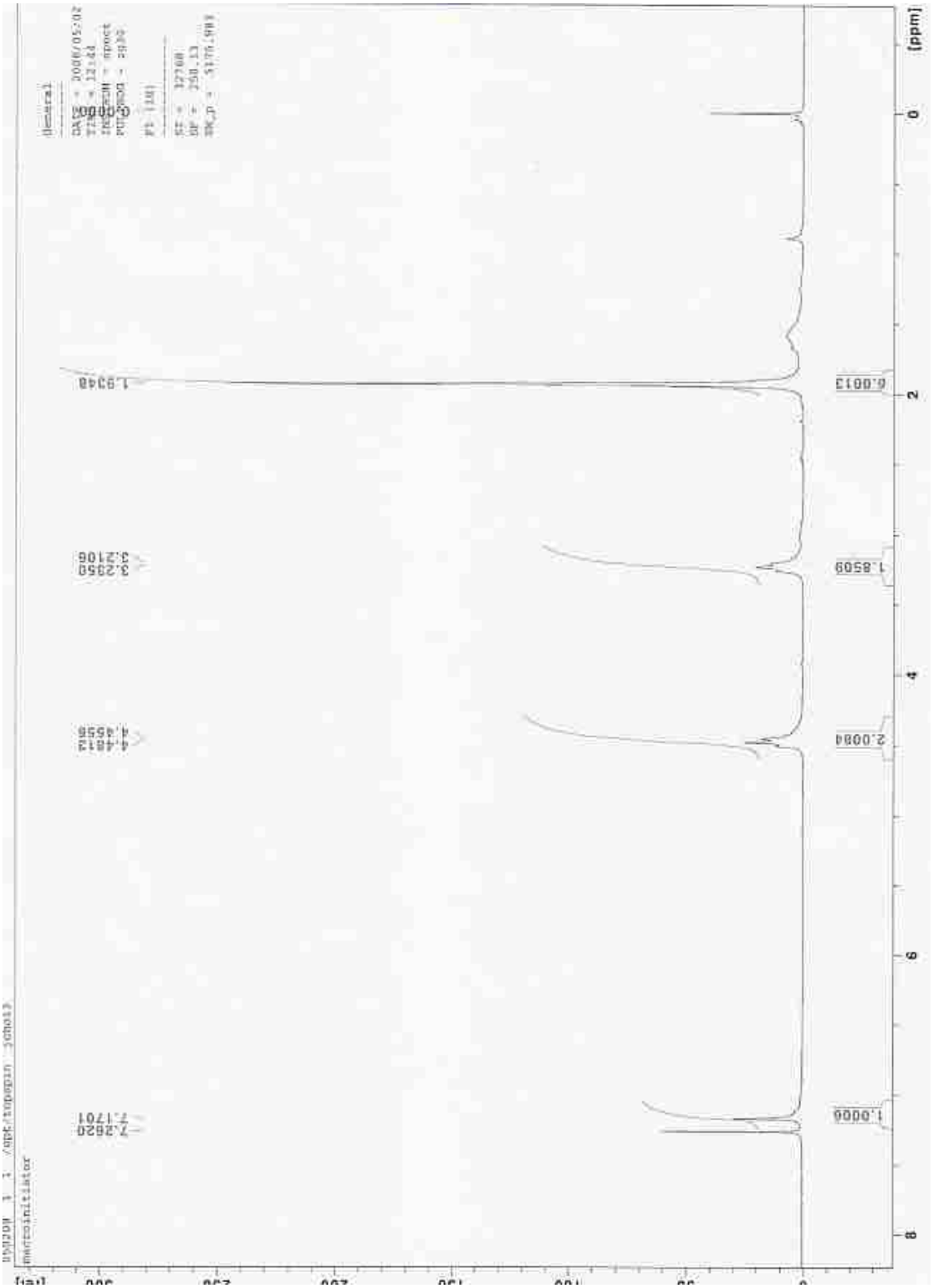

Figure A-7. ^{1}H NMR of polymer **2-7** (250 MHz, $CDCl_3$)

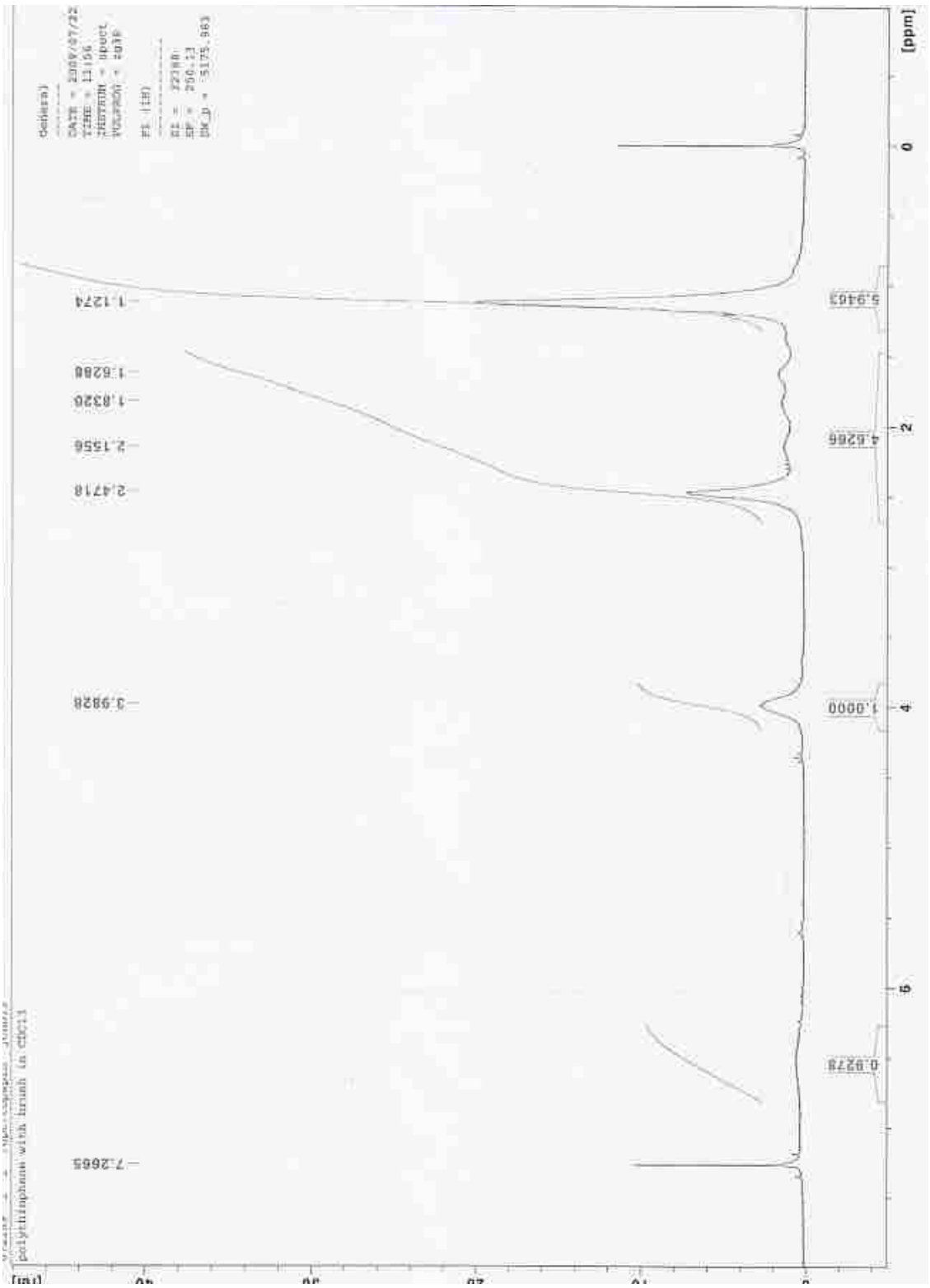

Figure A-8. ^{1}H NMR of polymer **2-8~10 (**All three polymers are identical**)** (250 MHz, $CDCl_3$)

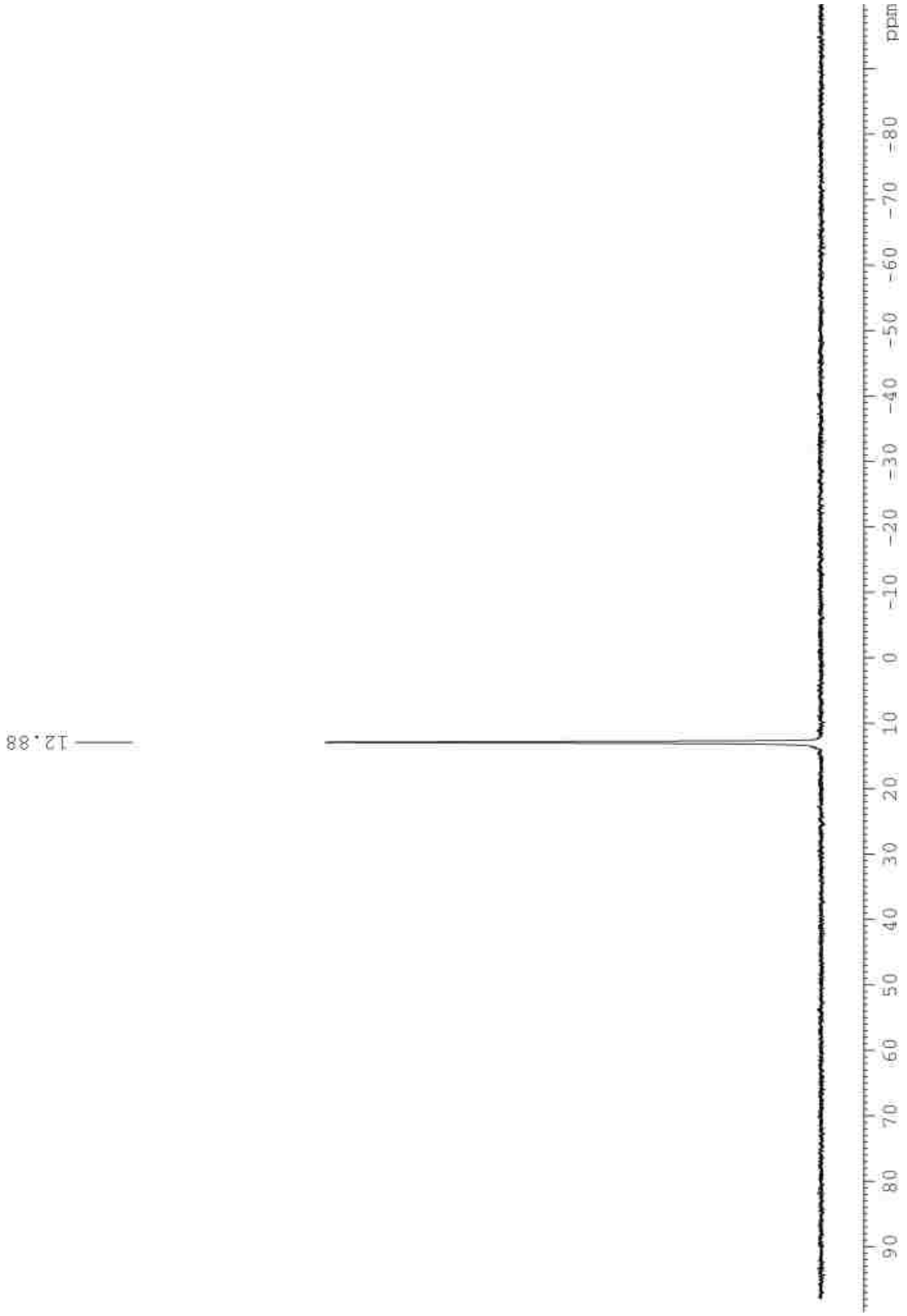

Figure A-9. ^{31}P NMR of $Ni(dppp)_2$ (162 MHz, toluene)

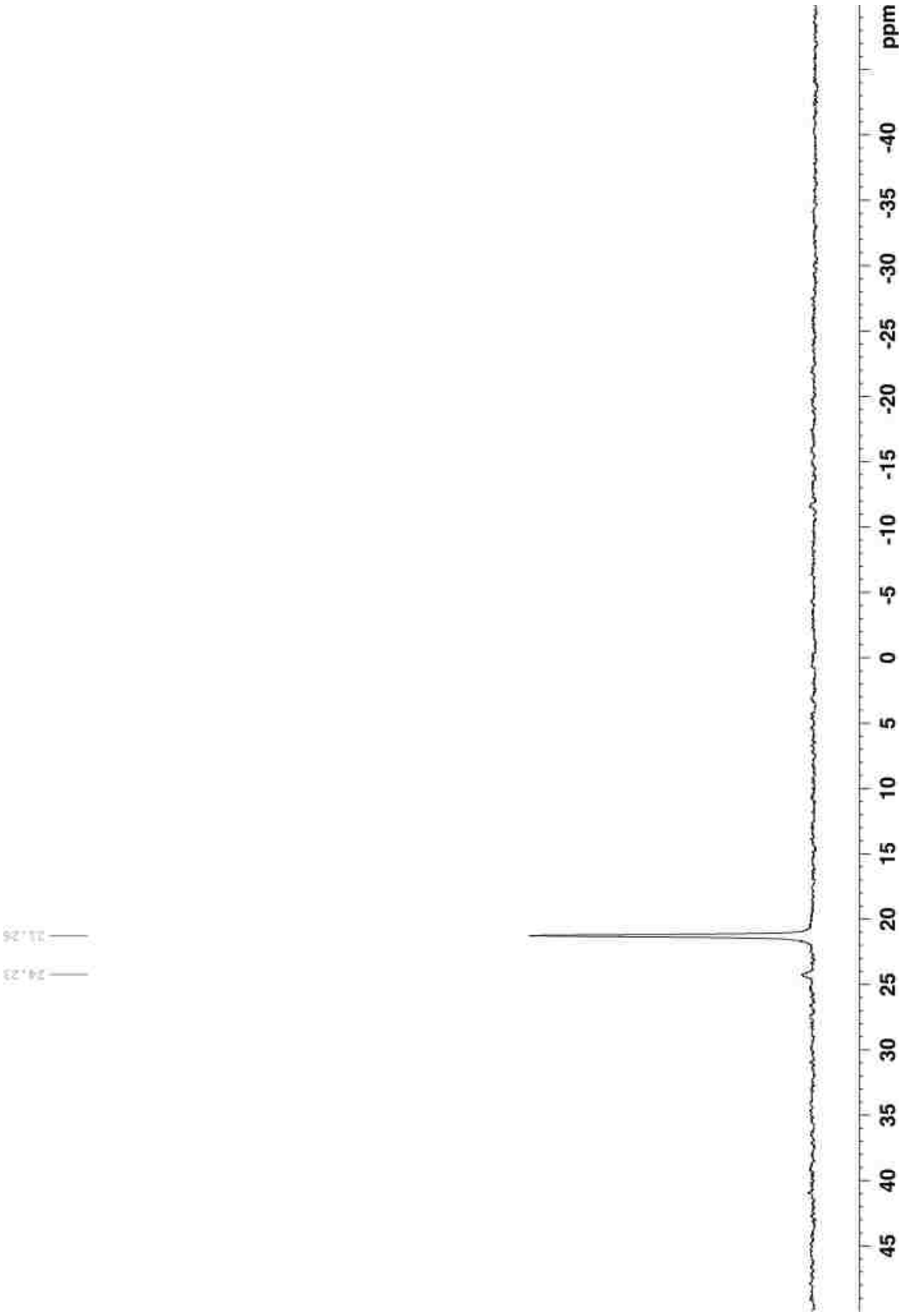

Figure A-10. ^{31}P NMR of $PhNi(PPh_3)_2Cl$ (162 MHz, chlorobenzene)

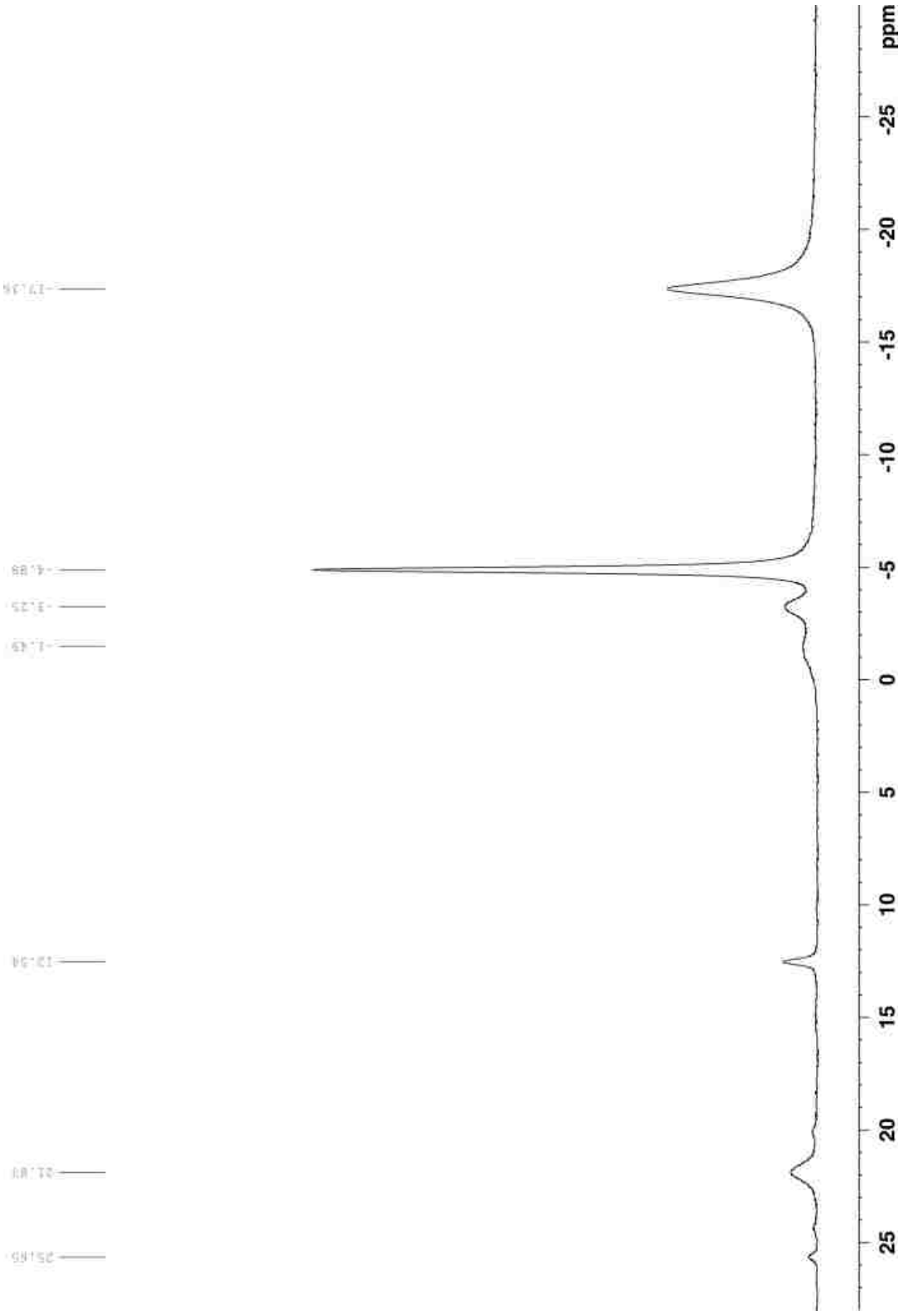

Figure A-11. ^{31}P NMR of **3-1** obtained by the "indirect" method (162 MHz, chlorobenzene)

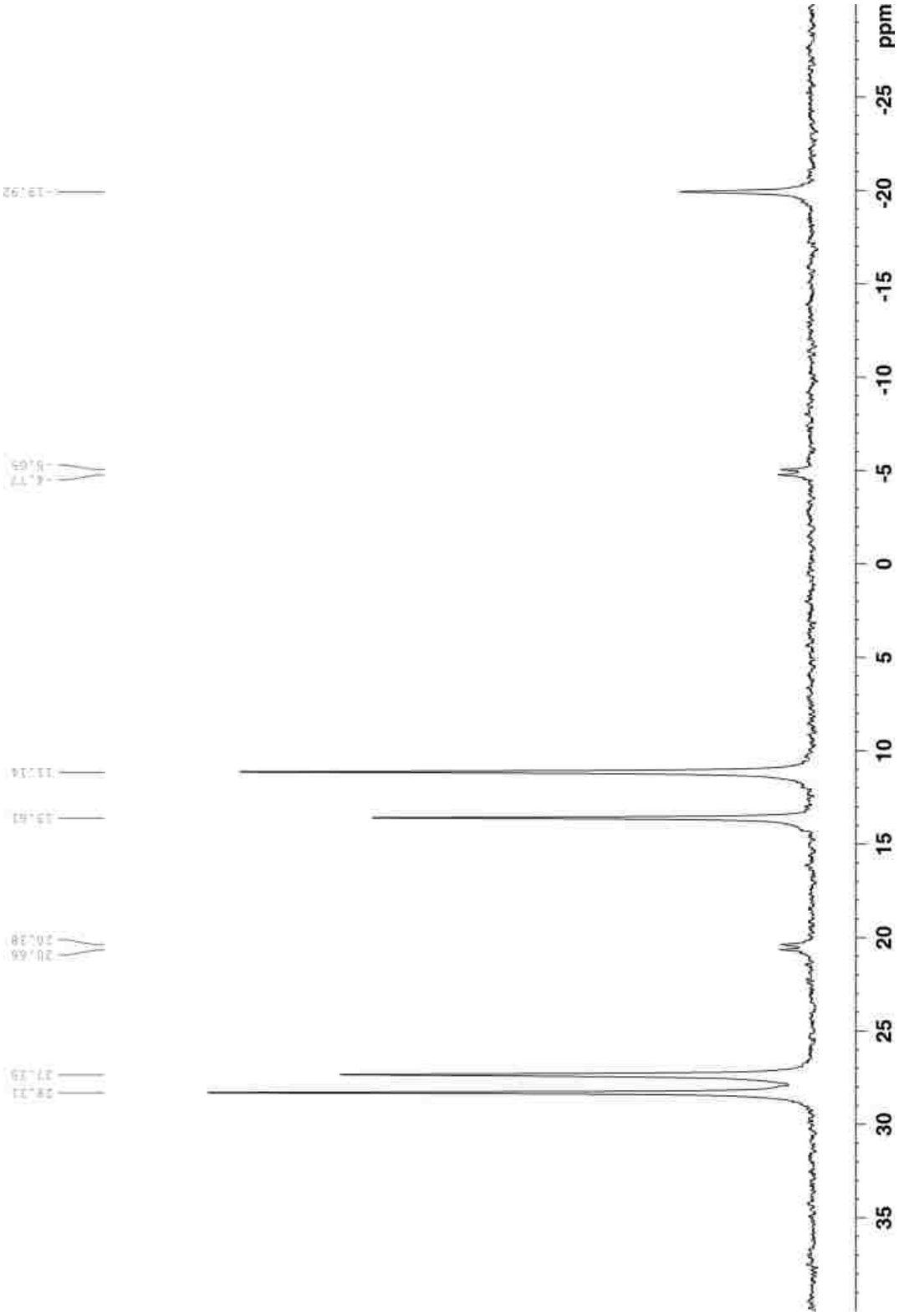

Figure A-12. ^{31}P NMR of **3-1** obtained by the "direct" method (162 MHz, chlorobenzene)

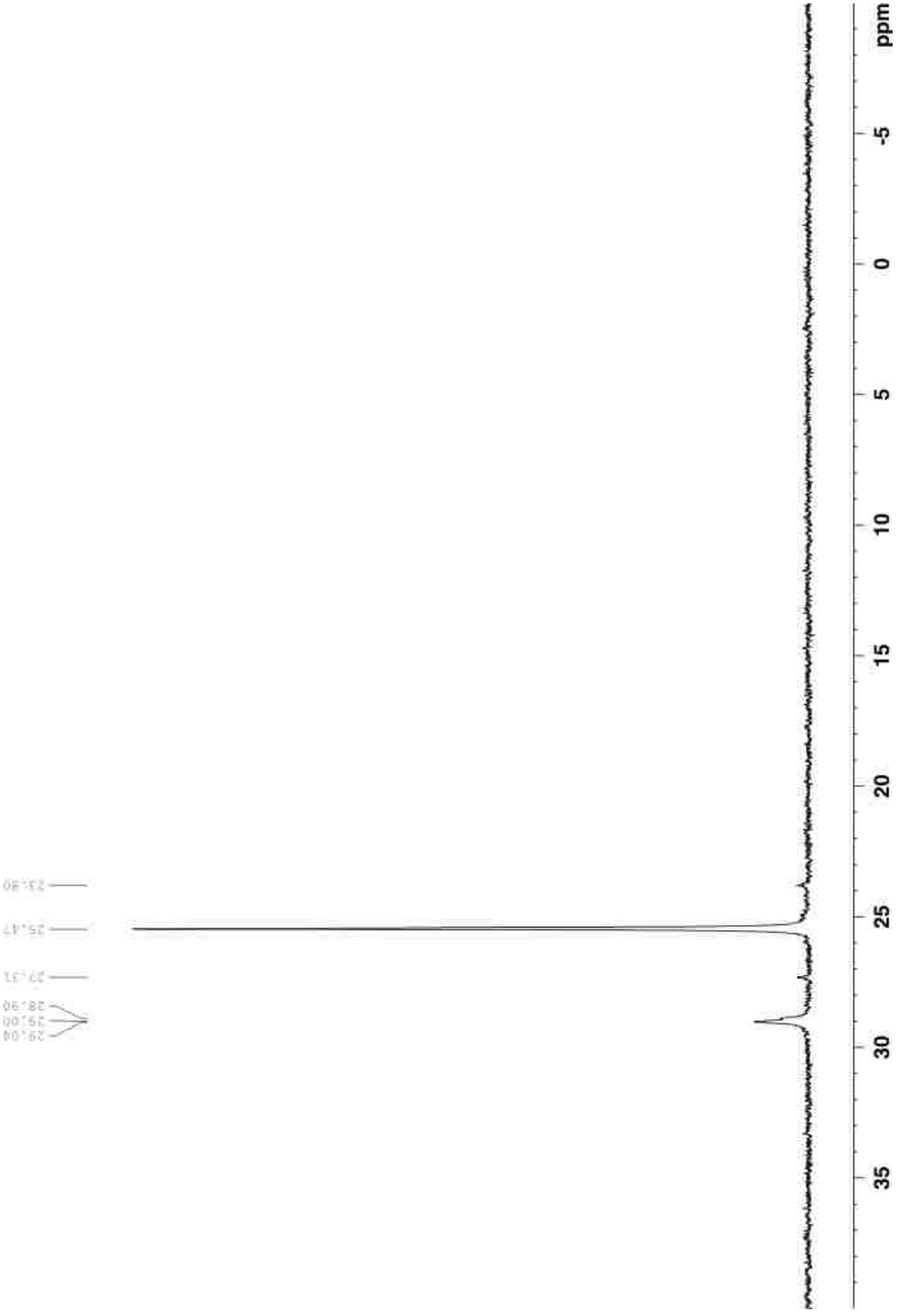

Figure A-13. ^{31}P NMR of Bithiophene-Ni(PPh_3)$_2$Br (162 MHz, toluene)

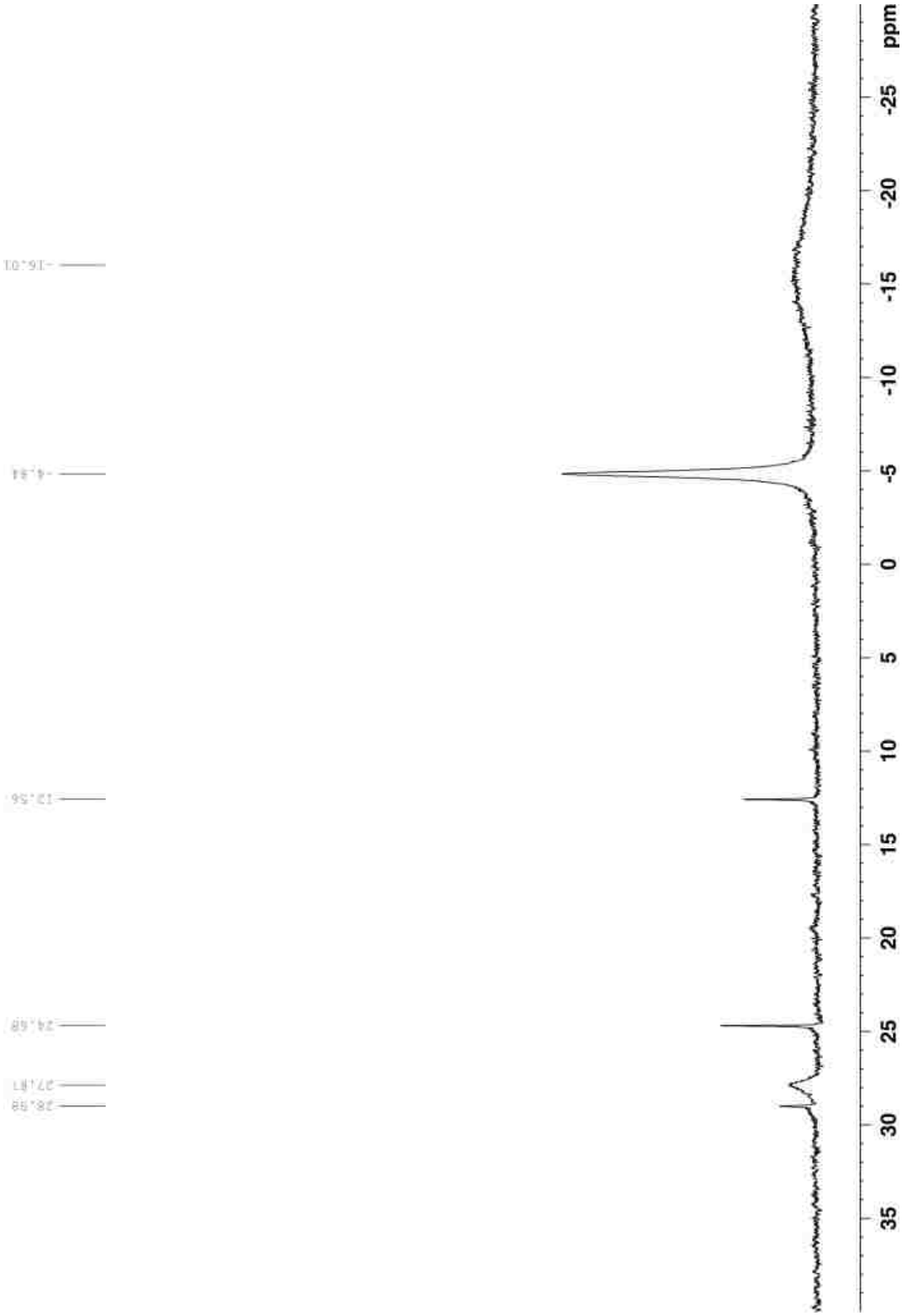

Figure A-14. ^{31}P NMR of the bithiophene initiator obtained by the "indirect" method (crude reaction mixture) (162 MHz, toluene)

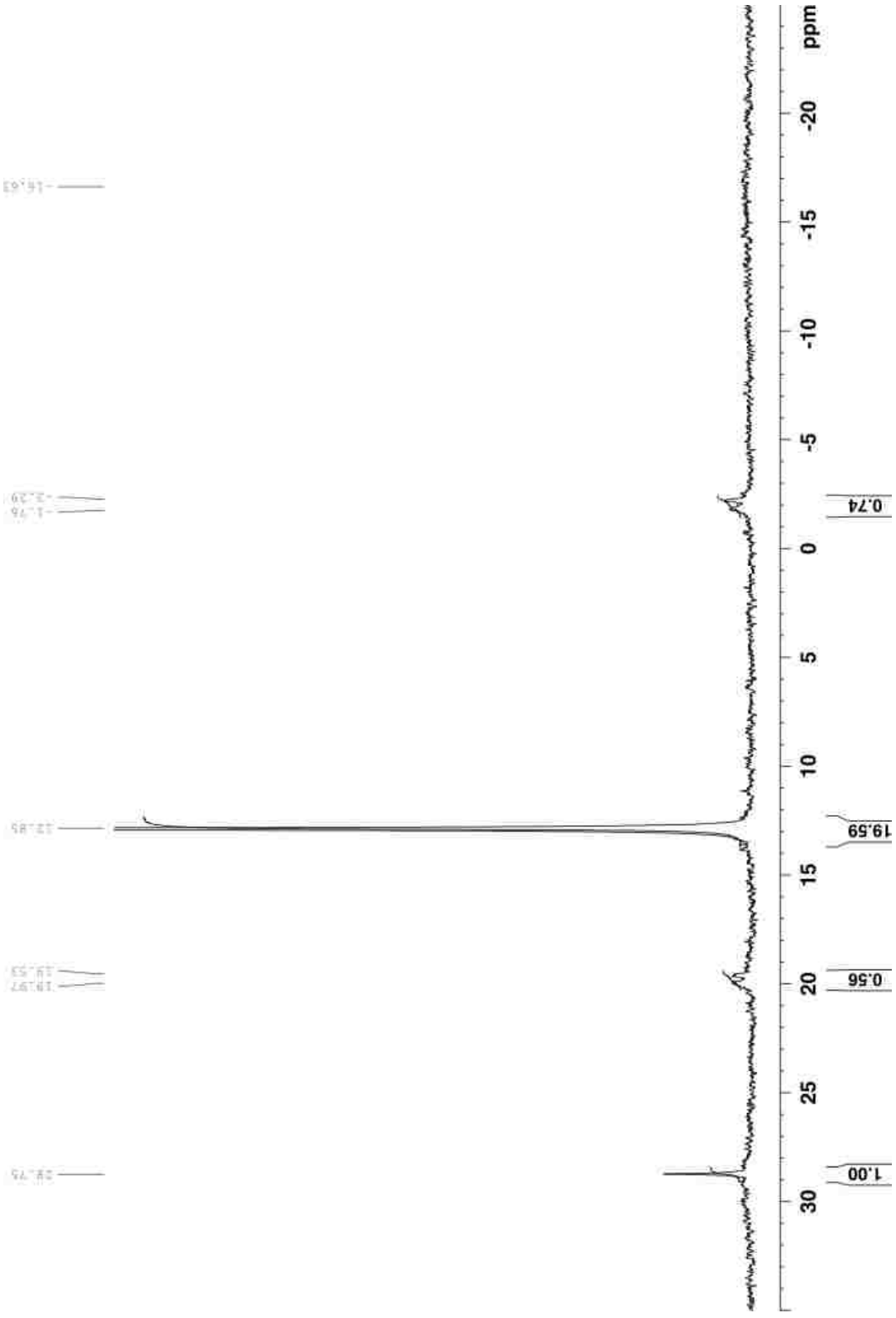

Figure A-15. ^{31}P NMR of **3-3** by the "direct" method (crude reaction mixture) (162 MHz, toluene)

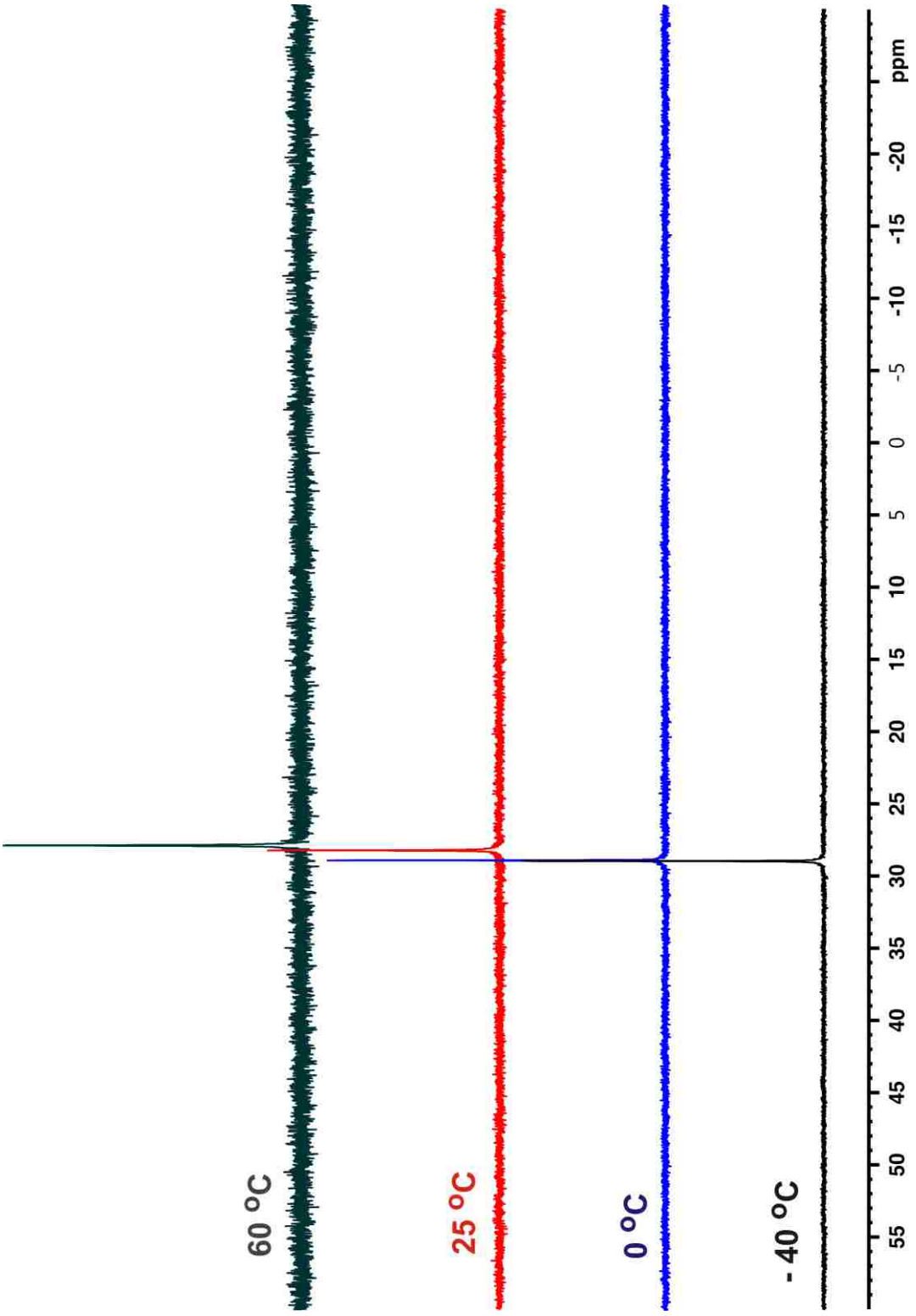

Figure A-16. Variable temperature ^{31}P NMR of **3-3** (162 MHz, toluene)

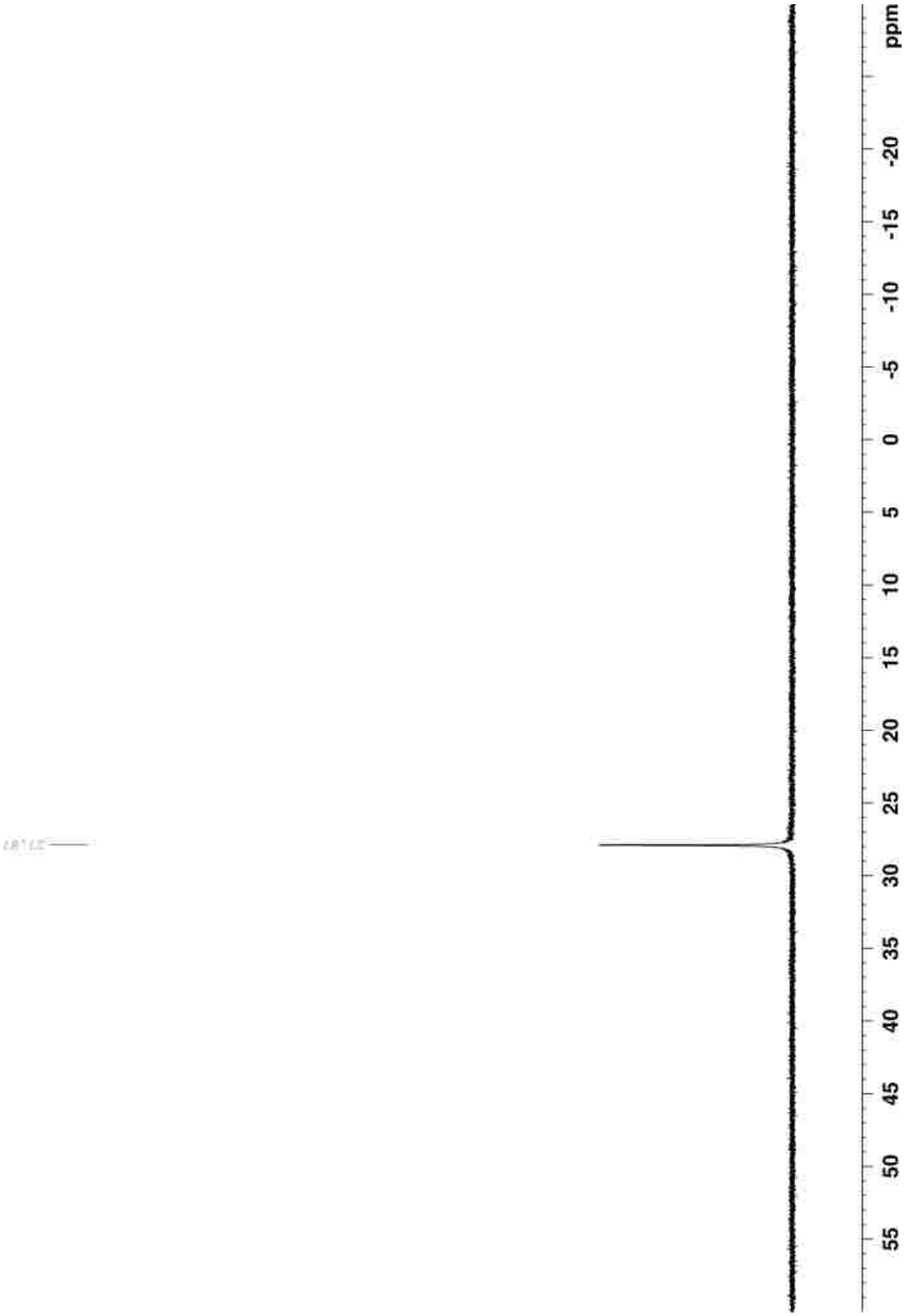

Figure A-17. ^{31}P NMR of **3-3** before addition of the Grignard monomer **3-6** solution (162 MHz, THF)

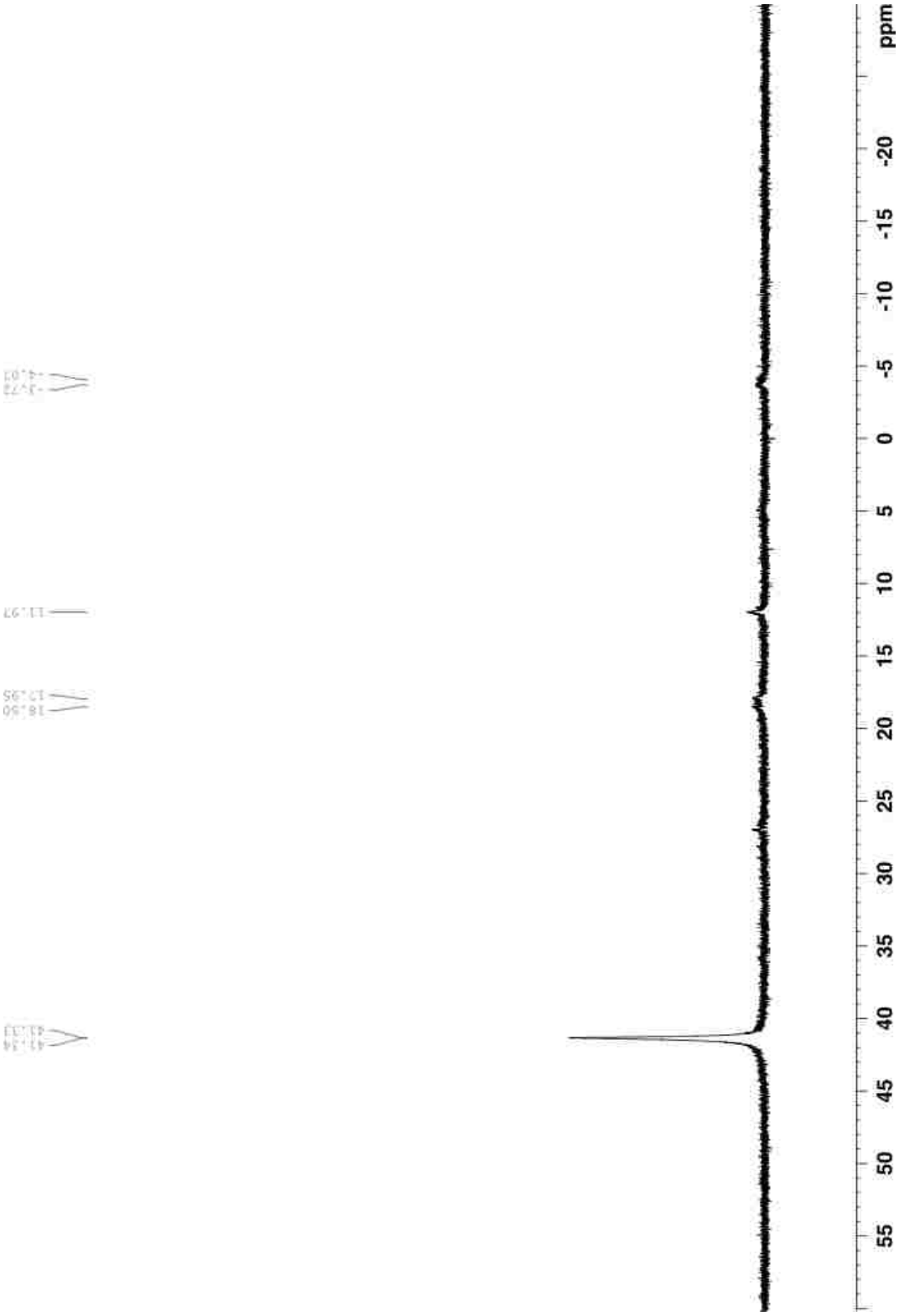

Figure A-18. ^{31}P NMR of **3-3** after addition of the Grignard monomer **3-6** solution (162 MHz, THF)

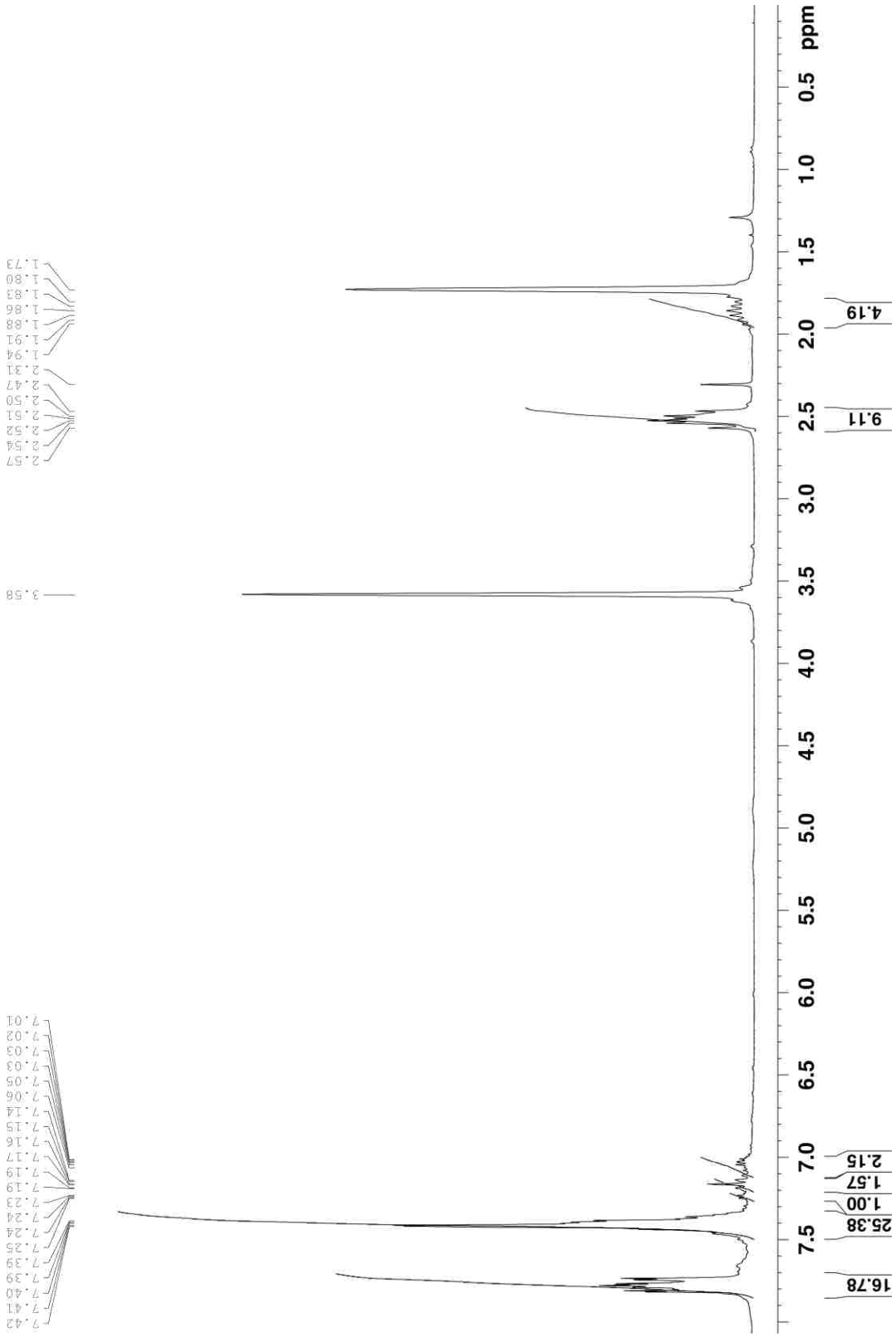

Figure A-19. ^{1}H NMR of the external bithiophene nickel catalyst **3-3** (400 MHz, THF-D_8)

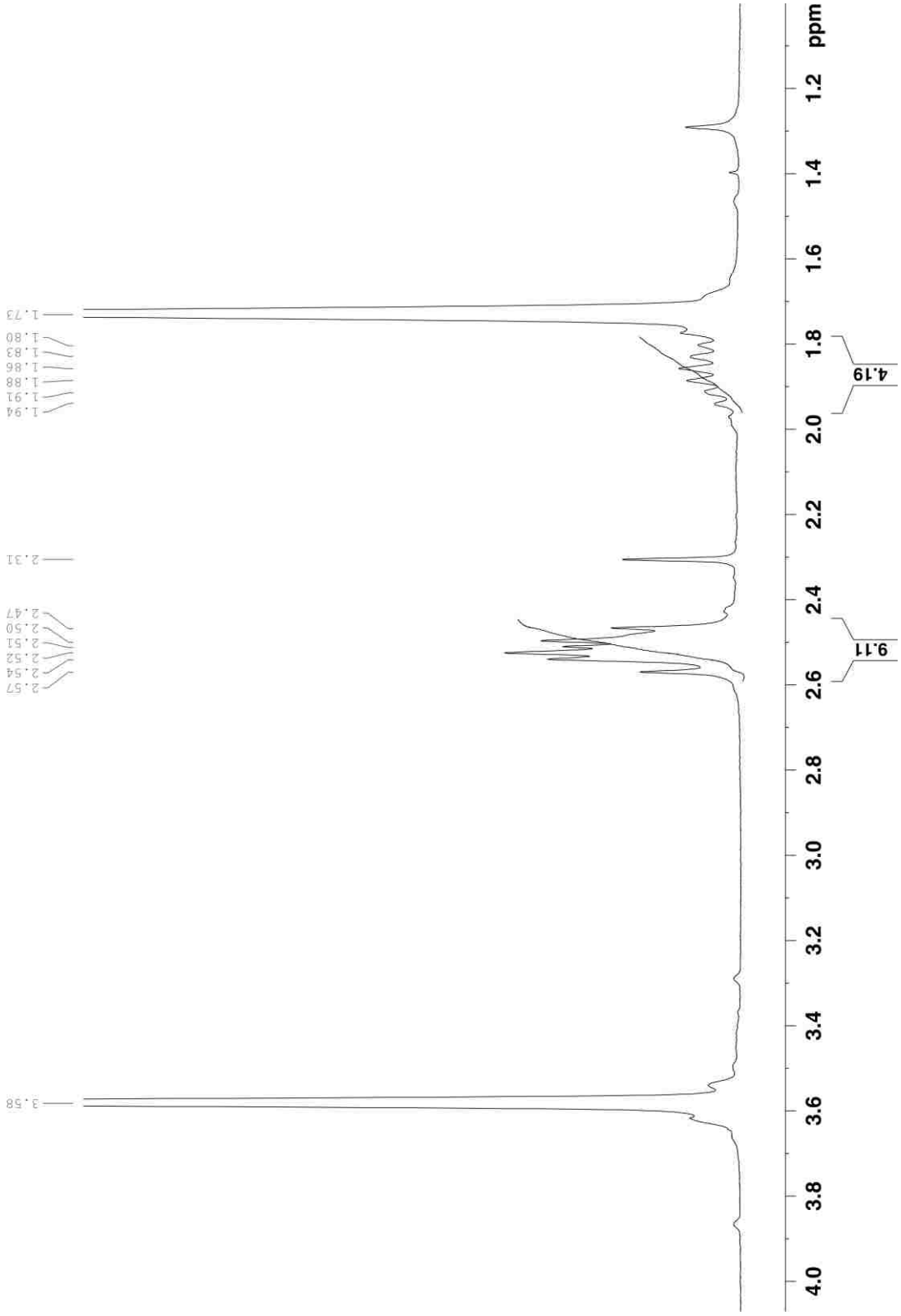

Figure A-20. ^{1}H NMR of the external bithiophene nickel catalyst **3-3** (extended aliphatic region) (400 MHz, THF-D_8)

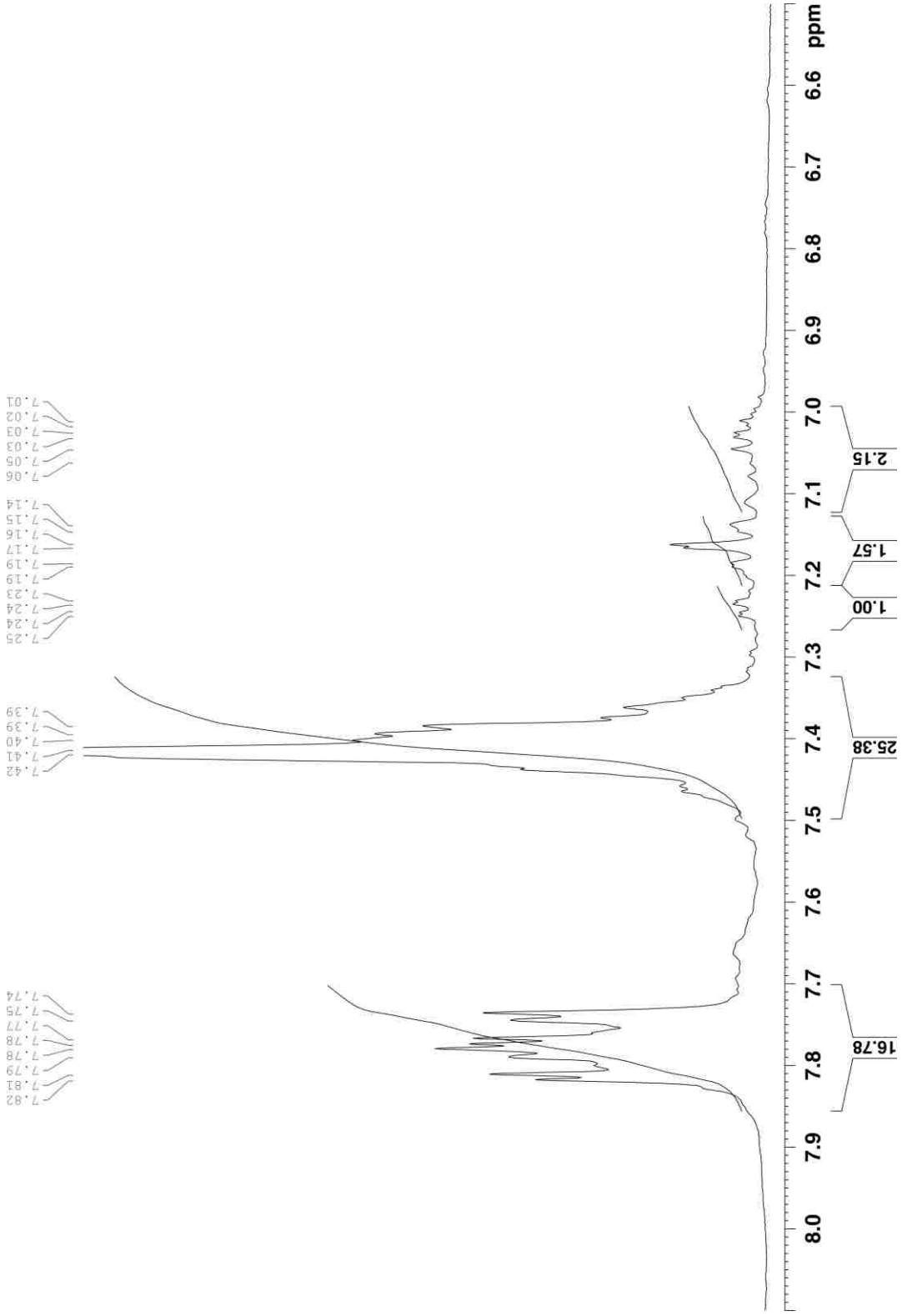

Figure A-21. ^{1}H NMR of the external bithiophene nickel catalyst **3-3** (extended aromatic region) (400 MHz, THF-D_8)

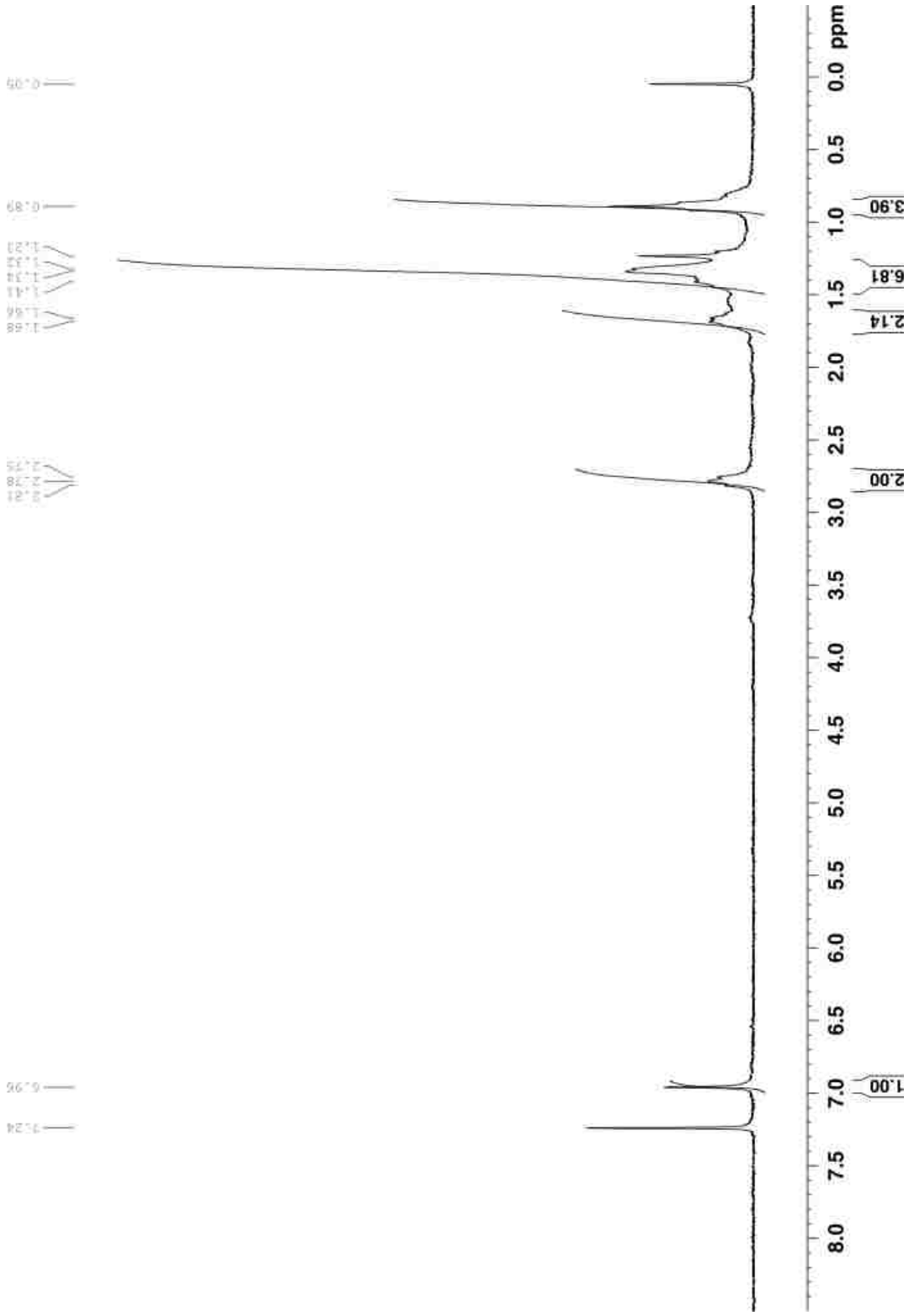

Figure A-22. ^{1}H NMR of **3-8** (M_n: 48kDa, PDI: 1.35, rr~100%) (400 MHz, $CDCl_3$)

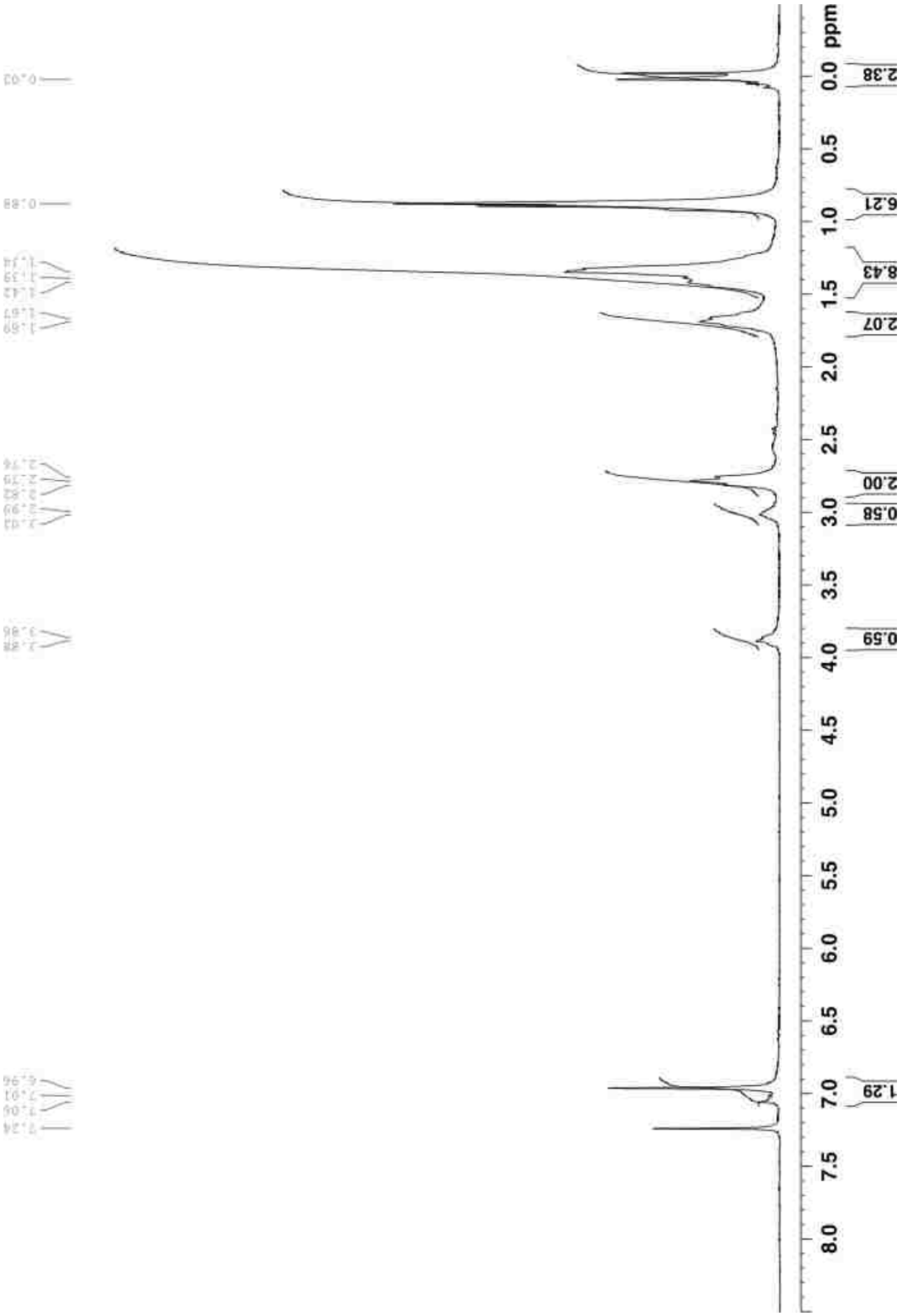

Figure A-23. ^{1}H NMR of **3-9-1** (M_n: 70kDa, PDI: 1.27, rr~100%); Ratio of poly(**3-6**) to poly(**3-7**) blocks 3.5:1 (250 MHz, $CDCl_3$)

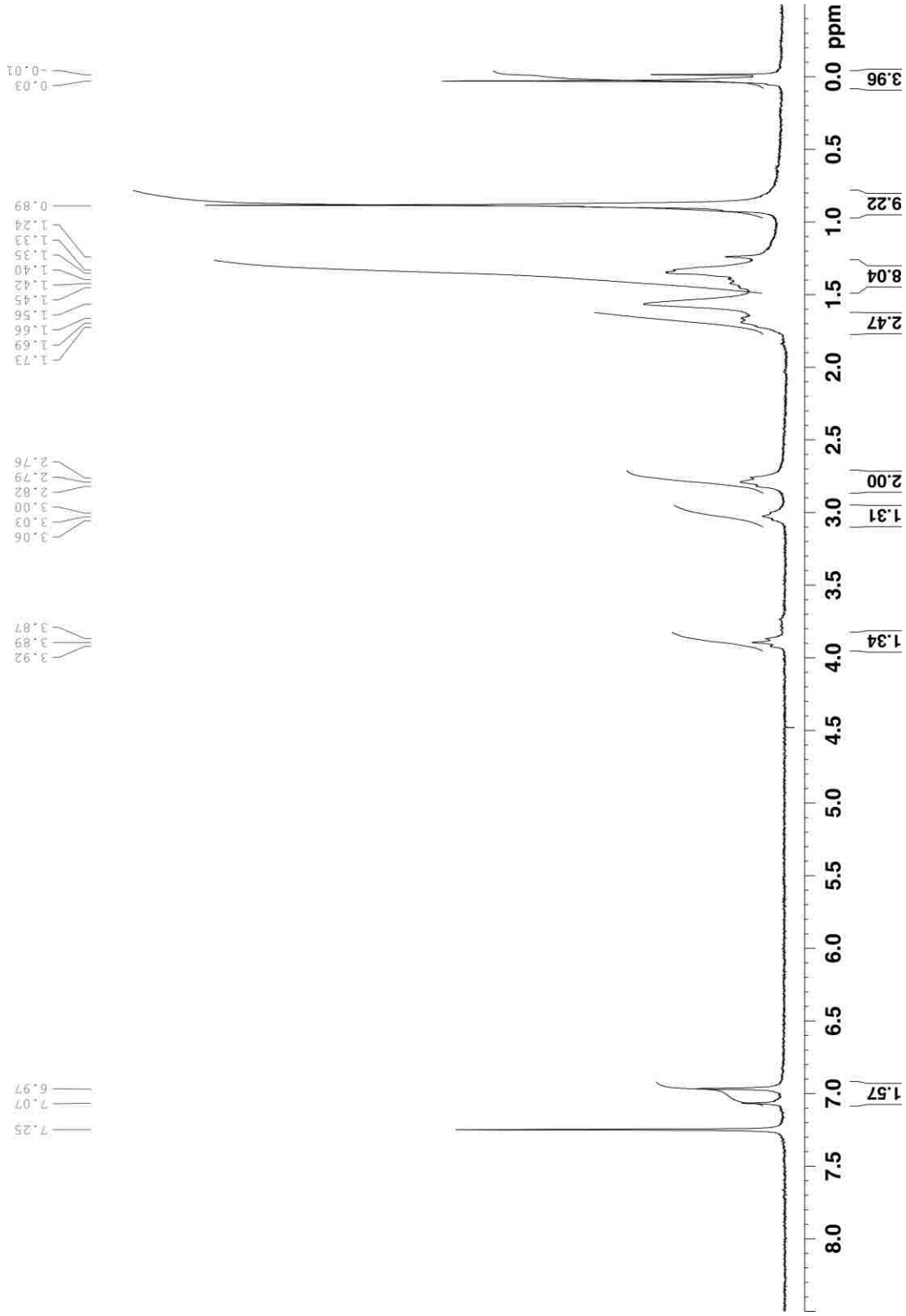

Figure A-24. ^{1}H NMR of **3-9-2** (M_n: 80kDa, PDI: 1.47, rr~100%); Ratio of poly(**3-6**) to poly(**3-7**) blocks 1.5:1 (250 MHz, $CDCl_3$)

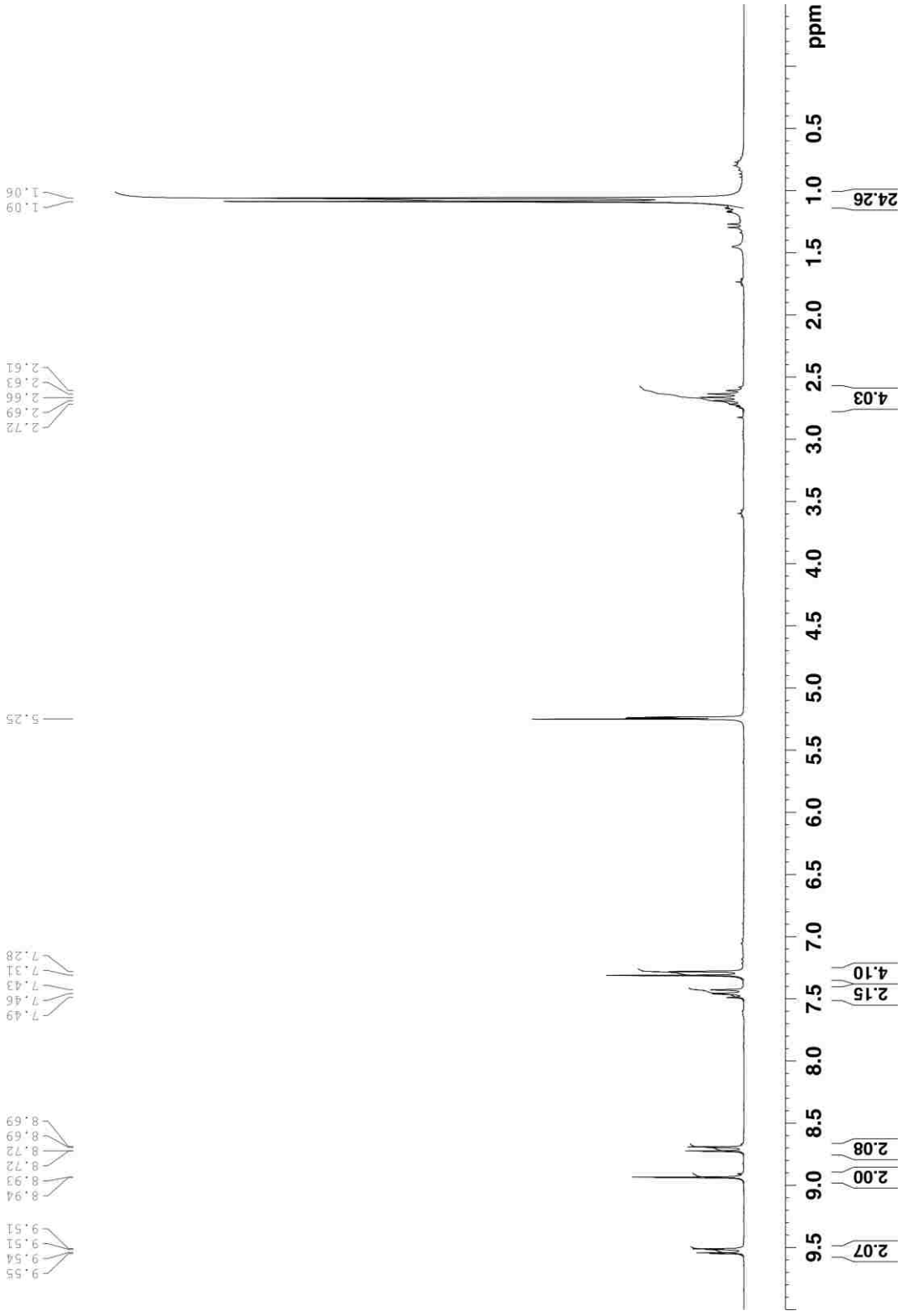

Figure A-25. ^{1}H NMR of compound **4-PDCI2** (250 MHz, CD_2Cl_2)

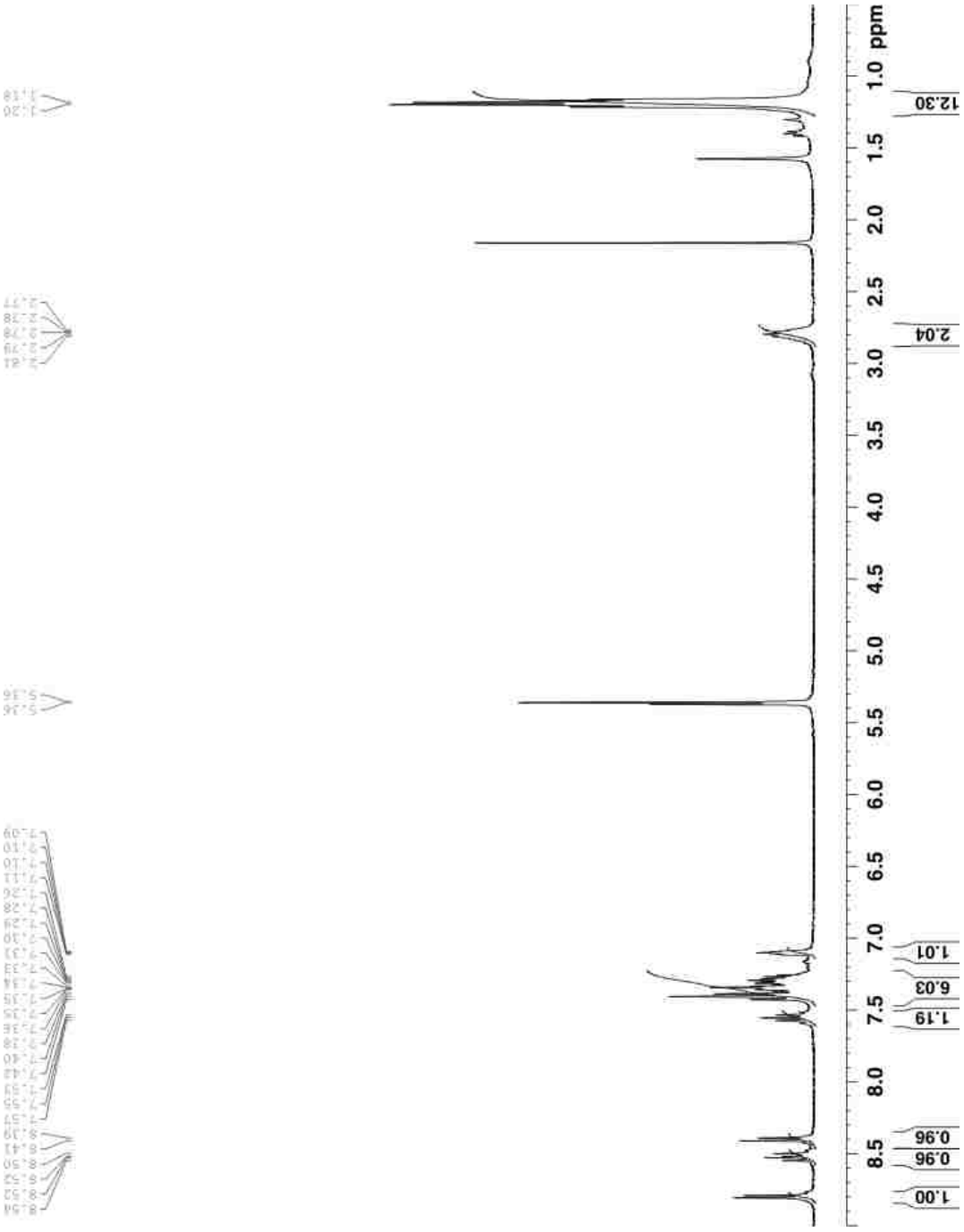

Figure A-26. ^{1}H NMR of compound **4-PDCI3** (400 MHz, CD_2Cl_2)

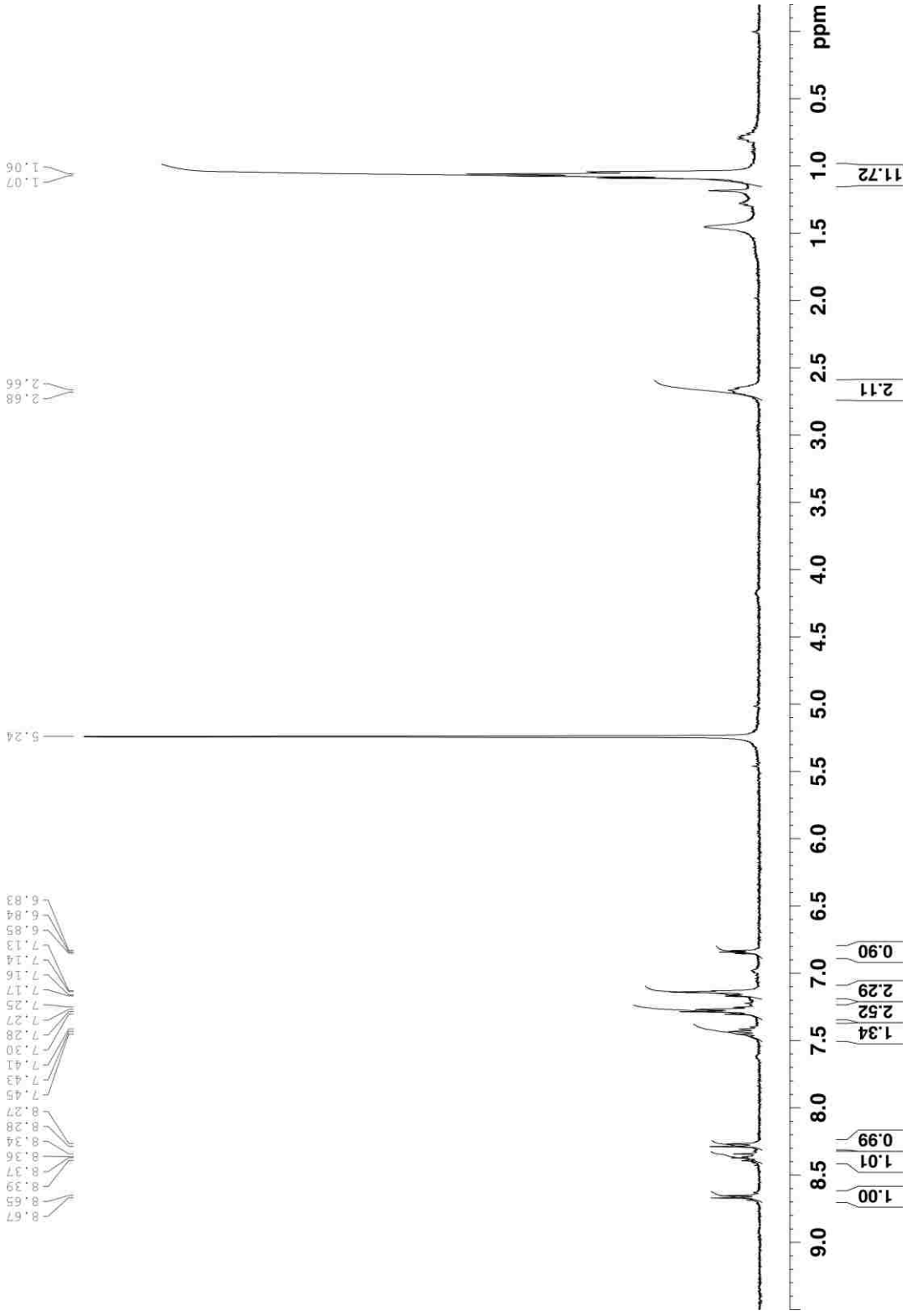

Figure A-27. ^{1}H NMR of compound **4-S1** (400 MHz, CD_2Cl_2)

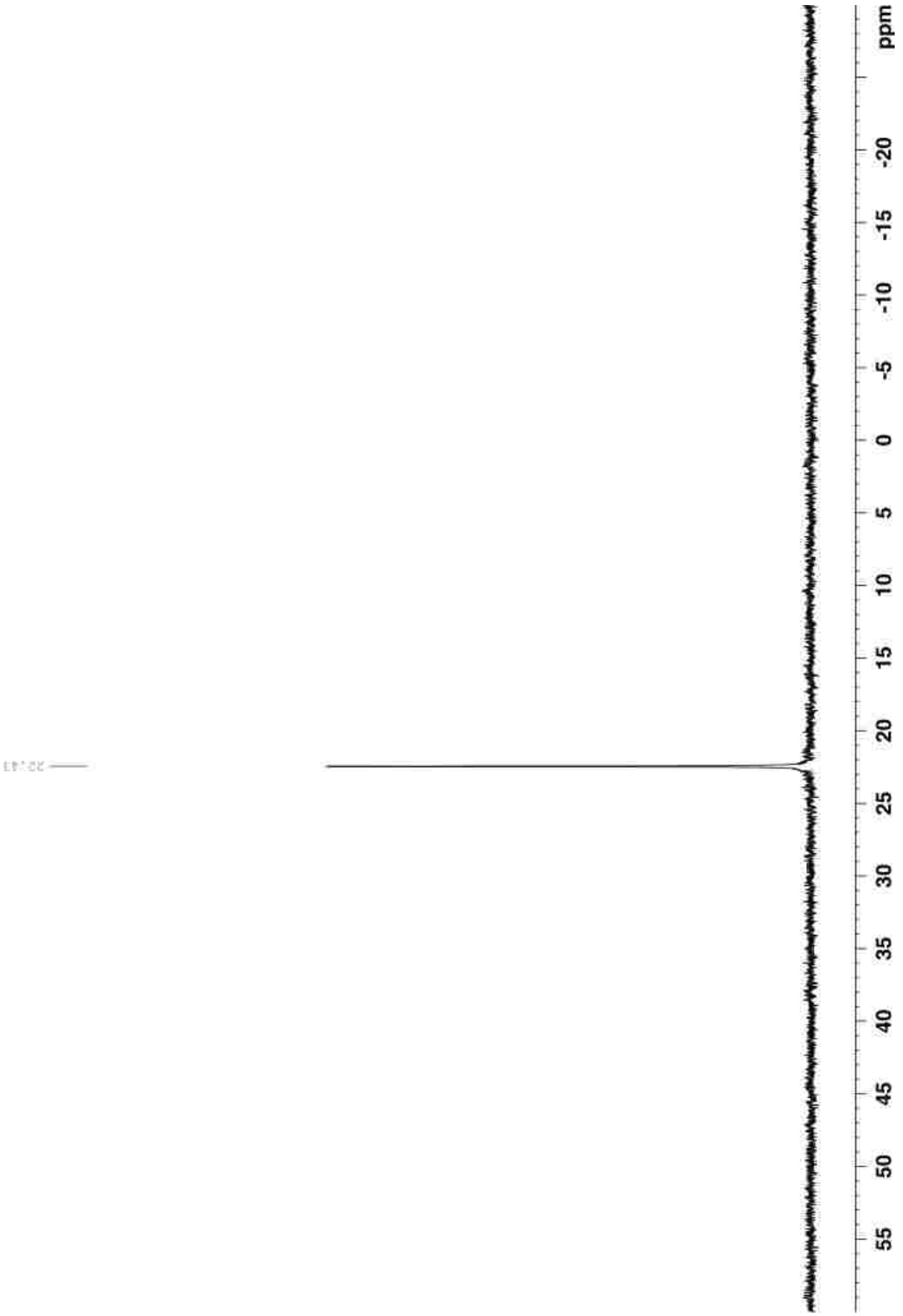

Figure A-28. ^{31}P NMR of the external PDCI initiator **4-S2** (162 MHz, THF)

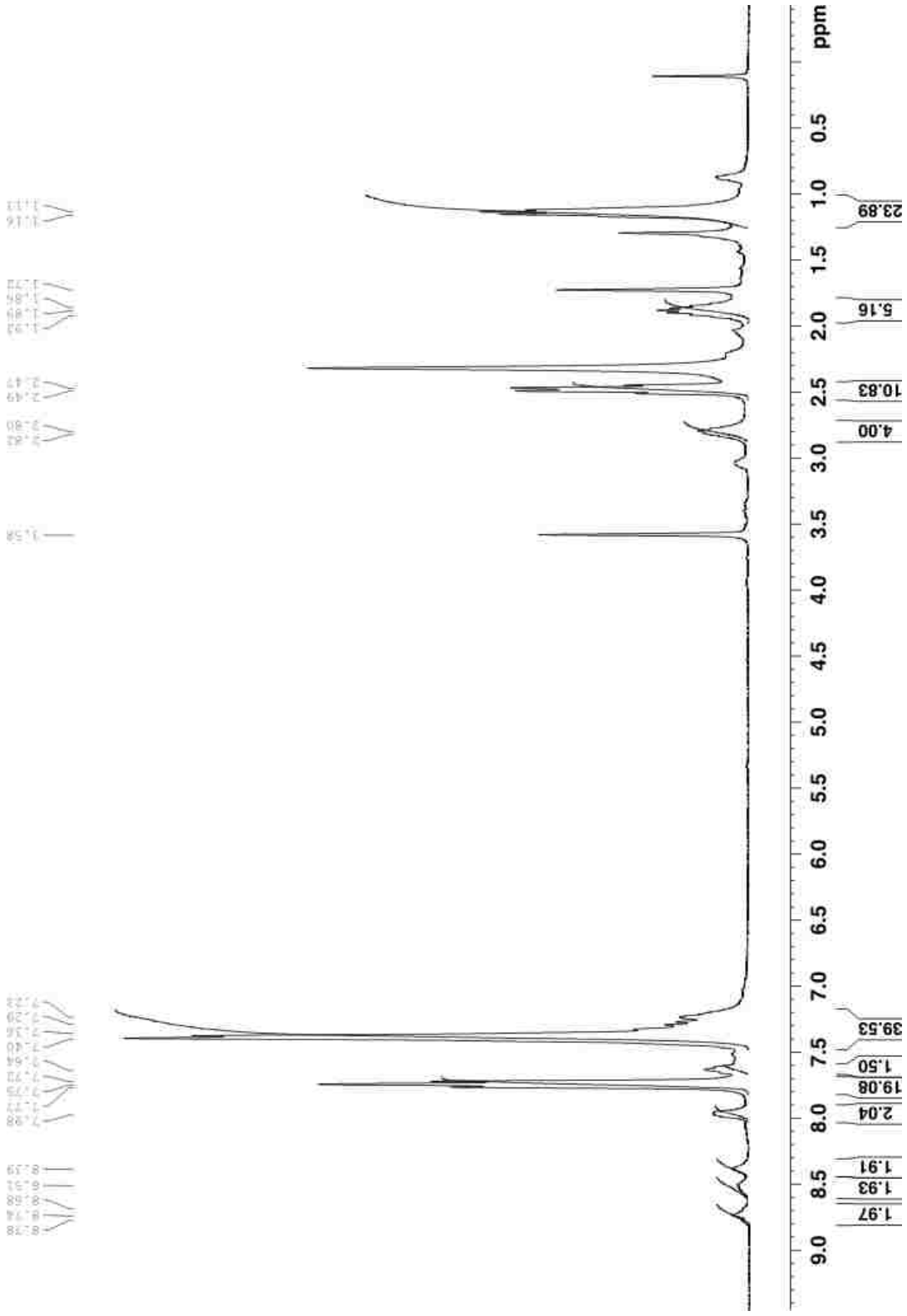

Figure A-29. ^{1}H NMR of the external PDCI initiator **4-S2** (400 MHz, THF-D_8)

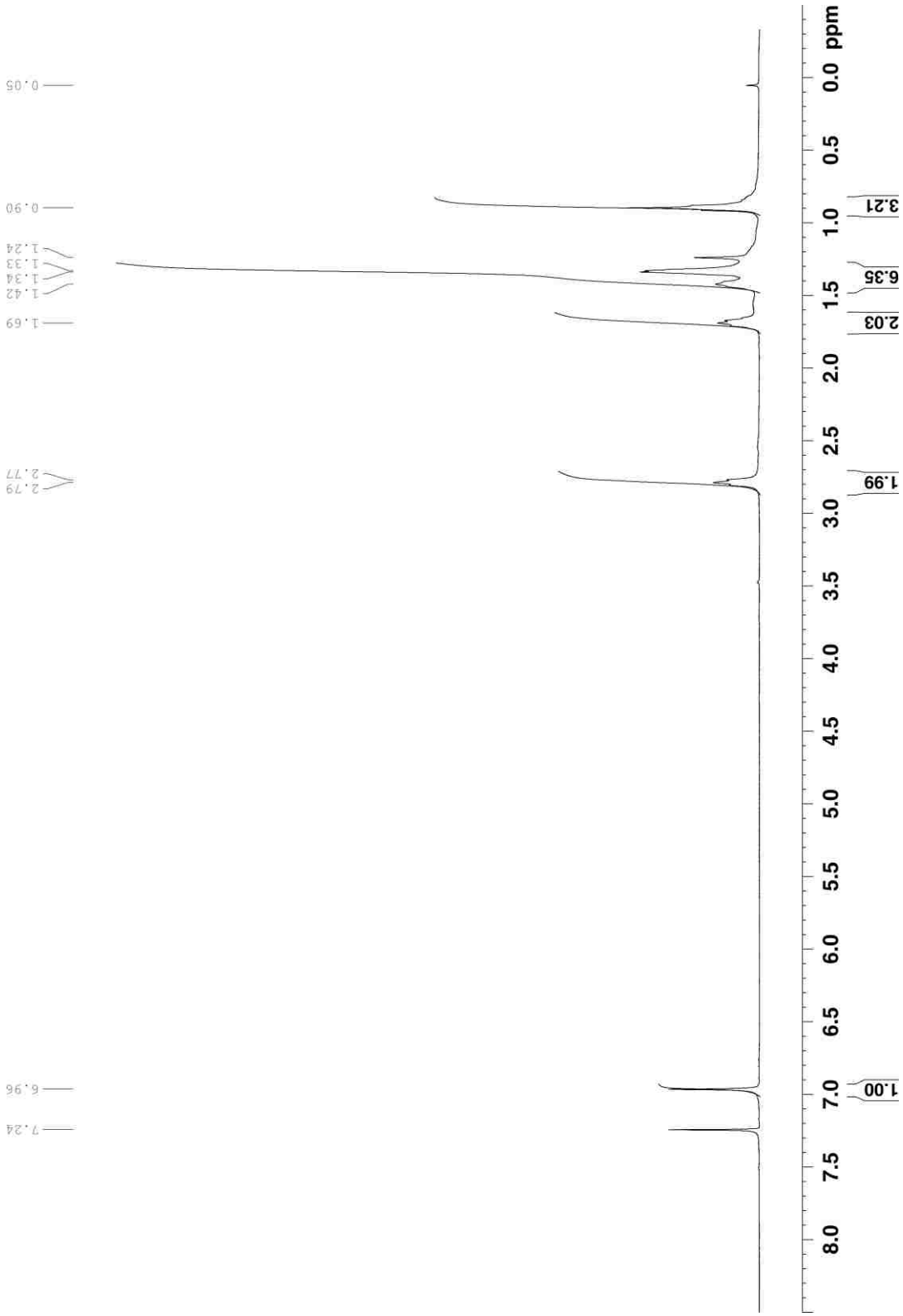

Figure A-30. ^{1}H NMR of high M_n **4-P1** (GPC: 53kDa, PDI: 1.34, rr: 100%) (400 MHz, $CDCl_3$)

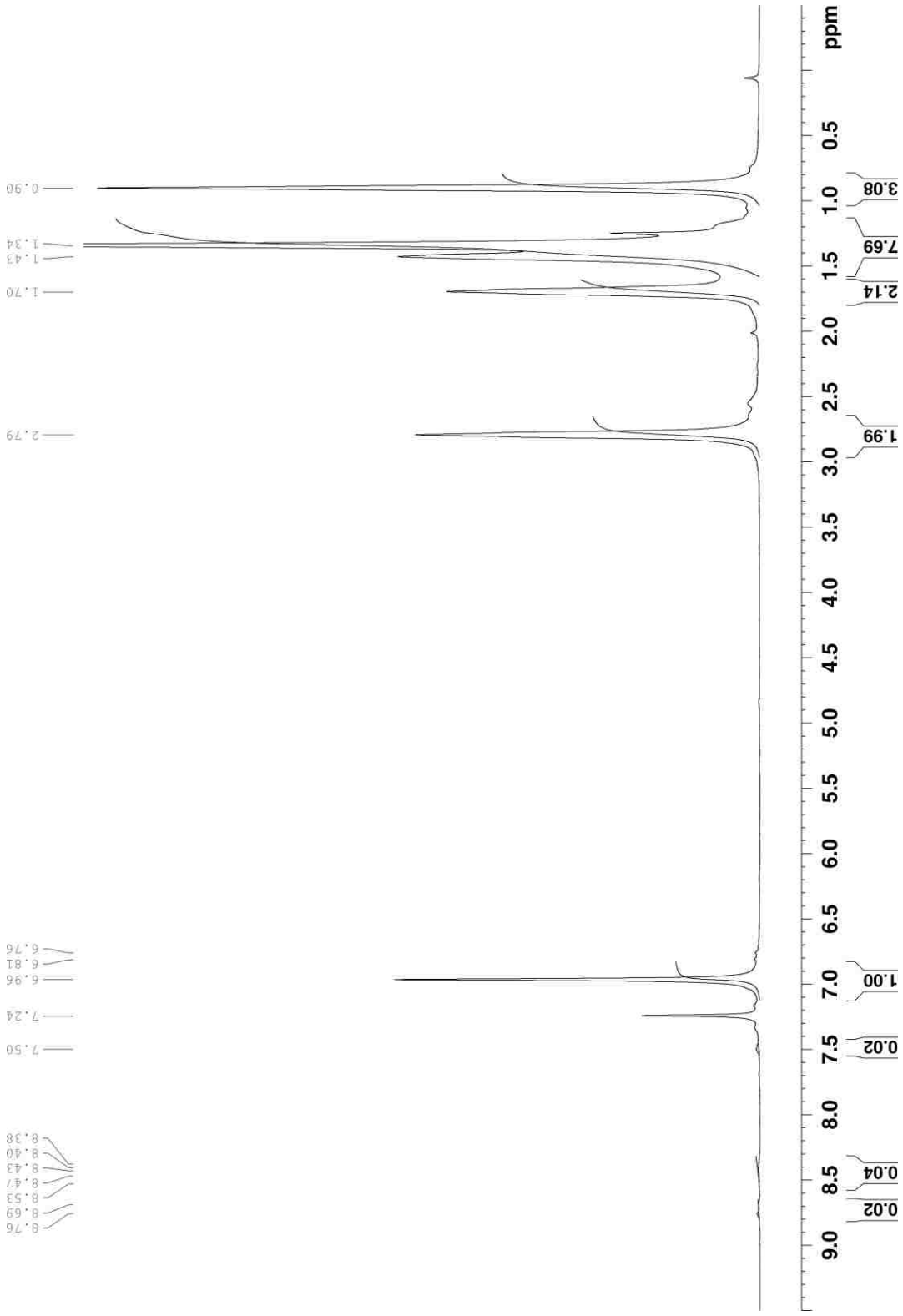

Figure A-31. ^{1}H NMR of low M_n **4-P1** (GPC: 24kDa and NMR: 19k) (400 MHz, $CDCl_3$)

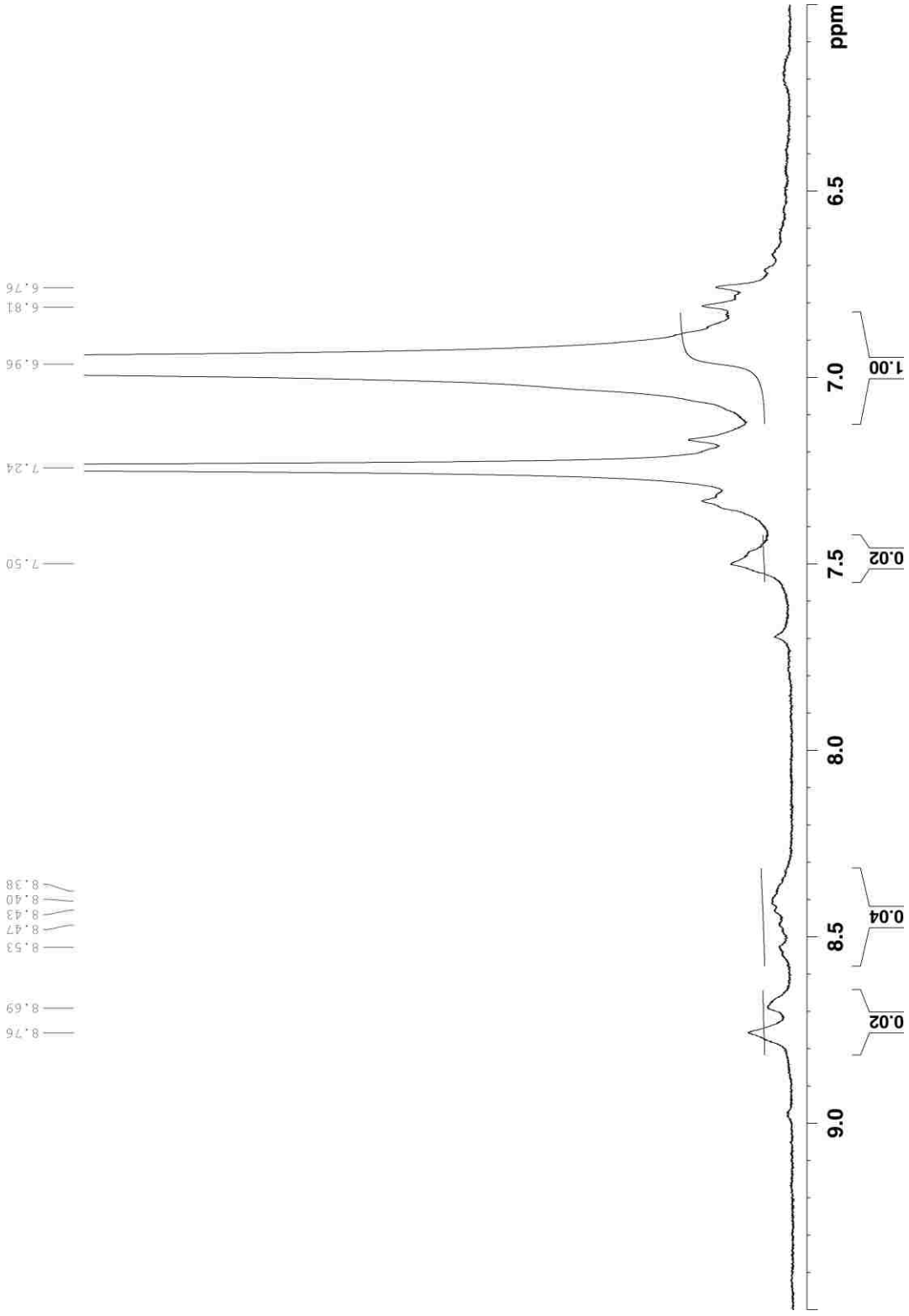

Figure A-32. ^{1}H NMR of low M_n **4-P1** (extended aromatic region)

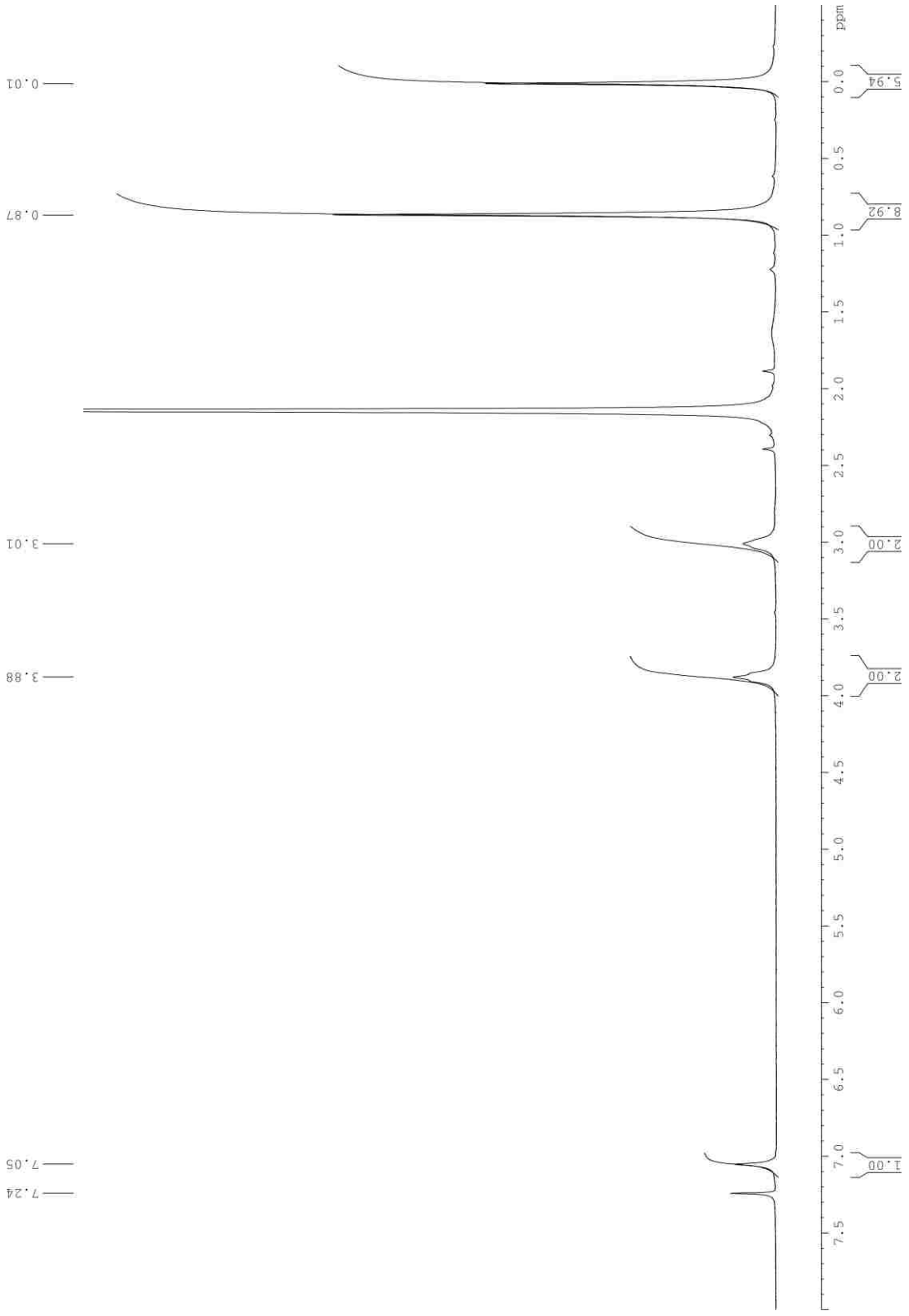

Figure A-33. ^{1}H NMR of **4-M1** (GPC: 31kDa, PDI: 1.46, rr: 100%) (400 MHz, $CDCl_3$)

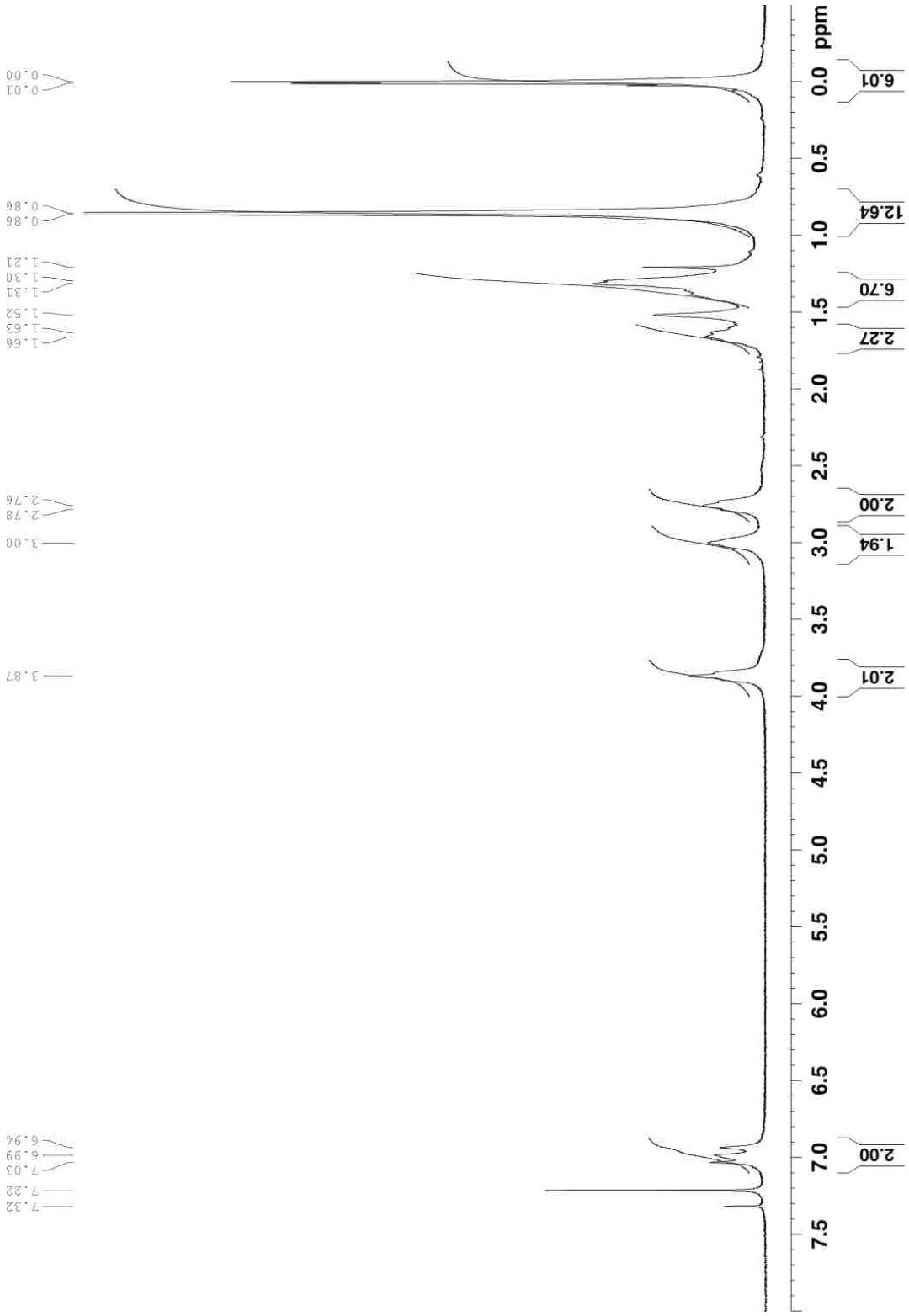

Figure A-34. ^{1}H NMR of **4-1-1** (M_n: 47kDa, PDI: 1.39, rr~100%); Ratio of poly(**3-6**) to poly(**3-7**) blocks 1:1 (250 MHz, $CDCl_3$)

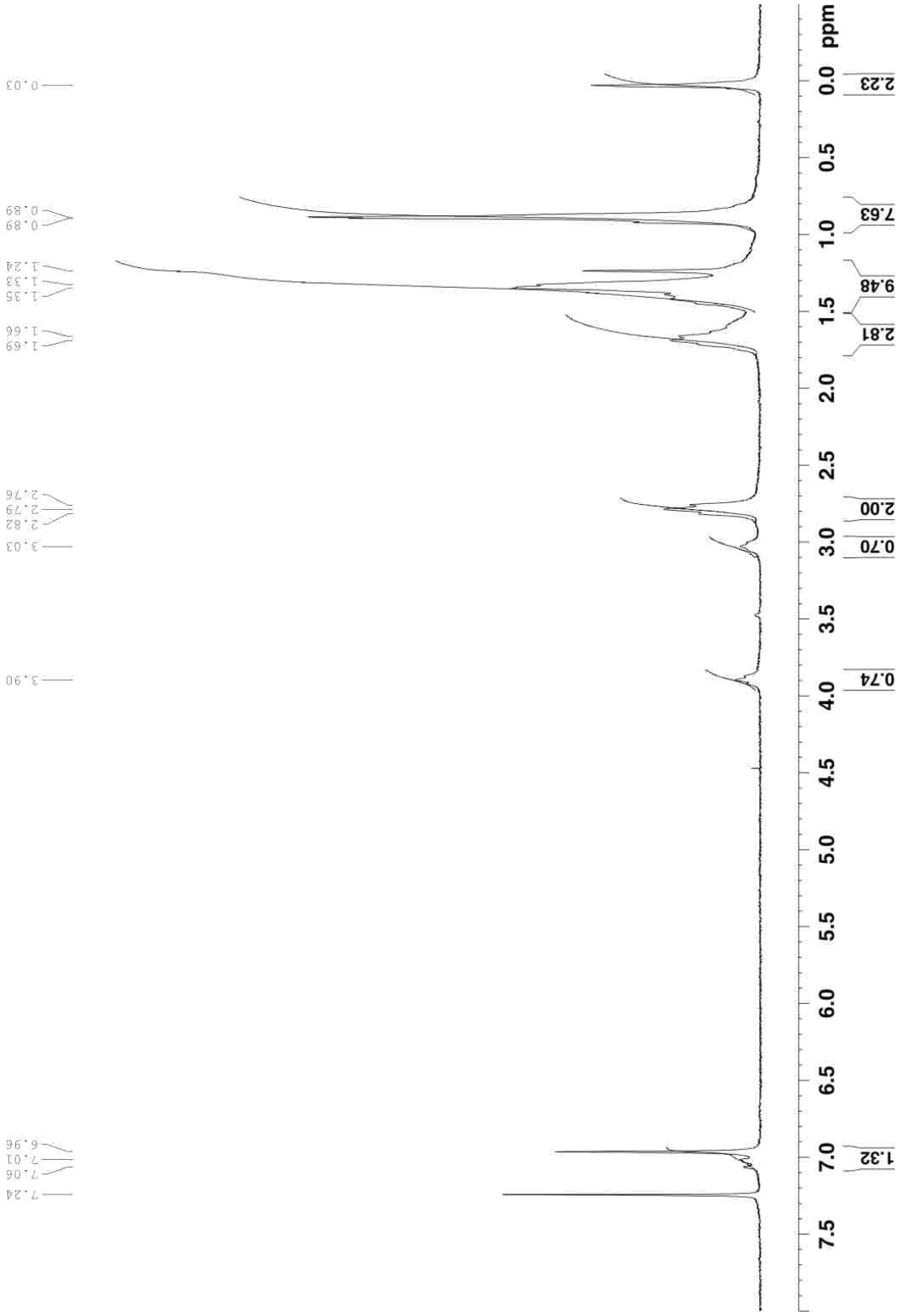

Figure A-35. ^{1}H NMR of **4-1-2** (M_n: 44kDa, PDI: 1.43, rr~100%); Ratio of poly(**3-6**) to poly(**3-7**) blocks 3:1 (250 MHz, $CDCl_3$)

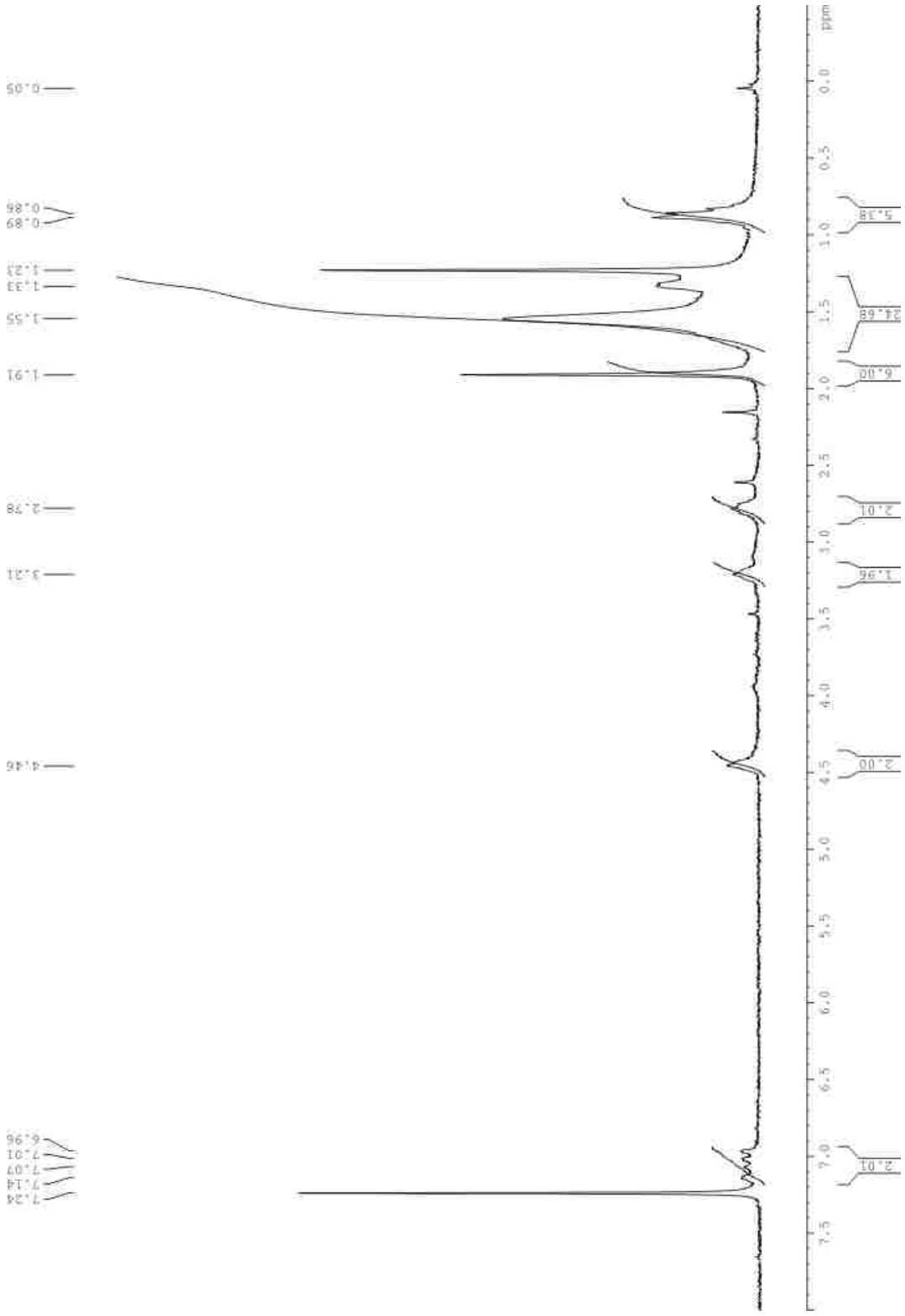

Figure A-36. ^{1}H NMR of macroinitiator **4-2-1** (250 MHz, $CDCl_3$)

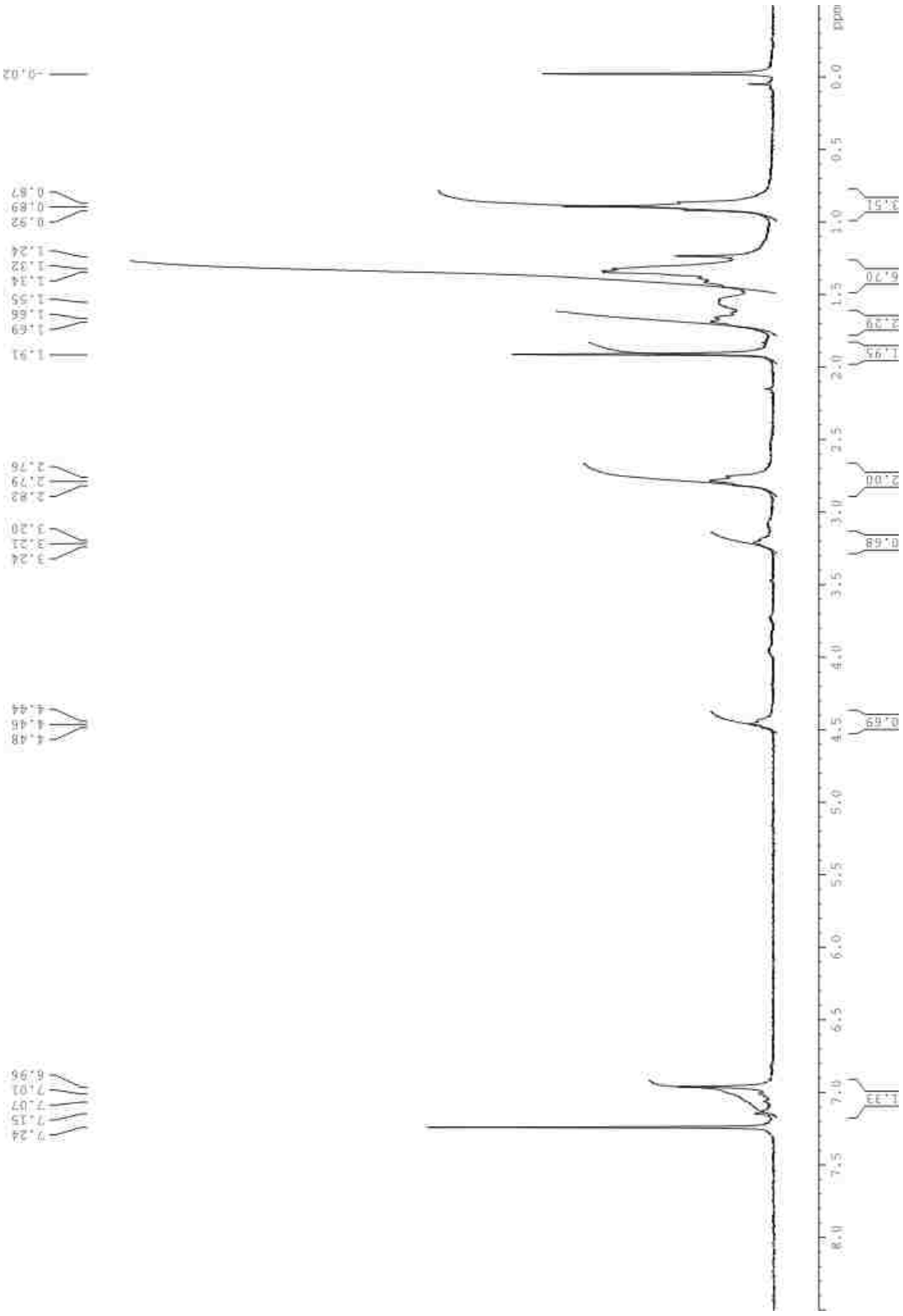

Figure A-37. ^{1}H NMR of macroinitiator **4-2-2** (250 MHz, $CDCl_3$)

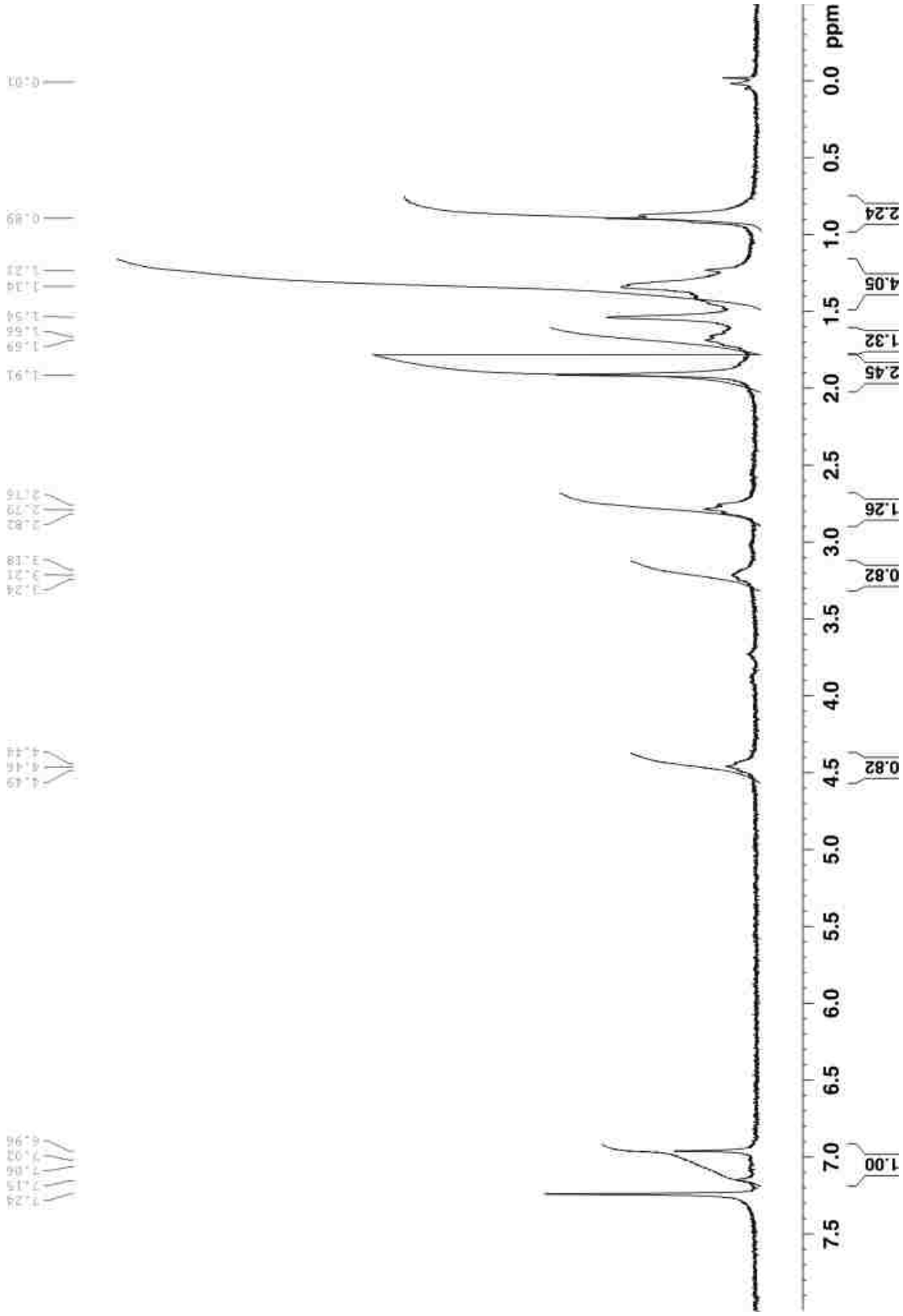

Figure A-38. ^{1}H NMR of macroinitiator **4-2-3** (250 MHz, $CDCl_3$)

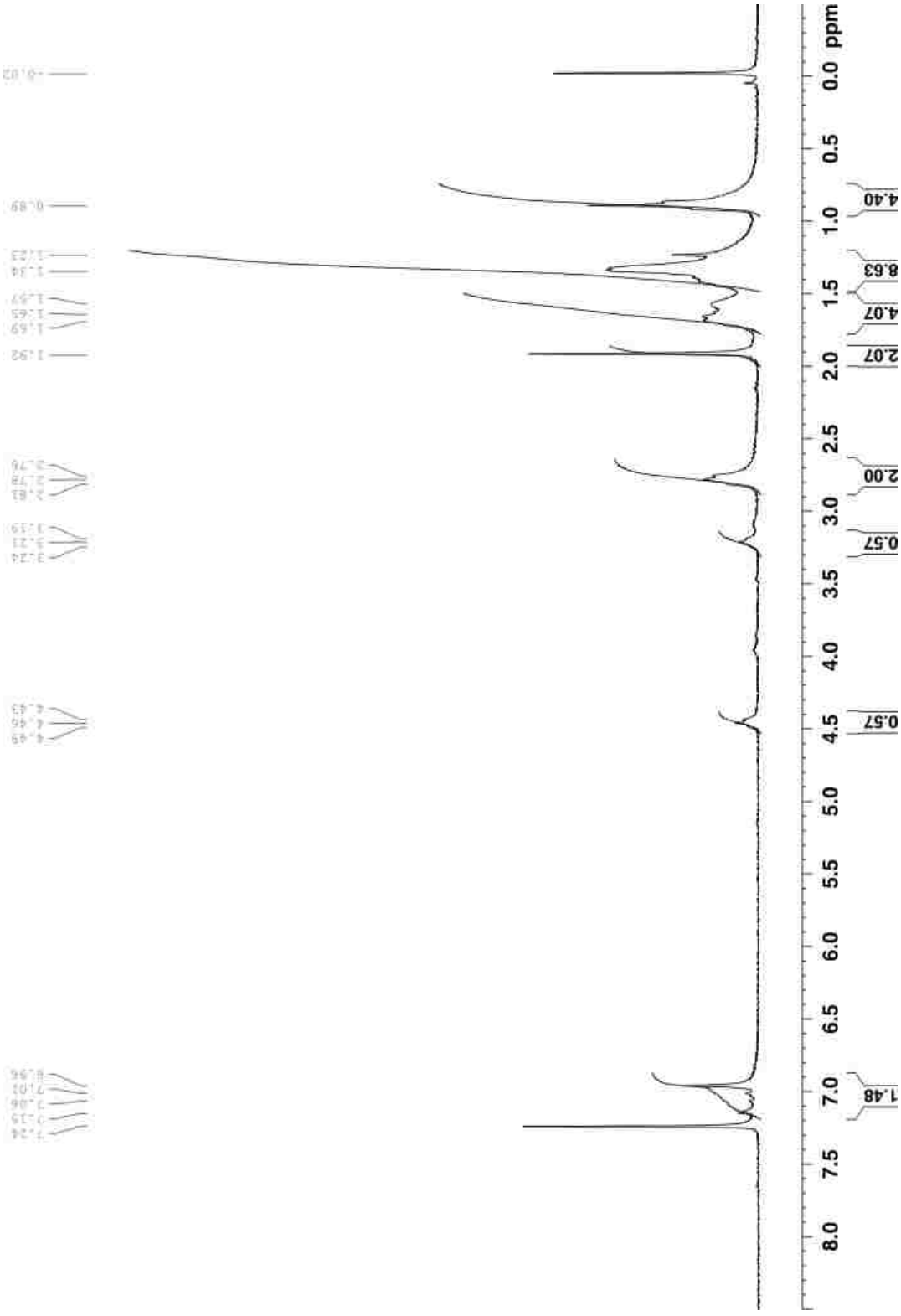

Figure A-39. ^{1}H NMR of macroinitiator **4-2-4** (250 MHz, $CDCl_3$)

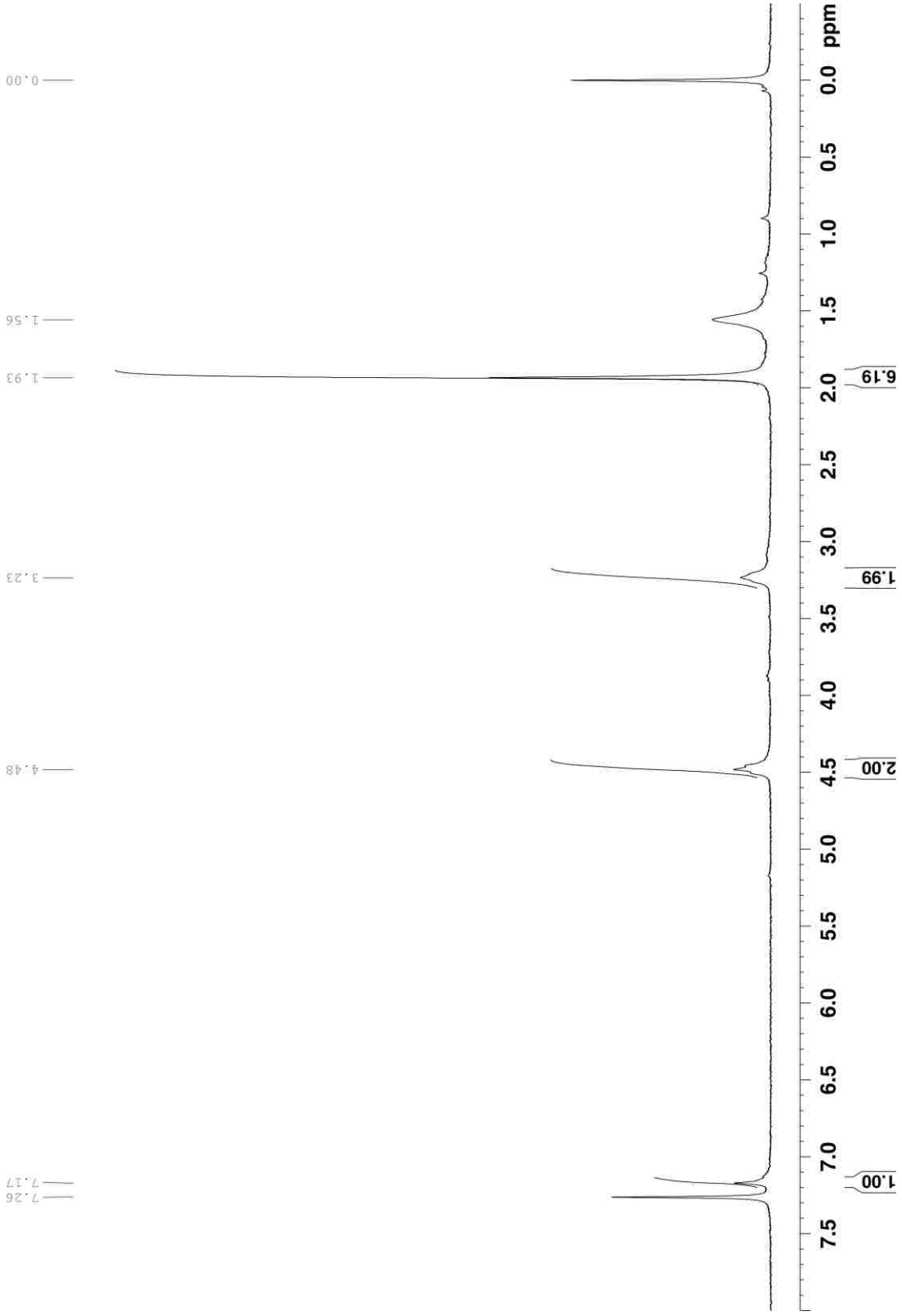

Figure A-40. ^{1}H NMR of macroinitiator **4-M2** (250 MHz, $CDCl_3$)

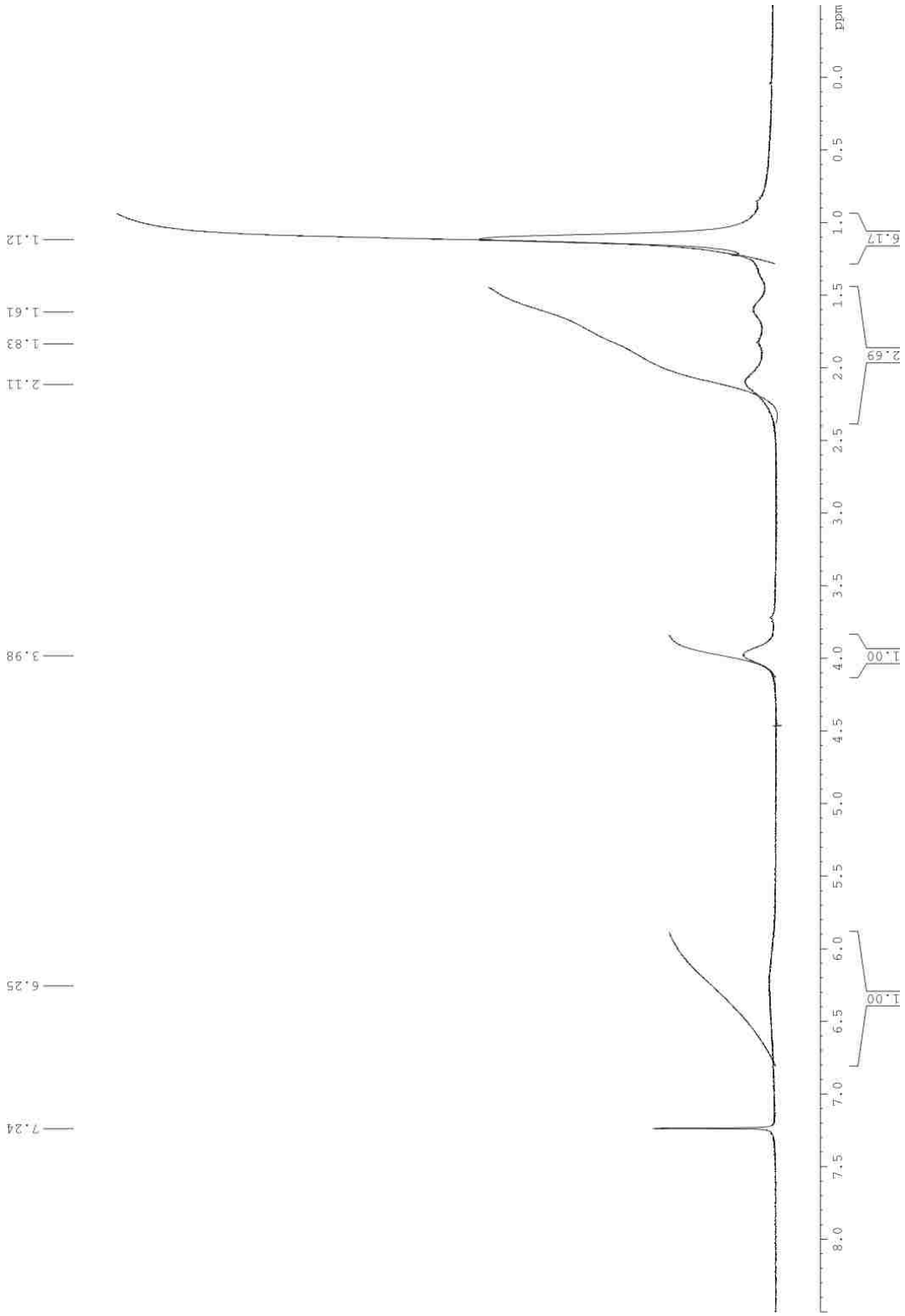

Figure A-41. ^{1}H NMR of amphiphilic diblock copolymer **4-3-1~4-3-4, 4-P2** (all are identical) (250 MHz, $CDCl_3$)

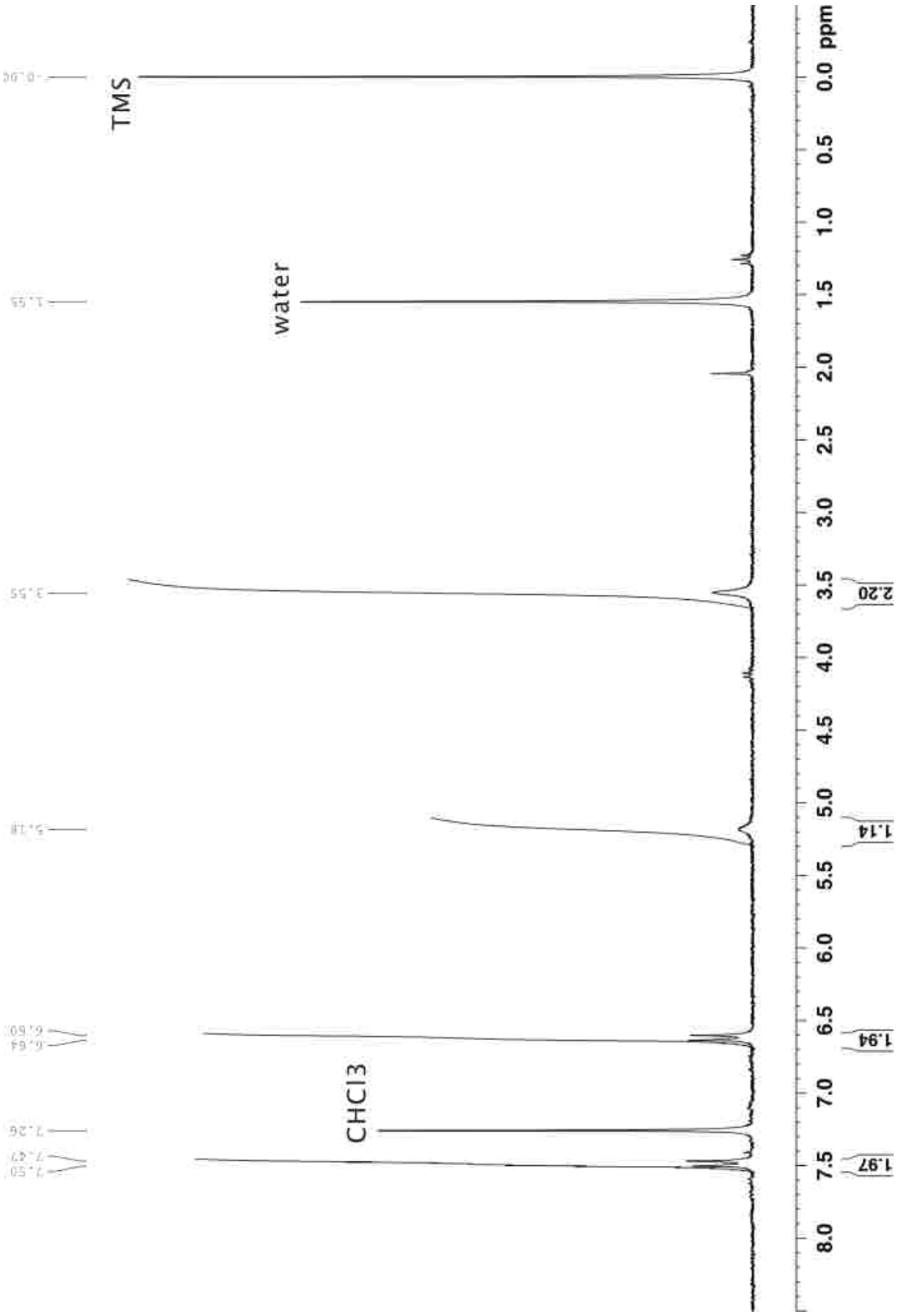

Figure A-42. ^{1}H NMR of **5-2** (250 MHz, $CDCl_3$)

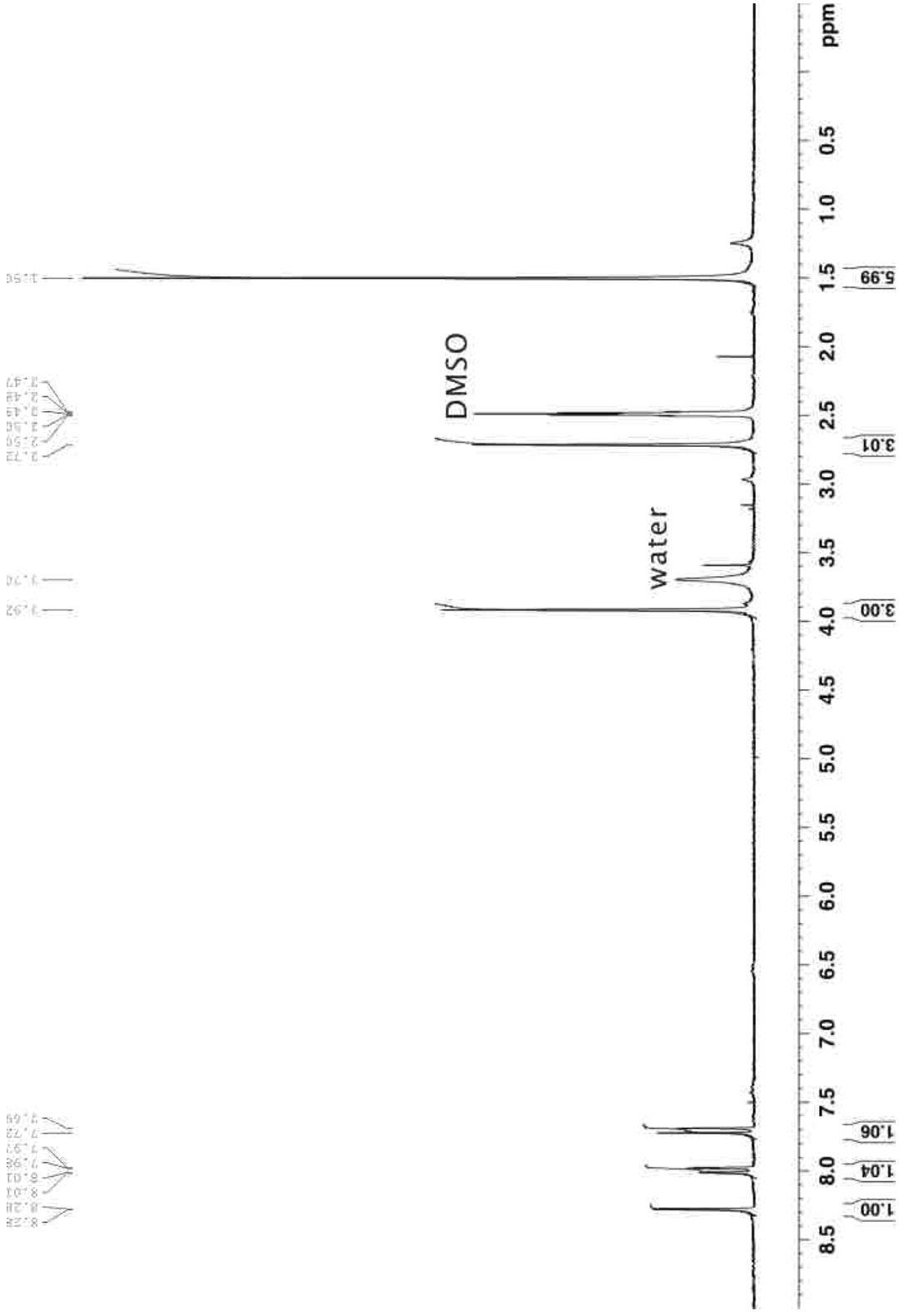

Figure A-43. ^{1}H NMR of **5-3** (250 MHz, DMSO-D_6)

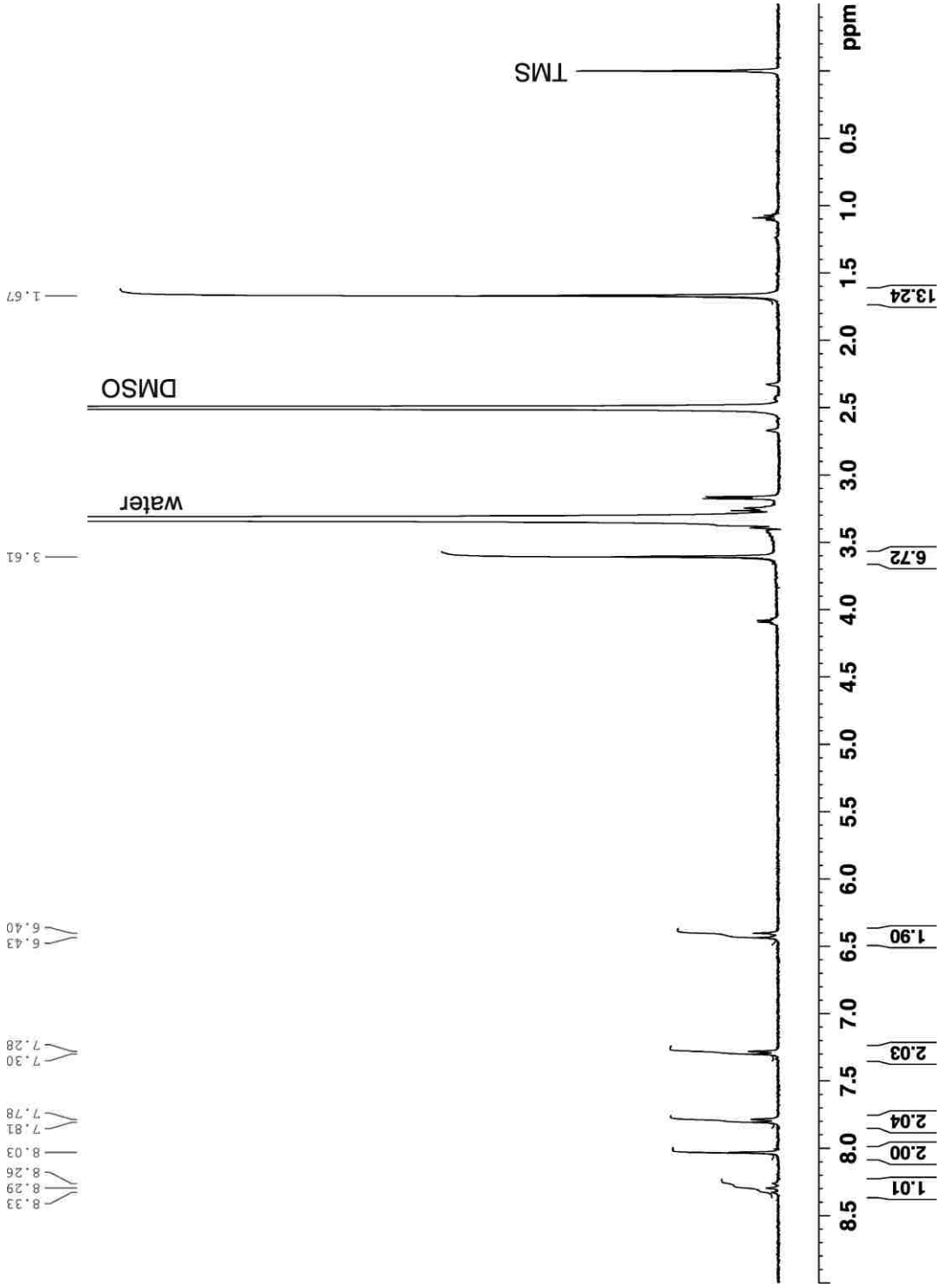

Figure A-44. ^{1}H NMR of mCy3 (diI-Cy3), **5-4** (400 MHz, DMSO-D_6)

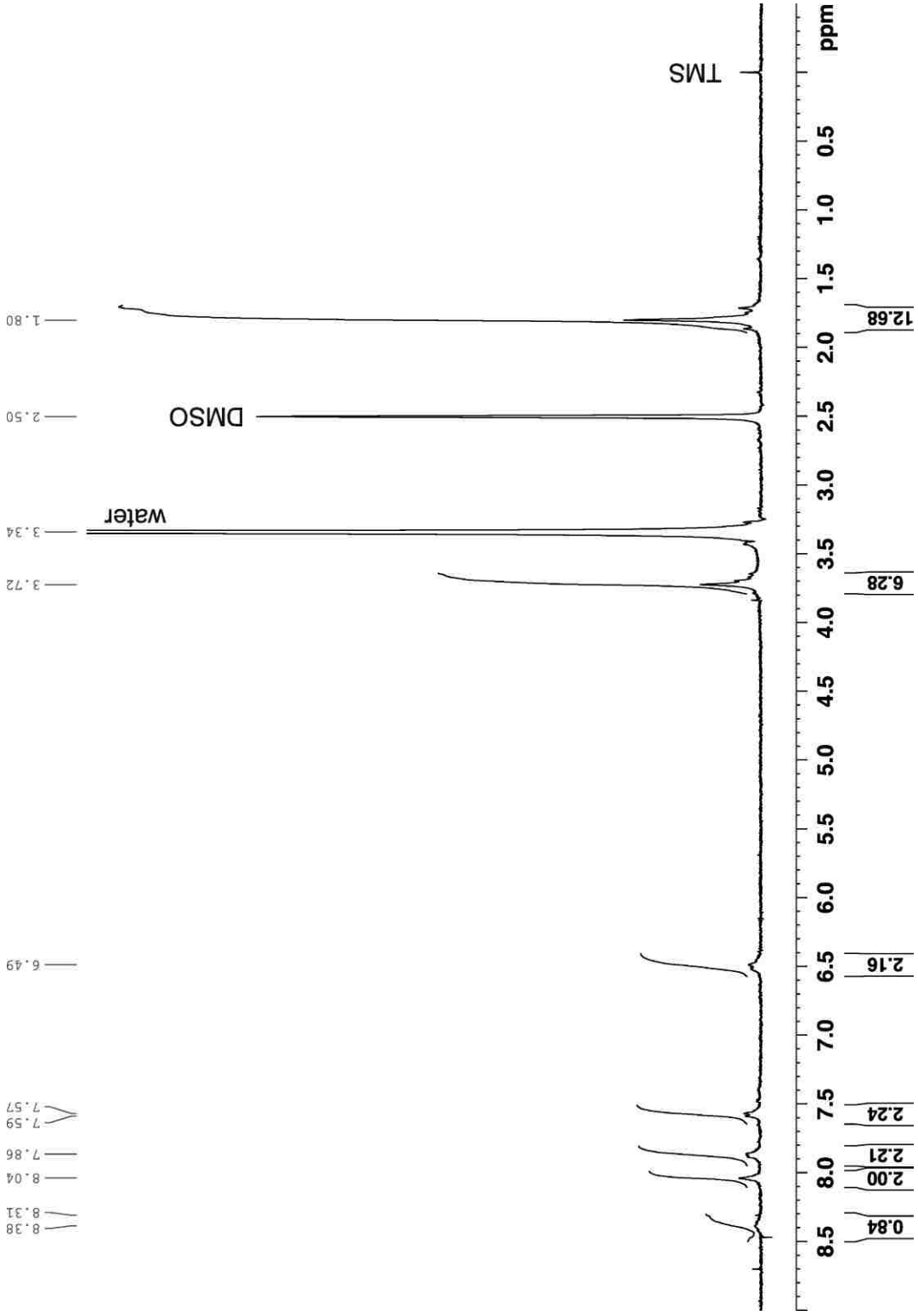

Figure A-45. ^{1}H NMR of poly(Cy3), **5-5** (400 MHz, DMSO-D_6)

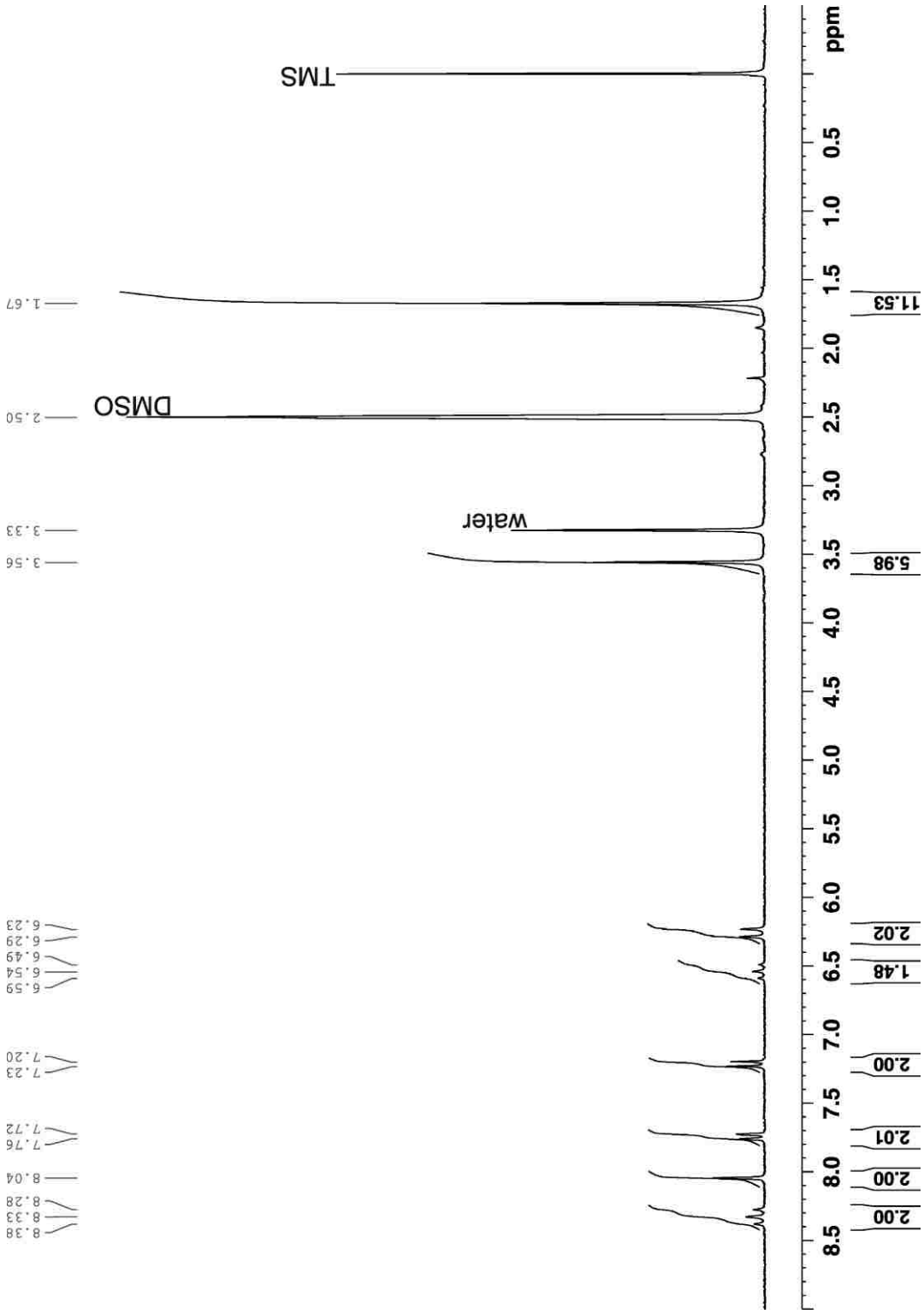

Figure A-46. ^{1}H NMR of mCy5 (diI-Cy5), **5-6** (250 MHz, DMSO-D_6)

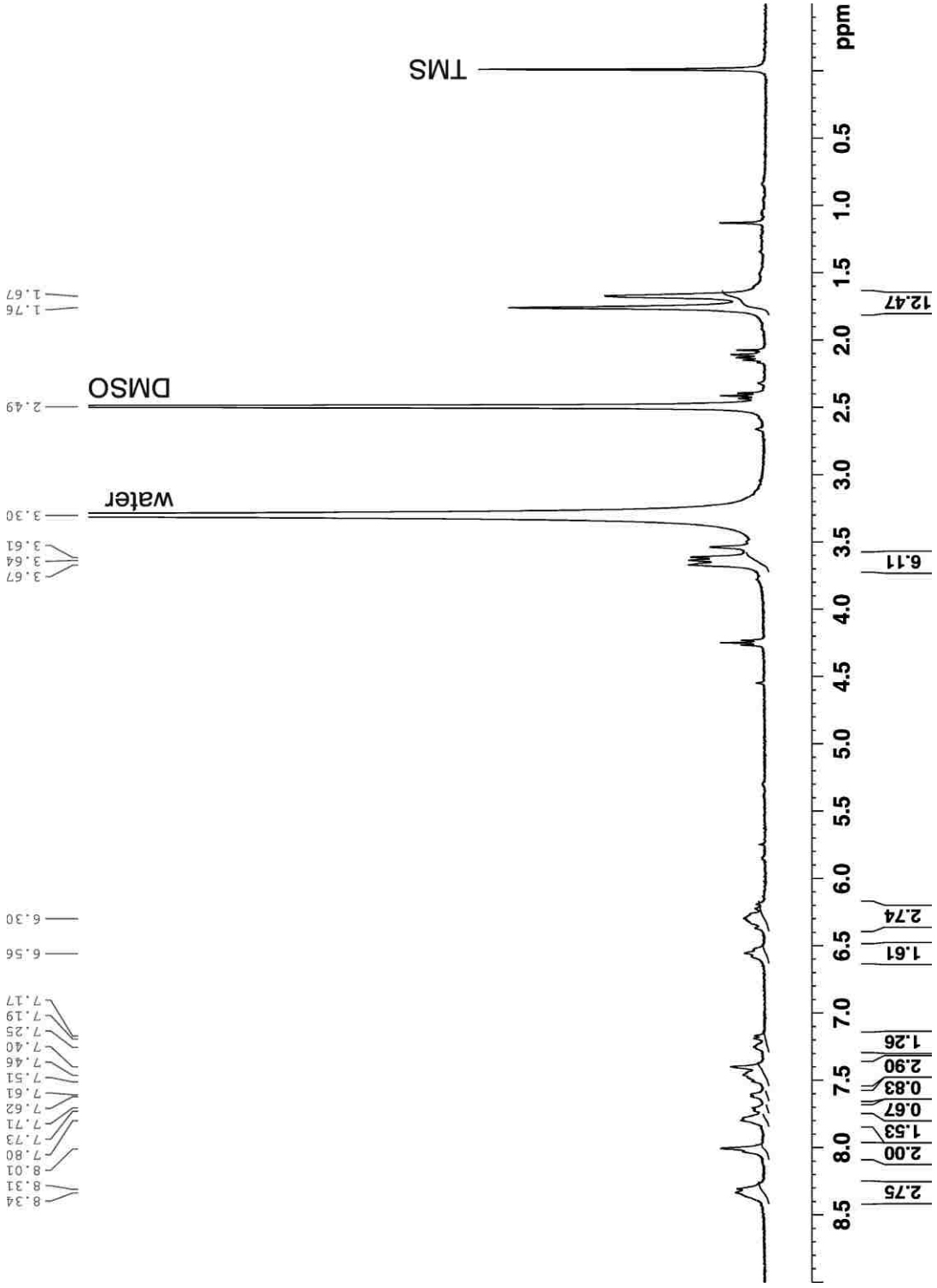

Figure A-47. ^{1}H NMR of poly(Cy5), **5-7** (400 MHz, DMSO-D_6)

APPENDIX B: PERMISSION TO REUSE CONTENTS FROM PUBLICATIONS

AMERICAN CHEMICAL SOCIETY LICENSE
TERMS AND CONDITIONS

Apr 20, 2011

This is a License Agreement between Jinwoo Choi ("You") and American Chemical Society ("American Chemical Society") provided by Copyright Clearance Center ("CCC"). The license consists of your order details, the terms and conditions provided by American Chemical Society, and the payment terms and conditions.

All payments must be made in full to CCC. For payment instructions, please see information listed at the bottom of this form.

License Number	2653340920542
License Date	Apr 20, 2011
Licensed content publisher	American Chemical Society
Licensed content publication	Journal of American Chemical Society
Licensed content title	Externally Initiated Regioregular P3HT with Controlled Molecular Weight and Narrow Polydispersity
Licensed content author	Hugo A. Bronstein et al.
Licensed content date	Sep 1, 2009
Volume number	131
Issue number	36
Type of Use	Thesis/Dissertation
Requestor type	Not specified
Format	Electronic
Portion	Table/Figure/Micrograph
Number of Table/Figure/Micrographs	1
Author of this ACS article	No
Order reference number	1
Title of the thesis / dissertation	SEMICONDUCTING POLYMERS AND DIBLOCK COPOLYMERS PREPARED BY LIVING POLYMERIZATION
Expected completion date	May 2011
Estimated size(pages)	120
Billing Type	Invoice
Billing Address	Choppin 212, dept. of chemistry, lsu Baton Rouge, LA 70803 United States
Customer reference info	
Total	0.00 USD
Terms and Conditions	

AMERICAN CHEMICAL SOCIETY LICENSE
TERMS AND CONDITIONS

Apr 13, 2011

This is a License Agreement between Jinwoo Choi ("You") and American Chemical Society ("American Chemical Society") provided by Copyright Clearance Center ("CCC"). The license consists of your order details, the terms and conditions provided by American Chemical Society, and the payment terms and conditions.

All payments must be made in full to CCC. For payment instructions, please see information listed at the bottom of this form.

License Number	2644291417329
License Date	Apr 08, 2011
Licensed content publisher	American Chemical Society
Licensed content publication	Macromolecules
Licensed content title	Temperature-Induced Control of Conformation and Conjugation Length in Water-Soluble Fluorescent Polythiophenes
Licensed content author	Jinwoo Choi et al.
Licensed content date	Feb 1, 2010
Volume number	43
Issue number	4
Type of Use	Thesis/Dissertation
Requestor type	Not specified
Format	Electronic
Portion	50% or more of original article
Author of this ACS article	Yes
Order reference number	
Title of the thesis / dissertation	SEMICONDUCTING POLYMERS AND DIBLOCK COPOLYMERS PREPARED BY LIVING POLYMERIZATION
Expected completion date	May 2011
Estimated size(pages)	150
Billing Type	Invoice
Billing Address	Choppin 212, dept. of chemistry, lsu Baton Rouge, LA 70803 United States
Customer reference info	
Total	0.00 USD
Terms and Conditions	

VITA

JinWoo Choi was born in Paltan, near Seoul, Korea. In his childhood, he spent time playing piano in order to become a musician; however, interest in chemistry allowed him to discover his ability toward organic chemistry drawing him to study in the college where he received Bachelor of Science degree in chemistry (2001) and Master of Science degree of organic materials chemistry (2003) in Korea University, Korea.

JinWoo worked on the total synthesis of biologically active organic compounds and drug compounds related to medicinal chemistry, synthetic organic chemistry and combinatorial organic chemistry method at Korea Institute of Science and Technology (KIST) in Korea from Jan, 2001 to Jul, 2004. Also, he worked on the methodological research employing environmentally favorable organometal catalysts, resulting in 12 peer-reviewed publications.

Under the financial support of NSF (National Science Foundation), KOSEF (Korea Science and Engineering Foundation), and LSU, Department of Chemistry, he received the degree of Doctor of Philosophy in Aug. 2011.